

M.Sc Chemistry



Inorganic Special Paper Semester IV

Course – 4101 B

Course Title – Spectral Techniques in Inorganic Chemistry

Nuclear Quadrupole Resonance (NQR) spectroscopy

- Nuclear quadrupole resonance spectroscopy is a branch of magnetic resonance spectroscopy and is concerned with the absorption of radio waves by matter in zero magnetic field. A unique feature of this kind of spectroscopy is the remarkably simple instrument that can be used to detect some signals, a circuit that can be constructed by anyone with some experience of radio techniques at a cost comparable to that of the cheapest transistor radio.
- A chemical detection technique used to measure molecules that have a magnetic dipole moment. The analysis is directed to nuclei which have a quadrupole moment which leads to an asymmetric electric charge distribution. The applied electric field, by frequency of radio waves, is directed into the atomic dipoles. The incident energy is to balance the fields between nuclei and electrons such that as the distribution returns to its natural state a spectrum is released. Analysis of the spectrum provides information for the determination of the particular chemical substance. NQR is applied to the detection of explosives and landmines such as TNT and RDX.

Introduction

Nuclear quadrupole resonance (NQR) spectroscopy is a method to characterize chemical compounds containing quadrupolar nuclei (QN). Similar as in nuclear magnetic resonance (NMR) the sample under investigation is irradiated with strong radiofrequency (RF) pulses to induce and detect transitions between sublevels of nuclear ground states. NMR refers to the situation where the sublevel energy splitting is predominantly due to nuclear interaction with an applied static magnetic field, while NQR refers to the case where the predominant splitting is due to an interaction with electric field gradients (EFG) within the material. Quadrupole splitting is possible if the charge distribution of the nucleus has an electric quadrupole moment. This is the case if the spin quantum-number I is greater than $1/2$. The electric quadrupole moment of the nucleus interacts with the EFG which is caused by a non-spherical charge distribution of the environment of the nucleus.

Acronyms, Synonyms

- Nuclear Quadrupole Resonance Spectroscopy
- Quadrupole Resonance
- Zero-Field Nuclear Magnetic Resonance Spectroscopy.

What is NQR?

- **Nuclear quadrupole resonance or NQR is a technique related to nuclear magnetic resonance (NMR) which is used to detect atoms whose nuclei have a nuclear quadrupole moment**
- **In NMR, nuclei with spin $\geq 1/2$ have a magnetic dipole moment so that their energies are split by a magnetic field, allowing resonance absorption of energy related to the difference between the ground state energy and the excited state.**
- **In NQR, on the other hand, nuclei with spin ≥ 1 , such as ^{14}N , ^{35}Cl and ^{63}Cu , also have an electric quadrupole moment so that their energies are split by an electric field gradient, created by the electronic bonds in the local environment.**

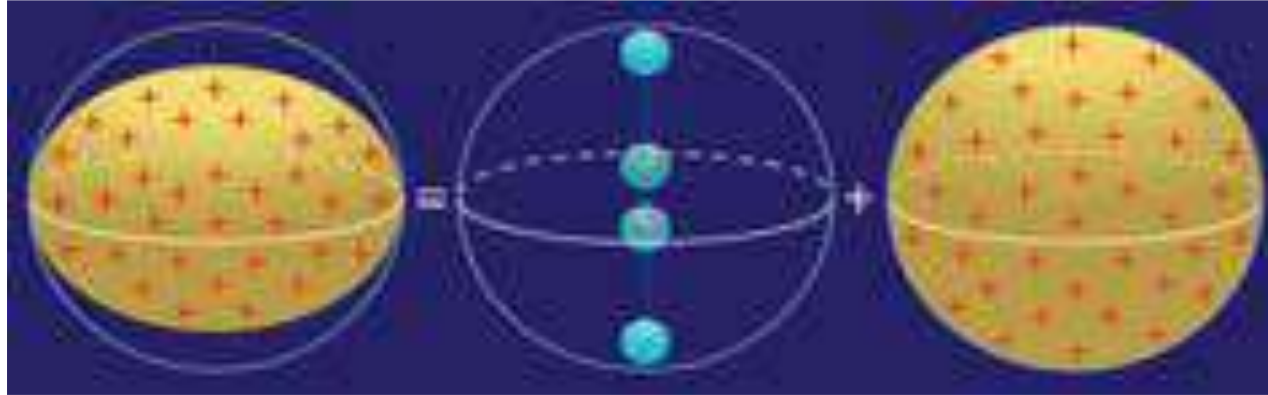
Quadrupole

- A quadrupole is one of a sequence of configurations of electric charge or gravitational mass that can exist in ideal form, but it is usually just part of a multipole expansion of a more complex structure reflecting various orders of complexity.
- To make a magnetic quadrupole we could place two identical bar magnets parallel to each other such that the North pole of one is next to the South of the other and vice versa.
- The result is a configuration like that in the figure with North poles in place of the positive charges and South in place of negative.
- Such a configuration would have **no dipole moment**, and its field will decrease at large distances faster than that of a dipole.
- Again, a changing magnetic quadrupole moment will lead to the production of electromagnetic radiation.

Orbital Symmetry

- Unlike NMR where a powerful external magnetic field is needed, quadrupole resonance takes advantage of a material's natural **electric field gradient**.
- The electrical gradients are available within certain asymmetrical atomic nuclei.
- These gradients are due to the distribution of the electrical charge and do therefore strongly depend on the chemical structure
- Why do some atomic nuclei have an electric quadrupole moment? Physicists would say because they have a spin quantum number greater than $1/2$.
- A more intuitive explanation is because the positive electric charge these nuclei carry is not distributed with **perfect spherical symmetry**.

Orbital Symmetry (Contd...)



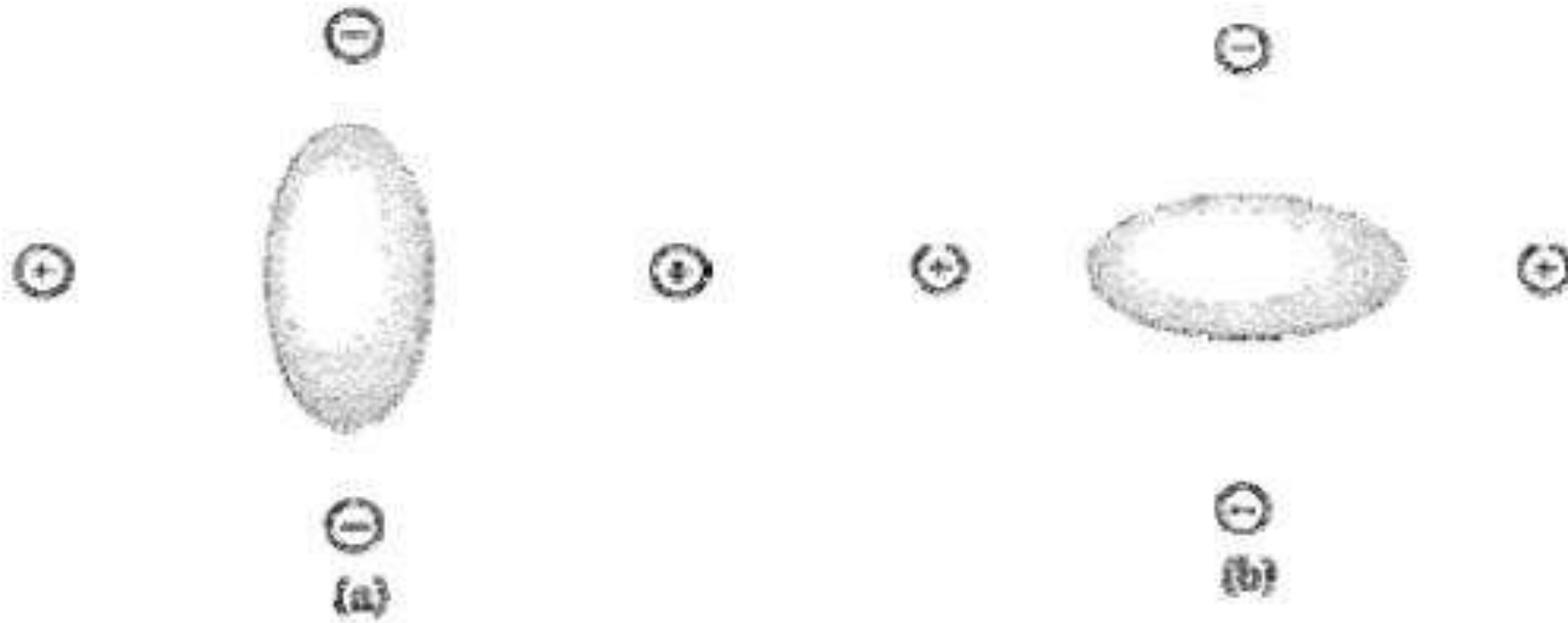
- Nuclear quadrupole resonance requires that the nuclei under scrutiny display electric quadrupole moments. Such quadrupole moments arise when the distribution of positive electric charge in the nucleus is not perfectly spherical.
- For example, a slightly oblate (pumpkin-like) distribution of positive charge (left) can be thought of as the sum of a quadrupolar distribution (center) and a spherical distribution (right).
- Consider for a moment a spherical nucleus with its positive charge distributed uniformly throughout.
- Now squeeze that nucleus in your mind's eye so that what was originally shaped like a basketball is flattened into a pumpkin.

Orbital Symmetry (Contd...)

- A pumpkin of positive charge can be thought of, to a rough approximation, as being the sum of a sphere of positive charge and two oppositely directed electric dipoles, one at the top and one at the bottom.
- That is, the only requirement for an electric quadrupole moment is that the nucleus be squashed (or stretched) along one axis.



Orbital Symmetry (Contd...)



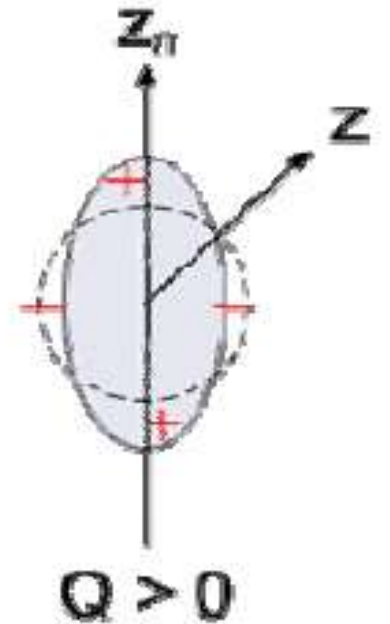
Torque Acting on the Nucleus

- Visualize quadrupole moment as two anti-parallel electric dipoles
- In a uniform electric field, net torque on the nucleus is zero
- An axial symmetric electric field gradient

$$\frac{\partial E_z}{\partial z} = -eq$$

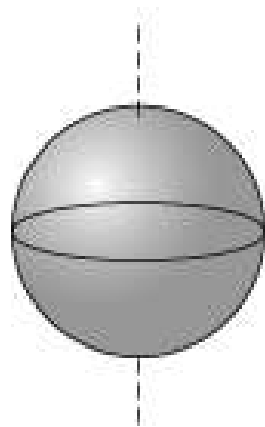
produces a net turning torque proportional to

$$|e^2 q Q|$$



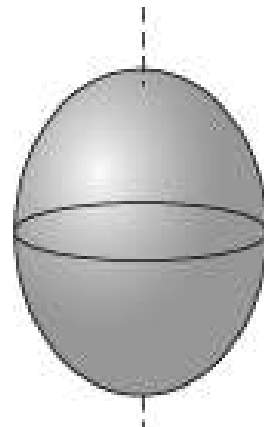
Electric Quadrupole Moment (EQM)

- eQ = electric quadrupole moment, EQM
- If $I > 1/2$, Nucleus has EQM. EQM measures deviation of nuclear charge distribution from spherical symmetry.



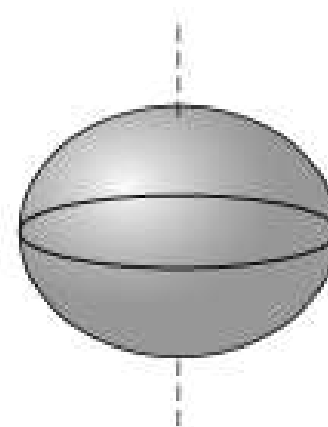
Spherical
 $Q = 0$

$I = 0, 1/2$



Elongated
 $Q > 0$

$I > 1/2$
 ${}^2\text{H}, {}^{14}\text{N}, {}^{27}\text{Al}$



Flattened
 $Q < 0$

$I > 1/2$
 ${}^{17}\text{O}, {}^{33}\text{S}$

A negative value for Q denotes a distribution of charge that is "football-shaped", i.e. a sphere elongated at the poles; a positive value corresponds to a flattened sphere.

Some examples of nuclear quadrupole moments

| Nucleus | I | $Q/10^{-28} \text{ m}^2$ |
|------------------|-------|--------------------------|
| ^2H | 1 | 2.8×10^{-3} |
| ^{14}N | 1 | 1.06×10^{-3} |
| ^{23}Na | $3/2$ | 9.7×10^{-2} |
| ^{35}Cl | $3/2$ | -7.9×10^{-2} |
| ^{63}Cu | $3/2$ | -0.157 |
| ^{93}Nb | $9/2$ | -0.2 |

The $(2I + 1)$ values of m_I that correspond to the different orientations of the nuclear "spin-axis" with respect to a defined direction are degenerate **unless**

(1) a magnetic field is applied (this is the NMR expt.) or

(2) there is a nonzero electric field gradient (EFG) at the nucleus.

The splitting of the m_I levels by the EFG is the nuclear analog of the zero-field splitting of m_s levels in ESR spectroscopy.

Electric Field Gradient

- The intrinsic electric quadrupole moment of the nucleus and the electric-field gradient imposed from outside together create distinct energy states.
- This result is analogous to the multiple energy states in NMR, where the critical ingredients were the intrinsic magnetic dipole moment of the nucleus and a magnetic field imposed from the outside.
- The key difference between NMR and NQR is the definition of "outside."
- In NMR, the outside magnetic field arises because the experimenter has invested considerable effort in setting it up, perhaps using a superconducting electromagnet.
- Since unlike NMR, NQR is done in an environment without a static (or DC) magnetic field, it is sometimes called "zero field NMR".
- In NQR, the required electric field (or, more precisely, the required electric-field gradient) comes free:
 - ✓ It reflects the local arrangement of electrons around the nucleus under study.
 - ✓ That arrangement, in turn, depends not only on the nature of the atom but also on its chemical environment.

Electric Field Gradient (Contd...)

- This feature accounts for one of the chief benefits of NQR -- the method is exquisitely sensitive to chemistry.
- Any nucleus with more than one unpaired nuclear particle (protons or neutrons) will have a quadrupolar charge distribution.
- The NQR effect results from the interaction of this quadrupole with an electric field gradient supplied by the non-uniform distribution electron density (from bonding electrons).
- So the technique is very sensitive to the nature of the bonding around the nucleus.
- Spinning nuclear charge has electric field, extends outside nucleus.
- Interacts with non-spherical (asymmetric) charge distribution caused by :

nonbonding electrons (lone pairs, p, d)

∨

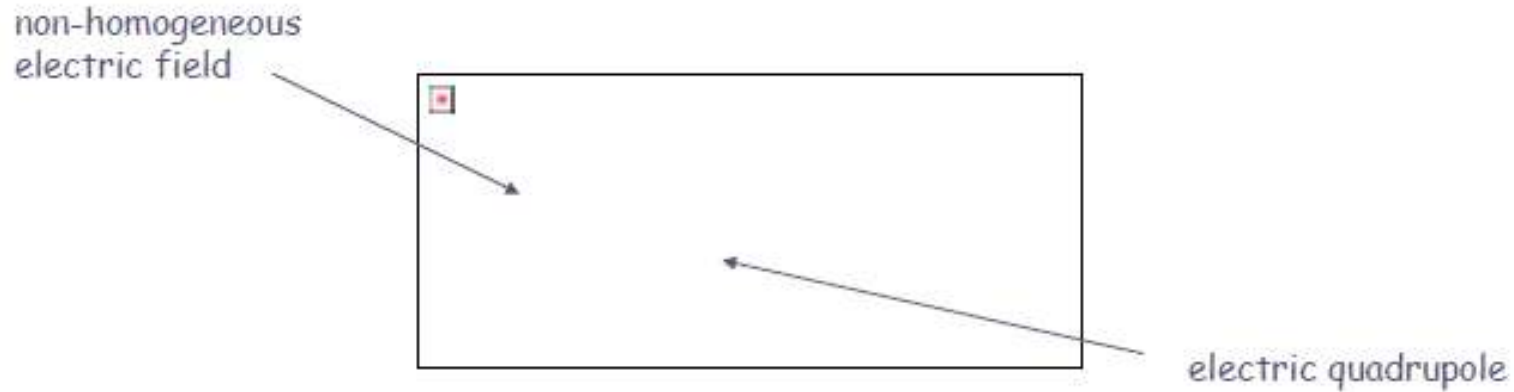
bonding electrons

∨

low symmetry environment, charges on neighboring ions

- So nucleus orients in certain quantized directions with respect to this field, with different energy.

Electric Field Gradient (Contd...)



Magnitude of asymmetric electric field indicated by EFG, electric field gradient along z : $eq = -d^2V/dz^2 = V_{zz}$.

Interaction between EQM and EFG measured by their product e^2Qq : quadrupole coupling constant, QCC. The different orientations cause - interaction with rotational levels, J - transitions between nuclear spin levels

NQR Spectra
(No External Magnetic Field)

NMR Spectra
(External Magnetic Field)

Energy Levels

The EFG can be described by a real, symmetric, traceless 3x3 tensor. Such a tensor can always be made diagonal by choosing an appropriate set of coordinate axes known as principal axes (V_{xx} , V_{yy} , V_{zz}). In the appropriate coordinate system, the electric field gradient has three components, V_{xx} , V_{yy} , and V_{zz} ,

$$\text{where } V_{xx} + V_{yy} + V_{zz} = 0$$

In an axially-symmetric situation, $V_{xx} = V_{yy}$, and the EFG is defined by V_{zz} , or

$$eq = V_{zz}$$

In a non-axial case, a second parameter (the "asymmetry parameter", η) is needed,

$$\eta = (V_{xx} - V_{yy}) / V_{zz}$$

where η is the asymmetry parameter which indicates the degree of the deviation of the EFG from its axisymmetric shape.

Energy Levels (Contd...)

Usually the principal axes are chosen as follows:

$$|V_{xx}| \leq |V_{yy}| \leq |V_{zz}|$$

There are two contributions to q

$$q = q_{\text{valence electrons}} + q_{\text{lattice}}$$

$$q_{\text{valence}} = K_p[-N_{p(z)} + \frac{1}{2}(N_{p(x)} + N_{p(y)})]$$

or

$$q_{\text{valence}} = K_d[-N_{d(z^2)} + N_{d(x^2-y^2)} + N_{d(xy)} - \frac{1}{2}(N_{d(xy)} + N_{d(yz)})]$$

where the N's are the populations of the orbitals indicated (taking into account any effects of covalency).

Note the sign convention that concentration of charge along the z axis contributes to a **negative** field gradient. q_{lattice} is affected by the symmetry of the neighboring atoms or ligands, e.g. an octahedron with two long trans bonds would have $q_{\text{lattice}} > 0$

Obviously, calculation of absolute q -values from structural data is virtually impossible because of the many contributing factors to q_{valence} and q_{lattice} .

Energy Levels (Contd...)

One of the goals of an NQR measurement is to determine the quadrupole coupling constant e^2qQ and the asymmetry parameter η , which contain information about the environment surrounding the nucleus. Based on these parameters conclusions with respect to changes of the crystallographic structures can be made. In case of axial symmetry, $\eta=0$, $2I+1$ quadrupole energy levels are observable. For ease of representation we define as follows:

$$A = e^2qQ / (4I (2I - 1))$$

The quadrupole energy levels can be calculated as follows:

$$E_Q(m) = A * (3m^2 - I (I + 1))$$

where m is the magnetic quantum number ($m = -I, -I+1, \dots, I-1, I$). The quadrupole frequencies $f_Q(m-m')$ are corresponding to the difference between two energy levels ($E_m - E_{m'}$). For the more general case of $\eta \neq 0$, a correction function f_η has to be multiplied with $f_Q(m-m')$. If $\eta=0$, $f_\eta=1$ for every kind of nucleus. For quadrupole nuclei with a higher spin quantum number I than $3/2$ an exact solution for f_η is not known. One option to get accurate results is to use tabulated iterative calculation results. The Landolt-Börnstein tables provide an easy and precise method to determine values for quadrupole frequencies and correction functions for nuclei with spin quantum number $I > 3/2$. Another possibility is just to diagonalize the quadrupolar Hamiltonian numerically and calculate the respective eigenvalues for arbitrary η .

The splitting of m_l levels

For axial cases ($\eta = 0$)

The general equation for the splitting of m_l levels in an efg (q) is

$$E_m = \frac{e^2 Qq [3m_l^2 - l(l+1)]}{4l(2l-1)}$$

where E is the energy of a specified m_l level.

Thus for $l = 1$

$$E(m_l = 0) = e^2 Qq(-2/4) = -e^2 Qq/2$$

$$E(m_l = \pm 1) = e^2 Qq(1/4) = (+)e^2 Qq/4$$

Energy separation = $\frac{3}{4}(e^2 Qq)$

$e^2 Qq$ is known as the Quadrupole Coupling Constant and can be positive or negative quantity depending upon the sign of Qq .

In NQR spectroscopy,
transitions are induced between the m_I states

Selection rule $\Delta m_I = \pm 1$

So for an $I=1$ sample, a single transition should be observed when

$$h\nu = \frac{3}{4}(e^2Qq).$$

We can also show that for $I = 3/2$, only two levels (one NQR transition) can be observed.

$$E(\pm 1/2) = -\frac{1}{4}(e^2Qq)$$

$$E(\pm 3/2) = (+)\frac{1}{4}(e^2Qq)$$

So in this case $h\nu = \frac{1}{2}(e^2Qq)$

The energy differences are very small, e.g. for some ^{35}Cl compounds e^2Qq may be 20 MHz, which corresponds to $7 \times 10^{-4} \text{ cm}^{-1}$

NOTE NQR must be done on solid samples, for molecular tumbling in liquids averages field gradients to zero. Sample must also be diamagnetic (unpaired electrons affect relaxation times of nuclei).

Zeeman Splitting

The presence of an external magnetic field B_0 results in Zeeman splitting. The eigenstates $E_Z(m)$ of a pure Zeeman splitting are defined as follows:

$$E_Z(m) = m * f_{\text{Larmor}} * h = m * \gamma * B_0 * h$$

where f_{Larmor} is the Larmor frequency at the presence of a static magnetic field B_0 . γ is the specific gyromagnetic constant of the nucleus.

Energy and Frequency Spectra

Spin 3/2 nuclei:

Spin 3/2 nuclei have two quadrupolar energy levels and therefore only one transition frequency. Fig. 1 shows the energy spectrum in case of $\eta=0$ in the absence (E_Q) and in the presence (E_{QZ}) of an external magnetic field B_0 . We here assume that the quadrupolar coupling is much stronger than the Zeeman interaction. The corresponding frequency spectrum is shown in fig. 2. In the presence of a weak B_0 the initial transition frequency (f_Q) is split into two distinct frequencies ($f_Q - f_0$, $f_Q + f_0$). The shift frequency f_0 depends on f_{Larmor} and on the angle α between the direction of V_{zz} and the direction of B_0 .

$$f_0 = f_{Larmor} * \cos(\alpha)$$

Two discrete frequency peaks are just observable if the compounds have perfect mono-crystalline structures. In case of powders or substances with many crystalline defects the spectrum shows a broad frequency distribution (pake-doublet).

The energy levels under the presence of an external magnetic field B_0 can be calculated as followed:

$$E_{QZ}(m) = E_Q(m) + E_Z(m) * \cos(\alpha)$$

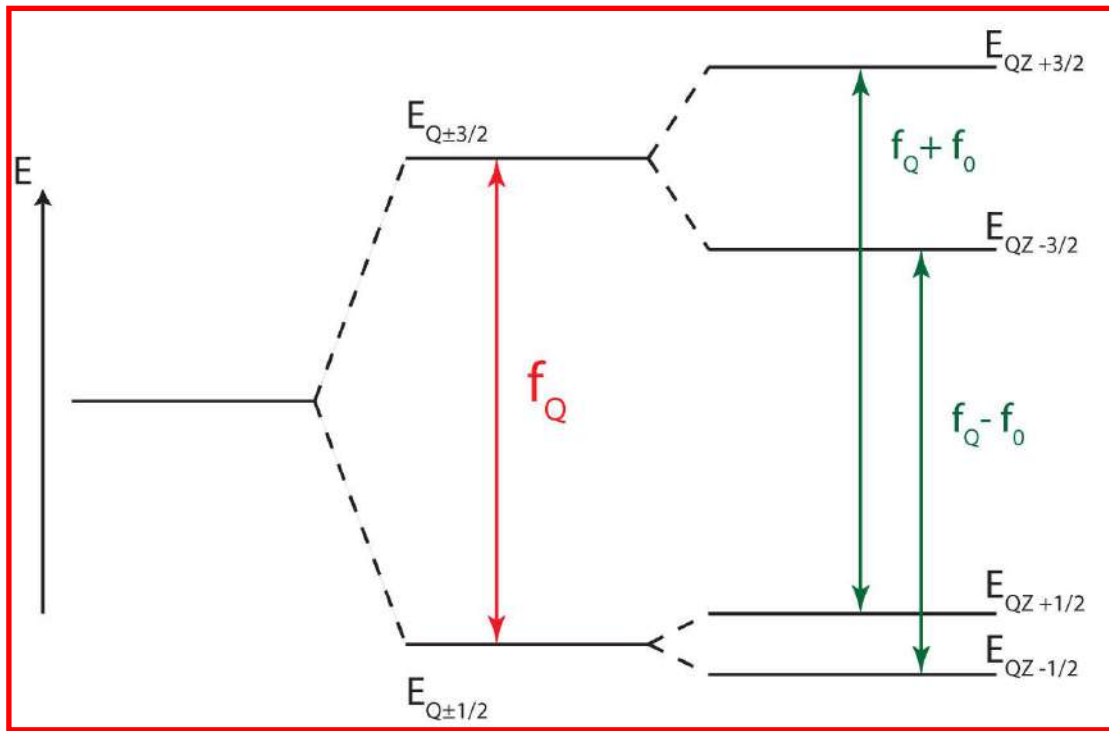


Figure 1 shows the energy spectrum of $l=3/2$ nuclei in the absence (left) and in the presence (right) of a weak external magnetic field.

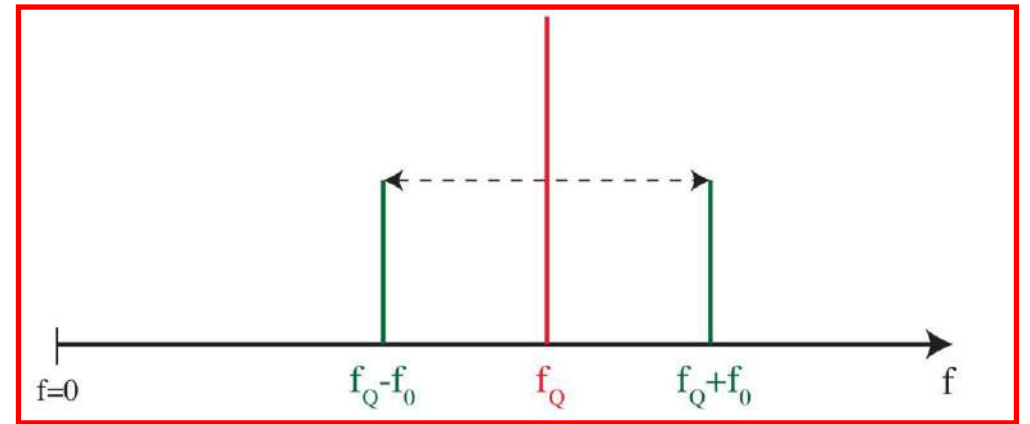


Figure 2 shows the frequency spectrum corresponding to the energy spectrum shown in fig.1.

The figures shows how the energy levels and the frequency spectrum of fig. 1 and 2 build up. It is clearly recognizable that the pure quadrupole frequency f_Q disappears under the presence of an external magnetic field B_0 .

Energy and Frequency Spectra (Contd...)

Spin $> 3/2$ nuclei

Fig. 3 shows the energy levels in the absence (E_Q) and in the presence (E_{QZ}) of a weak external magnetic field \mathbf{B}_0 for quadrupole nuclei with a spin quantum number of $I=9/2$ ($\eta=0$). The frequency spectrum corresponding to the energy spectrum is shown in fig 4. In the presence of \mathbf{B}_0 the pure quadrupole frequencies disappear (brown) and twice as many peaks are detectable. This is just valid for systems with perfect mono-crystalline structures. In case of powders or substances with many crystalline each peak is converted to a broad frequency distribution (pake-doublet).

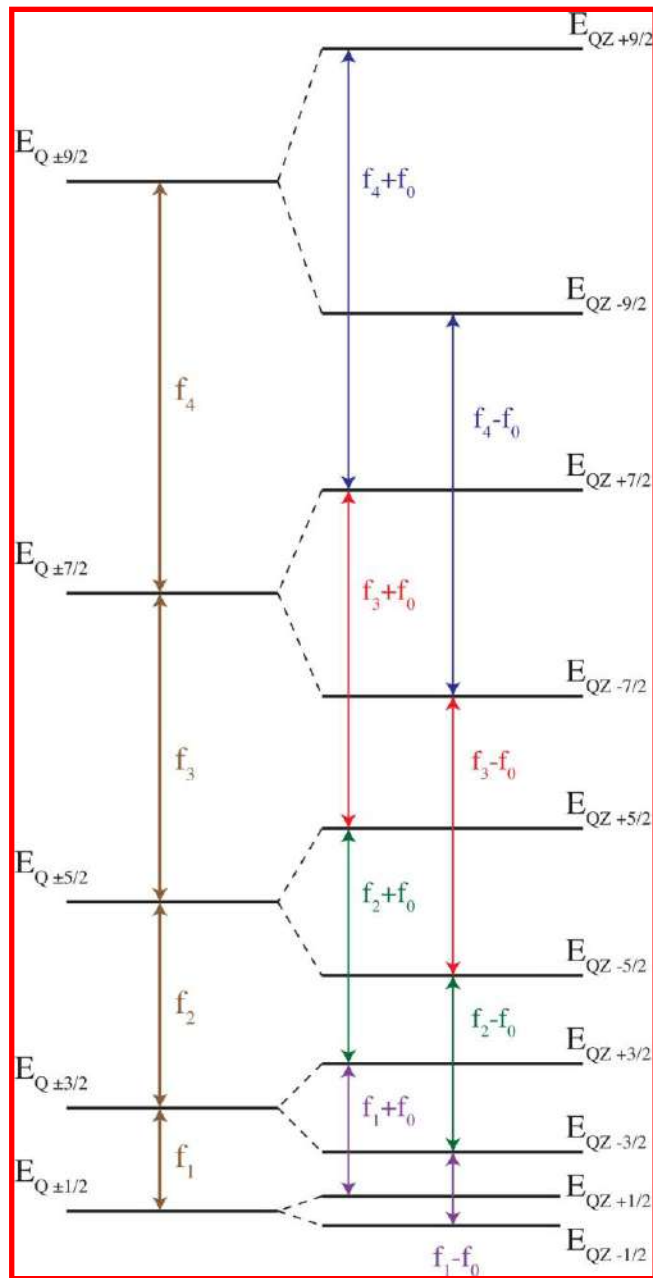


Figure 3 shows the energy spectrum of $l=9/2$ nuclei in the absence (left) and in the presence (right) of a weak external magnetic field.

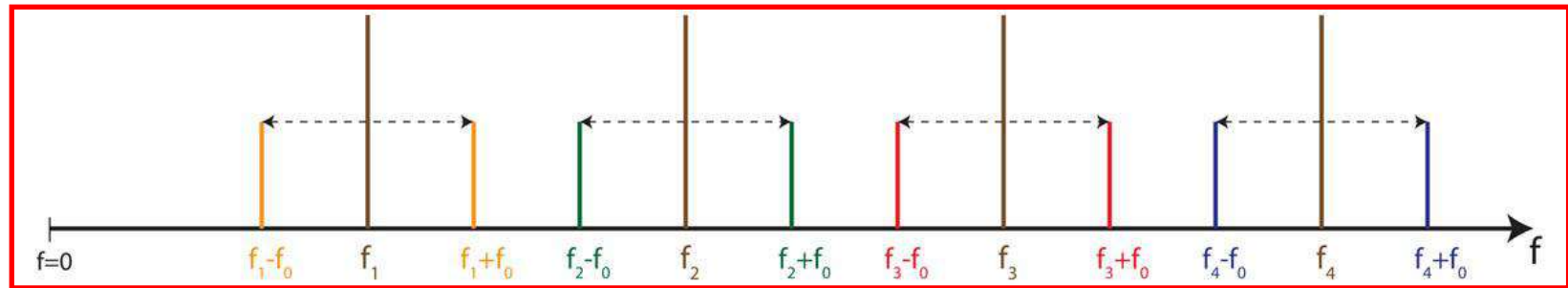


Figure 4 shows the frequency spectrum corresponding to the energy spectrum shown in fig.3.

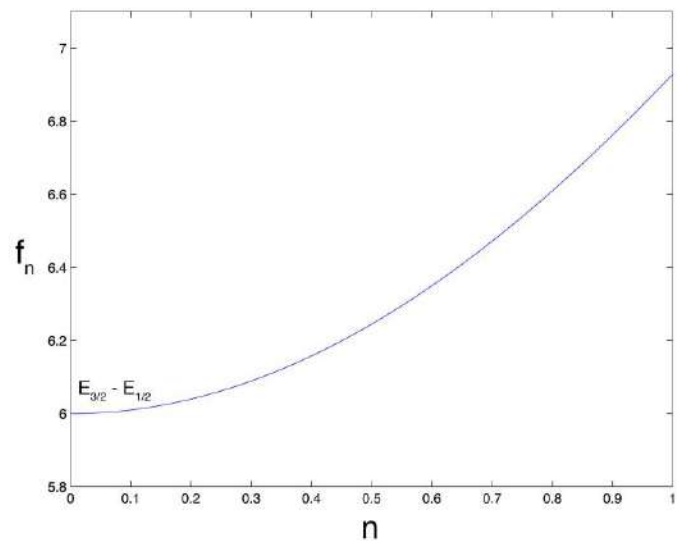
Correction Function

The correction function $f_\eta(m-m')$ depends on the asymmetry parameter η . The correct transition frequency can be calculated as follows:

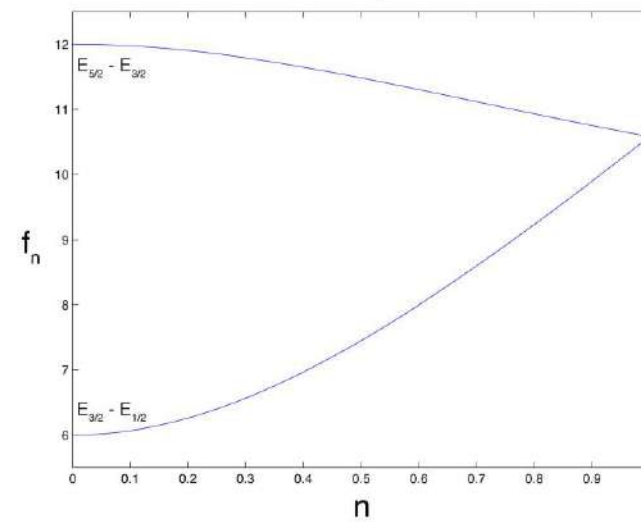
$$f_Q(m-m') = A/h * 3(m^2 - m'^2) * f_\eta(m-m')$$

In systems with small values of η only transitions of $\Delta m = \pm 1$ are allowed. Figures 5 show $f_\eta(m-m')$ depending on η for transitions of $\Delta m = \pm 1$.

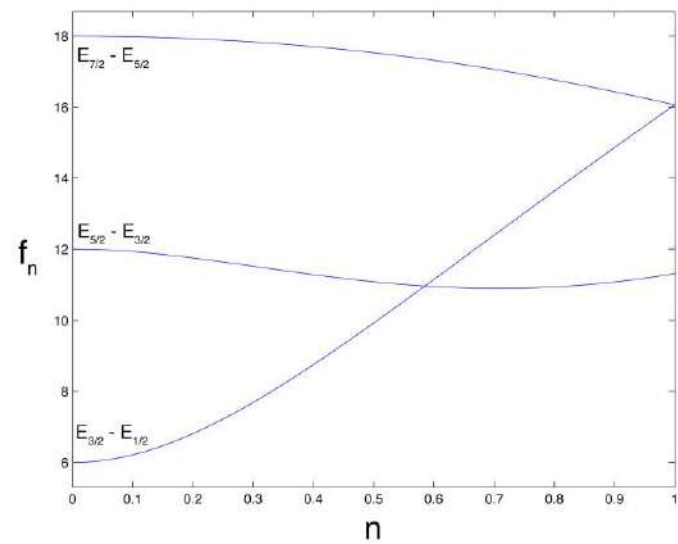
$l = 3/2$



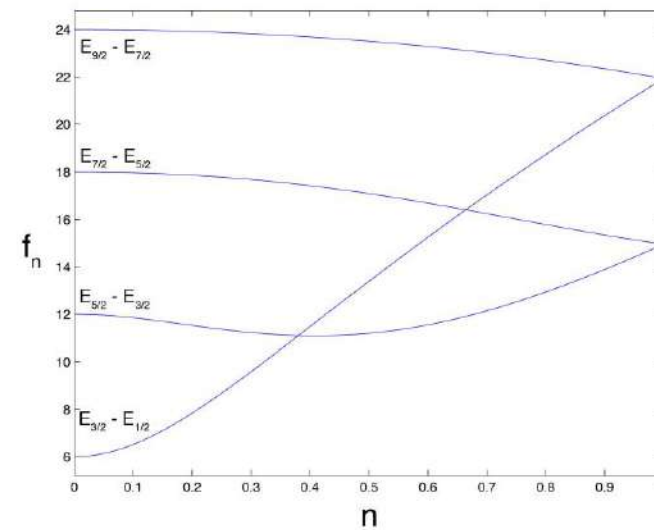
$l = 5/2$



$l = 7/2$



$l = 9/2$



Nuclear Quadrupole Resonance Applications

The NQR frequencies for the various nuclei vary from several kHz up to 1000 MHz. Their values depend on quadrupole moments of the nucleus, valent electrons state and type of chemical bond in which the studied atom participates. Using the NQR frequencies the quadrupole coupling constant (QCC) and asymmetry parameter (η) can be calculated according to the different exact or approximate equations (selected for the spin of the nuclei). For polyvalent atom NQR frequencies depend on coordination number and hybridization.

Structural Aspects of NQR Information

- When applied to structural investigations, NQR spectra may prove an effective tool for preliminary study of crystal structure in the absence of detailed X-Ray data. Such parameters as spectroscopic shifts, multiplicity, spectroscopic splitting, resonance line width, the temperature dependence of resonance frequencies and relaxation rates, afford useful structural information and provide insight into the factors determining the formation of certain structural types.
- The electronic structure of *chemically equivalent* atoms should be identical. The violation of chemical equivalence of resonance atoms due to a change in chemical bonding, such, as for example, dimerization IIIA groups halogenides, leads to a significant splitting of the spectroscopic multiplet caused by a difference in the electronic structure of bridging and terminal atoms.
- The intensities of spectroscopic lines are also important characteristics. They reflect the relative concentration of resonance nuclei at certain sites although one also has to take into account transition probabilities and life times of the energy states of the system investigated. The correspondence between the number and intensities of frequencies and the number of in-equivalent sites occupied by a resonant atom in a crystal lattice, is very helpful in a preliminary structure study made with the use of NQR.
- The NQR single-crystal Zeeman analysis can provide information about special point positions occupied by the quadrupole atoms. This Zeeman analysis determines the orientation of the EFG components with respect to the crystal axes, which essentially facilitates the most difficult and time-consuming stage of the X-Ray analysis.

Uses of NQR

- NQR has been used principally for investigating the electronic structure of molecules
- Information regarding hybridization and the ionic character of the bond can be determined by comparing the quadrupole coupling constant in atomic and molecular state in the same nuclei
- Study of the structure of charge transfer complexes
- Detection of crystal imperfections
- ✓ small imperfections destroy symmetry of internal electric field, lead to splitting or broadening of NQR lines.
 - Confirmation of nuclear spin Q. No. of an isotope from observed NQR lines.
- This technique is suitable for detecting land mines, an application for which it would be difficult to project a uniform magnetic field into the ground.
- Although many different technical measures are available to search for land mines and other kinds of hidden explosives (including trained dogs, electronic metal detectors and ground-penetrating radar), instruments based on nuclear quadrupole resonance offer some special advantages.
- In particular, they are highly discriminating, being able to sense the presence of various nitrogen rich compounds used in explosives.
- Nuclear quadrupole resonance offers the possibility of being applied to other tasks as well, including the nondestructive evaluation of materials.

Nuclear Quadrupole Resonance

- Unlike NMR where a powerful external magnetic field is needed, quadrupole resonance takes advantage of a material's natural electric field gradient,
 - ✓ i.e. the electrical gradients available within certain asymmetrical atomic nuclei.
- These gradients are due to the distribution of the electrical charge and do therefore strongly depend on the chemical structure
 - ✓ they will be different for RDX, for TNT, etc.

Bulk Explosive Detection Method

- When a low-intensity RF signal of the correct frequency is applied to the explosive, usually in the range 0.5 to 6 MHz, the energy state of some of the ^{14}N nuclei can be altered.
- After the RF stimulation is removed, the nuclei can return to their original state, releasing energy and producing a characteristic radio signal. The signal can be detected using a special radio receiver and be measured for analysis of the compounds present.
- Detecting the presence of explosives becomes similar to tuning a radio to a particular station and detecting the signal, and the uniqueness of a molecule's electric field allows NQR technology to be highly compound specific.
- This high selectivity is partly a disadvantage, as it is not straight forward to build a highly specific multichannel system necessary to cover a wide range of target substances, and the precise frequencies drift with temperature.

Applications of Nuclear Quadrupole Resonance Spectroscopy For Explosive detection

NQR as Detector

One significant advantage of NQR is the absence of a magnet: Even if the NMR approach were thought to give some advantage to detecting explosives, projecting a large static magnetic field into the ground is difficult. But the main advantage is that NQR provides a highly specific and arguably unique frequency signature for the material of interest. Although the chemical structure of RDX indicates that the three ring nitrogens are chemically equivalent and hence would be expected to have identical NQR frequencies, in fact the crystal packing is sufficient to remove this degeneracy, and indeed the chemically equivalent ring nitrogens are separated by the order of 100 kHz from one another. This demonstrates the specificity of NQR: Even such small effects from crystal packing are sufficient to resolve the NQR lines from nominally equivalent nitrogens. Because the bandwidth of excitation is only about 5 kHz for commercial NQR detectors, NQR lines more than 5 kHz away from the carrier will not be excited.

For landmine detection, TNT, RDX, and, to a lesser extent, tetryl are the most important explosives. The basic detection concept is particularly simple: Apply a pulse or series of RF pulses resonant at the appropriate NQR frequency of the explosives

Applications of Nuclear Quadrupole Resonance Spectroscopy in Drug Development

In this review, fundamentals of nuclear quadrupole resonance (NQR) spectroscopy are briefly outlined. Examples of its applications in drug development are discussed to demonstrate that the NQR method is a sophisticated, non-destructive and valuable analytical technique for studying pharmaceuticals, providing effective assistance at the two main steps of drug development: the physical and chemical characterization of the active pharmaceutical ingredients (API) at the analytical step and API development. This review covers different aspects of the use of NQR spectroscopy for drug development and analysis and illustrates the power and versatility of this method in the determination of impurities, polymorphic forms, the drug's structure and conformation, characterization of the interactions between the drug and ligands, search for analogs (second- or third-generation drugs) and the drug's thermal stability. Lastly, NQR advantages and restrictions in the aspect of application in drug development studies are summarized.

Authentication of Dietary Supplements through Nuclear Quadrupole Resonance (NQR) Spectroscopy

As the industry grows, adulteration of many products by mislabeling, re-branding, and false advertising are becoming prevalent practice. Existing solutions for analysis often require extensive sample preparation or are limited in terms of detecting different types of integrity issues. In this paper, a novel authentication method based on Nuclear Quadrupole Resonance (NQR) spectroscopy which is quantitative, non-invasive, and non-destructive is described. It is sensitive to small deviation in the solid-state chemical structure of a product, which changes the NQR signal properties. These characteristics are unique for different manufacturers, resulting in manufacturer-specific watermarks. We show that nominally-identical dietary supplements from different manufacturers can be accurately classified based on features from NQR spectra. Specifically, a machine learning-based classification called support vector machines (SVMs) is used to verify the authenticity of products under test. This approach has been evaluated on three products using semi-custom hardware and shows promising results, with typical classification accuracy of over 95%

Thank you!



This article was downloaded by: [Emory University]

On: 13 August 2015, At: 14:40

Publisher: Taylor & Francis

Informa Ltd Registered in England and Wales Registered Number: 1072954 Registered office: 5 Howick Place, London, SW1P 1WG



Expert Opinion on Drug Discovery

Publication details, including instructions for authors and subscription information:
<http://www.tandfonline.com/loi/iedc20>

Applications of nuclear quadrupole resonance spectroscopy in drug development

Jolanta N Latosińska^a

^a Adam Mickiewicz University, Institute of Physics, Umultowska 85, 61-614 Poznań, Poland.

Published online: 31 Mar 2015.

To cite this article: Jolanta N Latosińska (2007) Applications of nuclear quadrupole resonance spectroscopy in drug development, *Expert Opinion on Drug Discovery*, 2:2, 225-248

To link to this article: <http://dx.doi.org/10.1517/17460441.2.2.225>

PLEASE SCROLL DOWN FOR ARTICLE

Taylor & Francis makes every effort to ensure the accuracy of all the information (the "Content") contained in the publications on our platform. However, Taylor & Francis, our agents, and our licensors make no representations or warranties whatsoever as to the accuracy, completeness, or suitability for any purpose of the Content. Any opinions and views expressed in this publication are the opinions and views of the authors, and are not the views of or endorsed by Taylor & Francis. The accuracy of the Content should not be relied upon and should be independently verified with primary sources of information. Taylor and Francis shall not be liable for any losses, actions, claims, proceedings, demands, costs, expenses, damages, and other liabilities whatsoever or howsoever caused arising directly or indirectly in connection with, in relation to or arising out of the use of the Content.

This article may be used for research, teaching, and private study purposes. Any substantial or systematic reproduction, redistribution, reselling, loan, sub-licensing, systematic supply, or distribution in any form to anyone is expressly forbidden. Terms & Conditions of access and use can be found at <http://www.tandfonline.com/page/terms-and-conditions>

Expert Opinion

1. Introduction
2. Nuclear quadrupole resonance spectroscopy fundamentals
3. Nuclear quadrupole resonance spectroscopy experimental methods
4. Nuclear quadrupole resonance in drug development
5. An example of systematic studies – thiazides
6. Other examples
7. Drug–ligand interactions
8. Advantages and disadvantages of nuclear quadrupole resonance for drug investigation
9. Expert opinion

informa
healthcare

Applications of nuclear quadrupole resonance spectroscopy in drug development

Jolanta N Latosinska

Adam Mickiewicz University, Institute of Physics, Umultowska 85, 61-614 Poznan, Poland

In this review, fundamentals of nuclear quadrupole resonance (NQR) spectroscopy are briefly outlined. Examples of its applications in drug development are discussed to demonstrate that the NQR method is a sophisticated, non-destructive and valuable analytical technique for studying pharmaceuticals, providing effective assistance at the two main steps of drug development: the physical and chemical characterization of the active pharmaceutical ingredients (API) at the analytical step and API development. This review covers different aspects of the use of NQR spectroscopy for drug development and analysis and illustrates the power and versatility of this method in the determination of impurities, polymorphic forms, the drug's structure and conformation, characterization of the interactions between the drug and ligands, search for analogs (second- or third-generation drugs) and the drug's thermal stability. Lastly, NQR advantages and restrictions in the aspect of application in drug development studies are summarized.

Keywords: analytical method, API development, drug development, drug–ligand, NQR fundamentals, nuclear quadrupole resonance, polymorphism, stability, structure–activity, structure–conformation, thermal stability

Expert Opin. Drug Discov. (2007) 2(2):225-248

1. Introduction

Although each day thousands of new prospective drugs are synthesized, only a few actually become implemented in medical therapy. Only 1 per 5000 compounds reaches the final stage and is introduced as a therapeutic drug, although the process of discovering a new drug and its investigation needs an average of ~ 10 – 15 years of intense interdisciplinary research. When a successful drug has been discovered for the treatment of a particular disease the process of searching for its analogs, that is the second-generation drugs expected to improve on the efficacy and the toxicity profile relative to those of the original drug, begins. Lower doses of the second-generation drugs should produce the same or even greater beneficial effect at much lower toxic side effects and possibly extended modes of administration. After the efficacy and toxicity profiles of the second-generation analogs have been obtained, more analogs, the so-called third-generation drugs, are synthesized and studied. The complexity of this process implies the need to look for methods that would increase the speed and efficiency of the drug discovery process.

Approximately 90% of pharmaceuticals are marketed as solid dosage formulations [1], although the majority of commonly used methods used to study them are the solution-based organic chemical analysis techniques such as high performance liquid chromatography (HPLC), mass spectrometry (MS), ultraviolet (UV) spectroscopy, infrared (IR) spectroscopy or nuclear magnetic resonance (NMR). These methods provide reliable information on the purity of the drug substance, but are not non-destructive, and in addition, molecular interactions between the solvent

Table 1. Properties of nuclei most useful for drug studies [10].

| Isotope | Natural abundance (%) | Spin I | Q [barns] |
|------------------|-----------------------|--------|-----------|
| ¹ H | 99.9 | 1/2 | * |
| ² H | 0.0115 | 1 | 0.0028 |
| ¹³ C | 1.1 | 1/2 | * |
| ¹⁴ N | 99.634 | 1 | 0.00201 |
| ¹⁷ O | 0.038 | 5/2 | -0.02578 |
| ²³ Na | 100 | 3/2 | 0.1006 |
| ²⁵ Mg | 10.05 | 5/2 | 0.201 |
| ³⁵ Cl | 75.77 | 3/2 | 0.0819 |
| ³⁷ Cl | 24.23 | 3/2 | -0.068 |
| ³⁹ K | 93.08 | 3/2 | 0.049 |
| ⁴¹ K | 6.91 | 3/2 | 0.060 |
| ³³ S | 0.75 | 3/2 | -0.678 |
| ⁶⁷ Zn | 4.12 | 5/2 | 0.150 |
| ⁷⁹ Br | 50.57 | 3/2 | 0.331 |
| ⁸¹ Br | 49.43 | 3/2 | 0.276 |

*Non-quadrupolar nuclei.

and the solute often lead to conformational changes, which means that instead of the actual drug, its isomorphous compound is studied. Moreover, the use of solvents means that certain information that is specific of the solid-state such as the presence of isomers, conformation, polymorphism and intermolecular interactions are irreversibly lost.

Physical characterization of the active pharmaceutical ingredient (API) is an integral aspect of the drug development process and, furthermore, is crucial for successful development of the final drug product [2-4]. Most often, the most thermodynamically stable form is chosen to be developed into the final product. However, sometimes, for example, because of the enhanced dissolution or bioavailability profiles, metastable forms are also used [5]. In any case, exact determination of the chemical and physical properties of the material of API is necessary as they are directly related to the possibilities of processing and/or manufacture of the API and the drug product. Thus, the physical and chemical properties of a given compound can affect the quality, safety and efficacy of the final drug product.

It has been known for a long time [6] that > 70% of pharmaceutical solids (e.g., 67% of steroids, 40% of sulfonamides and 63% of barbiturates) occur in more than one solid polymorphic form (crystal or amorphous), which can have significantly different physical and chemical properties, including stability, chemical reactivity, dissolution rate and bioavailability [7]. As these properties directly affect the drug potency and effectiveness, the US FDA approves crystalline drugs only in a specific crystal structure or polymorph and demands constant monitoring of their solid-state properties by pharmaceutical companies [3,4].

In this context, nuclear quadrupole resonance (NQR) is the most sensitive to changes in the crystalline or electronic structure out of all the resonance spectroscopies [8], which permits solid-state investigation and so seems very promising in drug development. In particular it can be successfully used in the search for second- or third-generation drugs, in evaluation of purity of the drug substance and it can provide information on the API structure, stability and polymorphism.

NQR spectroscopy is very similar to NMR and was developed by Dehmelt and Krüger in 1949, shortly after NMR discovery [9], as an alternative to NMR that does not require a magnetic field. Since the first recording of the NQR signal, this technique has been developed to a sophisticated method for the investigation of bonding, structural features, phase transitions and molecular dynamics in compounds and at present is treated as an independent branch of radio-frequency spectroscopy concerned with magnetic resonance absorption in the solid state [10].

Although NQR spectroscopy was discovered at around the same time as NMR, it has rarely been applied to drug analysis. Moreover, in the past, starting from the early 1950s, the studies of drugs even if performed did not take into account the pharmaceutical aspect of compounds (Livingstone in 1951 [11,12], Allen in 1953 [13], Gutowsky in 1960 [14], Smirnov in 1970 [15], Kume in 1976 [16], Bray and Kim in 1977 and 1984 [17,18], Hiyama in 1980 [19], Lucken in 1981 [20] and Semin in 1985 [21]). Drugs were treated as any other chemical compounds, only their physical and chemical properties were determined and the scope of these studies was limited to substituent effects as well as molecular dynamics. By the end of the 1970s, Bray

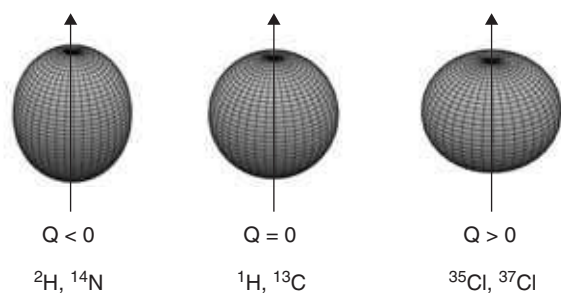


Figure 1. Spatial charge distribution for quadrupolar nuclei.

made the first attempts at relating the biological activity of drugs with their NQR signals, reaching a success for one group of drugs (i.e., sulfonamides [22]). Although by the end of the 1980s this rather new field of NQR was considered fruitful in biochemistry, the breakthrough and really intense study of drugs by this method began only recently, and since then the interest in the NQR possibilities in drug detection or development has substantially increased.

This review covers different aspects of the use of NQR spectroscopy for drug development and analysis and illustrates the power and versatility of this method in the determination of impurities, polymorphic forms, the drug's structure and conformation, characterization of the interactions between the drug and ligands, search for analogs (second- or third-generation drugs) and the drug's thermal stability.

2. Nuclear quadrupole resonance spectroscopy fundamentals

2.1 Introduction

NQR is a technique related to NMR, but, unlike NMR, NQR is done exclusively in solid state and in an environment without a static (or DC) magnetic field; therefore, it is sometimes referred to (although incorrectly) as the 'zero-field NMR'.

NQR is used to detect atoms whose nuclei have spins higher than a half, such as ^{14}N , ^{35}Cl , ^{17}O , ^2H , ^{127}I and ^{63}Cu (Table 1) [23]. Approximately 130 isotopes meet these requirements. In addition to the dipole moment these nuclei have a nuclear electric quadrupole moment (eQ) reflecting the deviations from the spherically symmetric charge distribution (Figure 1). The quadrupole moment eQ describes the effective shape of the ellipsoid of the nuclear charge distribution (Equation 1):

(1)

$$eQ = \int e\rho(3z^2 - r^2)dV$$

and a non-zero eQ value indicates that the positive electric charge distribution on the nuclei is not spherically symmetric. By convention, the value of eQ is taken to be positive if the

ellipsoid is prolate (^2H , ^{14}N) and negative if it is oblate (^{35}Cl , ^{37}Cl). The electric quadrupole moments of nuclei can be measured, for example, from the hyperfine splitting of atomic spectral lines, from the quadrupole hyperfine splitting of molecular rotational spectra or from the spin-polarized radioactive nuclear beams.

2.2 Hamiltonian of the quadrupole interaction

The energy of interactions of the nuclear electric charge distribution $\rho(\vec{r})$ in an external inhomogeneous electric field described by the potential $V(\vec{r})$ is given by Equation 2 [24-29]:

(2)

$$E = \int \rho(\vec{r})V(\vec{r})d\vec{r}^3$$

and when the electrostatic potential varies weakly over the nuclear charge distribution it can be expanded into a Taylor series (Equation 3):

(3)

$$E = V_0 \int \rho(\vec{r})d\vec{r}^3 + \sum_k \left(\frac{\partial V}{\partial x_k} \right)_0 \int x_k \rho(\vec{r})d\vec{r}^3 + \frac{1}{2} \sum_{k,l} \left(\frac{\partial^2 V}{\partial x_k \partial x_l} \right)_0 \int x_k x_l \rho(\vec{r})d\vec{r}^3 + \dots$$

The first term in the energy (Equation 3), the so-called monopole term, does not depend on the orientation, and the second term, known as the dipole term, vanishes because a nucleus in a ground state has the electric dipole moment equal to zero. The third term in Equation 3 is the so-called quadrupole term and is the first non-zero, orientation-dependent and strongest anisotropic term of the energy expansion that can be rewritten as a quantum-mechanical expression (Equation 4):

(4)

$$H_Q = \frac{1}{6} \sum_{k,l} Q_{kl} V_{kl}$$

where Q_{kl} is the operator of the nuclear electric quadrupole moment tensor (Equation 5):

(5)

$$Q_{kl} = \int (3x_k x_l - r^2 \delta_{kl}) \rho(\vec{r}) d\vec{r}^3$$

and V_{kl} is electric field gradient (EFG) tensor (or more accurately the hessian matrix, i.e., the matrix of the second derivatives of the electrical potential; Equation 6):

$$V_{kl} = \left(\frac{\partial^2 V}{\partial x_k \partial x_l} \right)_0 \tag{6}$$

The quadrupole term (Equation 4) does not disappear if the nuclear electric quadrupole moment tensor (Equation 5) is non-zero, so only if the charge distribution on the nucleus is not spherically symmetric and when EFG (Equation 6) is non-zero, that is, only if the charges surrounding the nucleus violate cubic symmetry and can, therefore, generate an inhomogeneous electric field at the position of the nucleus. Both tensors in Equations 5 and 6 are symmetric traceless second rank.

The quadrupole term/Hamiltonian (Equation 4) describes the quadrupolar interactions between two electric charge distributions: that of the nucleus described by the operator of the nuclear quadrupole moment tensor Q_{kl} (a property of the nucleus) and that of all electric charges surrounding the quadrupole nucleus described by the EFG tensor V_{kl} at the site occupied by the resonant quadrupole nucleus (a property of the sample).

To be able to determine the nuclear quadrupole energy levels and the corresponding NQR frequencies it is necessary to evaluate the Q_{kl} operator using Equation 7:

$$Q_{kl} = \frac{eQ}{I(2I-1)} \left[\frac{3}{2} (I_k I_l + I_l I_k) + \delta_{kl} I^2 \right] \tag{7}$$

where eQ is a scalar constant given by Equation 1 and I_k, I_l are the components of the nuclear angular momentum vector I .

The quadrupole Hamiltonian may be expressed as Equation 8:

$$H_Q = \frac{eQ}{6I(2I-1)} \sum_{k,l} V_{kl} \left[\frac{3}{2} (I_k I_l + I_l I_k) - \delta_{kl} I^2 \right] \tag{8}$$

The EFG tensor (Equation 6) is a symmetric tensor of rank 2 and it consists of only five independent components. However, in the Cartesian tensor representation, in which the coordinate axes xyz coincide with the principal axis system of the EFG tensor, the EFG tensor is diagonal and can be characterized by the three principal components V_{xx}, V_{yy}, V_{zz} (labelled according to the convention: $|V_{zz}| \geq |V_{yy}| \geq |V_{xx}|$ meeting the Laplace equation $V_{xx} + V_{yy} + V_{zz} = 0$ that requires the tracelessness of the EFG tensor).

Due to the tracelessness of EFG, only two independent parameters are required to characterize the magnitudes of the

principal components of EFG tensor.

The parameters usually chosen are (Equation 9):

$$eq = V_{zz} \eta = \frac{eq_{xx} - eq_{yy}}{eq_{zz}} \tag{9}$$

where eq is the largest principal value of EFG and η is the dimensionless asymmetry parameter being a measure of the departure of EFG from the cylindrical geometry (i.e., the biaxiality of the EFG tensor).

Taking into regard Equation (9), the quadrupole Hamiltonian H_Q (Equation 8) assumes a simple form in the principal axis system (Equation 10):

$$H_Q = \frac{e^2 Qq}{4I(2I-1)} [I_z^2 - I^2 + \eta(I_x^2 - I_y^2)] \tag{10}$$

where (Equation 11):

$$QCC = \frac{e^2 Qq}{h} = \frac{e^2 Qq_{zz}}{h} \tag{11}$$

is called the quadrupole coupling constant (QCC), which measures the magnitude of quadrupolar interactions and should not be identified with the quadrupolar frequency observed in NQR experiments. For example, in the NQR spectra on 2H , the asymmetry parameter η defines the powder sample NQR lineshape and QCC is related to the line width.

For the solid NMR purposes, when H_Q represents a perturbation of the Zeeman interactions, the z axis is selected to be parallel to the external magnetic field and then H_Q can be rewritten in a more convenient form (Equation 12):

$$H_Q = \frac{eQ}{4I(2I-1)} [V_0(3I_z^2 - I^2) + V_{+1}(I_+ I_z - I_z I_+) + V_{-1}(I_+ I_z - I_z I_+) + V_{+2} I_-^2 + V_{-2} I_+^2] \tag{12}$$

where (Equation 13):

$$\begin{aligned} V_0 &= V_{zz} \\ V_{\pm 1} &= V_{zz} \pm i V_{yx} \\ V_{\pm 2} &= (V_{zz} - V_{yy}) / 2 \pm i V_{xy} \\ I_{\pm} &= I_x \pm i I_y \end{aligned} \tag{13}$$

and where I_x , I_y and I_z are the three components of the nuclear angular momentum vector I in Cartesian coordinates.

2.3 Nuclear quadrupole levels and resonance frequencies

The NQR frequencies characterizing the transitions between the nuclear quadrupole energy levels of a given nucleus are determined by the methods of the perturbation calculus.

For the spin $I = 1$ (^{14}N or ^2D), when the levels are not degenerated (i.e., for $\eta \neq 0$), there are three transitions at the frequencies (Equation 14):

$$\begin{aligned} \nu_+ &= \frac{e^2 Qq}{h} \frac{(3 + \eta)}{4} \\ \nu_- &= \frac{e^2 Qq}{h} \frac{(3 - \eta)}{4} \\ \nu_0 &= \nu_+ - \nu_- = \frac{e^2 Qq}{h} \frac{\eta}{2} \end{aligned} \quad (14)$$

However, when the upper level is doubly degenerated (i.e., for $\eta = 0$), only one transition is observed (Equation 15):

$$\nu = \frac{3}{4} \frac{e^2 Qq}{h} \quad (15)$$

For the spin $I = 3/2$ (^{35}Cl , ^{37}Cl , ^{23}Na , ^{33}S), because the levels are doubly degenerated, irrespective of η , there is only a single transition at the frequency (Equation 16):

$$\nu = \frac{e^2 Qq}{2h} \sqrt{1 + \frac{\eta^2}{3}} \quad (16)$$

For the nuclei of higher spins, the equations for the transition frequencies are more complicated [30,31].

For $I = 1$ and $\eta \neq 0$, the NQR parameters such as the quadrupole coupling constant QCC and η can be calculated knowing the resonance frequencies (Equation 14) from the following formulae (Equation 17):

$$\frac{e^2 Qq}{h} = \frac{2(\nu_+ - \nu_-)}{3} \quad \eta = 3 \frac{\nu_+ - \nu_-}{\nu_+ + \nu_-} \quad (17)$$

As follows from Equations 13 and 14, a standard pure NQR experiment does not always permit a separation of QCC from the η parameter.

For ^{35}Cl , ^{23}Na or other spin-3/2 nuclei, two common methods to separate these two parameters are the mutation

technique (for ^{35}Cl) [32] and the observation of the transition between the $-1/2$ and $1/2$ states in high-field NMR experiments if a second-order, quadrupolar-broadened pattern is observed (Zeeman effect) (^{23}Na) [33].

As follows from Equations 12 – 14, NQR frequency depends only on the spin I and two parameters: QCC $e^2 Qq/h$ and asymmetry parameter η , both related to the EFG tensor. As the internal EFGs are a characteristic feature of the material, each material has characteristic resonance frequencies. In general, NQR spectra have been observed in the approximate range of 0.0009 – 1000 MHz, with the highest frequencies for ^{127}I and the lowest for ^2H . For ^{35}Cl NQR, the spectra are in the range of 0 – 120 MHz, whereas for ^{14}N , the spectra are in the range of 0 – 6 MHz and for ^2H in the range of 0 – 2.6 MHz. This feature makes NQR an obvious candidate method for the analytical purposes.

2.4 Temperature effects

Disturbances to the charge distribution in a molecule, due to the molecular torsional vibrations, change the directions of the principal axes of EFG, which causes a reduction in the EFG tensor [34–36] and a variation of NQR frequency and consequently, in the NQR parameters [37]. In addition to torsional motions, other motions such as hidden rotations can cause thermal averaging of the Hamiltonian and the reduction in the effective EFG. The mathematical analysis of the temperature dependence of the NQR resonance frequency permits the determination of the parameters characterizing molecular dynamics such as activation energy of librations, frequency of librations, anharmonicity or moments of inertia.

To be able to determine the values of these parameters for the compounds studied, the results are fitted by different models. The so-called Bayer model [34] describes exclusively only one mode of librations. The Kushida–Benedek–Bloembergen model [35], an extension of Bayer model, takes into account the different vibrations of the crystal lattice and the change in the crystal volume; the Brown model [36] describes different anharmonic vibrations of the crystal lattice, assuming that the frequency of the mode of vibrations is a linear function of temperature (the assumption is correct at high temperatures) and neglects thermal expansion; the revision of the Brown model, referring to low temperatures takes into account the vibration mode frequency being a square function of temperature. A comprehensive summary of different theories can be found in [38].

The temperature dependencies of the resonance frequencies mainly provide information on the torsional motions and permit detection of structural phase transitions. However, these rarely bring information on full molecular dynamics in the solid state. On the other hand, they can still be very useful in the investigation of thermal stability of pharmaceutical compounds, aimed at checking the effect of temperature on the drug stability and not at identification of particular molecular motions. Much more suitable for the investigation of molecular dynamics are the temperature dependencies of the

Table 2. Experimental (frequency, FWDH, T_1 and T_2) and calculated NQR parameters (QCC and η) used in investigation of drugs.

| NQR parameter | Structure | Dynamics | Imaging | Area of use |
|--------------------------------------|-----------|----------|---------|--|
| ν , NQR frequency | +++ | + | ++ | Identification Polymorphism Stability Search for analogs Drug–ligand interaction Complexation |
| QCC | +++ | + | ++ | Identification Polymorphism Stability Search for analogs Drug–ligand interaction Complexation |
| Asymetry parameter η | +++ | + | ++ | Identification Polymorphism Stability Search for analogs Drug–ligand interaction Complexation |
| FWDH, line width | - | ++ | + | Quality control Polymorphism Stability |
| T_1 , spin–lattice relaxation time | - | +++ | ++ | Quality control Polymorphism Phase transitions Molecular dynamics |
| T_2 spin–spin relaxation time | - | +++ | ++ | Quality control Polymorphism Phase transitions Molecular dynamics |

FWDH: Full width at half-maximum; NQR: Nuclear quadrupole resonance; QCC: Quadrupole coupling constant.

relaxation times, although their measurement needs a high signal-to-noise ratio (SNR) and is much more time consuming. Quadrupole relaxation can be characterized by the spin–lattice or longitudinal relaxation time T_1 , the spin–spin or the transverse relaxation time T_2 or the global true spin–spin relaxation T_2^* , describing the spin–spin relaxation and dephasing due to inhomogeneities. The spin–lattice relaxation described by T_1 is determined by the interactions between the nucleus of interest and the unexcited nuclei and electric fields in the environment, the spin–spin relaxation described by T_2 is determined by the interactions between the spinning nuclei that are already excited and the true spin–spin relaxation T_2^* is further determined by differences in the chemical environment that can lead to a distribution of resonance frequencies. As a general rule, the following inequality holds: $T_1 > T_2 > T_2^*$.

Temperature dependencies of the relaxation times permit determination of the activation energies of molecular motions such as reorientations or rotations of molecular fragments [39,40]. For example, a sharp decrease of the spin lattice relaxation time T_1 is usually attributed to the onset of reorientation of the group over a potential barrier [41] whereas

T_1 minimum is usually ascribed to the modulation effect of the EFG due to motion of a molecular fragments such as a sudden jump reorientation of an atomic group [42].

For pharmaceuticals, a temperature study of relaxation times is rarely performed in the full range. However, measurements of the relaxation times at selected temperatures provide information about the compound purity and are used for quality control.

The NQR parameters most often used in pharmaceutical studies and the areas that they are used in are displayed in Table 2.

3. Nuclear quadrupole resonance spectroscopy experimental methods

3.1 Nuclear quadrupole resonance spectroscopy direct and indirect methods

The NQR signal detection is mainly performed by the direct NQR (i.e., pure NQR) and the indirect NQR methods. Direct NQR methods are based on the nuclear energy level splittings appearing as a result of the electric field gradients internal to the sample and that is why, in contrast to the NMR method, they

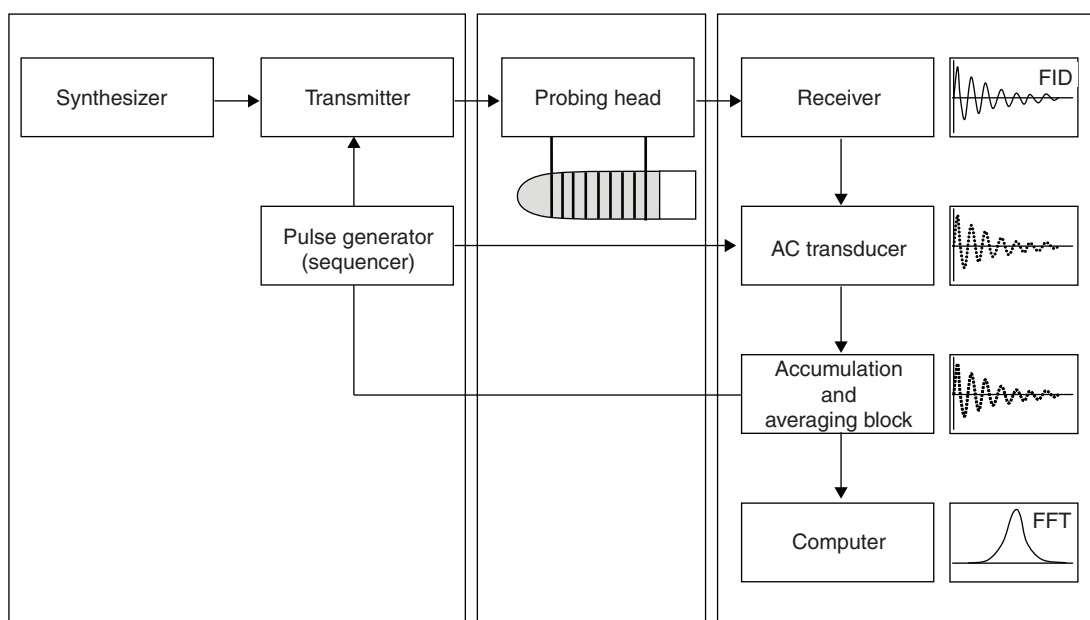


Figure 2. A simplified block diagram of a pulse NQR spectrometer.

FFT: Fast Fourier transform; FID: Free induction decay; NQR: Nuclear quadrupole resonance.

do not require a strong external DC magnetic field. Direct NQR (pure NQR) methods consist of the oscillator–detector techniques (simple and inexpensive continuous wave and super-regenerative techniques), presently of historical importance and the pulsed and multipulsed techniques used much more often because they ensure better sensitivity (i.e., higher the SNR) and the possibility of sweeping a much greater range of frequencies, especially in the detection of signals from ^{35}Cl and ^{81}Br (including the fast Fourier transform with digital filtering). The detection is most often realised using multipulsed sequences such as spin-locking spin-echo [43], phase alternated Hahn sequences, steady-state free precession [44], or a strong off-resonance comb [45]. The use of these multipulse sequences permits an increase in the NQR sensitivity (SNR) and a shortening of the experiment duration, which is particularly advantageous in the search for the signal or in temperature measurements of relaxation times. The direct NQR methods are used for the investigation of compounds consisting of ^{35}Cl or ^{81}Br nuclei.

Indirect detection methods include the techniques known from the application in the NMR detection, based on the use of a strong signal from one type of nuclei (most often ^1H) for the detection of a weak signal from another type of nuclei (most often ^{17}O or ^{15}N). Indirect methods [46–51] include different modifications of double resonance NMR-NQR and cross-relaxation spectroscopy techniques used successfully for the detection of signals from light nuclei (such as ^2H , ^{15}N) or weak signals (in particular those from the low-frequency range of 0 – 10 MHz) from the nuclei ^{17}O , ^{23}Na , ^{25}Mg and ^{27}Al often found in API pharmaceuticals. The use of indirect

methods in the investigation of pharmaceuticals is of growing popularity mainly because of a significant increase in the NQR sensitivity in the detection of weak signals from ^{17}O and ^{15}N nuclei, often present in pharmaceuticals.

Recently, several special NQR techniques effective in the detection of weak NQR signals for some lower abundant isotopes have also been developed, among which superconducting quantum interference (SQUID) [52,53], NQR with the use of volume coils [54] and field cycling methods should all be mentioned [55–57]. The experimental NQR parameters can be obtained not only with the direct or indirect detection methods, but in an indirect way by using other spectroscopies in which the quadrupolar interaction disturbs the main phenomenon. For example, in the high-field NMR used for the detection of signals from low-abundant nuclei (^2H), EPR or electron nuclear double resonance (ENDOR), nuclear acoustic resonance, Mössbauer effect, antiferromagnetic nuclear resonance electron spin-echo envelope modulation spectroscopy, time-differential perturbed-angular-distribution method (used for detection of heavy quadrupole nuclei and rare earth elements) and specific heat measurements in low temperatures. From among these methods only the high-field NMR has found a significant use in the investigation of pharmaceuticals.

For investigation of pharmaceuticals, the most suitable are the pure NQR methods (^{35}Cl , ^{81}Br) and the double resonance NMR-NQR and cross-relaxation spectroscopy techniques, permitting detection of weak signals from the nuclei: ^{17}O , ^{23}Na , ^{25}Mg and ^{27}Al .

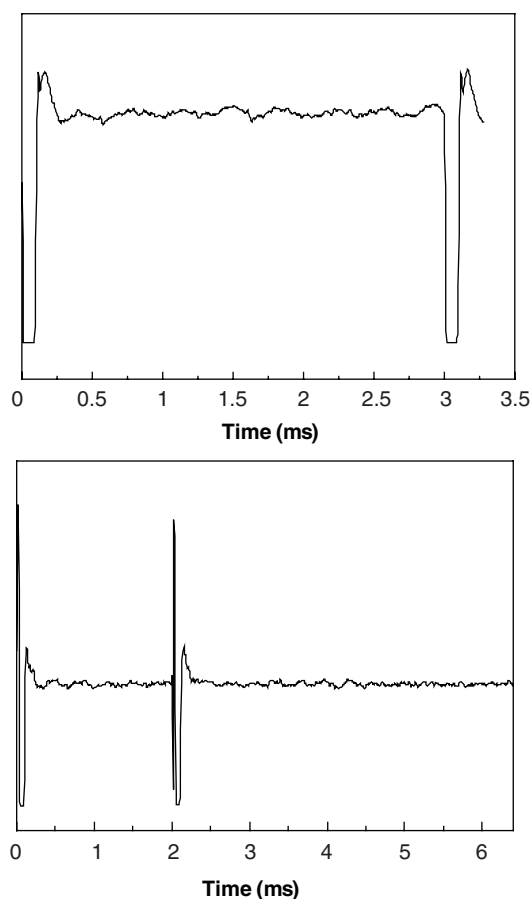


Figure 3. Typical NQR signals: ^{14}N -NQR for sulfanilamide, Hahn sequence, echo, 2000 accumulations ^{14}N -NQR for sulfanilamide, SLSE sequence, echo, 2000 accumulations. NQR: Nuclear quadrupole resonance; SLSE: Spin-locking spin-echo.

3.2 Nuclear quadrupole resonance spectrometer

Figure 2 shows a simplified block diagram of a pulse NQR spectrometer. The first important part of spectrometer is the system exciting the NQR signal, which includes a transmitter, a generator of pulses with a sequencer and a synthesizer. The second part of the spectrometer contains the probing head with the sample and a temperature-stabilising system equipped with a cryostat. The receiver block contains a digital receiver with low-pass filters and output amplifiers, an analog-to-digital converter and the accumulation and averaging block. The principle of quadrature detection is used in all receivers. An integral part of a modern spectrometer is a computer used first of all for programming and controlling of the spectrometer work, then programming the pulses and their sequences, the processing of results (Fourier transform, filtering) and their transmission and collection (the spectra and Fourier transforms). In addition, double resonance spectrometers require a special sample transit system and often a source

of DC magnetic field. A comprehensive review of different spectrometers can be found in [58].

3.3 Nuclear quadrupole resonance spectroscopy imaging

It is well known that MRI is a method of imaging-based on NMR, that is used for medical purposes. In contrast to NMR, the NQR method is principally a non-imaging technique. However, the high selectivity of the NQR method (permitting easy differentiation of the resonance signals from the same type nuclei and from different quadrupole nuclei) seems very promising in this application, but the possibility of investigation of solid state is still an important restriction. This problem can be solved by freezing in liquid nitrogen, but it is a serious drawback from the medical – not from the pharmaceutical – point of view. Attempts at making images based on the NQR data, the so-called three-dimensional NQR or quadrupole resonance imaging (QRI), have been performed at a few laboratories including those of GS Harbisson (University of Nebraska at Lincoln, US), DJ Pusiol (National University of Córdoba, Argentina), R Kimmich (Ulm University, Germany) and BH Suits (Michigan Technological University, US). However, the results only permitted the presentation of the potential of NQR imaging, mainly for the spatial localization of strain or dynamics [59-67]. In application to pharmaceutical analysis, QRI not only permits the detection of the presence of all types of anomalies such as areas with a different degree of vitrification, oxidation or hydration or different polymorphous forms in the sample volume, but also provides information on their localization. Moreover, if NQR permitted the detection of narcotics or toxic materials, the QRI method would also give their localization.

3.4 Measurement of nuclear quadrupole resonance frequency and line width

The NQR parameters such as NQR resonance frequency and line width can be found directly from the signal of free induction decay, Hahn echo or multipulse sequence (Figure 3), (Table 3) after the Fourier transform (Figure 4). The nuclear quadrupole resonance (NQR) resonance frequency is characteristic of a given type of nuclei and a given compound and it determines the absorption line position in the NQR spectrum on a given nucleus, but the intensity and shape of the NQR resonance line can change depending on the the experimental conditions. The parameter commonly used for description of the line shape is the full width at half maximum (FWHM) usually given in kHz units.

The NQR parameters QCC and possibly η calculated from relevant formulae (Equation 17) knowing the resonance frequencies from ^{14}N -NQR spectra provide information about the electron density distribution in the neighborhood of the nuclei studied, on the bonds in which a given atom is involved and, thus, on the population of the free electron pair or the bonds [23]. On the other hand,

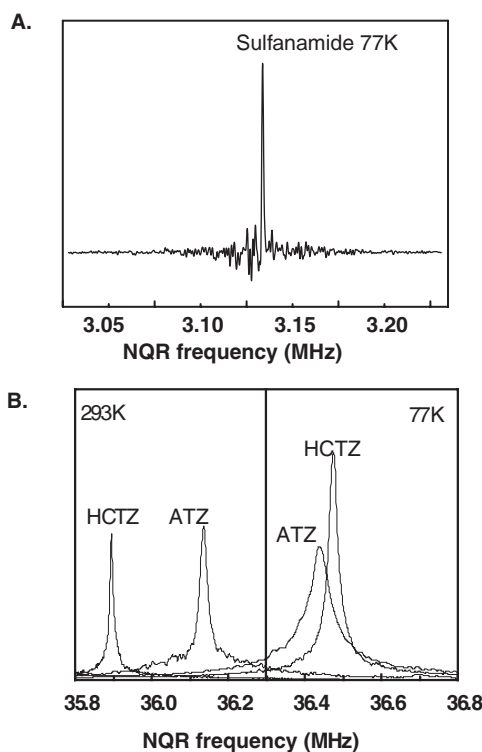


Figure 4. Typical NQR spectra. A. ^{14}N -NQR for sulphanilamide and **B.** ^{35}Cl -NQR for HCTZ and ATZ.

ATZ: Althiazide; HCTZ: Hydrochlorothiazide; NQR: Nuclear quadrupole resonance.

^{35}Cl -NQR spectra provides information about the double bond characteristics of the single bond in which a chlorine is involved [23].

3.5 Measurement of T_1 and T_2 relaxation times

The line width in the NQR spectrum is determined by the relaxation time T_2^* and the line intensity depends on the relaxation time T_1 . The methods most often used for precise measurements of the spin–lattice or longitudinal relaxation time, T_1 , are the inversion–recovery ones. The best known of these is the zero method with two pulse π - t - $\pi/2$ or three pulse π - t - $\pi/2$ - τ - π sequence. Here, the amplitude of the free induction signal is measured after probing pulse $\pi/2$ as a function of the distance between the π and $\pi/2$ pulses. Alternatively, the amplitude of the quadrupole spin–echo is measured as a function of the distance between the first π pulse and the pair of the $\pi/2$ - π probing pulses and permits calculating T_1 from the relation (Equation 18):

(18)

$$M(t) = M_0[1 - 2\exp(-t/T_1)]$$

The frequently used inversion–recovery method uses two impulses π - t - $\pi/2$ - τ sequence, in which the sequence interval remains constant, whereas the time of repetition of the pair of the pulses changes, although the method only gives good results for NQR lines of great SNR.

The method most frequently used for the measurement of the spin–spin or transverse relaxation time, T_2 , is the two-pulse method in which the amplitude of the quadrupole spin–echo depends on the time interval between the $\pi/2$ and π pulses according to the relation (Equation 19):

(19)

$$M(t) = M_0\exp[-(2t/T_2)^2]$$

where M_0 is the initial value of the transversal component of the nuclear magnetisation of the spin system and $M(t)$ is the magnetisation after the time $t = 2\tau$.

The measurement of the true spin–spin relaxation T_2^* time is most often performed by refocusing the two impulse $\pi/2$ - τ - π sequence, in which the two-pulse experiment is repeated with a number of different values of t interval between the pulses, whereas the relaxation time T_2 is determined in the same way as T_1 .

The spin–spin relaxation T_2^* time can be estimated from the FWHM of the resonance line or it can be measured using the following equation describing the rate of the free induction decay after the $\pi/2$ pulse (Equation 20):

(20)

$$M(t) = M_0\exp(-t/T_2^*)$$

The most often used methods of the relaxation time measurements are characterized in (Table 3).

4. Nuclear quadrupole resonance in drug development

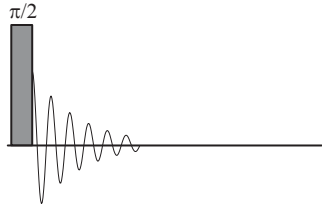
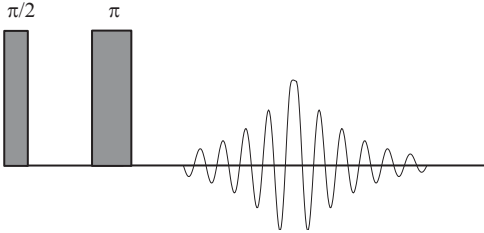
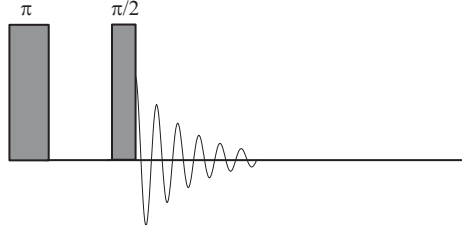
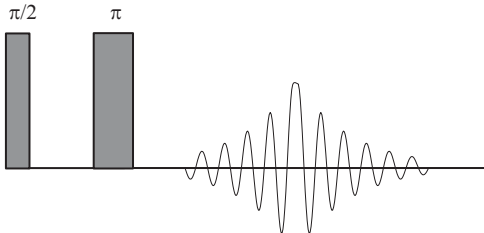
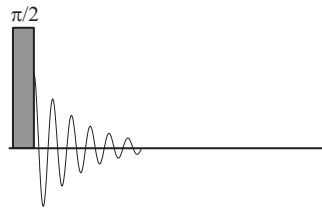
NQR is a sophisticated technique that can be applied in two ways in the process of drug development, namely: i) analytical, which covers the physical and chemical characterization of the API (identification, quality control, polymorphism and crystal structure) and ii) API development – structure and (second- or third-generation drugs).

4.1 Analytical step

4.1.1 Identification

As mentioned above, EFG is a characteristic of the material and, thus, it can be expected that the NQR frequency is unique for every chemical compound. That is why NQR has

Table 3. Selected pulse sequences for FID, echo, T_1 , T_2 and T_2^* measurements.

| Parameter | Pulse sequence | Formula |
|-----------|---|---------------------------------|
| FID |  | FFT |
| Echo |  | FFT |
| T_1 |  | $M(t) = M_0[1 - 2\exp(-t/T_1)]$ |
| T_2 |  | $M(t) = M_0\exp(-[2t/T_2]^2)$ |
| T_2^* |  | $M(t) = M_0\exp(-t/T_2^*)$ |

FFT: Fast Fourier transform; FID: Free induction decay.

Table 4. The differences in the NQR data (line width, relaxation time, NQR frequency) originating from defects, crystalline imperfections and for selected drugs and its complexes

| Drug | Nucleus | T (K) | Frequency (MHz) | Line width (Hz) | T ₁ | T ₂ | QCC | η | Ref. | | | | | | | | | | | | | | | | | | | | | | | | | | | | | | | | | | | | | | | | | | | | | | | | | | | | | | | | | | | | | | | | | | | | | | | | | | | | | | | | | | | | | | | | | | | | | | | | | | | | | | | | | | | | | | | | | | | | | | | | | | | | | | | | | | | | | | | | | | | | | | | | | | | | | | | | | | | | | | | | | | | | | | | | | | | | | | | | | | | | | | | | | | | | | | | | | | | | | | | | | | | | | | | | | | | | | | | | | | | | | | | | | | | | | | | | | | | | | | | | | | | | | | | | | | | | | | | | | | | | | | | | | | | | | | | | | | | | | | | | | | | | | | | | | | | | | | | | | |
|--|-----------------|------------------|-------------------------|-----------------|----------------|----------------|--------|--------|------|-----------------------------|-----------------|-----|----------------|------|-----|-----|--------|--------|------|--------------|-----------------|------|-------|-----------------------------|-----------------|-----|----------------|-------|------|-----------------------------|-----------------|--------|-------|--------------|-----------------|------|-------|-----------------------------|-----------------|-------|--------|-------|------|-----------------------------|-----------------|--------|-------|--------------|-----------------|-------|-------|----------------|-----------------|-------|-------|-------|-------|-----------------------------|-----------------|------|-------|-----------------------------|-----------------|---------|-----------------|-------|-------|-------|--------|--------|-------|-----------------------------|-----------------|--|-----------------|-----------------------------|-----------------|---------|-----------------|-------|-------|-------|--------|---------|-----------------|--------|-----------------|--|-----------------|----------------|-----------------|---------|-----------------|-------|-----------------|-----------------------------|-------------------------|---------|-----------------|--------|-----------------|--|-----------------|-----------|-----------------|---------|-----------------|-------|-----------------|-----------------------------|-------------------------|---------|-----------------|-------|-------------|--|-----------------|-----------|-----------------|-------|-------|-------|-----------------|-------|-------------------------|---------|-----------------|-------|-------------|---------|-----------------|-----------|-----------------|-------|-------|-------|-----------------|-------|-------------------------|--|-----------------|-----------------|-------|-------|-------|-----------|-----------------|------|-------|---------|--|-----------------|-------------|-------|-------|-------|-------|-------|-------|-------|-----------------|-----------------|-------------------------|-------------|-------|-------|-------|-------|-------|-----------|-----------------|-----------------|-------|-------------------------|-------|-------|-------|--------|-------|-------|-----------|-----------------|--------|---------------|-------|------------------|--------|-------|-------|--------|-------|--------|-------|--------|----------|-------|--------|-------|--------|---------------|--------|------------------|-------|--------|-------|---------------|-------|------------------|----------|-------|--------|--------|--------------|-------|------------------|----|--------|-------|--------|--------|--------|---------------|------|------------------|---------------|----|------------------|--------|------------------|------|----------|-------|--------|----------|--------|------------|----|--------|--------|--------|--------------|--------|------------------|------|--------|--------|--------------|-------|------------------|------------|----|--------|--------|----------------|------|----------------|--------|--------|-------|-------|--------|--------|--------------|--------------|------------------|------------------|---|----------------|--------|----------------|-------|------------|------------|-------|--------|--------|---|---|--------|--------|--------|----------------|--------|----------------|---|--------|--------|----------------|--------|----------------|---|---|---|-------|-------|--------|--------|--|--|--|--|--|----------------|----------------|----------------|----------------|
| Cocaine base (raw) | ¹⁴ N | 77 | 3.740 | 2300 | - | - | 5.046 | 0.0013 | [71] | | | | | | | | | | | | | | | | | | | | | | | | | | | | | | | | | | | | | | | | | | | | | | | | | | | | | | | | | | | | | | | | | | | | | | | | | | | | | | | | | | | | | | | | | | | | | | | | | | | | | | | | | | | | | | | | | | | | | | | | | | | | | | | | | | | | | | | | | | | | | | | | | | | | | | | | | | | | | | | | | | | | | | | | | | | | | | | | | | | | | | | | | | | | | | | | | | | | | | | | | | | | | | | | | | | | | | | | | | | | | | | | | | | | | | | | | | | | | | | | | | | | | | | | | | | | | | | | | | | | | | | | | | | | | | | | | | | | | | | | | | | | | | | | | | | | | | | | | |
| | | | 3.829 | 2300 | - | - | | | | Cocaine base | ¹⁴ N | 295 | 3.7176 | 870 | - | - | 5.0229 | 0.0395 | [71] | 3.8168 | 860 | 210 | 85 | Cocaine base | ¹⁴ N | 295 | 3.865 3.757 | | | | 5.081 | 0.043 | [72] | Cocaine. HCl | ¹⁴ N | 77 | 0.960 | 5000 | 370 | 25 | 1.182 | 0.250 | [71] | 0.811 | 5000 | 360 | 22 | Cocaine. HCl | ¹⁴ N | 295 | 0.960 | | | | 1.178 | 0.263 | [72] | 0.809 | | | | Cocaine. HCl | ¹⁴ N | 295 | 0.961 | 5000 | 700 | 1.5 | 1.178 | 0.263 | [71] | 0.806 | 4000 | 2000 | 0.3 | Cocaine base recrystallized | ¹⁴ N | 295 | 3.7175 | 270 | 75 | 75 | 5.0228 | 0.0395 | [71] | 3.8168 | 260 | 160 | 81 | MDMA (ecstasy) | ¹⁴ N | 295 | 2.712 | - | - | - | - | - | [74] | Heroin | ¹⁴ N | 295 | 4.026 | 3.950 | | | 5.031 | 0.028 | [72] | Heroin.HCl.H ₂ O | ¹⁴ N | 4.2 | 0.957 | - | - | - | 1.328 | 0.108 | [74] | 1.035 | | | | 1.329 | 0.128 | | 0.954 | | | | 3.801 | 0.4 | | 1.032 | | | | 3.830 | 0.4 | | Codeine | ¹⁴ N | 295 | 4.028 | 3.980 | - | - | - | 0.02 | [72] | Codeine.H ₃ PO ₄ | ¹⁴ N | 295 | 1.017 | 0.785 | - | - | 1.200 | 0.35 | [72] | Hashish | ¹⁴ N | 295 | Line series | - | - | - | - | - | [72] | Opium | ¹⁴ N | 295 | 3.0 – 4.0 many lines | - | - | - | - | - | [72] | Lidocaine | ¹⁴ N | 77 | 3.034 | 2.134 | - | - | 3.334 | 0.508 | [18] | 2.969 | 2.095 | | | 5.485 | 0.059 | 2.871 | 2.083 | | | 2.823 | 1.998 | | | 4.227 | 4.094 | | | 4.218 | 4.064 | | | 4.209 | 4.051 | | | 4.129 | 3.925 | | | | | | | Lidocaine.HCl | 77 | 2.5130 1.8267 | - | - | - | 2.8931 | 0.474 | [18] | Procaine | 77 | 3.0313 | - | - | - | 3.6823 | 0.293 | [18] | 2.4922 | | | | 5.3971 | 0.038 | | 4.0994 | | | | | | | 3.9962 | | | | | | | Procaine.HCl | 77 | 2.9352 2.2887 | - | - | - | 3.4826 | 0.371 | [18] | Tetracaine | 77 | 3.4010 | - | - | - | 4.1913 | 0.246 | [18] | 2.8860 | | | | 5.1930 | 0.0187 | | 3.9190 | | | | | | | 3.8705 | | | | | | | Tetracaine.HCl | 77 | 3.304 2.793 | - |
| Cocaine base | ¹⁴ N | 295 | 3.7176 | 870 | - | - | 5.0229 | 0.0395 | [71] | | | | | | | | | | | | | | | | | | | | | | | | | | | | | | | | | | | | | | | | | | | | | | | | | | | | | | | | | | | | | | | | | | | | | | | | | | | | | | | | | | | | | | | | | | | | | | | | | | | | | | | | | | | | | | | | | | | | | | | | | | | | | | | | | | | | | | | | | | | | | | | | | | | | | | | | | | | | | | | | | | | | | | | | | | | | | | | | | | | | | | | | | | | | | | | | | | | | | | | | | | | | | | | | | | | | | | | | | | | | | | | | | | | | | | | | | | | | | | | | | | | | | | | | | | | | | | | | | | | | | | | | | | | | | | | | | | | | | | | | | | | | | | | | | | | | | | | | | |
| | | | 3.8168 | 860 | 210 | 85 | | | | Cocaine base | ¹⁴ N | 295 | 3.865 3.757 | | | | 5.081 | 0.043 | [72] | Cocaine. HCl | ¹⁴ N | 77 | 0.960 | 5000 | 370 | 25 | 1.182 | 0.250 | [71] | 0.811 | 5000 | 360 | 22 | Cocaine. HCl | ¹⁴ N | 295 | 0.960 | | | | 1.178 | 0.263 | [72] | 0.809 | | | | Cocaine. HCl | ¹⁴ N | 295 | 0.961 | 5000 | 700 | 1.5 | 1.178 | 0.263 | [71] | 0.806 | 4000 | 2000 | 0.3 | Cocaine base recrystallized | ¹⁴ N | 295 | 3.7175 | 270 | 75 | 75 | 5.0228 | 0.0395 | [71] | 3.8168 | 260 | 160 | 81 | MDMA (ecstasy) | ¹⁴ N | 295 | 2.712 | - | - | - | - | - | [74] | Heroin | ¹⁴ N | 295 | 4.026 | 3.950 | | | 5.031 | 0.028 | [72] | Heroin.HCl.H ₂ O | ¹⁴ N | 4.2 | 0.957 | - | - | - | 1.328 | 0.108 | [74] | 1.035 | | | | | | | 1.329 | 0.128 | | 0.954 | | | | 3.801 | 0.4 | | 1.032 | | | | 3.830 | 0.4 | | Codeine | ¹⁴ N | 295 | 4.028 | 3.980 | - | - | - | 0.02 | [72] | Codeine.H ₃ PO ₄ | ¹⁴ N | 295 | 1.017 | 0.785 | - | - | 1.200 | 0.35 | [72] | Hashish | ¹⁴ N | 295 | Line series | - | - | - | - | - | [72] | Opium | ¹⁴ N | 295 | 3.0 – 4.0 many lines | - | - | - | - | - | [72] | Lidocaine | ¹⁴ N | 77 | 3.034 | 2.134 | - | - | 3.334 | 0.508 | [18] | 2.969 | | | | 2.095 | | | 5.485 | | | | 0.059 | 2.871 | 2.083 | | | | | 2.823 | 1.998 | | | 4.227 | 4.094 | | | 4.218 | 4.064 | | | 4.209 | 4.051 | | | 4.129 | 3.925 | | | | | | | Lidocaine.HCl | 77 | 2.5130 1.8267 | - | - | - | 2.8931 | 0.474 | [18] | Procaine | 77 | 3.0313 | | | - | - | - | 3.6823 | 0.293 | [18] | 2.4922 | | | | 5.3971 | 0.038 | | 4.0994 | | | | | | | 3.9962 | | | | | | | Procaine.HCl | 77 | 2.9352 2.2887 | - | - | - | 3.4826 | 0.371 | [18] | Tetracaine | | | 77 | 3.4010 | - | - | - | 4.1913 | 0.246 | [18] | 2.8860 | | | | 5.1930 | 0.0187 | | 3.9190 | | | | | | | 3.8705 | | | | | | | Tetracaine.HCl | 77 | 3.304 2.793 |
| Cocaine base | ¹⁴ N | 295 | 3.865 3.757 | | | | 5.081 | 0.043 | [72] | | | | | | | | | | | | | | | | | | | | | | | | | | | | | | | | | | | | | | | | | | | | | | | | | | | | | | | | | | | | | | | | | | | | | | | | | | | | | | | | | | | | | | | | | | | | | | | | | | | | | | | | | | | | | | | | | | | | | | | | | | | | | | | | | | | | | | | | | | | | | | | | | | | | | | | | | | | | | | | | | | | | | | | | | | | | | | | | | | | | | | | | | | | | | | | | | | | | | | | | | | | | | | | | | | | | | | | | | | | | | | | | | | | | | | | | | | | | | | | | | | | | | | | | | | | | | | | | | | | | | | | | | | | | | | | | | | | | | | | | | | | | | | | | | | | | | | | | | |
| Cocaine. HCl | ¹⁴ N | 77 | 0.960 | 5000 | 370 | 25 | 1.182 | 0.250 | [71] | | | | | | | | | | | | | | | | | | | | | | | | | | | | | | | | | | | | | | | | | | | | | | | | | | | | | | | | | | | | | | | | | | | | | | | | | | | | | | | | | | | | | | | | | | | | | | | | | | | | | | | | | | | | | | | | | | | | | | | | | | | | | | | | | | | | | | | | | | | | | | | | | | | | | | | | | | | | | | | | | | | | | | | | | | | | | | | | | | | | | | | | | | | | | | | | | | | | | | | | | | | | | | | | | | | | | | | | | | | | | | | | | | | | | | | | | | | | | | | | | | | | | | | | | | | | | | | | | | | | | | | | | | | | | | | | | | | | | | | | | | | | | | | | | | | | | | | | | |
| | | | 0.811 | 5000 | 360 | 22 | | | | Cocaine. HCl | ¹⁴ N | 295 | 0.960 | | | | 1.178 | 0.263 | [72] | 0.809 | | | | Cocaine. HCl | ¹⁴ N | 295 | 0.961 | 5000 | 700 | 1.5 | 1.178 | 0.263 | [71] | 0.806 | 4000 | 2000 | 0.3 | Cocaine base recrystallized | ¹⁴ N | 295 | 3.7175 | 270 | 75 | 75 | 5.0228 | 0.0395 | [71] | 3.8168 | 260 | 160 | 81 | MDMA (ecstasy) | ¹⁴ N | 295 | 2.712 | - | - | - | - | - | [74] | Heroin | ¹⁴ N | 295 | 4.026 | 3.950 | | | 5.031 | 0.028 | [72] | Heroin.HCl.H ₂ O | ¹⁴ N | 4.2 | 0.957 | - | - | - | 1.328 | 0.108 | [74] | 1.035 | | | | 1.329 | 0.128 | | 0.954 | | | | 3.801 | 0.4 | | | | | 1.032 | | | | 3.830 | 0.4 | | Codeine | ¹⁴ N | 295 | 4.028 | 3.980 | - | - | - | 0.02 | [72] | Codeine.H ₃ PO ₄ | ¹⁴ N | 295 | 1.017 | 0.785 | - | - | 1.200 | 0.35 | [72] | Hashish | ¹⁴ N | 295 | Line series | - | - | - | - | - | [72] | Opium | ¹⁴ N | 295 | 3.0 – 4.0 many lines | - | - | - | - | - | [72] | Lidocaine | ¹⁴ N | 77 | 3.034 | 2.134 | - | - | 3.334 | 0.508 | [18] | 2.969 | 2.095 | | | 5.485 | 0.059 | 2.871 | 2.083 | | | 2.823 | 1.998 | | | | | | 4.227 | 4.094 | | | | | | 4.218 | | | | 4.064 | | | | | | | | 4.209 | 4.051 | | | | | 4.129 | 3.925 | | | | | | | Lidocaine.HCl | 77 | 2.5130 1.8267 | - | - | - | 2.8931 | 0.474 | [18] | Procaine | 77 | 3.0313 | - | - | - | 3.6823 | 0.293 | [18] | 2.4922 | | | | 5.3971 | 0.038 | | | | 4.0994 | | | | | | | 3.9962 | | | | | | | Procaine.HCl | 77 | 2.9352 2.2887 | - | - | - | 3.4826 | 0.371 | [18] | Tetracaine | 77 | 3.4010 | - | - | - | 4.1913 | 0.246 | [18] | 2.8860 | | | | 5.1930 | 0.0187 | | | 3.9190 | | | | | | | | 3.8705 | | | | | | | Tetracaine.HCl | 77 | 3.304 2.793 | - | - | - | 4.065 | 0.251 | [18] | | | | | | | | | | |
| Cocaine. HCl | ¹⁴ N | 295 | 0.960 | | | | 1.178 | 0.263 | [72] | | | | | | | | | | | | | | | | | | | | | | | | | | | | | | | | | | | | | | | | | | | | | | | | | | | | | | | | | | | | | | | | | | | | | | | | | | | | | | | | | | | | | | | | | | | | | | | | | | | | | | | | | | | | | | | | | | | | | | | | | | | | | | | | | | | | | | | | | | | | | | | | | | | | | | | | | | | | | | | | | | | | | | | | | | | | | | | | | | | | | | | | | | | | | | | | | | | | | | | | | | | | | | | | | | | | | | | | | | | | | | | | | | | | | | | | | | | | | | | | | | | | | | | | | | | | | | | | | | | | | | | | | | | | | | | | | | | | | | | | | | | | | | | | | | | | | | | | | |
| | | | 0.809 | | | | | | | Cocaine. HCl | ¹⁴ N | 295 | 0.961 | 5000 | 700 | 1.5 | 1.178 | 0.263 | [71] | 0.806 | 4000 | 2000 | 0.3 | Cocaine base recrystallized | ¹⁴ N | 295 | 3.7175 | 270 | 75 | 75 | 5.0228 | 0.0395 | [71] | 3.8168 | 260 | 160 | 81 | MDMA (ecstasy) | ¹⁴ N | 295 | 2.712 | - | - | - | - | - | [74] | Heroin | ¹⁴ N | 295 | 4.026 | 3.950 | | | 5.031 | 0.028 | [72] | Heroin.HCl.H ₂ O | ¹⁴ N | 4.2 | 0.957 | - | - | - | 1.328 | 0.108 | [74] | 1.035 | | | | | | | 1.329 | 0.128 | | 0.954 | | | | 3.801 | 0.4 | | 1.032 | | | | 3.830 | 0.4 | | Codeine | ¹⁴ N | 295 | 4.028 | 3.980 | - | - | - | 0.02 | [72] | Codeine.H ₃ PO ₄ | ¹⁴ N | 295 | 1.017 | 0.785 | - | - | 1.200 | 0.35 | [72] | Hashish | ¹⁴ N | 295 | Line series | - | - | - | - | - | [72] | Opium | ¹⁴ N | 295 | 3.0 – 4.0 many lines | - | - | - | - | - | [72] | Lidocaine | ¹⁴ N | 77 | 3.034 | 2.134 | - | - | 3.334 | 0.508 | [18] | 2.969 | 2.095 | | | | | | 5.485 | 0.059 | 2.871 | 2.083 | | | | | | 2.823 | 1.998 | | | | | 4.227 | 4.094 | | | 4.218 | 4.064 | | | | | | 4.209 | 4.051 | | | | | | | | | 4.129 | 3.925 | | | | | | | | | | | | | | Lidocaine.HCl | 77 | 2.5130 1.8267 | - | - | - | 2.8931 | 0.474 | [18] | Procaine | 77 | 3.0313 | - | - | - | | | 3.6823 | 0.293 | [18] | 2.4922 | | | | 5.3971 | 0.038 | | 4.0994 | | | | | | | 3.9962 | | | | | | | Procaine.HCl | 77 | 2.9352 2.2887 | - | - | - | 3.4826 | 0.371 | [18] | Tetracaine | 77 | 3.4010 | - | - | - | | | 4.1913 | 0.246 | [18] | 2.8860 | | | | 5.1930 | 0.0187 | | 3.9190 | | | | | | | 3.8705 | | | | | | | Tetracaine.HCl | 77 | 3.304 2.793 | - | - | - | 4.065 | 0.251 | [18] | | | | | | | | | | | | | | | | |
| Cocaine. HCl | ¹⁴ N | 295 | 0.961 | 5000 | 700 | 1.5 | 1.178 | 0.263 | [71] | | | | | | | | | | | | | | | | | | | | | | | | | | | | | | | | | | | | | | | | | | | | | | | | | | | | | | | | | | | | | | | | | | | | | | | | | | | | | | | | | | | | | | | | | | | | | | | | | | | | | | | | | | | | | | | | | | | | | | | | | | | | | | | | | | | | | | | | | | | | | | | | | | | | | | | | | | | | | | | | | | | | | | | | | | | | | | | | | | | | | | | | | | | | | | | | | | | | | | | | | | | | | | | | | | | | | | | | | | | | | | | | | | | | | | | | | | | | | | | | | | | | | | | | | | | | | | | | | | | | | | | | | | | | | | | | | | | | | | | | | | | | | | | | | | | | | | | | | |
| | | | 0.806 | 4000 | 2000 | 0.3 | | | | Cocaine base recrystallized | ¹⁴ N | 295 | 3.7175 | 270 | 75 | 75 | 5.0228 | 0.0395 | [71] | 3.8168 | 260 | 160 | 81 | MDMA (ecstasy) | ¹⁴ N | 295 | 2.712 | - | - | - | - | - | [74] | Heroin | ¹⁴ N | 295 | 4.026 | 3.950 | | | 5.031 | 0.028 | [72] | Heroin.HCl.H ₂ O | ¹⁴ N | 4.2 | 0.957 | - | - | - | 1.328 | 0.108 | [74] | 1.035 | | | | | | | 1.329 | 0.128 | | 0.954 | | | | 3.801 | 0.4 | | 1.032 | | | | 3.830 | 0.4 | | Codeine | ¹⁴ N | 295 | 4.028 | 3.980 | - | - | - | 0.02 | [72] | Codeine.H ₃ PO ₄ | ¹⁴ N | 295 | 1.017 | 0.785 | - | - | 1.200 | 0.35 | [72] | Hashish | ¹⁴ N | 295 | Line series | - | - | - | - | - | [72] | Opium | ¹⁴ N | 295 | 3.0 – 4.0 many lines | - | - | - | - | - | [72] | Lidocaine | ¹⁴ N | 77 | 3.034 | 2.134 | - | - | 3.334 | 0.508 | [18] | 2.969 | 2.095 | | | | | | 5.485 | 0.059 | 2.871 | 2.083 | | | | | | 2.823 | 1.998 | | | | | | | | | | | 4.227 | 4.094 | | | | | 4.218 | 4.064 | | | 4.209 | 4.051 | | | | | | 4.129 | 3.925 | | | | | | | | | | Lidocaine.HCl | 77 | 2.5130 1.8267 | | - | - | - | | 2.8931 | 0.474 | [18] | Procaine | 77 | 3.0313 | - | - | - | 3.6823 | 0.293 | [18] | 2.4922 | | | | 5.3971 | | | 0.038 | | 4.0994 | | | | | | | 3.9962 | | | | | | | Procaine.HCl | 77 | 2.9352 2.2887 | - | - | - | 3.4826 | 0.371 | [18] | Tetracaine | 77 | 3.4010 | - | - | - | 4.1913 | 0.246 | [18] | 2.8860 | | | | 5.1930 | | | 0.0187 | | 3.9190 | | | | | | | 3.8705 | | | | | | | Tetracaine.HCl | 77 | 3.304 2.793 | - | - | - | 4.065 | 0.251 | [18] | | | | | | | | | | | | | | | | | | | | | | | | | | | | | | |
| Cocaine base recrystallized | ¹⁴ N | 295 | 3.7175 | 270 | 75 | 75 | 5.0228 | 0.0395 | [71] | | | | | | | | | | | | | | | | | | | | | | | | | | | | | | | | | | | | | | | | | | | | | | | | | | | | | | | | | | | | | | | | | | | | | | | | | | | | | | | | | | | | | | | | | | | | | | | | | | | | | | | | | | | | | | | | | | | | | | | | | | | | | | | | | | | | | | | | | | | | | | | | | | | | | | | | | | | | | | | | | | | | | | | | | | | | | | | | | | | | | | | | | | | | | | | | | | | | | | | | | | | | | | | | | | | | | | | | | | | | | | | | | | | | | | | | | | | | | | | | | | | | | | | | | | | | | | | | | | | | | | | | | | | | | | | | | | | | | | | | | | | | | | | | | | | | | | | | | |
| | | | 3.8168 | 260 | 160 | 81 | | | | MDMA (ecstasy) | ¹⁴ N | 295 | 2.712 | - | - | - | - | - | [74] | Heroin | ¹⁴ N | 295 | 4.026 | 3.950 | | | 5.031 | 0.028 | [72] | Heroin.HCl.H ₂ O | ¹⁴ N | 4.2 | 0.957 | - | - | - | 1.328 | 0.108 | [74] | 1.035 | | | | | | | 1.329 | 0.128 | | 0.954 | | | | 3.801 | 0.4 | | 1.032 | | | | 3.830 | 0.4 | | Codeine | ¹⁴ N | 295 | 4.028 | 3.980 | - | - | - | 0.02 | [72] | Codeine.H ₃ PO ₄ | ¹⁴ N | 295 | 1.017 | 0.785 | - | - | 1.200 | 0.35 | [72] | Hashish | ¹⁴ N | 295 | Line series | - | - | - | - | - | [72] | Opium | ¹⁴ N | 295 | 3.0 – 4.0 many lines | - | - | - | - | - | [72] | Lidocaine | ¹⁴ N | 77 | 3.034 | 2.134 | - | - | 3.334 | 0.508 | [18] | 2.969 | 2.095 | | | | | | 5.485 | 0.059 | 2.871 | 2.083 | | | | | | 2.823 | 1.998 | | | | | | | | | | | 4.227 | 4.094 | | | | | | | | 4.218 | 4.064 | | | | | | 4.209 | 4.051 | | | | | 4.129 | 3.925 | | | | | | | Lidocaine.HCl | 77 | 2.5130 1.8267 | - | - | - | 2.8931 | 0.474 | [18] | Procaine | 77 | 3.0313 | - | - | - | 3.6823 | 0.293 | [18] | 2.4922 | | | | 5.3971 | | | 0.038 | | 4.0994 | | | | | | | 3.9962 | | | | | | | Procaine.HCl | 77 | 2.9352 2.2887 | - | - | - | 3.4826 | 0.371 | [18] | Tetracaine | 77 | 3.4010 | - | - | - | 4.1913 | 0.246 | [18] | 2.8860 | | | | 5.1930 | | | 0.0187 | | 3.9190 | | | | | | | 3.8705 | | | | | | | Tetracaine.HCl | 77 | 3.304 2.793 | - | - | - | 4.065 | 0.251 | [18] | | | | | | | | | | | | | | | | | | | | | | | | | | | | | | | | | | | | | | | | | | | | |
| MDMA (ecstasy) | ¹⁴ N | 295 | 2.712 | - | - | - | - | - | [74] | | | | | | | | | | | | | | | | | | | | | | | | | | | | | | | | | | | | | | | | | | | | | | | | | | | | | | | | | | | | | | | | | | | | | | | | | | | | | | | | | | | | | | | | | | | | | | | | | | | | | | | | | | | | | | | | | | | | | | | | | | | | | | | | | | | | | | | | | | | | | | | | | | | | | | | | | | | | | | | | | | | | | | | | | | | | | | | | | | | | | | | | | | | | | | | | | | | | | | | | | | | | | | | | | | | | | | | | | | | | | | | | | | | | | | | | | | | | | | | | | | | | | | | | | | | | | | | | | | | | | | | | | | | | | | | | | | | | | | | | | | | | | | | | | | | | | | | | | |
| Heroin | ¹⁴ N | 295 | 4.026 | 3.950 | | | 5.031 | 0.028 | [72] | | | | | | | | | | | | | | | | | | | | | | | | | | | | | | | | | | | | | | | | | | | | | | | | | | | | | | | | | | | | | | | | | | | | | | | | | | | | | | | | | | | | | | | | | | | | | | | | | | | | | | | | | | | | | | | | | | | | | | | | | | | | | | | | | | | | | | | | | | | | | | | | | | | | | | | | | | | | | | | | | | | | | | | | | | | | | | | | | | | | | | | | | | | | | | | | | | | | | | | | | | | | | | | | | | | | | | | | | | | | | | | | | | | | | | | | | | | | | | | | | | | | | | | | | | | | | | | | | | | | | | | | | | | | | | | | | | | | | | | | | | | | | | | | | | | | | | | | | |
| Heroin.HCl.H ₂ O | ¹⁴ N | 4.2 | 0.957 | - | - | - | 1.328 | 0.108 | [74] | | | | | | | | | | | | | | | | | | | | | | | | | | | | | | | | | | | | | | | | | | | | | | | | | | | | | | | | | | | | | | | | | | | | | | | | | | | | | | | | | | | | | | | | | | | | | | | | | | | | | | | | | | | | | | | | | | | | | | | | | | | | | | | | | | | | | | | | | | | | | | | | | | | | | | | | | | | | | | | | | | | | | | | | | | | | | | | | | | | | | | | | | | | | | | | | | | | | | | | | | | | | | | | | | | | | | | | | | | | | | | | | | | | | | | | | | | | | | | | | | | | | | | | | | | | | | | | | | | | | | | | | | | | | | | | | | | | | | | | | | | | | | | | | | | | | | | | | | |
| | | | 1.035 | | | | 1.329 | 0.128 | | | | | | | | | | | | | | | | | | | | | | | | | | | | | | | | | | | | | | | | | | | | | | | | | | | | | | | | | | | | | | | | | | | | | | | | | | | | | | | | | | | | | | | | | | | | | | | | | | | | | | | | | | | | | | | | | | | | | | | | | | | | | | | | | | | | | | | | | | | | | | | | | | | | | | | | | | | | | | | | | | | | | | | | | | | | | | | | | | | | | | | | | | | | | | | | | | | | | | | | | | | | | | | | | | | | | | | | | | | | | | | | | | | | | | | | | | | | | | | | | | | | | | | | | | | | | | | | | | | | | | | | | | | | | | | | | | | | | | | | | | | | | | | | | | | | | | | | | | |
| | | | 0.954 | | | | 3.801 | 0.4 | | | | | | | | | | | | | | | | | | | | | | | | | | | | | | | | | | | | | | | | | | | | | | | | | | | | | | | | | | | | | | | | | | | | | | | | | | | | | | | | | | | | | | | | | | | | | | | | | | | | | | | | | | | | | | | | | | | | | | | | | | | | | | | | | | | | | | | | | | | | | | | | | | | | | | | | | | | | | | | | | | | | | | | | | | | | | | | | | | | | | | | | | | | | | | | | | | | | | | | | | | | | | | | | | | | | | | | | | | | | | | | | | | | | | | | | | | | | | | | | | | | | | | | | | | | | | | | | | | | | | | | | | | | | | | | | | | | | | | | | | | | | | | | | | | | | | | | | | | |
| | | | 1.032 | | | | 3.830 | 0.4 | | | | | | | | | | | | | | | | | | | | | | | | | | | | | | | | | | | | | | | | | | | | | | | | | | | | | | | | | | | | | | | | | | | | | | | | | | | | | | | | | | | | | | | | | | | | | | | | | | | | | | | | | | | | | | | | | | | | | | | | | | | | | | | | | | | | | | | | | | | | | | | | | | | | | | | | | | | | | | | | | | | | | | | | | | | | | | | | | | | | | | | | | | | | | | | | | | | | | | | | | | | | | | | | | | | | | | | | | | | | | | | | | | | | | | | | | | | | | | | | | | | | | | | | | | | | | | | | | | | | | | | | | | | | | | | | | | | | | | | | | | | | | | | | | | | | | | | | | | |
| Codeine | ¹⁴ N | 295 | 4.028 | 3.980 | - | - | - | 0.02 | [72] | | | | | | | | | | | | | | | | | | | | | | | | | | | | | | | | | | | | | | | | | | | | | | | | | | | | | | | | | | | | | | | | | | | | | | | | | | | | | | | | | | | | | | | | | | | | | | | | | | | | | | | | | | | | | | | | | | | | | | | | | | | | | | | | | | | | | | | | | | | | | | | | | | | | | | | | | | | | | | | | | | | | | | | | | | | | | | | | | | | | | | | | | | | | | | | | | | | | | | | | | | | | | | | | | | | | | | | | | | | | | | | | | | | | | | | | | | | | | | | | | | | | | | | | | | | | | | | | | | | | | | | | | | | | | | | | | | | | | | | | | | | | | | | | | | | | | | | | | |
| Codeine.H ₃ PO ₄ | ¹⁴ N | 295 | 1.017 | 0.785 | - | - | 1.200 | 0.35 | [72] | | | | | | | | | | | | | | | | | | | | | | | | | | | | | | | | | | | | | | | | | | | | | | | | | | | | | | | | | | | | | | | | | | | | | | | | | | | | | | | | | | | | | | | | | | | | | | | | | | | | | | | | | | | | | | | | | | | | | | | | | | | | | | | | | | | | | | | | | | | | | | | | | | | | | | | | | | | | | | | | | | | | | | | | | | | | | | | | | | | | | | | | | | | | | | | | | | | | | | | | | | | | | | | | | | | | | | | | | | | | | | | | | | | | | | | | | | | | | | | | | | | | | | | | | | | | | | | | | | | | | | | | | | | | | | | | | | | | | | | | | | | | | | | | | | | | | | | | | |
| Hashish | ¹⁴ N | 295 | Line series | - | - | - | - | - | [72] | | | | | | | | | | | | | | | | | | | | | | | | | | | | | | | | | | | | | | | | | | | | | | | | | | | | | | | | | | | | | | | | | | | | | | | | | | | | | | | | | | | | | | | | | | | | | | | | | | | | | | | | | | | | | | | | | | | | | | | | | | | | | | | | | | | | | | | | | | | | | | | | | | | | | | | | | | | | | | | | | | | | | | | | | | | | | | | | | | | | | | | | | | | | | | | | | | | | | | | | | | | | | | | | | | | | | | | | | | | | | | | | | | | | | | | | | | | | | | | | | | | | | | | | | | | | | | | | | | | | | | | | | | | | | | | | | | | | | | | | | | | | | | | | | | | | | | | | | |
| Opium | ¹⁴ N | 295 | 3.0 – 4.0 many lines | - | - | - | - | - | [72] | | | | | | | | | | | | | | | | | | | | | | | | | | | | | | | | | | | | | | | | | | | | | | | | | | | | | | | | | | | | | | | | | | | | | | | | | | | | | | | | | | | | | | | | | | | | | | | | | | | | | | | | | | | | | | | | | | | | | | | | | | | | | | | | | | | | | | | | | | | | | | | | | | | | | | | | | | | | | | | | | | | | | | | | | | | | | | | | | | | | | | | | | | | | | | | | | | | | | | | | | | | | | | | | | | | | | | | | | | | | | | | | | | | | | | | | | | | | | | | | | | | | | | | | | | | | | | | | | | | | | | | | | | | | | | | | | | | | | | | | | | | | | | | | | | | | | | | | | |
| Lidocaine | ¹⁴ N | 77 | 3.034 | 2.134 | - | - | 3.334 | 0.508 | [18] | | | | | | | | | | | | | | | | | | | | | | | | | | | | | | | | | | | | | | | | | | | | | | | | | | | | | | | | | | | | | | | | | | | | | | | | | | | | | | | | | | | | | | | | | | | | | | | | | | | | | | | | | | | | | | | | | | | | | | | | | | | | | | | | | | | | | | | | | | | | | | | | | | | | | | | | | | | | | | | | | | | | | | | | | | | | | | | | | | | | | | | | | | | | | | | | | | | | | | | | | | | | | | | | | | | | | | | | | | | | | | | | | | | | | | | | | | | | | | | | | | | | | | | | | | | | | | | | | | | | | | | | | | | | | | | | | | | | | | | | | | | | | | | | | | | | | | | | | |
| | | | 2.969 | 2.095 | | | | | | 5.485 | 0.059 | | | | | | | | | | | | | | | | | | | | | | | | | | | | | | | | | | | | | | | | | | | | | | | | | | | | | | | | | | | | | | | | | | | | | | | | | | | | | | | | | | | | | | | | | | | | | | | | | | | | | | | | | | | | | | | | | | | | | | | | | | | | | | | | | | | | | | | | | | | | | | | | | | | | | | | | | | | | | | | | | | | | | | | | | | | | | | | | | | | | | | | | | | | | | | | | | | | | | | | | | | | | | | | | | | | | | | | | | | | | | | | | | | | | | | | | | | | | | | | | | | | | | | | | | | | | | | | | | | | | | | | | | | | | | | | | | | | | | | | | | | | | | | | | | | | | | | | |
| | | | 2.871 | 2.083 | | | | | | | | | | | | | | | | | | | | | | | | | | | | | | | | | | | | | | | | | | | | | | | | | | | | | | | | | | | | | | | | | | | | | | | | | | | | | | | | | | | | | | | | | | | | | | | | | | | | | | | | | | | | | | | | | | | | | | | | | | | | | | | | | | | | | | | | | | | | | | | | | | | | | | | | | | | | | | | | | | | | | | | | | | | | | | | | | | | | | | | | | | | | | | | | | | | | | | | | | | | | | | | | | | | | | | | | | | | | | | | | | | | | | | | | | | | | | | | | | | | | | | | | | | | | | | | | | | | | | | | | | | | | | | | | | | | | | | | | | | | | | | | | | | | | | | | | | | | | | | |
| | | | 2.823 | 1.998 | | | | | | | | | | | | | | | | | | | | | | | | | | | | | | | | | | | | | | | | | | | | | | | | | | | | | | | | | | | | | | | | | | | | | | | | | | | | | | | | | | | | | | | | | | | | | | | | | | | | | | | | | | | | | | | | | | | | | | | | | | | | | | | | | | | | | | | | | | | | | | | | | | | | | | | | | | | | | | | | | | | | | | | | | | | | | | | | | | | | | | | | | | | | | | | | | | | | | | | | | | | | | | | | | | | | | | | | | | | | | | | | | | | | | | | | | | | | | | | | | | | | | | | | | | | | | | | | | | | | | | | | | | | | | | | | | | | | | | | | | | | | | | | | | | | | | | | | | | | | | | |
| | | | 4.227 | 4.094 | | | | | | | | | | | | | | | | | | | | | | | | | | | | | | | | | | | | | | | | | | | | | | | | | | | | | | | | | | | | | | | | | | | | | | | | | | | | | | | | | | | | | | | | | | | | | | | | | | | | | | | | | | | | | | | | | | | | | | | | | | | | | | | | | | | | | | | | | | | | | | | | | | | | | | | | | | | | | | | | | | | | | | | | | | | | | | | | | | | | | | | | | | | | | | | | | | | | | | | | | | | | | | | | | | | | | | | | | | | | | | | | | | | | | | | | | | | | | | | | | | | | | | | | | | | | | | | | | | | | | | | | | | | | | | | | | | | | | | | | | | | | | | | | | | | | | | | | | | | | | | |
| | | | 4.218 | 4.064 | | | | | | | | | | | | | | | | | | | | | | | | | | | | | | | | | | | | | | | | | | | | | | | | | | | | | | | | | | | | | | | | | | | | | | | | | | | | | | | | | | | | | | | | | | | | | | | | | | | | | | | | | | | | | | | | | | | | | | | | | | | | | | | | | | | | | | | | | | | | | | | | | | | | | | | | | | | | | | | | | | | | | | | | | | | | | | | | | | | | | | | | | | | | | | | | | | | | | | | | | | | | | | | | | | | | | | | | | | | | | | | | | | | | | | | | | | | | | | | | | | | | | | | | | | | | | | | | | | | | | | | | | | | | | | | | | | | | | | | | | | | | | | | | | | | | | | | | | | | | | | |
| | | | 4.209 | 4.051 | | | | | | | | | | | | | | | | | | | | | | | | | | | | | | | | | | | | | | | | | | | | | | | | | | | | | | | | | | | | | | | | | | | | | | | | | | | | | | | | | | | | | | | | | | | | | | | | | | | | | | | | | | | | | | | | | | | | | | | | | | | | | | | | | | | | | | | | | | | | | | | | | | | | | | | | | | | | | | | | | | | | | | | | | | | | | | | | | | | | | | | | | | | | | | | | | | | | | | | | | | | | | | | | | | | | | | | | | | | | | | | | | | | | | | | | | | | | | | | | | | | | | | | | | | | | | | | | | | | | | | | | | | | | | | | | | | | | | | | | | | | | | | | | | | | | | | | | | | | | | | |
| | | | 4.129 | 3.925 | | | | | | | | | | | | | | | | | | | | | | | | | | | | | | | | | | | | | | | | | | | | | | | | | | | | | | | | | | | | | | | | | | | | | | | | | | | | | | | | | | | | | | | | | | | | | | | | | | | | | | | | | | | | | | | | | | | | | | | | | | | | | | | | | | | | | | | | | | | | | | | | | | | | | | | | | | | | | | | | | | | | | | | | | | | | | | | | | | | | | | | | | | | | | | | | | | | | | | | | | | | | | | | | | | | | | | | | | | | | | | | | | | | | | | | | | | | | | | | | | | | | | | | | | | | | | | | | | | | | | | | | | | | | | | | | | | | | | | | | | | | | | | | | | | | | | | | | | | | | | | |
| | | | | | | | | | | | | | | | | | | | | | | | | | | | | | | | | | | | | | | | | | | | | | | | | | | | | | | | | | | | | | | | | | | | | | | | | | | | | | | | | | | | | | | | | | | | | | | | | | | | | | | | | | | | | | | | | | | | | | | | | | | | | | | | | | | | | | | | | | | | | | | | | | | | | | | | | | | | | | | | | | | | | | | | | | | | | | | | | | | | | | | | | | | | | | | | | | | | | | | | | | | | | | | | | | | | | | | | | | | | | | | | | | | | | | | | | | | | | | | | | | | | | | | | | | | | | | | | | | | | | | | | | | | | | | | | | | | | | | | | | | | | | | | | | | | | | | | | | | | | | | | | | | | |
| Lidocaine.HCl | 77 | 2.5130 1.8267 | - | - | - | 2.8931 | 0.474 | [18] | | | | | | | | | | | | | | | | | | | | | | | | | | | | | | | | | | | | | | | | | | | | | | | | | | | | | | | | | | | | | | | | | | | | | | | | | | | | | | | | | | | | | | | | | | | | | | | | | | | | | | | | | | | | | | | | | | | | | | | | | | | | | | | | | | | | | | | | | | | | | | | | | | | | | | | | | | | | | | | | | | | | | | | | | | | | | | | | | | | | | | | | | | | | | | | | | | | | | | | | | | | | | | | | | | | | | | | | | | | | | | | | | | | | | | | | | | | | | | | | | | | | | | | | | | | | | | | | | | | | | | | | | | | | | | | | | | | | | | | | | | | | | | | | | | | | | | | | | | |
| Procaine | 77 | 3.0313 | - | - | - | 3.6823 | 0.293 | [18] | | | | | | | | | | | | | | | | | | | | | | | | | | | | | | | | | | | | | | | | | | | | | | | | | | | | | | | | | | | | | | | | | | | | | | | | | | | | | | | | | | | | | | | | | | | | | | | | | | | | | | | | | | | | | | | | | | | | | | | | | | | | | | | | | | | | | | | | | | | | | | | | | | | | | | | | | | | | | | | | | | | | | | | | | | | | | | | | | | | | | | | | | | | | | | | | | | | | | | | | | | | | | | | | | | | | | | | | | | | | | | | | | | | | | | | | | | | | | | | | | | | | | | | | | | | | | | | | | | | | | | | | | | | | | | | | | | | | | | | | | | | | | | | | | | | | | | | | | | |
| | | 2.4922 | | | | 5.3971 | 0.038 | | | | | | | | | | | | | | | | | | | | | | | | | | | | | | | | | | | | | | | | | | | | | | | | | | | | | | | | | | | | | | | | | | | | | | | | | | | | | | | | | | | | | | | | | | | | | | | | | | | | | | | | | | | | | | | | | | | | | | | | | | | | | | | | | | | | | | | | | | | | | | | | | | | | | | | | | | | | | | | | | | | | | | | | | | | | | | | | | | | | | | | | | | | | | | | | | | | | | | | | | | | | | | | | | | | | | | | | | | | | | | | | | | | | | | | | | | | | | | | | | | | | | | | | | | | | | | | | | | | | | | | | | | | | | | | | | | | | | | | | | | | | | | | | | | | | | | | | | | | |
| | | 4.0994 | | | | | | | | | | | | | | | | | | | | | | | | | | | | | | | | | | | | | | | | | | | | | | | | | | | | | | | | | | | | | | | | | | | | | | | | | | | | | | | | | | | | | | | | | | | | | | | | | | | | | | | | | | | | | | | | | | | | | | | | | | | | | | | | | | | | | | | | | | | | | | | | | | | | | | | | | | | | | | | | | | | | | | | | | | | | | | | | | | | | | | | | | | | | | | | | | | | | | | | | | | | | | | | | | | | | | | | | | | | | | | | | | | | | | | | | | | | | | | | | | | | | | | | | | | | | | | | | | | | | | | | | | | | | | | | | | | | | | | | | | | | | | | | | | | | | | | | | | | | | | | | | |
| | | 3.9962 | | | | | | | | | | | | | | | | | | | | | | | | | | | | | | | | | | | | | | | | | | | | | | | | | | | | | | | | | | | | | | | | | | | | | | | | | | | | | | | | | | | | | | | | | | | | | | | | | | | | | | | | | | | | | | | | | | | | | | | | | | | | | | | | | | | | | | | | | | | | | | | | | | | | | | | | | | | | | | | | | | | | | | | | | | | | | | | | | | | | | | | | | | | | | | | | | | | | | | | | | | | | | | | | | | | | | | | | | | | | | | | | | | | | | | | | | | | | | | | | | | | | | | | | | | | | | | | | | | | | | | | | | | | | | | | | | | | | | | | | | | | | | | | | | | | | | | | | | | | | | | | | |
| Procaine.HCl | 77 | 2.9352 2.2887 | - | - | - | 3.4826 | 0.371 | [18] | | | | | | | | | | | | | | | | | | | | | | | | | | | | | | | | | | | | | | | | | | | | | | | | | | | | | | | | | | | | | | | | | | | | | | | | | | | | | | | | | | | | | | | | | | | | | | | | | | | | | | | | | | | | | | | | | | | | | | | | | | | | | | | | | | | | | | | | | | | | | | | | | | | | | | | | | | | | | | | | | | | | | | | | | | | | | | | | | | | | | | | | | | | | | | | | | | | | | | | | | | | | | | | | | | | | | | | | | | | | | | | | | | | | | | | | | | | | | | | | | | | | | | | | | | | | | | | | | | | | | | | | | | | | | | | | | | | | | | | | | | | | | | | | | | | | | | | | | | |
| Tetracaine | 77 | 3.4010 | - | - | - | 4.1913 | 0.246 | [18] | | | | | | | | | | | | | | | | | | | | | | | | | | | | | | | | | | | | | | | | | | | | | | | | | | | | | | | | | | | | | | | | | | | | | | | | | | | | | | | | | | | | | | | | | | | | | | | | | | | | | | | | | | | | | | | | | | | | | | | | | | | | | | | | | | | | | | | | | | | | | | | | | | | | | | | | | | | | | | | | | | | | | | | | | | | | | | | | | | | | | | | | | | | | | | | | | | | | | | | | | | | | | | | | | | | | | | | | | | | | | | | | | | | | | | | | | | | | | | | | | | | | | | | | | | | | | | | | | | | | | | | | | | | | | | | | | | | | | | | | | | | | | | | | | | | | | | | | | | |
| | | 2.8860 | | | | 5.1930 | 0.0187 | | | | | | | | | | | | | | | | | | | | | | | | | | | | | | | | | | | | | | | | | | | | | | | | | | | | | | | | | | | | | | | | | | | | | | | | | | | | | | | | | | | | | | | | | | | | | | | | | | | | | | | | | | | | | | | | | | | | | | | | | | | | | | | | | | | | | | | | | | | | | | | | | | | | | | | | | | | | | | | | | | | | | | | | | | | | | | | | | | | | | | | | | | | | | | | | | | | | | | | | | | | | | | | | | | | | | | | | | | | | | | | | | | | | | | | | | | | | | | | | | | | | | | | | | | | | | | | | | | | | | | | | | | | | | | | | | | | | | | | | | | | | | | | | | | | | | | | | | | | |
| | | 3.9190 | | | | | | | | | | | | | | | | | | | | | | | | | | | | | | | | | | | | | | | | | | | | | | | | | | | | | | | | | | | | | | | | | | | | | | | | | | | | | | | | | | | | | | | | | | | | | | | | | | | | | | | | | | | | | | | | | | | | | | | | | | | | | | | | | | | | | | | | | | | | | | | | | | | | | | | | | | | | | | | | | | | | | | | | | | | | | | | | | | | | | | | | | | | | | | | | | | | | | | | | | | | | | | | | | | | | | | | | | | | | | | | | | | | | | | | | | | | | | | | | | | | | | | | | | | | | | | | | | | | | | | | | | | | | | | | | | | | | | | | | | | | | | | | | | | | | | | | | | | | | | | | | |
| | | 3.8705 | | | | | | | | | | | | | | | | | | | | | | | | | | | | | | | | | | | | | | | | | | | | | | | | | | | | | | | | | | | | | | | | | | | | | | | | | | | | | | | | | | | | | | | | | | | | | | | | | | | | | | | | | | | | | | | | | | | | | | | | | | | | | | | | | | | | | | | | | | | | | | | | | | | | | | | | | | | | | | | | | | | | | | | | | | | | | | | | | | | | | | | | | | | | | | | | | | | | | | | | | | | | | | | | | | | | | | | | | | | | | | | | | | | | | | | | | | | | | | | | | | | | | | | | | | | | | | | | | | | | | | | | | | | | | | | | | | | | | | | | | | | | | | | | | | | | | | | | | | | | | | | | |
| Tetracaine.HCl | 77 | 3.304 2.793 | - | - | - | 4.065 | 0.251 | [18] | | | | | | | | | | | | | | | | | | | | | | | | | | | | | | | | | | | | | | | | | | | | | | | | | | | | | | | | | | | | | | | | | | | | | | | | | | | | | | | | | | | | | | | | | | | | | | | | | | | | | | | | | | | | | | | | | | | | | | | | | | | | | | | | | | | | | | | | | | | | | | | | | | | | | | | | | | | | | | | | | | | | | | | | | | | | | | | | | | | | | | | | | | | | | | | | | | | | | | | | | | | | | | | | | | | | | | | | | | | | | | | | | | | | | | | | | | | | | | | | | | | | | | | | | | | | | | | | | | | | | | | | | | | | | | | | | | | | | | | | | | | | | | | | | | | | | | | | | | |

MDMA: 3,4-Methylenedioxy-methamphetamine; NQR: Nuclear quadrupole resonance; QCC: Quadrupole coupling constant.

Table 4. The differences in the NQR data (line width, relaxation time, NQR frequency) originating from defects, crystalline imperfections and for selected drugs and its complexes (continued)

| Drug | Nucleus | T (K) | Frequency (MHz) | Line width (Hz) | T ₁ | T ₂ | QCC | η | Ref. |
|---------------|---------|-------|-----------------|-----------------|----------------|----------------|-----|-------|------|
| Dibucaine | 77 | 2.041 | - | - | - | 3.127 | | 0.390 | [18] |
| | | 3.855 | | | | 5.204 | | 0.037 | |
| | | 3.034 | | | | 4.002 | | 0.032 | |
| | | 2.969 | | | | | | | |
| Dibucaine.HCl | 77 | 2.735 | - | - | - | 3.025 | | 0.366 | [18] |
| | | 2.140 | | | | 3.867 | | 0.072 | |
| | | 2.970 | | | | | | | |
| | | 2.830 | | | | | | | |

MDMA: 3,4-Methylenedioxy-methamphetamine; NQR: Nuclear quadrupole resonance; QCC: Quadrupole coupling constant.

been successfully applied for the detection of the presence of explosives and narcotics; moreover, of such compounds whose resonance frequencies ¹⁴N-NQR are in a certain range (68 – 70). ¹⁴N pure NQR offers an opportunity of quantitative identification of narcotic drugs such as cocaine [71-73], heroin [71,72], hashish, opium [72], 3,4-methylenedioxy-methamphetamine (ecstasy) [74], antitussive and antidiarrheal codeine and its phosphate [72], heroin monohydrate [72], as well as bacteriostatic, sympathicoplegic and coagulant drug urotropine (hexamethylenetetramine, HMT) [39,40], whereas ³⁵Cl pure NQR can be used to identify hydrochlorides [71,72] of these compounds (Table 4). Several special NQR techniques have been improved and applied, among which it is worth mentioning SQUID [52,53], NQR with the use of volume coils [54], field cycling methods [55-57] and different modifications of the double resonance NQR [46-51]. The inherent specificity of NQR is its extremely high sensitivity to local environment changes and weak interactions [8,75] (which is especially important in regard of the so-called added mass in drugs) and a possibility of remote [76,77], non-invasive and non-destructive detection [78]. These features suggest the applicability of NQR for the contactless detection of strongly toxic or carcinogenic substances.

The NQR spectra of ¹⁴N (spin I = 1) contain three lines assigned to each inequivalent nucleus, which seems sufficient for the identification of a compound (as yet, no compounds have been found for which the system of 3 lines, two of them independent and the one whose position depends on the positions of the other two (Equation 2), would be identical, but the number of compounds investigated by this methods is close to 2000). However, the NQR spectra of the nuclei ³⁵Cl, ⁷⁹Br, NQR (I = 3/2) contains only one line assigned to each inequivalent nuclei (Figure 4). Consequently, it is easy to find from among ~ 7000 compounds hitherto studied by ³⁵Cl-NQR [79], such compounds that give a single resonance line and whose frequencies at a given temperature are the same within the experimental error; for example, 35.004 and 35.006 MHz, for 1-chloro-4-[(phenylmethyl)thio]-benzene and [N-(3-chlorophenyl)benzenesulfonamido-N]phenyl-mercury, respectively [80]; 35.016 and 35.015 MHz for the 1:1 complex of 4-chloro-N,N,N-trimethyl-benzenaminium with

chloroacetic acid [81] and N-[4-chlorophenyl]-2,2,2-trifluoro-acetamide [82] and 4,6-dichloro-2-methyl-5-[phenylmethyl]-pyrimidine, respectively [83].

Besides the sometimes unreliable identification of compounds, another serious drawback of NQR is that it does not permit a determination of the chemical composition of a given compound, as the detectable components have to contain the quadrupole nuclei and the range of frequency scanning on a measurement is not large (~ 10 kHz for ¹⁴N and 100 kHz for ³⁵Cl); moreover, the search for the resonance lines is time consuming. However, attempts to use NQR frequency resonances for structure determinations of unknown compounds, although theoretically sound, have been rare and have been met with only qualitative success [84]. In the field of chemical composition determination the NQR method is not competitive to IR, UV or NMR.

4.1.2 Quality control

The extremely high sensitivity of NQR to local environment changes (e.g., due to impurities) [85] suggests its potential application for quality control in the chemical and pharmaceutical industries. Moreover, NQR measurements are characterized by high spectral resolution, precision and specificity, and NQR spectroscopy is highly sensitive to inhomogeneities and changes in the local environment – more sensitive than NMR or powder x-ray diffraction (PXRD). The differences in the line widths originating from defects and crystalline imperfections as well as the presence of impurities or even strain can be threefold (Table 4). Usually, recrystallization is applied to improve the SNR and to eliminate the impurities of a substance in solid phase. In extreme cases NQR measurements demand recrystallization of the sample to improve SNR.

By using NQR, it is relatively easy to detect the presence of impurities causing considerable line width broadening, but it is difficult to identify them. Because of the high sensitivity, the NQR method can be used not only for determination and monitoring of the purity of medical drugs, but as the intensity of the NQR signal is directly proportional to the number of equivalent nuclei and to the amount of a given substance, the

Table 5. ^{35}Cl NQR parameters for different polymorphic forms of drugs.

| Compound | Phase I | | | | Phase II | | Phase III | | | | No. polymorphs | T (K) | Ref. |
|-----------------|-------------|------------------|---------------------|---------------------|-------------|-------------|------------------|---------------------|---------------------|---|----------------|-------|------|
| | Freq. (MHz) | Line width (kHz) | T ₁ (ms) | T ₂ (μs) | Freq. (MHz) | Freq. (MHz) | Line width (kHz) | T ₁ (ms) | T ₂ (μs) | | | | |
| Chloral hydrate | 39.806 | - | - | - | 39.4330 | - | - | - | - | 2 | 77 | [88] | |
| | 39.769 | | | | 38.1894 | | | | | | | | |
| | 39.450 | | | | 39.515 | | | | | | | | |
| | 39.302 | | | | 39.429 | | | | | | | | |
| | 39.184 | | | | 38.190 | | | | | | | | |
| | 39.131 | | | | | | | | | | | | |
| | 38.979 | | | | | | | | | | | | |
| | 38.946 | | | | | | | | | | | | |
| | 38.697 | | | | | | | | | | | | |
| | 38.530 | | | | | | | | | | | | |
| | 38.508 | | | | | | | | | | | | |
| | 38.498 | | | | | | | | | | | | |
| Diclofenac | 34.997 | - | - | - | 34.997 | - | - | - | - | 2 | RT | [86] | |
| | 35.269 | | | | 35.445 | | | | | | | | |
| Chlorpropamide | 34.325 | 18 | 3.5 | 720 | no data | 34.631 | 8 | 1.5 | 630 | 3 | RT | [86] | |

NQR: Nuclear quadrupole resonance; RT: Room temperature.

method can be applied for a fast and accurate measurement of the API concentration in a drug substance. The interest in this field of NQR application has been rather low. The tests that have been performed for chlorpropamide [86] and furosemide [87] have shown that the differences in measurements of API concentration by NQR and by mass do not exceed 5%.

4.1.3 Polymorphism

It is well known that NQR permits an easy identification of the number of crystallographically inequivalent molecules in the unit cell on the basis of the number of peaks for each nucleus [23]. Because different polymorphic forms of a crystal have different crystal lattices the polymorphs can be easily identified and their contribution can be accurately evaluated.

There are a number of methods that can be used to characterize polymorphs of a drug substance [7], but the single crystal X-ray diffraction (XRD) is presently regarded as the definitive evidence of polymorphism. In many cases NQR can be much more effective. In contrast to XRD, the NQR method can be applied even to amorphous material after freezing in liquid nitrogen, although it is not easy because of great line widths. Unfortunately, only a few authors have discussed the NQR spectroscopy application for revealing and characterization of polymorphism of drugs [86,87] and from > 200 compounds whose polymorphism has been studied by this method [79] only 11 are drugs.

Results of the NQR study of different drugs known from the X-ray studies to exist in polymorphs are presented in Tables 5 and 6; the drugs include a sedative and hypnotic chloral hydrate (trichloroacetaldehyde monohydrate, 2,2,2-trichloro-1,1-ethanediol) [88] one of the oldest synthetic agents, anticancer and

chronic multiple sclerosis and schizophrenia drug glycine [89,90], bacteriostatic sulfapyridine (4-amino-*N*-pyridinylbenzene sulfonamide) [86,91], sulfanilamide, sulfadiazine, sulfamerazine, sulfamethazine and sulfathiazole [92], non-steroidal anti-inflammatory diclofenac (2-[2-(2,6-dichlorophenyl) aminophenyl] acetic acid) [86], anticancer chlorpropamide (1-(4-chlorophenyl)sulfonyl-3-propyl-urea) [86] or diuretic furosemide (4-chloro-2-furfurylamino-5-sulfamoyl-benzoic acid) [87]. Differentiation of the polymorphic forms of these compounds is not difficult because of distinct shift of the ^{35}Cl -NQR line; for example by 0.287 MHz for chloral hydrate, 0.176 MHz for and diclofenac and 0.306 MHz for chlorpropamide, whereas the ^{14}N -NQR line by, for example, 0.136 and 0.108 MHz for sulfapyridine, 0.555, 0.522, 0.410 and 0.693 MHz for sulfanilamide, 0.65, 0.425, 0.58 and 0.18 MHz for sulfamerazine, 0.23, 0.48, 0.42, 0.30, 0.10 and 0.08 MHz for sulfathiazole, 0.033 and 0.044 MHz for glycine and 0.142 MHz for FSE, at the accuracy of determination is not > 10 kHz (^{35}Cl NQR) and 1 kHz (^{14}N NQR) even for broad lines.

In addition, polymorphs are often readily identified on the basis of changes in the NQR line width (1.5 kHz for sulfapyridine, 10 kHz for chlorpropamide) or in the spin-lattice (sulfapyridine 70-fold, chlorpropamide 2-fold) or spin-spin (chlorpropamide 10%) relaxation times. The differences between the QCCs and asymmetry parameters are also significant (glycine, sulfanilamide, sulfamerazine, sulfathiazole).

NQR results suggest the polymorphism of the anticancer drug chloronafazine [93], *N,N*-bis(2-chloroethyl)-4-methyl-benzenesulfonamide and anesthetic lidocaine [57], although in their spectra the presence of additional resonance lines not resulting from the crystalline inequivalence had been explained by the presence of impurities.

Table 6. ¹⁴N-NQR parameters for different polymorphic forms of drugs.

| Compound | Phase I | | | Phase II | | | Phase III | | | No. polymorphs | T (K) | Ref. |
|--|-------------|-----------|--------|-------------|-----------|--------|-------------|-----------|--------|----------------|--------------|------|
| | Freq. (MHz) | QCC (MHz) | η: (-) | Freq. (MHz) | QCC (MHz) | η: (-) | Freq. (MHz) | QCC (MHz) | η: (-) | | | |
| Glycine | 1.100 | 1.257 | 0.501 | 1.133 | 1.317 | 0.440 | 1.044 | 1.244 | 0.3 | 3 | 77 | [89] |
| | 0.785 | | | 0.843 | | | 0.822 | | 57 | | | |
| | 0.315 | | | 0.290 | | | 0.222 | | | | | |
| | 0.705 | 1.129 | 0.501 | - | - | - | - | - | - | - | | [90] |
| Sulfapyridine (4-amino- <i>N</i> -pyridiny lbenzene sulfonamide) | 2.393 | - | - | 3.060 | - | - | - | - | - | 6 | RT | [86] |
| | 2.284 | | | 2.895 | | | | | | | | |
| | 2.924 | | | | | | | | | | | |
| | 2.787 | | | | | | | | | | | |
| | 2.917 | 3.553 | 0.284 | - | - | - | - | - | - | - | 77 | [91] |
| | 2.807 | 3.375 | 0.327 | | | | | | | | | |
| | 2.412 | | | | | | | | | | | |
| | 2.255 | | | | | | | | | | | |
| Sulfanilamide | 3.460 | 3.990 | 0.47 | 2.905 | 3.270 | 0.55 | | | | 5 | Form I | [92] |
| | 2.527 | 3.810 | 0.27 | 2.005 | 3.080 | 0.51 | | | | | 210 | |
| | 0.933 | | | 0.900 | | | | | | | Form II | |
| | 3.115 | | | 2.705 | | | | | | | 255 | |
| | 2.603 | | | 1.910 | | | | | | | | |
| | 0.512 | | | 0.790 | | | | | | | | |
| Sulfadiazine | 3.530 | 4.055 | 0.48 | | | | | | | many | 233 | [92] |
| | 2.555 | 3.616 | 0.34 | | | | | | | | | |
| | 0.975 | | | | | | | | | | | |
| | 3.015 | | | | | | | | | | | |
| | 2.405 | | | | | | | | | | | |
| | 0.610 | | | | | | | | | | | |
| Sulfamerazine | 3.440 | 3.950 | 0.48 | 2.790 | 3.230 | 0.45 | | | | 2 | Form I | [92] |
| | 2.485 | 3.670 | 0.31 | 2.060 | 3.160 | 0.11 | | | | | 295 | |
| | 0.955 | | | 0.730 | | | | | | | Form II | |
| | 3.040 | | | 2.460 | | | | | | | 183K | |
| | 2.460 | | | 2.280 | | | | | | | | |
| | 0.580 | | | 0.180 | | | | | | | | |
| Sulfamethazine | 3.763 | 4.435 | 0.39 | | | | | | | many | 233 | [92] |
| | 2.888 | 3.775 | 0.27 | | | | | | | | | |
| | 0.875 | | | | | | | | | | | |
| | 3.090 | | | | | | | | | | | |
| | 2.575 | | | | | | | | | | | |
| | 0.515 | | | | | | | | | | | |
| Sulfathiazole | 2.940 | 3.410 | 0.45 | 3.170 | 3.880 | 0.27 | | | | 2 | Form I | [92] |
| | 2.170 | 3.340 | 0.45 | 2.650 | 3.640 | 0.33 | | | | | 233 | |
| | 0.770 | 2.330 | 0.50 | 0.520 | 2.290 | 0.59 | | | | | [stable] | |
| | 2.880 | 2.180 | 0.56 | 3.30 | | | | | | | Form II | |
| | 2.130 | | | 2.430 | | | | | | | 233 | |
| | 0.750 | | | 0.600 | | | | | | | [metastable] | |
| | 2.040 | | | 2.050 | | | | | | | | |
| | 1.460 | | | 1.380 | | | | | | | | |
| | 0.580 | | | 0.670 | | | | | | | | |
| | 1.940 | | | | | | | | | | | |
| | 1.330 | | | | | | | | | | | |
| | 0.610 | | | | | | | | | | | |
| Furosemide | 3.564 | - | - | 3.422 | - | - | - | - | - | 6 | RT | [87] |
| | 3.561 | | | | | | | | | | | |

NQR: Nuclear quadrupole resonance; QCC: Quadrupole coupling constant; RT: Room temperature.

4.1.4 Thermal stability

Temperature studies of NQR frequencies provides information on the compounds stability, not only on the presence of polymorphic species, but also on the phase transitions (changes in the crystallographic structure and ordering). For many drugs, such as antiseptics used for the prophylaxis of urinary tract infections (urotropine [HMT]) or a local anaesthetic (chloral hydrate), the temperature dependence of NQR frequency has been studied more or less systematically [39,94,95], but not in the pharmaceutical context. Typical temperature changes in the NQR frequency [39] for HMT (axially symmetric EFG tensor, i.e., $\eta = 0$) are shown in Figure 5A, although typical temperature changes in the NQR frequency [96], QCC and asymmetry parameter, which unfortunately cannot be presented for drugs because of the scarcity of data, are exemplified in Figure 5B, for non-drug hexamethyltetramine (1,3,5,7-tetranitro-1,3,5,7-tetrazocyclooctane) produced by nitration of HMT in the presence of acetic anhydride, paraformaldehyde and ammonium nitrate.

Interesting results have been obtained for a diuretic drug applied to treat high blood pressure and heart failure, that is for hydrochlorothiazide (HCTZ). As follows from the results obtained for HCTZ, NQR was found to be much more sensitive to phase transitions than NMR or density functional theory (DTA) [38,97]. The anomalies in the temperature dependence of the ^{35}Cl -NQR frequency for HCTZ, the change in the line width (as a result of an increase in the spin-lattice relaxation time) (Figure 6), the small, but notable, changes in the slope and the jump in the frequency observed at 253 K, not exceeding 0.05 MHz, together with the lack of hysteresis (which distinguishes the first- and second-order transitions) indicated a second-order transition, not revealed by the temperature dependencies of the second moment or spin-lattice (NMR) and only weakly indicated by the results of DTA measurements [97].

Another interesting example of the ability of the molecular dynamic NQR studies are the results obtained for an intermediate chemical in the manufacture of a psychiatric drug – phenothiazine [98]. ^{14}N -NQR frequencies measured in both the low- and high-temperature phases show the presence of large thermal librations of the phenothiazine molecules in both crystallographic phases as well as an order-disorder phase transition associated with the reorientations of the phenothiazine molecules around the orthorhombic axis.

The results discussed in the analytical step section have illustrated the power of NQR as an analytical technique (i.e., the ability of NQR spectroscopy to identify compounds, characterize formulations, to differentiate and quantify polymorphic forms and to complement the information provided by other analytical techniques). When applied to polymorphism investigations, NQR spectra may prove to be an effective tool for preliminary study of crystal structure in the absence of detail X-ray data. Such parameters as spectroscopic shifts, multiplicity, spectroscopic splitting, resonance line width, the temperature dependence of resonance

frequencies and relaxation times afford useful structural information and provide insight into the factors determining the formation of certain structural types.

4.1.5 Other aspects of stability

The other aspects of stability concern the effects of ageing and include such processes as oxidation, exposure to water or decomposition. These processes can be observed with NQR spectroscopy. However, the attempts to do so have rarely been undertaken. It is known that NQR is suitable for the determination of the degree of ^{35}Cl release from a given pharmaceutical under the effect of UV irradiation, which is manifested as a decrease in the signal intensity or even as its disappearance (e.g., for furosemide). However, when the radicals formed undergo fast recombination changes in the NQR spectra are undetectable (e.g., for thiazides) and the hydration of a given compound, related to a change or a decrease in the resonance frequency, is usually observed as a decrease in the signal intensity or the lack of signal at the frequency at which it has been earlier observed.

4.2 Active pharmaceutical ingredient development stage

4.2.1 Search for active pharmaceutical ingredient analogs

To facilitate the process of drug development, in particular in the phase of the search for analogs (second- or third-generation drugs), new methods are being devised to predict biological activity of certain compounds on the basis of their structure and physical and chemical properties. It is known that a well-designed study narrows the search for the optimum molecule and permits the prediction of the possible efficacy or toxicity of a potential drug. NQR offers a unique possibility of determining QCC proportional to the effective charges on the atom containing the resonant nuclei and the atomic bond's population (only for spins $I = 1$). This information permits a conclusion about the redistribution of the electron density in the molecule taking place as a result of conformational changes, intramolecular interactions (i.e., electron effects [polarisation or delocalisation] or complexation).

4.2.2 Structure and conformation

NQR spectroscopy can be applied to provide detailed information on the structure and conformation of chemical compounds. The occurrence of a number of conformations often related to polymorphism is a very important problem from the point of view of drug development.

A good illustration of the problem is cisplatin *cis*-diamminedichloroplatinum (II), one of the most widely used and most effective cytotoxic agents in the treatment of epithelial malignancies such as lung, head and neck, ovarian, bladder and testicular cancers. Although cisplatin and its complexes are widely used as anticancer drugs, neither its isomer (transplatin) nor its complexes have therapeutic

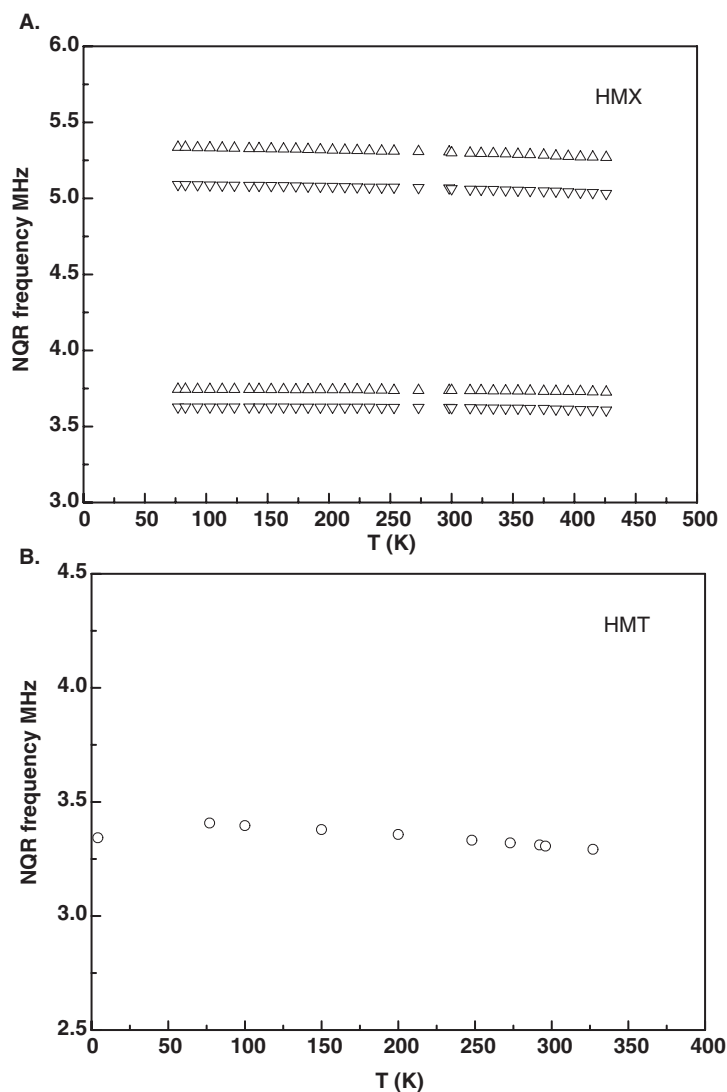


Figure 5. Temperature dependence of: A. frequency for HMT and B. frequencies, quadrupole coupling constants, asymmetry parameters for HMX.

HMT: Hexamethylenetetramine; HMX: Hexamethyltetramine; NQR: Nuclear quadrupole resonance.

properties. Possible explanations of the different biological activity of the *cis* and *trans* isomers are that *cis* compounds make platinum–DNA adducts inhibiting DNA replication or transcription to a greater extent than those formed by transplatin, and alternatively, that DNA adducts formed by *trans* compounds may be repaired more efficiently [99]. Thus, differentiation between the *cis* and *trans* isomers is essential. The ^{35}Cl -NQR permits their easy distinction. The difference in the resonance frequencies is evident and reaches as much as 2.13 MHz (16.18 MHz for *cis*-platinum and 18.31 MHz for *trans*-platinum [100]). Differences of the same order occur for all platinum compounds showing the *trans-cis* isomer trend.

Similarly, a good illustration of the differences in the biological activity of structurally similar compounds are two diuretic drugs (1,2,4-derivatives of benzothiadiazine), used to treat hypertension, congestive heart failure, symptomatic oedema and prevention of kidney stones, namely: chlorothiazide (CTZ) and hydrochlorothiazide (HCTZ). They differ only in one bond: in CTZ either the bond N(2)–C(3) or C(3)–N(4) is double, whereas in HCTZ one hydrogen atom occurs at N(2) and N(4) and the two bonds N(2)–C(3) and C(3)–N(4) are single. The appearance of the delocalization effect on coming from HCTZ to CTZ was found to be accompanied by a significant (1.26 MHz) increase in the QCC spectroscopic parameter, which

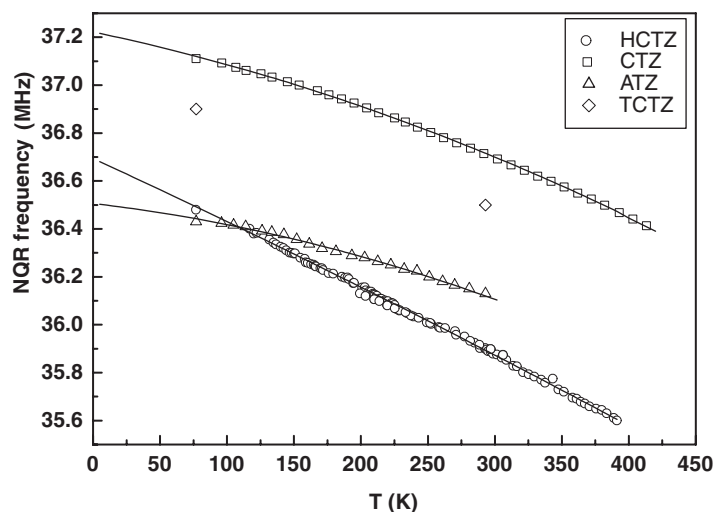


Figure 6. Temperature dependence of the NQR resonance frequency for HCTZ, CTZ, TCTZ and ATZ.

ATZ: Althiazide; CTZ: Chlorothiazide; HCTZ: Hydrochlorothiazide; NQR: Nuclear quadrupole resonance; TCTZ: Trichloromethiazide.

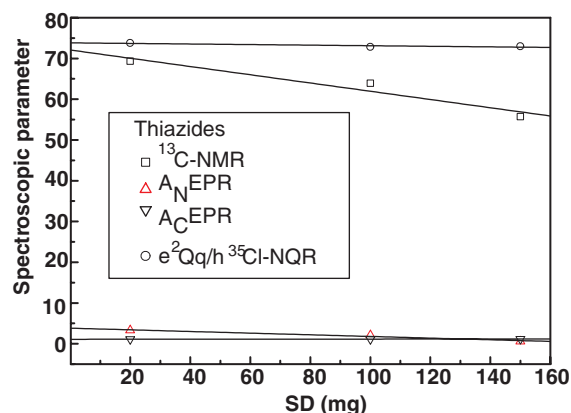


Figure 7. Correlation between the spectroscopic parameter describing the polarization effect and biological activity of thiazides.

EPR: Electron paramagnetic resonance; NQR: Nuclear quadrupole resonance; RT: Room temperature; SD: Single dose.

induces a significant increase in the single dose (from 25 – 150 mg to 1 – 2 g) and, thus, a drastic decrease in the biological activity [101]. Although HCTZ is widely used, the less-active CTZ is used in addition to furosemide to alter the mode of its activity.

5. An example of systematic studies – thiazides

As yet, systematic NQR studies of the correlation between structure and activity have only been performed for

diuretic thiazides (1,2,4-benzothiadiazine derivatives) used for the treatment of treat heart failure, liver cirrhosis, hypertension, certain kidney diseases, osteoporosis or even cancer [38,97,102-106]. The studies were prompted by the contrasting opinions on the electron density distribution and reactive sites in the thiazide molecules. Shinagawa *et al.* [107], related the biological activity of thiazides with the π -electron density on the nitrogen atoms N(2), N(4) and the carbon atom C(7), Wohl [108,109] thought that it was determined by the positive charge on the nitrogen atom N(4). The rotational symmetry of the substituent, according to Cragoe [2], was considered as a consequence of the hydrophobic properties of the substituent, according to Beyer [110] to chlorouretic properties of thiazides, according to Orita to the formal charge on the atom at C-7 [111] and according to Toplis to the parameters of the octanol–water division [112]. Theoretical works based on the results of calculations performed by simplified methods (Hückel method [108,109] and semiempirical CNDO/2 [111]) and only a few experimental reports on the physicochemical properties of thiazides (parameters of octanol–water division [111]) have been published. In the earlier review papers on thiazides [113-121] this problem was left unsolved and the authors emphasized that the mechanism of the thiazides activity was still unknown. In the papers published up until 1997, the diuretic activity of thiazides was related to the inhibition of carbonic anhydrase (CA) [113]. Later the diuretic properties of thiazides were linked to the reflux absorption of sodium and chlorine based on the inhibition of the 115-kDa protein (composed of 1021 amino acids) of the Na^+Cl^- co-transporter sensitive to thiazides (TSC, NCC or SLC12A3) [114,115]. In 1999, Chang [122,123]

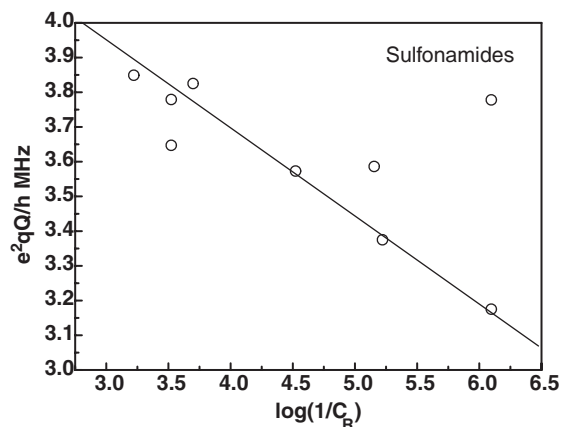


Figure 8. Correlation between quadrupole coupling constant and biological activity of sulfonamides.

SD: Single dose.

proposed a model explaining the diuretic activity of thiazides based on the activity of membranes assuming that thiazides compete with chlorine in the process of bond formation with the cotransporter Na^+Cl^- . It was experimentally proven [114] that the Na^+Cl^- co-transporter with a thiazide instead of chlorine cannot permeate through cell membranes. The Chang model, later developed by Lloyd [201], could not explain the way of bonding a thiazide with the Na^+Cl^- co-transporter. The problem seems important as, according to the recent literature reports, thiazides are successful in therapy of osteoporosis and the interest in them is growing [118,120,121].

Only a correlated spectroscopic and quantum-mechanical research [102] has permitted a comprehensive analysis of the electron density distribution and identification of the reactive sites in thiazide molecules. Lastly, it has been established that the biological activity of thiazides is determined by the electron density distribution in the region N(2)–C(3)–N(4), which has been concluded from the results of the ^{35}Cl -NQR experimental study on the chlorine atom at the position C(7) [103] and NMR on all carbon atoms [104] in the ground state, as well as electron paramagnetic resonance (EPR) in direct neighborhood of the radical (i.e., on the chlorine atoms N(2) and N(4), the chlorine atom from $-\text{CHCl}_2$ and C(3) from the radical [105]) and the density functional theory (DFT) calculations [106].

It was found that the delocalization effects decrease the biological activity of thiazides, whereas the inductive effects modify it (cause its decrease or increase depending on the substituent being an electron donor or acceptor) and the density changes of the free electron pair at N(4) play the most important role N(4) [103-106]. It is worth emphasizing that the changes in the ^{35}Cl QCC constant detected by NQR at the chlorine atom Cl(7) localized far from the substitution site show the same tendency as the changes in the chemical shifts

at C(6) and C(3) detected by ^{13}C P/MAS NMR and the changes in the isotropic hyperfine coupling constants at C(3) detected by EPR, but the ^{35}Cl -NQR spectroscopy is the most sensitive to the polarization (inductive) electronic effects.

As reported in [102] with an increasing single dose of the administered drug, (corresponding to its decreasing biological activity) the spectroscopic parameter describing the polarization effect also decreases. The same conclusion has been drawn irrespectively of the spectroscopic parameter analyzed: QCC, chemical shift, hyperfine coupling constants (Figure 7). Although the number of points presented in the figure illustrating the character of the dependence of spectroscopic parameters on the single dose is small (the small number of compounds studied), the tendency is clear.

A sufficient support of the conclusion comes from the fact that analogous relationships have been obtained when analysing a correlation of the spectroscopic parameters determined by three different methods (NMR, EPR, NQR) with biological activity. The intercorrelation of the spectroscopic parameters for thiazides has been analyzed in detail on the basis of the spectroscopic theories and confirmed by DFT calculations [8,102]. As indicated by the results of a biological study, the weakest among the thiazides studied is CTZ, whereas the strongest diuretic is trichloromethiazide (TCTZ) with the electron-acceptor group $-\text{CHCl}_2$ at C(3), whose replacement by hydrogen (HCTZ) or $-\text{CH}_2-\text{SCH}_2=\text{CH}-\text{CH}_2$ (ATZ) significantly reduces its biological activity. The Parr reactivities determined for thiazides by the DFT method in [8] suggest the highest chemical reactivity of TCTZ and the lowest of CTZ, although the electronegativity calculated for TCTZ is close to that of a chlorine atom, which in the light of the Chang model explains the highest biological activity of TCTZ. The results given in [102] suggest that the source of the reactive electrons is the nitrogen atom N(4) and because of the type of radical formed following γ -irradiation, the most active site in the molecule is the carbon atom C(3) and these atoms play the main role in the process of the thiazide bonding with the Na^+Cl^- co-transporter.

The above example illustrates the potential of the NQR spectroscopy supported with the DFT calculations in drug investigation aimed at revealing the mechanisms of their action. Moreover, the detailed study of thiazides has indicated that the NQR spectroscopy is the most sensitive to electronic effects of the resonance methods applied [8].

6. Other examples

For a group of sulfonamides, a correlation between NQR data and their biological activity *in vitro* was found (Figure 8) [22]. It is supportive of the Seydel's conclusion [124,125] about a relation between the electronic properties of amine groups in anilines and the biological activity of sulfonamide prompted

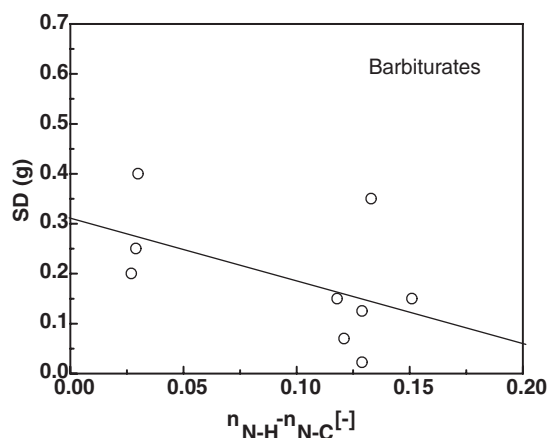


Figure 9. Correlation between the differences in nitrogen bond populations and biological activity of barbiturates.

by the correlation diagrams between the chemical shifts from the $^1\text{H-NMR}$ spectra and the biological activity [124]. Similar attempts were undertaken for anticancer drugs (nitrogen mustard derivatives). However, the number of compounds studied in this group have proven to be insufficient.

Although in the past, drugs other than sulfonamides (halogen derivatives of methane, barbiturates, bromide salts, derivatives of *p*-aminobenzoic acid, etc.) have been studied by NQR [11,12,15-18,125-129], a relationship between the electronic properties and the biological activity has been only recently discovered [130]. The toxicity of halons, expressed in the maximum admissible concentrations in mg/l for CCl_4 , chloroform, di- and monochloromethane was found to decrease with decreasing QCC obtained from $^{35}\text{Cl-NQR}$ spectra, except for chloromethane (which could be useful for the assessment of a halons toxicity). A similar correlation was found between the QCC determined from the spectra of $^{81}\text{Br-NQR}$ and the single doses expressed in grams for bromide salts. It is probable that the enhanced tolerance to a given bromide salt is related to an increasing QCC because the effectiveness of the bromide salts increased with growing QCC. Halons or bromide salts are compounds of simple chemical structure, but the structure-activity correlation observed for them proved valid also for more complex drugs such as derivatives of common amino amide-type local anaesthetics (derivatives of *p*-aminobenzoic acid) or anaesthetic, anticonvulsant and hypnotic barbiturates (5,5-bisubstituted derivatives of barbituric acid). The differences in the electron density of the free electron pair on the nitrogen and populations of nitrogen atom bonds determined from the $^{14}\text{N-NQR}$ data for *p*-aminobenzoic acid and barbiturates were found to be correlated with single doses *pro disi* as well as the toxicity LD_{50} in mg/kg. Particularly interesting results have been obtained [130] for derivatives of barbituric acid containing higher aliphatic or aromatic substituents, in which the extension of the chain leads to a decrease in the electric

density of the free pair and introduction of alkyl substituents causes a decrease in the population of the free pair of electrons and an increase in the population of the inequivalent bond of the nitrogen atom (Figure 9). The differences in the activity of barbital and phenobarbital, containing aliphatic and aromatic groups as substituents, are mainly a result of differences in the population of the inequivalent nitrogen atom.

These results suggest that the NQR parameter being significant from the point of view of drug activity is the QCC or the difference in the population of inequivalent atom bonds. However, it is not always possible to correlate the parameters obtained from NQR spectra with the data describing biological activity because of the lack of exact data on the latter. Fortunately, in some cases an increase or decrease in biological activity of some compounds (depending on the type of substituent) can be predicted by analyzing the distribution of electron density on the basis of the NQR data. For example, in the search for anticancerous drugs from the group of 4N derivatives of cytosine, the more effective will be those in which the aromatic substituents are strongly separated by a $-\text{CH}_2-\text{CH}_2$ chain [131], whereas the substitution at position 1H of imidazole, anticancerous through bacteriostatic activity depending on the substituents, leads to the redistribution of the electron density from the nitrogen atom $-\text{N}$ onto $-\text{NR}$ (where both N atoms are in the imidazole ring and its R is a substituent at the three-substituted nitrogen) [132]. On the basis of the results performed for two groups of compounds: 4N-derivatives of cytosine and 1H derivatives of imidazole it was found that redistribution of π -electron density caused by a change in the substituent led to a change in biological activity of the compounds.

As shown in [8] the results of these studies can be generalized not only for drugs, but for other biologically active systems as well.

7. Drug-ligand interaction

Many drugs occur in the form of complexes, mainly with HCl because salts of HCl are easily dissolved in the stomach and intestine media. On the basis of the NQR spectra it is easy to discern if a given drug occurs as a complex or not (Table 4). The complexation with HCl, H_2O or H_3PO_4 leads to a characteristically significant decrease in the resonance frequency $^{14}\text{N-NQR}$ [71,72] as a result of the nitrogen atom protonation. The effect of complexation is also manifested in the NQR parameters: a decrease in QCC and an increase in the asymmetry parameter. Moreover, the complexation with HCl results in the appearance of the $^{35}\text{Cl-NQR}$ resonance line in the low-frequency range. These features suggest the possible application of NQR for structural characterizations of drug-ligand complexes, which can be helpful in understanding the drug-target interactions.

Another striking example of NQR application is the direct observation of the Zn^{2+} in CA, the first enzyme recognized to have a biological function for Zn^{2+} , which was

postulated as the activator of bound H₂O. Commonly occurring in all mammalian tissues, plants, algae and bacteria, CA is perhaps one of the best-recognised metalloproteins, although the mechanism of action assumed hitherto for human CA has been proven to be incorrect. The ⁶⁷Zn QCC values, being sensitive to changes in the structure and bonding associated with water or hydroxide have been found independent of pH over the range of 5 – 8.5 [133], whereas, according to the hitherto assumed model, Zn²⁺ should be coordinated by H₂O, and as a result, the ⁶⁷Zn-NQR spectrum should be three- to five-times broader than that at pH 8.5. This observation is contradictory to the accepted mechanism, but consistent with an alternative mechanism proposed by Merz *et al.* [134]. The above example demonstrates the significance of zinc NQR spectroscopy in delineating the structure and action mechanism of this class of metalloproteins.

The examples of the structure–activity correlation in a broad sense presented in the section on API development have shown the applicability of NQR in the search for other optimal drugs from the same class at atomic resolution and in the investigation of the molecular mechanism of drug activity or drug resistance. The advantage of the NQR method over other spectroscopies has been particularly well illustrated by the results obtained for thiazides.

8. Advantages and disadvantages of nuclear quadrupole resonance for drug investigation

Pure NQR spectroscopy has a large number of merits making it an useful analytical technique for drug investigation, namely it is: i) highly specific with regard to the chemical and crystalline form of a substance; ii) non-destructive; iii) quantitative; iv) focused on a specific nucleus; v) capable of detecting compounds heterogeneously distributed over large volumes; vi) able to yield results quickly (in favorable cases) as it does not need sample preparation; vii) sensitive to the presence of impurities in the sample; viii) temperature dependent on NQR results; ix) not limited by the requirement of an extreme magnetic field (as is the case with other magnetic resonance techniques); x) relatively inexpensive (does not need reagents) and xi) non-invasive.

Some of these advantages (i – viii) are simultaneously restricted from other points of view. In general, the most important restrictions of NQR as an analytical method for drug investigation include: i) the possibility of measurements in the solid phase only; ii) the necessity for the use of large samples (many grams or tens of grams) of the compound studied; iii) very low SNR, which requires the use of accumulation and methods of sensitivity enhancement (especially for ¹⁴N); iv) time consuming (especially when looking for the unknown NQR transition frequencies); v) possibility of interferences (NQR signal is somewhat above the conventional AM radio band); vi) the occurrence of spurious signals (due to piezoelectric responses as well as ‘acoustic ringing’ effects due

to certain metals and metal coatings); vii) the fact that it is a non-imaging technique as QRI is still in the laboratory test phase and viii) temperature dependence on NQR results.

Although the specificity of NQR is a major advantage over other spectroscopic methods, the NQR signal is very weak in comparison with the thermal noise, which is not observed in any other magnetic resonance spectroscopies. In view of the above, attempts have been undertaken to develop the techniques of sensitivity enhancement [52-73,135-140] and effective detection of the NQR signals, which should lead to a wider use of NQR as a modern analytical method for the investigation of a greater variety of substances.

9. Expert opinion

Pharmaceutical scientists have been using several analytical techniques, sometimes providing unsatisfactory or contradictory information and, hence, they have been continuously looking for new more reliable research tools. It seems that the NQR spectroscopy can soon become such a tool, despite the fact that its application in drug development studies definitely has a short history. Although in some fields, such as that of chemical composition determination, the NQR method is not competitive with IR, UV or NMR, in many others it can be successfully applied and is more sensitive than NMR, EPR or PXRD. Using this highly sensitive technique, researchers can obtain more accurate information than by using any other magnetic resonance methods. Moreover, NQR, being highly sensitive to subtle changes in electron density distribution, provides diverse information on the structural and chemical properties of drugs.

From this review, it is evident that NQR is a sophisticated, non-destructive, valuable analytic technique for studying pharmaceuticals, which can be applied at two main steps of drug development: analysis and the search for drug analogs.

NQR spectroscopy can readily detect and identify drugs, distinguish conformers, isomers, polymorphic and amorphous forms, reveal polymorphic transitions or phase transitions. Moreover, NQR data in combination with DFT calculations can be helpful in searching for new drugs from the same class (second- or third-generation drugs) and for explaining the molecular mechanism of the drug activity. A good illustration of the NQR possibilities in this direction of research is the investigation of thiazides.

In view of the widespread occurrence of nitrogen in pharmaceuticals, the ¹⁴N-NQR spectroscopy should be of particular interest in studying electron density distribution, molecular reorientations and intermolecular time-dependent interactions. It seems that such studies will acquire more and more importance in future and will be more and more frequent, especially after the improvements to the NQR technique in terms of sensitivity, speed and ease of use have been made. The reason for the present relatively limited practical application of NQR in pharmacy seems to lie in the lack of sufficiently sophisticated equipment.

Bibliography

- BUGAY DE: Solid-state nuclear magnetic resonance spectroscopy: theory and pharmaceutical applications. *Pharm. Res.* (1993) **10**:317-327.
- BYRN S, PFEIFFER R, GANEY M, HOIBERG C, POOCHIKIAN G: Pharmaceuticals solids, a strategic approach to regulatory considerations. *Pharm. Res.* (1995) **12**:945-954.
- US GOVERNMENT: 6A specifications, test procedures and acceptance criteria for new drug substances and new drug products, chemical substances. *Federal Register* (2000) **65**(251):83041-83063.
- NO AUTHORS LISTED: Q3A[®] impurities in new drug substances, Q3C impurities: residual solvents, and Q6A Specifications: test procedures and acceptance criteria for new drugs. *Federal Register* (2003) **68**(68):6924-6925.
- URAKAMI K: Characterization of pharmaceutical polymorphs by isothermal calorimetry. *Curr. Pharm. Biotechnol.* (2005) **6**:193-203.
- HALEBLIAN JK: Characterization of habits and crystalline modification of solids and their pharmaceutical applications. *J. Pharm. Sci.* (1975) **64**:1269-1288
- BRITTAİN H: Methods for the characterization of polymorphs and solvates. In: *Polymorphism in Pharmaceutical Solids*. Marcel Dekker, Inc., New York, USA (1999):227-278.
- LATOSINSKA JN: A correlation of spectroscopic parameters from different magnetic resonance spectroscopies for thiazides. A study by NQR, NMR, EPR and DFT methods. *Chem. Phys. Lett.* (2004) **398**:324-329.
- DEHMELT HG, KRUGER H: Quadrupol-resonanzfrequenzen von Cl- und Br-kernen in kristallinem dichloräthylen und methylbromid. *Z. Physik* (1951) **129**:401-415
- POLESHCHUK OK, LATOSINSKA JN: Magnetic resonance: nuclear quadrupole resonance, applications. In: *Encyclopedia of spectroscopy and spectrometry (volume 2)*. Lindon JC, Tranter GE, Holmes JL (Eds), Academic Press, London, UK (1999):1653-1662.
- LIVINGSTONE R: Pure quadrupole spectra: the substituted methanes. *J. Chem. Phys.* (1951) **19**:1434.
- LIVINGSTONE R: Pure quadrupole spectra of solid chlorine compounds. *J. Phys. Chem.* (1953) **57**:496-201.
- ALLEN HC: Pure quadrupole spectra of molecular crystals. *J. Phys. Chem.* (1953) **57**:501-504.
- GUTOWSKY HS, MCCALL DW: Temperature dependence of the chlorine pure quadrupole resonance frequency in molecular crystals. *J. Chem. Phys.* (1960) **32**:548-552.
- SMIRNOV NI, VOLKOV AF: *Teor. EkspKhim.* (1970) **13**:88.
- KUME Y, NAKAMURA D: *J. Magn. Reson.* (1976) **21**:235.
- KIM NS, BRAY PJ: ¹⁴N nuclear quadrupole resonance in the barbiturates. *Phys. Lett. A.* (1977) **60A**:483-486.
- BUESS ML, BRAY PJ: ¹⁴N NQR study of some local anesthetics. *Org. Magn. Reson.* (1984) **22**:233-236.
- HIYAMA Y: Multinuclear quadrupole resonance studies of biological systems. *Zeit. Naturforsch. A* (1984) **22**:273-292.
- LITZISTORF G, SENGUPTA S, LUCKEN EAC: *J. Magn. Reson.* (1981) **42**:307-311.
- SEMIN GK, RAEVSKII AM, KUZNETSOV SI: *Izv. Akad. Nauk SSSR. Ser. Fiz.* (1985) **49**:1402-1411.
- SUBBARAO SN, BRAY PJ: Correlation of carbonic anhydrase inhibitory activities of benzenesulfonamides with the data obtained by use of nitrogen-14 nuclear quadrupole resonance. *J. Med. Chem.* (1979) **22**:111-114.
- STONE NJ: Table of nuclear magnetic dipole and electric quadrupole moments. *Data Nucl. Data Tables* (2005) **90**:75-176.
- DAS TP, HAHN EL: *Nuclear quadrupole resonance spectroscopy, solid state physics (Suppl. 1)*. Academic Press, New York, USA (1958).
- LUCKEN EAC: *Nuclear quadrupole coupling constants*. Academic Press, London, UK (1969).
- SCHEMPP E, BRAY PJ: Nuclear quadrupole resonance spectroscopy. In: *Physical chemistry and advanced treatise (Volume 4)*. Academic Press, New York, USA (1970):521-632.
- WEISS A: Crystal field effects in NQR. In: *Topics in current chemistry, nuclear quadrupole resonance*. Davison A, Dewar MJS, Hafner K *et al.* (Eds), Springer-Verlag, Heidelberg, Berlin, Germany and New York, USA (1972) **30**:1-76.
- SELIGER J: Magnetic resonance: nuclear quadrupole resonance, theory. In: *Encyclopedia of spectroscopy and spectrometry (Volume 2)*. Lindon JC, Tranter GE, Holmes JL (Eds), Academic Press, London, UK (1999):1672-1680.
- SUITS BH: Nuclear quadrupole resonance spectroscopy. In: *Handbook of Applied Solid State Spectroscopy*. Vij DR (Ed.), Kluwer Scientific (2006).
- BERSOHN R: Nuclear electric quadrupole spectra in solids. *J. Chem. Phys.* (1952) **20**:1505-1509.
- COHEN MH: Nuclear quadrupole spectra in solids. *Phys. Rev.* (1954) **96**:1278-1284.
- HARBISON GS, SLOKENBERGS A, BARBARA TM: Two-dimensional zero-field nutation spectroscopy. *J. Chem. Phys.* (1989) **90**:5292-5298.
- NAGARAJAN V: Zeeman effect in NQR. *Curr. Sci. Jpn.* (1962) **31**:233-235.
- BAYER H: Zur Theorie der Spin-Gitterrelaxation in Molekülkristallen. *Z. Phys.* (1951) **130**:227-238.
- KUSHIDA T, BENEDECK GB, BLOEMBERGEN N: Dependence of the pure quadrupole resonance frequency on pressure and temperature. *Phys. Rev.* (1956) **104**:1364-1377.
- BROWN RJC: Temperature dependence of quadrupole resonance frequencies under constant pressure. *J. Chem. Phys.* (1960) **32**:116-118.
- YOON JG, KWUN SI, YU I: ¹⁴N-NQR in ferroelectric NaNO₂ single crystals. *J. Korean Phys. Soc.* (1988) **21**(3):304-308.
- LATOSINSKA JN, KASPRZAK J, UTRECHT R: Molecular dynamics of thiazides studied by ³⁵Cl-NQR spectroscopy. *Appl. Magn. Reson.* (2002) **23**:193-210.
- ALEXANDER S, TZALMONA A: Relaxation by slow motional processes. Effect of molecular rotations in pure quadrupole resonance. *Phys. Rev.* (1965) **138**:A845-A855.
- ALEXANDER S, TZALMONA A: Measurement of molecular rotation by N¹⁴ nuclear quadrupole resonance. *Phys. Rev. Lett.* (1964) **13**:546-547.
- PUSIOL DJ, BRUNETTI AH: Temperature dependence of the spin-lattice relaxation of ³⁵Cl nuclei in solid *p*-chlorobenzenesulphonyl chloride. *J. Phys. C. Solid State Phys.* (1984) **17**:4487-4491.
- SCHNEIDER J, WOLFENSON A, SCHÜRRER C, BRUNETTI A, DE O NUNES LA: Partial disorder and molecular motion of 4-chlorobiphenyl studied by ³⁵Cl

- NQR and Raman spectroscopy. *Phys. Rev. B* (1996) **53**:9045-9051.
43. MARICQ MM: Quasistationary state and its decay to equilibrium in the pulsed spin locking of a nuclear quadrupole resonance. *Phys. Rev. B* (1986) **33**:4501-4513.
 44. RUDAKOV TN, MIKHALTSEVICH VT: Steady-state free-precession in nitrogen-14 quadrupolar spin-system with axially symmetric electric field gradient tensor. *Chem. Phys. Lett.* (2000) **324**:69.
 45. KIM SS, JAYAKODY JRP, MARINO RA: Experimental investigations of the strong off-resonant comb (SORC) pulse sequence in ^{14}N NQR. *Z. Naturforsch.* (1992) **47a**:415-420.
 46. GRECHISHKIN VS, SINJAVSKY NJ: Local NQR in solid state. *Phys. Usp.* (1993) **163**:95-120.
 47. HARTMANN SR, HAHN EL: Nuclear double resonance in the rotating frame. *Phys. Rev.* (1962) **128**:2042-2053.
 48. LEPPELMEIER GW, HAHN EL: Nuclear dipole field quenching of integer spins. *Phys. Rev.* (1966) **141**:724-731.
 49. JONES EP, HARTMANN SR: Steady-state nuclear double resonance: an application to the study of the quadrupole resonances of K^{39} , K^{40} , and K^{41} in KClO_3 . *Phys. Rev.* (1972) **B6**:757-771.
 50. EDMONDS DT: Nuclear quadrupole double resonance. *Phys. Rep.* (1977) **C29**:233-290.
 51. SELIGER J, BLINC R, MALI M, OSREDKAR R, PRELESNIK A: Nuclear magnetic double resonance based on strong rf magnetic-field-induced coupling between spin systems. *Phys. Rev.* (1975) **B11**:27-36.
 52. HÜRLIMANN MD, PENNINGTON CH, FAN NQ, CLARKE J, PINES A, HAHN EL: Pulsed Fourier-transform NQR of ^{14}N with a dc SQUID. *Phys. Rev. Lett.* (1992) **69**:684-687.
 53. CONNOR C, CHANG J, PINES A: Magnetic resonance spectrometer with a dc SQUID detector. *Rev. Sci. Instrum.* (1990) **61**:1059-1063.
 54. GRECHISHKIN VS: Detection of NQR in explosives. *Rus. Phys. J.* (1993) **35**:637-640.
 55. REDFIELD AG: Pure nuclear electric quadrupole resonance in impure copper. *Phys. Rev.* (1963) **130**:589-585.
 56. SLUSHER RE, HAHN EL: Sensitive detection of nuclear quadrupole interactions in solids. *Phys. Rev.* (1968) **166**:332-347.
 57. IVANOV D, REDFIELD AG: Field-cycling method with central transition readout for pure quadrupole resonance detection in dilute systems. *J. Magn. Reson.* (2004) **166**:19-27.
 58. RUDAKOV TN: Magnetic resonance: nuclear quadrupole resonance, instrumentation. In: *Encyclopedia of spectroscopy and spectrometry (Volume 2)*. Lindon JC, Tranter GE, Holmes JL (Eds), Academic Press, London, UK (1999):1663-1671.
 59. LIAO MY, SUBRAMANIAN R, YUNG RL, HARBISON GS: Two and three dimensional nuclear quadrupole resonance in the investigation of structure and bonding. *Z. Naturforsch. A* (2000) **55**:29-36.
 60. ROBERT H, MINUZZI R, PUSIOL DJ: A fast method for the spatial encoding in rotating-frame NQR imaging. *J. Magn. Reson. A* (1996) **118**:189-194.
 61. CASANOVA F, ROBERT H, PUSIOL DJ: Mapping molecular orientation in solids by rotating-frame NQR techniques. *J. Magn. Reson.* (1998) **133**:129-133.
 62. ROBERT H, PUSIOL DJ: Fast NQR imaging with slice selection. *Z. Naturforsch.* (1996) **51a**:353-356.
 63. ROBERT H, PUSIOL D: Slice selection in NQR spatially resolved spectroscopy. *J. Magn. Reson.* (1996) **A118**:279-281.
 64. ROBERT H, MINUZZI R, PUSIOL DJ: A fast method for the spatial encoding in rotating-frame NQR imaging. *J. Magn. Reson. A* (1996) **118**:189-194.
 65. NICKEL P, ROBERT H, KIMMICH R, PUSIOL D: NQR method for stress and pressure imaging. *J. Magn. Reson.* (1994) **A111**:191-194.
 66. KIMMICH R, ROMMEL E, NICKEL P, PUSIOL D: NQR imaging. *Z. Naturforsch.* (1992) **47a**:361-366.
 67. SUITS BH, PLUDE GY: Gradient coils and NQR imaging of powders. *J. Magn. Reson. A* (1995) **117**:84-87.
 68. MARINO RA: Detection and identification of explosives by ^{14}N NQR. *New Concepts Symp. Workshop Detect. Identif. Explosives* (1978) 339-403.
 69. GARROWAY AN, BUSS ML, YESINOWSKI JP, MILLER JB: Narcotics and explosives detection by ^{14}N pure nuclear quadrupole resonance. *Proceedings of SPIE – The International Society for Optical Engineering* (1994) **2092**:318-327.
 70. GARROWAY AN, MILLER JB, ZAX DB, LIAO MY: A means for detecting explosives and narcotics by stochastic nuclear quadrupole resonance (NQR). *US Patent 5* (1997) **608**:321-324.
 71. YESINOWSKI JP, BUSS ML, GARROWAY AN, ZEIGEWIED M, PINES A: Detection of ^{14}N and ^{35}Cl in cocaine base and hydrochloride using NQR, NMR and SQUID techniques. *Anal. Chem.* (1995) **34**:2256-2263.
 72. GRECHISHKIN VS, YA SINYAVSKII N: New technologies: nuclear quadrupole resonance as an explosive and narcotic detection technique. *Phys. Usp.* (1997) **40**:393-403.
 73. GRECHISHKIN VS, KUTAIEVA IR: Double NQR and cross-relaxation spectroscopy of cocaine hydrochloride. *J. Struct. Chem.* (1996) **37**:686-687.
 74. BALCHIN E, MALCOLME-LAWES DJ, ROWE MD *et al.*: The unusual solid state structure of heroin hydrochloride monohydrate and its selective detection using NQR spectroscopy. *New J. Chem.* (2004) **28**:1309-1314.
 75. LIAO MY, HARBISON GS: Three-dimensional zero-field correlation spectroscopy: accurately measuring the hexadecapole coupling. *J. Chem. Phys.* (1994) **100**:1895-1901.
 76. GRECHISHKIN VS: Application of multipulse sequences in remote NQR. *J. Appl. Phys.* (1994) **58**:63-66.
 77. GARROWAY AN, BUSS ML, MILLER JB *et al.*: Remote sensing by nuclear quadrupole resonance. *IEEE Transactions on Geoscience and Remote Sensing* (2001) **39**:1108-1118.
 78. VIERKÖTTER SA, WARD CR, GREGORY DM, MENON SM, ROACH DP: NDE of composites via quadrupole resonance spectroscopy. *Proceedings of SPIE* (2003) **5046**:176-184.
 79. CHIHARA H, NAKAMURA N: *NQR spectroscopy data in landolt-boernstein new series III*. Madelung O (Ed.), Springer, Berlin, Germany (1982 – 1997):495.
 80. SEMIN GK, BABUSHKINA TA, YAKOBSON GG: *Nuclear Quadrupole Resonance in Chemistry*. John Wiley & Sons (1975):495.
 81. NOWAK N, PIES W, WEISS A: *Proceedings of the International Symposium*

- on NQR/NQI Spectroscopy 2nd. (1971) 5:165.
82. WIGAND S, ASAJI T, IKEDA R, NAKAMURA D: Reorientational motion of trihalomethyl groups in organic compounds as studied by chlorine-35 NQR and fluorine-19 NMR spectroscopy. *Z. Naturforsch* (1992) **47a**:265-273.
 83. DEWAR MJS, LUCKEN EAC: Chemical applications of nuclear quadrupole resonance spectroscopy. Part I. Some chloro-derivatives of nitrogen heterocycles. *J. Chem. Soc.* (1958) 3:2653-2658.
 84. KOZIMA K, SAITO S: Nuclear quadrupole resonance of dichlorocyclohexanone. *J. Chem. Phys.* (1959) **31**:560-561.
 85. JUNG JK, SEO YM, CHOH SH: Characteristics of impurity effects in isomorphous crystals and anisomorphous mixtures observed by ¹⁴N nuclear quadrupole resonance. *J. Chem. Phys.* (1999) **110**:3913-3918.
 86. BALCHIN E, MALCOLME-LAWES DJ, POPLETT IJF, SMITH MJAS, PEARCE GES, WREN SAC: Potential of nuclear quadrupole resonance pharmaceutical analysis. *Anal. Chem.* (2005) **77**:3925-3930.
 87. PEREZ SC, CERIONI L, WOLFENSON AE, FAUDONE S, CUFFINI SL: Utilization of pure nuclear quadrupole resonance spectroscopy for the study of pharmaceutical crystal forms. *Int. J. Pharm.* (2005) **298**:143-152.
 88. BIEDENKAPP D, WEISS A: *Z. Naturforsch.* (1967) **A22**:1124-1133.
 89. EDMONDS DT, SUMMERS CP: Quadrupole resonance of ¹⁴N and ²D in glycine a model compound. *Chem. Phys. Lett.* (1976) **41**:482-485.
 90. RABBANI SR, EDMONDS DT, GOSLING P, PALMER MH: Measurement of the ¹⁴N quadrupole coupling constants in glycine, diglycine, triglycine, and tetraglycine and a comparison with calculation. *J. Magn. Reson.* (1987) **72**:230-237.
 91. SUBBARAO SN, BRAY PJ: Correlation of nitrogen-14 nuclear quadrupole resonance data in sulfanilamides with the *in vitro* activities. *Org. Magn. Reson.* (1981) **15**:307-310.
 92. BLINC R, SELIGER J, ZIDANSEK A, ZAGAR V, MILIA F, ROBERTS H: ¹⁴N nuclear quadrupole resonance of some sulfa drugs. *Solid State NMR* (2006) **30**:61-68.
 93. HOOPER HO, BRAY PJ: Induction studies in several groups of halogen-containing organic compounds by their Cl³⁵, Br⁷⁹, or Br⁸¹ pure quadrupole resonance spectra. *J. Chem. Phys.* (1960) **33**:334-361.
 94. MACKOWIAK M: Multidimensional NQR spectroscopy – a new tool in studies of molecular dynamics. *Acta Physica Polonica A* (2006) **108**:61-72.
 95. SINYAVSKY N, MACKOWIAK M, BLUMICH B: Two-dimensional exchange Cl NQR spectroscopy of chloral hydrate. *Z. Naturforsch.* (2002) **57a**:53-57.
 96. LANDERS AG, BRILL TB, MARINO RA: ¹⁴N nuclear quadrupole resonance study of mechanism of the β-δ-HMX phase transition. *J. Phys. Chem.* (1981) **85**:2618-2623.
 97. LATOSINSKA JN, LATOSINSKA M, UTRECHT R, MIELCAREK S, PIETRZAK J: Molecular dynamics of solid benzothiadiazine derivatives (thiazides). A study by NMR, DTA and DFT methods. *J. Mol. Struct.* (2004) **694**:211-277.
 98. ZAGAR V, SELIGER J: ¹⁴N nuclear quadrupole resonance study of the structural phase transition in phenothiazine. *J. Phys. Condens. Matter* (1994) **6**:6027-6033.
 99. JOHNSON NP, LAPETOULE P, RAZAKA H, VILLANI G: *Biochemical mechanisms of platinum antitumor drugs*. McBrien DC, Slatter T (Eds), IRL Press, Oxford, UK (1986):1-28.
 100. PATTERSON HH, TEWKSBUURY JC, MARTIN M *et al.*: Luminescence, absorption, MCD and NQR study of *cis* and *trans* isomers of dichlorodiammineplatinum (II) *Inorg. Chem.* (1981) **20**:2297.
 101. ARANDJELOVIC S, TESIC Z, JURANIC Z *et al.*: Antiproliferative activity of some *cis/trans*-platinum(II) complexes on HeLa cells. *J. Exp. Clin. Cancer Res.* (2002) **21**:519-526.
 102. LATOSINSKA JN: Structure–activity study of thiazides by magnetic resonance methods (NQR, NMR, EPR) and DFT calculations. *J. Mol. Graph. Modell.* (2005) **23**:329-337.
 103. LATOSINSKA JN: Electronic structure of thiazides studied by ³⁵Cl-NQR spectroscopy and DFT calculations. *Magn. Reson. Chem.* (2003) **41**:395-405.
 104. LATOSINSKA JN: ¹³C CP/MAS NMR and DFT studies of thiazides. *J. Mol. Struct.* (2003) **646**:211-225.
 105. LATOSINSKA JN, PIETRZAK J: EPR study of free radicals in γ-irradiated thiazide compounds. *Appl. Magn. Reson.* (2004) **26**:345-336.
 106. LATOSINSKA JN: Studies of thiazide compounds in terms of the density functional theory. *Int. J. Quantum Chem.* (2003) **91**:339-349.
 107. SHINAGAWA Y, SHINAGAWA Y: A quantum pharmacological study on diuretics. *Int. J. Quantum Chem. Quantum Biol. Symp.* (1974) **1**:169-178.
 108. WOHL A: Electronic molecular pharmacology: the benzothiadiazine antihypertensive agents. I. Pharmacological aspects of tautomerism and conformation. *Mol. Pharm.* (1970) **6**:189-194.
 109. WOHL A: Electronic molecular pharmacology: the benzothiadiazine antihypertensive agents. II. Multiple regression analyses relating biological potency and electronic structure. *Mol. Pharm.* (1970) **6**:195-205.
 110. BEYER KH, BAER JE: Physiological basis for the action of newer diuretic agents. *Pharm. Rev.* (1961) **13**:517-562.
 111. ORITA Y, ANDO A, YAMABE S, NAKANISHI T, ARAKAWA Y, ABE H: *Arzneim. Forsch. Drug Res.* (1983) **33**:688-691.
 112. TOPLISS JG, YUDIS MD: Correlation of antihypertensive activity with structure in a series of 2*H*-1,2,4-benzothiadiazine 1,1-dioxides using the substituent constant approach. *J. Med. Chem.* (1972) **15**:394-400.
 113. KLEEMAN A, ENGEL J, KUTSCHER B, REICHERT D: *Pharmaceutical substances, synthesis, patents, applications*. Thieme, Stuttgart, Germany and New York, USA (1995).
 114. MOUNT DE, DELPIRE E, GAMBA G *et al.*: The electroneutral cation-chloride cotransporters. *J. Exp. Biol.* (1998) **201**:2091-2102.
 115. OBERMULLER N, BERNSTEIN P, VELASQUEZ H *et al.*: Expression of the thiazide-sensitive Na–Cl cotransporter in rat and human kidney. *Am. J. Physiol.* (1995) **269**:900-910.
 116. PUSCAS I, COLTAU M, BACAIN M, PASCA R, DOMUTA G: The inhibitory effect of diuretics on carbonic anhydrases.

- Res. Commun. Mol. Pathol. Pharmacol.* (1999) :105: 213-236.
117. SEBASTIAN A: Thiazides and bone. *Am. J. Med.* (2000) **109**:427-430.
118. SEBASTIAN A: Effect of low dose thiazide diuretics on plasma lipids : results from double blind, randomized clinical trial. *Harv. Heart Lett.* (2001) **6**:11.
119. STOELTING RK: *Antihypertensive drugs: pharmacology and physiology in anesthetic practice.* Lippincott-Raven Publishers (1999):302-312.
120. KAMEL HK, LACROIX AZ, OTT SM: Low-dose thiazide and bone density. *Ann. Intern. Med.* (2002) **136**:252-253.
121. LACROIX AZ, OTT SM, ICHIKAWA L, SCHOLES D, BARLOW WE: Low-dose hydrochlorothiazide and preservation of bone mineral density in older adults: a randomized, double-blind, placebo-controlled trial. *Ann. Intern. Med.* (2000) **133**:516-526.
122. CHANG CH, FUJITA T: A numerical model of the renal distal tubule. *Am. J. Phys. Renal Physiol.* (2001) **281**:222-243.
123. CHANG H, FUJITA T: A kinetic model of the thiazide-sensitive Na-Cl cotransporter. *Am. J. Phys. Renal Physiol.* (1999) **276**:952-959.
124. SEYDEL JK, SCHAPER KJ: *Chemische struktur und biologische aktivität von wirkstoffen.* Verlag Chemie, Weinheim, Germany (1979):359.
125. MILLER GJ, DOUKAS PH, SEYDEL JK: Structure-activity relationships between antibacterial activities and physicochemical properties of sulfonamides. *J. Med. Chem.* (1972) **15**:700-706.
126. BRAY PJ, MULKERN RV, GREENBAUM SG: ¹⁴N NQR in substituted isatin compounds. *Magn. Reson. Chem.* (1985) **23**:801-804.
127. GREENBAUM SG, BRAY PJ: ¹⁴N nuclear quadrupole resonance in weakly paramagnetic organic dye cations. *J. Magn. Reson.* (1981) **44**:189-192.
128. BRAY PJ, GREENBAUM SG: Pulsed NQR studies of electron distributions in organic molecules. *J. Mol. Struct.* (1982) **83**:35-38.
129. BRAY PJ, GREENBAUM SG: ¹⁴N nuclear quadrupole resonance in carcinostatic phosphamides. *Phys. Lett.* (1980) **75A**:438-440.
130. LATOSINSKA JN: Nuclear quadrupole resonance spectroscopy in studies of biologically active molecular systems – a review. *J. Pharm. Biomed. Anal.* (2005) **38**:557-587.
131. LATOSINSKA JN, SELIGER J, GRECHISHKIN V: NMR-NQR double resonance study of the electronic structure of 4*N*-cytosine derivatives. *Magn. Reson. Chem.* (1999) **37**:881-884.
132. LATOSINSKA JN, SELIGER J, NOGAJ B: Electron density distribution in 2-nitro-5-methylimidazole derivatives studied by NMR-NQR double resonance. *Magn. Reson. Chem.* (1999) **37**:878-881.
133. LIPTON AS, HECK RW, ELLIS PD: Solid-state NMR spectroscopy of human carbonic anhydrase: implications for the enzymatic mechanism. *J. Am. Chem. Soc.* (2004) **126**:4735-4739.
134. MERZ KM, HOFFMANN R, DEWAR MJS: The model of action of carbonic anhydrase. *J. Am. Chem. Soc.* (1989) **111**:5636-5649.
135. JAKOBSSON A, MOSSBERG M, ROWE MD, SMITH JAS: Exploiting temperature dependency in the detection of NQR signals. *IEEE Transactions on Signal Processing* (2006)**54**:1610-1616.
136. PIRNAT J, TRONTEJL Z: Correlation-based method form improvement NQR signals utilising signal shape information. *Appl. Magn. Reson.* (2004) **27**:343-357.
137. MIKHALTSEVITCH VT, RUDAKOV TN, FLEXMAN JH, HAYES PA, CHISHOLM WP: Multipulse sequences for explosives detection by NQR under conditions of magnetoacoustic and piezoelectric ringing. *Appl. Magn. Reson.* (2004) **25**:449-467.
138. JACOBSSON A, MOSSBERG M, ROWE M, SMITH MD: Frequency-selective detection of nuclear quadrupole resonance signals frequency-selective approximate maximum-likelihood (FSAML) detector. *IEEE Transactions on Geoscience and Remote Sensing* (2005) **43**:2659-2666.
139. WANG J-H, LIAO M-Y: Sensitivity-enhanced nuclear quadrupole correlation spectroscopy: application of single transition operators in nuclear quadrupole resonance of half-integer nucleus. *J. Chem. Phys.* (2002) **116**:3270-3276.
140. POLETTI GE, OSAN TM, PUSIOL DJ: Pulsed N-14 NQR device designed to detect substances in the presence of environmental noise. *Hyperf. Inter.* (2004) **159**:127-130.

Website

201. http://www.cellml.org/examples/repository/c hang_model_1999_doc.html
CellML webiste (2004).

Affiliation

Jolanta N Latosinska
Adam Mickiewicz University, Institute of Physics,
Umultowska 85, 61-614 Poznan, Poland
Tel: +48 61 829 5277; Fax: +48 61 825 7758;
E-mail: Jolanta.Latosinska@amu.edu.pl

APPLICATIONS OF NUCLEAR QUADRUPOLE RESONANCE SPECTROSCOPY TO METAL COMPLEXES

THEODORE L. BROWN

School of Chemical Sciences, University of Illinois, Urbana, Illinois 61801 (U.S.A.)

ABSTRACT

Nuclear quadrupole resonance (NQR) spectroscopy provides information on the ground state charge distribution about a quadrupolar nucleus, because the NQR spectrum is determined by the components of the electric field gradient (EFG) tensor. Metal complexes may be studied via NQR methods by observation of the spectra of quadrupolar metal nuclei. Interpretation of the data in terms of metal-ligand interactions is often difficult because of the large number of counterbalancing contributions. The NQR spectra of ligand nuclei can often provide a more direct access to details of the metal-ligand bonding. It has recently become possible to study the ^{14}N NQR spectra of coordinated nitrogen, and a substantial body of data for several nitrogen-containing ligands has been obtained. These NQR results can be interpreted in terms of the "coordinated nitrogen" model, an adaptation of the Townes-Dailey model. Using this approach it is possible to obtain an estimate of the population of the nitrogen donor orbital directed toward the metal ion or other Lewis acid. Thus the NQR experiment provides information on the extent of charge transfer from the ligand to the Lewis acid center in the ground electronic state.

INTRODUCTION

Nuclear quadrupole resonance (NQR) spectroscopy is a tool of considerable potential value in the study of metal complexes. In applying the NQR technique to such systems, one might hope to obtain greater insights into the metal-ligand interaction, particularly with regard to the extent of charge transfer from metal to ligand. Because the NQR spectra are determined by the components of the electric field gradient (EFG) tensor at the nuclei under study, the NQR experiment provides information about the ground state charge distribution. This is so because each component of the field gradient is the expectation value of a one-electron operator. Few spectroscopic techniques provide such information. Nearly always the observable is connected in some way with the properties of electronic excited states, e.g., electronic absorption spectra in which the transition energies are determined by the energies of the electronically excited states, or ESCA, in which relaxation effects which accompany photoionization play a role.

We might hope to learn from the NQR spectra something of the coordination number or gross geometry of a metal complex. When this information is available from other sources, the NQR data may help to establish isomerism, as in the distinction between cis and trans isomers in a six-coordinate complex. The NQR data may provide information about the solid state structure, for example the number of non-equivalent sites in the unit cell, or about phase transitions from the temperature dependence of the NQR spectra.

A great many metallic elements possess nuclides in reasonable abundance which might themselves serve as NQR probes in metal complexes. Among these are ^{59}Co , ^{27}Al , ^{69}Ga , ^{25}Mg , ^{55}Mn , $^{63,65}\text{Cu}$. Quadrupole transitions have been observed for these and other metallic nuclei, but it must be admitted that the body of NQR data for metallic elements is not very large. Several experimental difficulties impede the acquisition of NQR data for the metallic nuclei. Among these are the fact that many metal complexes are paramagnetic. The presence of unpaired electron spins results in exceedingly short relaxation times for the nuclear spins, and this precludes detection of their quadrupole transitions by the usual techniques. Even in diamagnetic complexes, relaxation times may be unfavorably short when the quadrupole coupling constants are large. In addition, the fact that the quadrupole transition frequencies may vary over a wide range makes the search for these transitions laborious and difficult.

Information about metal complexes may also be obtained by observation of the NQR spectra of the nuclei of coordinated atoms. Among the ligand elements which might lend themselves to such study are $^{35,37}\text{Cl}$, $^{79,81}\text{Br}$, ^{127}I , ^{14}N , ^{33}S , ^{17}O and ^{75}As . The nature of the metal-ligand interaction can be inferred from the NQR spectra of the coordinated ligands, by comparison of the spectra of the ligands in reference environments, e.g., the free ligand.

Application of the NQR technique to the study of metal complexes is controlled by several factors:

(a) Sample Form

The sample must be a polycrystalline material or a single crystal. It is a relatively straightforward matter to obtain polycrystalline samples of most metal complexes, although many complexes which may exist in solution are not obtainable as crystalline solids because of disproportionation reactions. In addition, because the equilibria in solution are often rapid, solubility factors may determine which species is recovered from solution when more than one complex is present.

(b) Sensitivity of Detection

Depending upon the experimental technique employed (vide infra), the sensitivity for detection of the NQR transitions may be very low. Unless double resonance methods of high sensitivity are employed, the low abundance of a particular nucleus of interest in the sample may make its detection difficult. Certainly it is true that one experiences many failures in the use of marginal oscillator or super-regenerative

oscillator-detector spectrometers in the search for NQR spectra of transition elements in complexes. In those instances in which the nuclei of interest are present in relatively low natural abundance, use of a double resonance method is mandatory. Similarly, in the study of ligand nuclei which are present in low natural abundance (^{33}S , 0.74% natural abundance, ^{17}O , 0.037% natural abundance), or for which the NQR transitions lie in the low frequency range (^{14}N , ^{17}O), use of double resonance methods is required.

(c) Sensitivity of EFG Parameters to the Coordination Phenomenon

For the NQR technique to be a useful probe of the metal-ligand interaction, the EFG parameters which determine the observed transition frequencies must be sensitive to chemically interesting aspects of the coordination, such as the extent of metal-ligand charge transfer or geometry. In this regard the NQR technique is on solid grounds in most cases. The quadrupole coupling constant, e^2Qq/h and asymmetry parameter, η , are observed to vary over a wide range in the inorganic and organometallic complexes of several metallic elements (1,2). In addition, it is well established that for both halogens and nitrogen, the EFG parameters of the coordinated ligand are a sensitive function of the nature of the metal-ligand interaction.

(d) Interpretation of the NQR Data

Given that the required sensitivity to coordination environment is present, there remains the question of whether the NQR data can be reasonably interpreted in terms of chemically interesting aspects of the coordination. Interpretation of the NQR data may be carried out at various levels, ranging from ab initio molecular orbital calculations to the most empirical correlations of the NQR data with other spectroscopic observables. Calculations involving SCF methods with fairly extended basis sets which might be presumed to give reasonable representations of the ground state charge distribution (3) are not appropriate for large, complex systems. While more empirical molecular orbital approaches might provide some guidance, such computational methods will not yield much of predictive value. On a more empirical level, adaptations of the classic Townes-Dailey model may be employed in interpreting the NQR data both for metal centers and for coordinated ligand nuclei. Application of such a model to the metal center is often a dubious procedure because there are too many unknown terms. Each metal-ligand interaction involves an unknown degree of ionic-covalent mixing, and there may be a substantial cancelling of contributions from different ligands due to geometrical factors. Thus the EFG tensor may consist of relatively small EFG components as the net sum over all metal-ligand interactions. In many cases a point charge type of model, such as the "donated charge" model (4-6), may be satisfactory in interpreting the EFG parameters at the metal center. Such a model lends itself well to correlating the data for a series of closely related complexes in terms of parameters which may be associated with the surrounding ligands (6,7).

It is well worth keeping in mind that the NQR technique, in company with most other spectroscopic techniques, is not a generally good method for deducing geometrical aspects of structure. Because the technique is related to both electronic and nuclear charge distribution, it is most valuable in determining the electronic distribution once the nuclear configuration of the system is known, for example, from an X-ray structure determination. Thus it is best to view the NQR technique as a probe of electronic, not nuclear, structure. Of course, gross aspects of the structure, such as the distinction between cis and trans isomers may be deduced from the NQR data in favorable cases. In addition, empirical correlations with geometrical structure may be developed as the body of data for a given nucleus becomes larger.

RESULTS FOR METALLIC NUCLEI

As indicated above, the body of NQR data for metallic nuclei is not large. The NQR spectra of coordination compounds have recently been reviewed (1). The NQR spectroscopy of ^{59}Co provides good examples of the limitations and capabilities inherent in the study of metal complexes by this technique; the results have been reviewed elsewhere (6). The limitations in this area are largely experimental. Sensitivity is often poor, particularly when the metal nuclei constitute a small fraction of the total sample. Many of the most interesting metal nuclei which possess non-zero quadrupole moments are of half-integer spin. Double resonance methods which involve field cycling and the establishment of thermal contact in the doubly rotating coordinate frame (8,9) are potentially applicable and would possess very high sensitivity. However, these methods have not yet been much used in the study of metal nuclei. Among the metal nuclei which are good prospects for the use of such techniques are ^{25}Mg , and ^{67}Zn . Both possess half-integer spins ($I = 5/2$), and relatively low frequencies are expected for their quadrupolar transitions. Among the nuclei of high natural abundance for which the NQR spectra can readily be obtained by the double resonance level crossing technique (10) are ^{27}Al , and the alkali metal nuclei, ^{23}Na , ^{39}K and ^{133}Cs .

NQR SPECTRA OF COORDINATED LIGANDS

The NQR spectra of coordinated halogens have been observed in a wide range of metal complexes. In the usual case the halogen atom is singly connected; however, NQR data for bridging halide ligands have also been obtained. The NQR spectra of halogen complexes provide information on the covalency in the metal-halogen bond; however, interpretation of the data in many instances is complicated by the possibility of π -bonding. The extensive literature on the NQR spectra of metal-halide complexes has been reviewed elsewhere (1, 11-13).

Nitrogen is perhaps the most important of all coordinating atoms, in terms of the number of known metal complexes, and because of the widespread occurrence of

nitrogen binding sites for metal ions in biological systems. However, the application of ^{14}N NQR spectroscopy to the study of such complexes has been limited because of the relatively low frequencies at which the nitrogen transitions occur in coordination compounds. The technique of double resonance via level crossing, pioneered by Hahn and coworkers (14), and advanced considerably by the work of Edmonds and coworkers (10), makes the study of the ^{14}N NQR spectra of such complexes relatively straightforward. The technique described elsewhere (10,15) requires as the detection system an abundant spin with relatively long spin-lattice relaxation time in high field. To date the sole spin system employed in the study of ^{14}N has been ^1H . A second requirement is that the ^{14}N spin lattice relaxation time in zero magnetic field, T_{1d} , must be long, i.e., on the order of a few seconds. These requirements preclude the study of paramagnetic samples since the presence of unpaired spins usually leads to unacceptably short spin lattice relaxation times.

Sample size requirement for the double resonance experiment is determined by the sensitivity in detecting the FID from the proton spin system following a 90° pulse. In addition, the heat capacity of ^{14}N spin system must be significant in relationship to the heat capacity of the proton spin bath. This means that any particular nitrogen which is to be detected must be present in numbers not less than perhaps 5 to 10 percent of the number of protons in the sample. With an apparatus capable of detecting the FID of the proton magnetization following a $\pi/2$ pulse in a field of perhaps 1.5-2 Tesla, the ^{14}N transitions in well-behaved samples should be observable with perhaps 50-200 mg total sample size, when the ratio of ^{14}N to ^1H is no less than about 1:5. A chief advantage of the technique is that the sensitivity is relatively independent of the frequencies of the ^{14}N transitions in the range from about 150 kHz upward. This is an especially important consideration in the study of metal complexes, because in these systems the ^{14}N quadrupole coupling constants are generally much lower than in the free ligands.

Essentially all of the NQR spectra of nitrogen directly coordinated to a metal or other Lewis acid center have been obtained using the double resonance technique. Table 1 lists some of the more important nitrogen ligands which have been studied, the number of distinct nitrogen complexation sites observed, and examples. It is evident that the technique is applicable to a wide variety of nitrogen-containing ligands.

Most of the substantial body of ^{14}N NQR data obtained to date for coordinated nitrogen can be interpreted in terms of a simple model which we term the coordinated nitrogen model (16-21). The geometrical aspects of this approach are illustrated in Figure 1. Coordination about the nitrogen is assumed to possess at minimum a mirror plane of symmetry. This means that two of the groups bonded to the nitrogen, B, are assumed equivalent. M represents the metal or other Lewis acid center to which the nitrogen is coordinated. A may represent another atom bonded to nitrogen; for example, in a coordinated amino group A represents the carbon to which the

NH₂ group is bound (21). However, in ligands such as pyridine, imidazole and phenanthroline, A represents a p_π orbital on the nitrogen. In these cases the group M lies in or near the BNB plane.

TABLE 1

Types of nitrogen ligands studied via the NQR double resonance method

| Ligand (refs) | Number of sites observed | Examples |
|---------------------------------|--------------------------|---|
| Pyridine (16,20) | 58 | [Ag(py) ₄]ClO ₄ ; M(py) ₂ Cl ₂ (M = Cd,Zn); cis-Mo(py) ₂ (CO) ₄ ; [I(py) ₂]ClO ₄ |
| Imidazole, histidine (17,18,21) | 24 | [M(Im) ₄]X ₂ (M = Zn,Cd, X = Cl,Br) Cd(Glygly)(Im)Br Zn(His) ₂ ·2H ₂ O |
| 1,10-phenanthroline (19) | 13 | Pd(phen)X ₂ (X = Cl,Br,etc.) |
| Amino (21) | 10 | M(gly) ₂ ·H ₂ O (M = Cd,Zn) |
| Glyoximes (22) | 4 | Ni(dmg) ₂ |

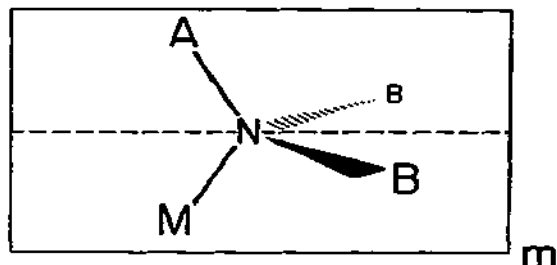


Figure 1. Environment about the coordinated nitrogen. A mirror plane *m* is assumed to be present.

In the Townes-Dailey model it is assumed that the major contribution to the field gradient at nitrogen arises from imbalances in the 2p orbital populations on the nitrogen atom itself. Application of this model to coordinated nitrogen implies that it is possible to describe the EFG at nitrogen in terms of the occupancies of the nitrogen valence orbitals used to form the N-A, N-B and N-M bonds. The data for metal complexes are interpreted in terms of the departures from the field gradient parameters characteristic of a reference system. For example, in the case of pyridine, imidazole, and other 3-coordinate nitrogen systems, the free ligand is chosen as reference. In the free ligand, the population of the nitrogen orbital directed toward M, termed the "donor" orbital, is taken to be 2. As charge is transferred from the nitrogen to the Lewis acid center, it is reasonable to expect that there will be some inductive flow of charge from the remainder of the molecule into the other nitrogen valence orbitals. Thus the populations of the N_A and N_B orbitals should increase in proportion to the extent of charge flow toward M.

Let \underline{a}_0 represent the population of the nitrogen orbital employed in bonding to A (This is the population of the p_π orbital when the ligand is a planar aromatic system such as pyridine). Similarly \underline{b}_0 represents the population of each nitrogen orbital in the bonds to B. These values become \underline{a} and \underline{b} in the coordinated ligand, in which the nitrogen donor orbital population is given the value σ . Then in the coordinated system,

$$\underline{a} = \underline{a}_0 + A(2-\sigma) \quad (1)$$

$$\underline{b} = \underline{b}_0 + B(2-\sigma) \quad (2)$$

where A and B are inductive parameters that reflect the flow of charge into the nitrogen orbitals as a result of charge withdrawal via the donor bond to the Lewis acid. A and B are assumed to be the same for all acid-base adducts of a particular ligand (16,20). Thus for any particular metal complex the EFG at nitrogen is related to that for the reference compound by three parameters: the inductive parameters associated with the groups A and B, and the population, σ , of the nitrogen orbital directed toward M. For a series of j complexes there are thus $j + 2$ disposable parameters. Since the NQR experiment provides two observables for each complex (e^2Qq/h and η), for a series of reasonable size the number of observables exceeds the number of parameters to be determined. Thus, it is possible to use the model to determine values of σ , the donor orbital occupancy of the nitrogen orbital directed towards the metal or other Lewis acid center, in a series of related complexes involving the same ligand.

To illustrate, Figure 2 shows the values of e^2Qq_{xx}/h , e^2Qq_{yy}/h , and e^2Qq_{zz}/h as a function of σ for a large number of pyridine complexes (20). The solid lines represent the values predicted from the application of the model described above, with an optimal choice of inductive parameters ($A = 0.446$, $B = 0.087$), and the points represent the EFG components calculated from the data. The data for each compound have been placed along the horizontal axis in such a manner as to minimize the vertical departures of the observed values of field gradient components from those predicted by the model. The fitting results in a very good agreement for the major field gradient component, defined as e^2Qq_{zz}/h in the tensor axis system, but the errors which accumulate in the fitting appear in a rather larger scatter of values predicted for η . This is shown in Figure 3 which shows a plot of the observed values of e^2Qq/h and η as a function of σ , in comparison with the variation in e^2Qq/h and σ predicted by the model. Clearly the fit to quadrupole coupling constants is excellent, whereas the scatter in asymmetry parameters is larger. The conclusion we may reach from this figure is that the value of quadrupole coupling constant itself is accurately related to the extent of charge transfer from nitrogen to the metal, as reflected in the donor orbital occupancy, σ .

Within the range of chemically interesting values, σ is double-valued. It is often possible on the basis of analogy with complexes already studied to determine which branch is appropriate for a given complex, but where this chemical intuition

fails the value observed for η provides in most cases a means of unambiguously assigning an appropriate value for σ .

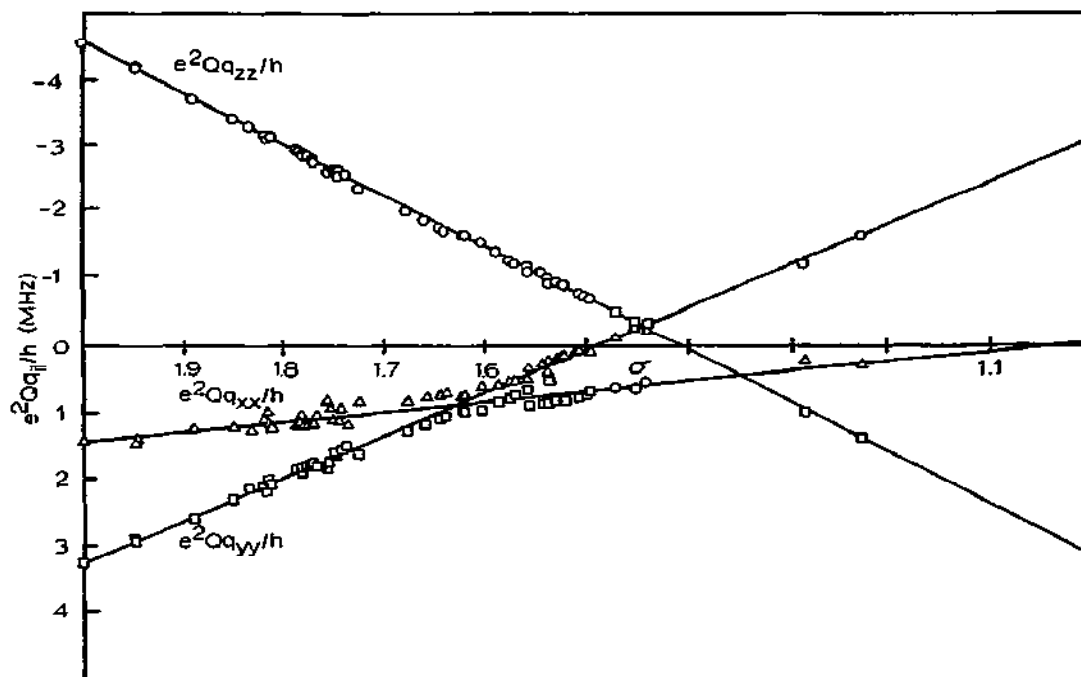


Figure 2. Values of the efg components as a function of donor orbital population σ for pyridine complexes. The solid lines represent the values calculated from the coordinated nitrogen model (20).

It should be pointed out that as the value for σ decreases from the value 2 for the free ligand, changes in the orientation of the major tensor axis occur. For ligands such as pyridine which contain an additional plane of symmetry normal to the mirror plane shown in Figure 1, the field gradient tensor axes are constrained to lie in the two planes; one axis along the intersection of the two planes, and the other two at directions normal to this. However, the relative magnitudes of the tensor components vary with σ , and the model predicts the values of σ at which the major component of the tensor axis shifts from lying along the N-M bond to a direction normal thereto. In the case of a coordinated amino group, which possesses only the mirror plane of symmetry, the orientation of the major tensor axis shifts continuously in the plane with an increase in the extent of charge donation to the metal. At still larger extent of charge donation to the metal, the major axis orientation shifts to a direction normal to the mirror plane. Predictions of the coordinated nitrogen model regarding the orientations of the various components of the field gradient tensor have not as yet been extensively tested. Nearly all of

the NQR data obtained to date have been obtained for polycrystalline materials. Studies of oriented crystals are required to determine the relative magnitudes and orientations of the major tensor axes (23). However, the excellent fit between the calculated and observed EFG components, as illustrated in Figure 2, provides reason to expect that the coordinated nitrogen model successfully predicts the orientations of the major field gradient components in the complexes.

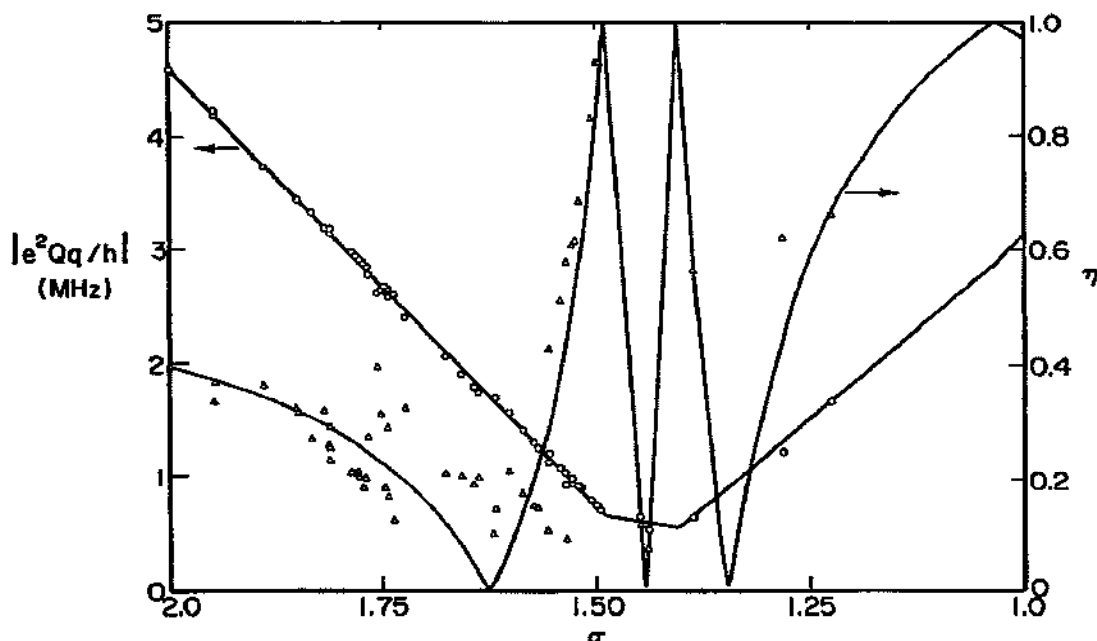


Figure 3. Quadrupole coupling constant and asymmetry parameter vs. the donor orbital population, σ , for coordinated pyridine (20).

A few examples of the calculated nitrogen donor orbital population σ for complexes of various ligands are given in Table 2. These donor orbital populations are model-related quantities, which do not correspond directly to an observable. Thus it is not possible to directly compare these numbers with other measures of charge transfer. However, to the extent that it is legitimate to partition the charge shared between two bonded atoms, the NQR-derived quantities should provide an exceptionally good measure of the charge transferred in the nitrogen-Lewis acid interaction. This is so because the NQR data correspond to the ground state charge distribution, and because the model used to derive the values of σ is relatively insensitive to reasonable variations in the choice of disposable parameters. Thus, the relative values of σ provide an accurate measure of the relative Lewis acidities of the sites to which the nitrogen is bound. As far as comparisons are possible, the ordering of Lewis acids as deduced from ^{14}N NQR data for various nitrogen

ligands is the same. The NQR-derived quantities provide a sensitive indication of the interplay between coordination number and the extent of charge transfer. For example, the extent of charge transfer is larger in $\text{Zn}(\text{Im})_4^{2+}$ ($\sigma = 1.69$) than in $\text{Zn}(\text{Im})_6^{2+}$ ($\sigma = 1.84$) (17). Furthermore, σ reflects the effects of metal ion charge and radius in the expected manner. Extensive data collected for pyridine enable a direct comparison for the first time, of the relative acidities of neutral and charged Lewis acids (20). This is possible because the nitrogen field gradient parameters are only slightly affected by the electrostatic contribution from an external charge located at the site of the Lewis acid. The predominant effect experienced at the nitrogen results from the change in valence orbital occupancy, regardless of whether the Lewis acid is neutral or charged overall. The NQR data for diamagnetic systems provides a basis for the interpretation of ENDOR data for paramagnetic complexes. The application to biological systems, in which the paramagnetic center may be present in low abundance, is especially interesting and exciting.

TABLE 2

Values of nitrogen donor orbital population, σ , derived from ^{14}N NQR data

| Complex | Ligand | σ |
|--|---------------------|----------|
| $\text{Zn}(\text{py})_2\text{Cl}_2$ | pyridine | 1.79 |
| $\text{Cd}(\text{py})_2\text{Cl}_2$ | pyridine | 1.87 |
| $\text{Zn}(\text{Im})_2\text{Cl}_2$ | imidazole | 1.72 |
| $\text{Cd}(\text{Im})_2\text{Cl}_2$ | imidazole | 1.76 |
| $\text{Pd}(\text{phen})\text{Cl}_2$ | 1,10-phenanthroline | 1.66 |
| $[\text{Zn}(\text{Im})_6](\text{NO}_3)_2$ | imidazole | 1.84 |
| $\text{Fe}(\text{py})(\text{CO})_4$ | pyridine | 1.72 |
| $\text{Zn}(\text{glygly})(\text{Im})(\text{NO}_3)$ | imidazole | 1.77 |
| | amino | 1.64 |

EXTENSIONS

The extensive body of ^{14}N NQR data already obtained for coordinated nitrogen establishes the utility of the NQR technique as a probe of metal-ligand interactions. It is expected that NQR spectroscopy will prove useful in the study of many other nitrogen-containing complexes. At the same time, however, the fact that ^{14}N is an integral spin nucleus places a severe limitation on the sensitivity obtainable by the double resonance method. Quenching of the dipolar interaction for integer spins in zero magnetic field precludes use of experiments involving multiple contacts in the rotating frame (24). Extension of double resonance methods to the observation of the NQR spectra of other coordinated atoms is worth considering. Both ^{33}S and ^{17}O are half integer spin systems, and both are present in relatively low natural abundance. Application of the technique pioneered by Slusher and Hahn (9), involving multiple irradiation of the rare quadrupolar spin system at zero

field in a field cycling experiment, makes it possible to observe these nuclear spin systems, even in natural abundance. In addition, if particular sites in very large molecules are highly enriched with the appropriate nuclide, it should be possible to study specific centers in large biomolecules using the NQR technique. The study of ^{33}S carries the limitation that in a $I = 3/2$ spin system, only one transition is observed. However, it may be possible to semi-empirically relate the ^{33}S NQR data to particular types of coordination; the distinction between free and coordinated sulfur should be possible.

One of the most important directions for future work is the extension of double resonance methods to experiments involving metal nuclides. Many of the metallic systems of considerable interest, for example, ^{25}Mg and ^{67}Zn , should exhibit relatively low quadrupole resonance transitions in their typical coordination environments. Observations of other transition element nuclei in diamagnetic coordination environments via double resonance methods have been few. Use of double resonance methods here requires a wide frequency range capability in the double resonance experiment, and that in turn presents a considerable experimental challenge.

ACKNOWLEDGEMENTS

I am indebted to Carol Ashby, C. P. Cheng, Gerald Rubenacker and Yu-Nian Hsieh for their major contributions to the work from our laboratory. This research was sponsored by the National Science Foundation through grants NSF CHE 76-17570 and DMR 77-23999, and the National Institutes of Health through research grant GM-23395.

REFERENCES

- 1 L. Ramakrishnan, S. Soundarajan, V.S.S. Sastry and J. Ramakrishna, *Coord. Chem. Revs.*, 22(1977)123-182.
- 2 T.B. Brill, *Adv. in Nucl. Quadrupole Res.*, 3(1978)131-183.
- 3 R. Moccia and M. Zandomenighi, *Adv. in Nucl. Quadrupole Res.*, 2(1975)135-178.
- 4 R. Parish, *Prog. Inorg. Chem.*, 15(1972)101-200.
- 5 G.M. Bancroft and R.H. Platt, *Adv. Inorg. Radiochem.*, 15(1972)59-258.
- 6 T.L. Brown, *Accts. Chem. Res.*, 7(1974)408-415.
- 7 G.M. Bancroft and E.T. Libbey, *J. Chem. Soc. Dalton Trans.*, (1973)2103-2111.
- 8 S.R. Hartmann and E.L. Hahn, *Phys. Rev.*, 128(1962)2042-2053.
- 9 R.E. Slusher and E.L. Hahn, *Phys. Rev.*, 166(1968)332-347.
- 10 D.T. Edmonds, *Phys. Repts.*, 29(1977)233-290.
- 11 H. Chihara and N. Nakamura, *MTP International Rev. Sci. Series 1*, C.A. McDowell, Editor, University Park Press (Baltimore), 4(1972)125-154.
- 12 R.L. Armstrong and H.M. van Driel, *Adv. in Nucl. Quadrupole Res.*, 2(1975)179-253.
- 13 D. Nakamura, R. Ikeda and M. Kubo, *Coord. Chem. Revs.*, 17(1975)281-316.
- 14 J.C. Koo and Y.N. Hsieh, *Chem. Phys. Lett.*, 9(1971)238-240.
- 15 R. Blinc, *Adv. in Nucl. Quadrupole Res.*, 2(1975)71-115.
- 16 Y.N. Hsieh, G.V. Rubenacker, C.P. Cheng and T.L. Brown, *J. Amer. Chem. Soc.*, 99(1977)1384-1389.
- 17 C.I.H. Ashby, C.P. Cheng and T.L. Brown, *J. Amer. Chem. Soc.*, 100(1978)6057-6063.
- 18 C.I.H. Ashby, C.P. Cheng, E.N. Duesler and T.L. Brown, *J. Amer. Chem. Soc.*, 100(1978)6063-6067.
- 19 C.P. Cheng, B. Plankey, J.V. Rund and T.L. Brown, *J. Amer. Chem. Soc.*, 99(1977)8413-8417.
- 20 G.V. Rubenacker and T.L. Brown, *Inorg. Chem.* (in press).

- 21 C.I.H. Ashby and T.L. Brown. J. Amer. Chem. Soc., (submitted); C.I.H. Ashby, Ph.D. Thesis, University of Illinois, Urbana, 1979.
- 22 Y.N. Hsieh, P.S. Ireland and T.L. Brown, J. Magn. Res., 21(1976)445-456.
- 23 A. Sasane and J.A.S. Smith, J. Magn. Res., 32(1978)265-287.
- 24 G.W. Leppelmeier and E.L. Hahn, Phys. Rev., 141(1966)724-731.

See discussions, stats, and author profiles for this publication at: <https://www.researchgate.net/publication/281939438>

Nuclear Quadrupole Resonance. Applications

Chapter · January 2010

CITATIONS

0

READS

7,288

2 authors:



Oleg Kh Poleshchuk

Tomsk Pedagogical University

130 PUBLICATIONS 487 CITATIONS

SEE PROFILE



Jolanta Natalia Latosińska

Adam Mickiewicz University

99 PUBLICATIONS 681 CITATIONS

SEE PROFILE

Some of the authors of this publication are also working on these related projects:



Molecular Oligogermanes and Related Compounds: Structure, Optical and Semiconductor Properties [View project](#)



Acetaldehyde-Ammonia Interaction [View project](#)

Poleshchuk O. Kh., Latosinska J. N. Encyclopedia of Spectroscopy and Spectrometry. Magnetic Resonance. Nuclear Quadrupole Resonance, Applications. Academic Press Ltd., London, 1999, V. 2, P. 1653-1662.

NUCLEAR QUADRUPOLE RESONANCE. APPLICATIONS

Oleg Kh.Poleshchuk, Jolanta N.Latosińska

The NQR frequencies for the various nuclei vary from several kHz up to 1000 MHz. Their values depend on quadrupole moments of the nucleus, valent electrons state and type of chemical bond in which the studied atom participates. Using the NQR frequencies the quadrupole coupling constant (QCC) and asymmetry parameter (η) can be calculated according to the different exact or approximate equations (selected for the spin of the nuclei). For polyvalent atom NQR frequencies depend on coordination number and hybridization. Classification of frequencies NQR shifts for a single-valent atom depending on a situation can be described as follows:

1. The greatest shifts of the NQR frequencies are determined by valent electrons state of the neighbour atoms and can reach 1200-1500%. The changes of the NQR frequencies occur largely naturally, and the lowest frequency corresponds to an ion Cl^- , whereas the highest - to the atom of chlorine in ClF_3 .
2. The changes within the limits of one type of chemical bond (with the same kind of atom) can reach already 40-50%. So the changes frequencies of bonds C-Cl vary from 29MHz to 44 MHz.
3. The range of possible shifts of the NQR frequencies is narrowed till 10-20 % in the case when only one class of compound is studied. Then shifts are determined by surroundings, amount and donor-acceptor properties of the substituents. For example, for halogen substituted benzene, the changes of the frequencies for the C-Cl bonds are about 9%, for the C-Br bonds - 12%, for the C-I bonds - 18%.
4. The changes of NQR frequencies caused by occurrence intra-molecular and inter-molecular interactions, lie within the limits of 3-40%.
5. The shifts of NQR frequencies at the expense of the crystal field effects in molecular

crystals reach maximum 1,5-2%. However with research of numbers of similar compounds this disorder, as a rule, does not exceed 0,3%.

Such classification of NQR frequencies shifts allow to give the definition of the structural nonequivalents in NQR spectra. Understanding last distinctions in gradients (and of course frequencies) on quadrupole atoms, caused by chemical in-equivalent and determined by distinctions in distribution of electronic density in a free molecule is very important. Moreover, it is observed crystallographically nonequivalencies, appearing as a result of distinction of the additional contributions into electric field gradient comes from chemically equivalent and nonequivalent atoms. It is obvious, that the division of structural nonequivalencies on chemical and crystal loses sense with transition to coordinative and ionic crystals, in which there are no individual molecules. The NQR, being highly sensitive to subtle changes in electron density distribution, provides diverse information on structural and chemical properties of compounds.

Structural Aspects of NQR Information

When applied to structural investigations, NQR spectra may prove an effective tool for preliminary study of crystal structure in the absence of detailed X-Ray data. Such parameters as spectroscopic shifts, multiplicity, spectroscopic splitting, resonance line width, the temperature dependence of resonance frequencies and relaxation rates, afford useful structural information and provide insight into the factors determining the formation of certain structural types.

As is evident from the previous, the electronic structure of *chemically equivalent* atoms should be identical. The violation of chemical equivalence of resonance atoms due to a change in chemical bonding, such, as for example, dimerization IIIA groups halogenides, leads to a significant splitting of the spectroscopic multiplet caused by a difference in the electronic structure of bridging and terminal atoms.

Aspects of Crystallographic Structure

For crystallografically in-equivalent atoms the corresponding components of the EFG at the respective sites differ from each other in magnitude and direction due to the crystal field effect. This generally includes contribution to the EFG of electrostatic forces between molecules, dispersion forces, intermolecular bonding and short-range repulsion forces. Physically inequivalent sites differ from each other only in the direction of the EFG components, their

magnitudes being identical. To distinguish between such sites, Zeeman analysis of the NQR spectrum is required.

The intensities of spectroscopic lines are also important characteristics. They reflect the relative concentration of resonance nuclei at certain sites although one also has to take into account transition probabilities and life times of the energy states of the system investigated. The correspondence between the number and intensities of frequencies and the number of in-equivalent sites occupied by a resonant atom in a crystal lattice, is very helpful in a preliminary structure study made with the use of NQR.

The NQR single-crystal Zeeman analysis can provide information about special point positions occupied by the quadrupole atoms. This Zeeman analysis determines the orientation of the EFG components with respect to the crystal axes, which essentially facilitates the most difficult and time-consuming stage of the X-Ray analysis. **Table 1** gives comparison of the angle values between the crystal axes and the EFG z-axis at the chlorine atoms in 1,3,5-trichlorobenzene, determined by the two methods.

<Table 1 near here>

As one can see from **Table 1** the angle values compared show rather good numerical agreement the others methods. In order to illustrate more completely the aspects of structure information which can be obtained by NQR spectroscopy, we consider in more detail an NQR study of BiCl_3 whose structure is known. The two chlorine atoms are involved in bridging to two other Bi atoms while another chlorine atom is involved in bridging to only one other Bi atom. The ^{35}Cl and ^{209}Bi NQR parameters of BiCl_3 measured by means of the single-crystal Zeeman method are listed in **Table 2**.

<Table 2 near here>

An example which illustrates useful information is provided by the ^{35}Cl results for phosphorus pentachloride. In the gas phase this is known to a trigonal bipyramid but the usual solid PCl_5 is likewise known to be an ionic crystal, $(\text{PCl}_4)^+(\text{PCl}_6)^-$. In accordance with this and the detailed crystal structure there are four resonances at high frequency corresponding to the $(\text{PCl}_4)^+$ group and six at a lower frequency corresponding to the $(\text{PCl}_6)^-$ group (**Table 3**).

<Table 3 near here>

It has recently been observed that quenching of the vapour of PCl_5 gives rise to a new metastable crystalline phase which can be preserved essentially indefinitely at low temperature. The resonance frequency of this is with two low frequencies corresponding to the axial chlorine atoms and three identical higher frequencies corresponding to the equatorial

substituents are strong evidence that this new phase is the corresponding molecular solid. Another example taken from the chemistry of the antimony pentachloride. It is known, that the molecule of antimony pentachloride with 210K has trigonal bipyramid structure, and with temperature 77K represents dimer. In **Table 3** the experimental frequencies ^{35}Cl -NQR and their assignment in equatorial and axial chlorine atoms are given. In dimer molecule bridging chlorine atoms have much lower NQR frequencies, as in dimer molecules of IIIA group compounds. From **Table 3** it is visible also, that in a molecule a monomer the NQR frequencies of equatorial chlorine atoms lies above, than axial ones.

In dimer a ratio of ^{35}Cl -NQR frequencies return, that was proved to us on the basis ab initio calculations. In dimers of transition elements, such as NbCl_5 and TaCl_5 the frequencies ^{35}Cl -NQR of equatorial atoms of chlorine are more, than axial, and bridging are higher, than on the average for terminal. The similar inversion of NQR frequencies in dimers of transition and non-transition elements is explained significant multiplicity metal-halogen bonds and thereof by essential electron transfer from p-valent orbital of halogen atom on vacant d-orbitals of central atom.

The fact that the difference between chemically non-equivalent atomic positions is readily revealed in NQR spectroscopic splitting may be utilized to identify geometric isomers. Octahedral complexes of tin tetrachloride, $\text{SnCl}_4 \cdot 2\text{L}$, form either cis- or trans-isomers. In cis-isomers the axial and equatorial inequivalence produces considerable splitting in the NQR spectra. In trans-complexes, all four chlorine atoms are chemically equivalent with identical electron density distribution. Splitting in the NQR spectra of these isomers, arises therefore from crystallographic inequivalence of the chlorine positions. Indeed, the observed NQR splitting of two complexes (**Table 4**) provides evidence for the cis-configuration of $\text{SnCl}_4 \cdot 2\text{OPCl}_3$ and the trans-configuration of $\text{SnCl}_4 \cdot 2\text{NC}_5\text{H}_5$ confirmed by X-Ray data.

<Table 4 near here>

However not always it is possible to carry out assignment of equatorial and axial chlorine atoms only on the basis of splitting ^{35}Cl -NQR frequencies. For cis-isomers of complexes the ratio of NQR frequencies of equatorial and axial chlorine atoms is determined by total action of the factors forming optimum crystal structure, among which the influence of donor molecules L is not determining. Practically in all structurally investigated complexes of this type of length of equatorial Sn-Cl bonds it is more axial, that corresponds, noticed in experiment,

to relative NQR frequencies downturn, of equatorial atoms in comparison with axial (**Table 4**). Except that large meaning have asymmetry parameters of chlorine atom, which (**Table 4**) considerably differ for axial and equatorial atoms. On the other hand result of donor ligands L influence on change - electron density of equatorial and axial Cl atoms is the relative downturn of frequencies of axial atoms in comparison with equatorial. Such relation of frequencies in cis-isomers is explained from the point of view of the mutual ligand influence concept in non-transition element complexes. In cis-complexes SnCl_4L_2 the interaction of -Sn-L bonds will be more with Sn-Cl bonds which are taking place in a trans-position to them, than with communications(connections) Sn-Cl. It points out that in these complexes the mutual ligand influence establishes the greater trans-effect, and, therefore, to redistribution of electronic density on atoms of chlorine. In complexes SbCl_5L (**Table 4**) for NQR frequencies axial and equatorial chlorine atoms assignment of besides the account of frequencies splittings and asymmetry parameters is necessary in a number of cases to use temperature dependences of NQR frequencies. In this case the NQR frequency is described square-law dependence: $\nu(T) = A + BT + CT^2$. The positive sign of C coefficient points to that such NQR frequency belongs to axial chlorine atom. Thus it appears, that in some complexes the frequency of axial chlorine atom lays above frequencies of equatorial atoms, in some - on the contrary. Apparently, in these complexes the spatial influence of the donors molecules on NQR frequencies of equatorial chlorine atoms is essential.

The width of the NQR signal also incorporates structural information. In molecular crystals of high order and purity, the line width is not much different from the value determined by the sum of the spin-lattice relaxation and spin-spin relaxation times. In the majority of inorganic compounds, the lines are however inhomogeneously broadened by lattice imperfections such as defects, vacancies, admixtures and dislocations, so that their widths are mainly determined by the crystal inhomogeneity. Systematic study of spectroscopic shifts and broadening produced by a continuous change of the relevant sources of broadening, makes an effective approach to the investigation of problems concerned with distribution of mixtures over a matrix, the nature of their interaction with matrix, the mechanisms of disorder, the local order in vitreous compounds, etc.

Aspects of Bonding from NQR Spectra

Townes-Dailey Approximation

The Townes and Dailey approach is the most widely used to provide a meaningful account of bonding trends within a series of related compounds.

The interpretation nuclear quadrupole interactions (NQI) in molecules is based on the

theory offered Townes and Dailey. The gradient of an electrical field in a place of a presence of a quadrupole nucleus (q_{zz}) forms mainly electrons of that atom, which possesses this nucleus. In the first approach it is possible to consider, that the internal electrons will form the closed environments with spherical symmetry and consequently do not give any contribution in EFG. Actually polarizability of the internal electrons is taken into account through Sternheimer antishielding factor (γ_{∞}), however, if the comparison NQR will be carried out only with the purpose of chemical interpretation and is not accompanied by discussion of their absolute meanings, the polarization of the internal electrons can be neglected. Among valent electrons those, that are on s-orbitals with spherical symmetry, do not give the contribution in EFG and the main contribution is caused by p-electrons; the contribution d- and f-electrons is much less significant because of their greater distance from a nucleus and smaller participation in hybridization.

The quantitative consideration of the contributions in EFG results in expressions of the following type applied to nuclei of chlorine in chloroorganic compounds:

$$q_{zz}^{Cl} = [(1-s^2 + d^2 - I - \pi) + I(s^2 + d^2)] q_{at}^{Cl},$$

where s^2 , d^2 -contributions s- and d-orbitals in hybridization chlorine atom bonding orbital, I- ionic character of the bond (the chlorine atom carries on itself a negative charge) and q_{at}^{Cl} is the gradient of p-electron on chlorine atom. The obvious account results others valent orbitals in the little bit modified expressions; some results are discussed with the account of the three nuclear p-orbitals populations, and the axes x, y, z usually get out so that the axis z coincided with a direction of the bond by consideration halogens or with any axis of system symmetry from several bonds by consideration of atoms such as nitrogen or arsenic; other results are more convenient for discussing with the account bonding and lone electron pair orbitals.

On the basis of told above interpretation NQR in the terms population orbitals can be represented rather unequivocal. Actually NQR spectroscopy allows to determine at the best two parameters (e^2Qqh^{-1} and η), and in many cases ($I = 3/2$) only approached meaning of

e^2Qqh^{-1} , whereas the above mentioned equation (1) contains four parameters (s, d, I, π), which cannot be determined from one or two experimental parameters. It is necessary to address to approximations, in which neglect d-orbital participation in hybridization, and in some cases as p-bonding and consider, that s-orbital's hybridization is small and remains constant in a number of researched compounds, so the changes of a constant e^2Qqh^{-1} directly contact to bond ionic character or p-electron transfer changes in case of hydrogen bond.

In case of nitrogen, which nucleus has spin $I = 1$, the situation is more favorable, as the experiment allows to determine two parameters, and about s-p-hybridization it is possible to judge on the basis of valent angle values, if the molecular geometry is known. However meaning nuclear NQI for ^{14}N p-electron is known not with such accuracy, as for chlorine, bromine or iodine, and approximately makes 9 - 10 MHz; the truth this estimation can be considered reliable, as it is based on the analysis of large number of experimental data. The even more difficult situation in case of antimony atom, for which exists a little considerably distinguished NQI values.

Donor-Acceptor Interactions

Except the marked above restrictions with discussion of experimental NQI meanings in the terms of orbital populations the certain role is played also by the physical contributions, which so change NQI, that their experimental meanings differ from expected for a hypothetical molecule or complex which are taking place in an isolated condition and in rest. In case of molecular complexes there is an additional contribution resulting in NQI changing in complex formation process, - change hybridization owing to change of donor and acceptor molecules geometry. The typical example is given by MX_3 complexes, where M is an element of IIIA or VB group of the periodic table, and X is halogen or methyl group. With complex formation the XMX angle values and appropriate hybridization change, that results in changes in NQI meanings even in absence of any charge transfer. It complicates unequivocal interpretation of experimental data.

The special importance has a question: whether the shifts of NQR frequencies, observable are caused with transition from pure, non-complexed of initial substances to

complexes, a charge transfer or other reason? This rather important question is necessary attentively to consider each time, as the answer to it depends on the several factors. With small a charge transfer there is a false representation about their reproduction frequency by shifts. In such cases frequency the shifts are defined mainly by crystal or solid-state effects, which are caused by distinctions in a crystal environment of molecules with transition from pure components of a complex to the complex (crystal electrical field, intermolecular interaction, thermal movement); the appropriate shifts can reach several hundreds kHz (in case of a resonance on a chlorine nucleus by a measure of similar effects the shift of the order 200 kHz) is considered. When the observable shifts have large value (one or several MHz), they already cannot be considered as the caused crystal effects and it is possible with confidence to attribute to electronic effects of a charge transfer. However it is necessary to take into account and other contributions, as for example, hybridization change. The hybridization change, accompanying deformation of a flat AlMe_3 molecule in pyramidal, formally results in NQI change on aluminium atom, even if there is no population change and ionic character of bonding orbitals; thus, the shift of NQR frequency in this case should be determined both carry of a charge, and hybridization change.

The more difficult situation meets, when in the free compounds there are strong intermolecular interactions: the infringement of these interactions by complex formation can result in increase NQI in a complex, that contradicts the usual simple circuit, predicted NQI reduction with transition to a complex. Such situation meets in complexes of mercury halogenides: HgBr_2 .dioxan and HgI_2 .dioxan. The further progress in discussion of experimental results can be achieved, if in a complex is present a little of quadrupole nucleuses, that allows to carry out comparison of shifts for each of them; frequently rather useful there are also structural data usually received by a X-Ray method. At last, for an estimation of a relative role of the various contributions in observable shifts of frequencies the theoretical discussion can assist.

Intermolecular Interactions

Another example presents the situation where the quadrupole atom halogen makes a

symmetrical bridge between two metal atoms, often the case in polymeric metal halides of composition MX_n ($n=3-5$). Dimers of metal halides, e. g. $AlCl_3$, $GaBr_3$, $TaCl_5$, $SbCl_5$, $[Al_2Br_7]$, have been attractive for NQR investigators, because of the differences between the resonance frequencies of bridging (X_b) and terminal (X_t) halogen atoms. The dimers have structures with either two bridging Me- X_b -Me bonds of about equal length, as in $GaBr_3$, or two bonds of significantly different length, as in complexes of oxygen donor ligands with mercuric halides, or one bridging bond as, e. g., in the aluminium heptabromide anion $[Al_2Br_7]$. **Figure 1** present the structure one of type of symmetric bridging dimeric halides.

<Figure 1 near here>

The spatial structure of the MeX_3 -type dimer is shown in **Figure 1a** whereas **Figure 1b** presents the same structure projected onto the plane of the bridging bonds. The halogen atoms involved in the bridges are together with metal atoms (Me) in one plane which is perpendicular to the plane of the other terminal halogen atoms (X_t) and the metal atoms.

Analysis of the Zeeman splitting of the NQR spectra of halides of non-transition metals from Group III of the periodic table permitted a determination of the directions of the main axes of the EFG tensor on the bridging halogen atoms. These directions are marked in **Figure 1b**. The axis of the greatest gradient of the electric field on the bridging halogen atom is perpendicular to the plane containing the metal atoms and the bridging halogen atoms. The same axis but on the terminal halogen atoms lies along the metal-halogen bond. The orientation of the main axes of the EFG tensor in the case of other types of bridging dimeric halides is similar.

We have been indicated that the NQR frequencies of the bridging halogen atoms in non-transition metal compounds are lower than those of the terminal atoms and this relationship is reversed in the case of transition metal compounds. **Table 5** includes the NQR frequencies of the bridging and terminal halogen atoms, the values of EFG asymmetry parameter for the bridging and terminal halogen atoms, as well as the angles at the bridging atoms (see **Figure 1b**) for some non-transition and transition dimers.

<Table 5 near here>

X-Ray structural and electron diffraction data indicate that, independently of the nature of the central Me atom, the length of the bridge is always greater than the distance between the terminal atoms. In non-transition metal compounds the effective negative charge on the bridging halogen atoms is smaller than that on the terminal atoms. The contrary situation takes place in transition metal halides. In these compounds the effective negative charge on the bridging atoms is greater than that on the terminal ones. The explanation lies in the nature of the metal valence shells (p - d transfer). In the framework of the Townes and Dailey theory this means an effective lowering of the resonance frequency due to the decrease in the p_x and p_y orbital population of the terminal halogens.

<Figure 2 near here>

Figure 2 presents a correlation found by the linear regression method between the values of unpaired p-electron densities for the bridging (U_p^b) and terminal (U_p^t) halogen atoms for the large number compounds. The existence of these correlations is connected with the influence of the p-electron distribution on NQR frequencies, and the bridging and terminal halogen atoms are connected through the central atom, which acts as «a buffer». One can see from **Figure 2** that the experimental points can be divided into two groups corresponding to non-transition and transition metal compounds. This is in a good agreement with the difference in NQR frequencies for the bridging and terminal halogen atoms, for all the compounds studied. As a consequence, the unpaired electron density differs for the compounds of both groups, although U_p^b increases with increasing U_p^t for all those studied. The observed correlations are approximate, which points to the influence of other factors, such as crystallographic uncertainty, position of the molecules in the elementary cell of the crystal, etc.

The NQR spectroscopy can be also used to provide detailed information on the structure and conformation of biologically active systems. It offers a unique possibility of determining the quadrupole coupling constants and in a consequence effective charges and in this way allows a determination of the electronic structure of the molecule. NQR spectroscopy appears to offer a powerful tool for the investigation of various chemical effects in the solid phase of many nitrogen-containing nitrogen compounds. Analysis of the quadrupole coupling constants on nitrogen

atoms allows an estimation of the electron density distribution on the nitrogen nuclei and enabled the analysis of the nitrogen bond's populations.

<Figure 3, Table 6 near here>

For example the effect of substitution of the 2-nitro-5-methylimidazole ring at the 1H position can be analysed (**Figure 3, Table 6**). Hitherto, different imidazole derivatives have been studied by NQR on ^{14}N nuclei (DLRC) by the continuous wave method, by ^{13}C NMR and ^{35}Cl NMR (pulse methods), however, the problem of the effect of a substituent at the 1H position on the electron distribution in 2-nitro-5- methylimidazole derivatives has not been considered. Results of the NMR-NQR double resonance studies are collected in **Tables 7**.

<Table 7 near here>

As follows from the **Table 7** data, the introduction of NO_2 and CH_3 at positions 2 and 5 of the imidazole ring, respectively, leads to an increase in e^2Qqh^{-1} constants on both nitrogens of the ring and a decrease in the value of this parameter on the nitrogen from the NO_2 group. Results of the bond population analysis carried out according to the Townes-Dailey method for imidazole and its derivatives are displayed in **Tables 8**.

<Table 8 near here>

According to the assumed notation n_{NC} and n_{NR} stand for the population of NC and NR bonds, n_a stand for the lone pair population of n atom, while π is the π -electron density. A comparison of the data collected in **Table 8**, shows that in the case of three- substituted nitrogen atom, the lone pair electron density and NR bond population increase with increasing length of a substituent at 1H position in the imidazole ring, both at 193 and 269 K. The substitution of NO_2 group at position 2 and a methyl group at position 5 of the imidazole ring lead to an insignificant redistribution of electron density (of an order of 2%) relative to that in pure imidazole. Only the introduction of a substituent at 1H position of the ring causes considerable changes. Similarly as for a three-substituted nitrogen, also for a two-substituted one, the bond population changes in the characteristic way - the π -electron density and population of the NC bond decrease with elongation of the substituent at 1H position of the imidazole ring, **Table 8**. Interestingly, a qualitatively the same but much more effective phenomenon is the electron redistribution on the nitrogen atoms of $-\text{NO}_2$ groups. Therefore it can be concluded that in the case of 2-nitro-5-methyl derivatives of imidazole with increasing length of the chain of the aliphatic substituent at the 1H position of the imidazole ring, the electron density from the π -orbital and σ -bond of the two-substituted atom as well as π -orbital and σ -bond of the NO_2 group towards the three-substituted nitrogen undergoes redistribution. Of essential importance is the character of substituents, i.e. $-\text{CH}_2\text{CH}_2\text{OH}$ and $-\text{CH}_2\text{CH}_2\text{OCOCH}_3$ groups are electron density acceptors, as for 1D-imidazole

and 1-acetyloimidazole the opposite tendency was observed, that is the π -electron density and population of σ -bond increased. The above presented results also indicate that the effect of temperature on the bond populations in the imidazole derivatives studied is negligible.

<Figure 4 near here>

The 4-N-derivatives of cytosine have aroused significant interest mainly because of their biological significance. 4N- methyl and 4N-acethylcytosine were found in nucleic acids among the rare bases. The structural formula is shown in **Figure 4**. Results of the analysis of bond population for cytosine and its derivatives performed by the Townes-Dailey is described below. On the -NH- nitrogen the changes in electron density distribution induced by substitution are insignificant. The symmetry of charge distribution at the -NH- nitrogen in 4N-thioethylcytosine is the lowest while in 4N-naphthalencytosine the highest. On the other hand the greatest value of the z-component of the EFG tensor was detected in the vicinity of -NH- in pure cytosine while the smallest in naphthalencytosine which implies that the electrons are drawn away from -NH- by the system of bonds depending on the substituent. Thus, it can be concluded that the introduction of a substituent at the amine group of cytosine at 4N does not cause any changes when the substituent contains a chain CH_2CH_2 which separates the aromatic system from the cytosine ring. However, when the aromatic system is separated only by CH_2 bond or is not separated at all, there occurs a strong inductive effect which is responsible for drawing π -electron density from the -NH- nitrogen. For a two-substituted nitrogen the symmetry of charge density at -N= is 50% lower - compare that of 4N-phenylmethylcytosine with that of 4N- thioethylcytosine, and about 20% lower than that of 4N-naphthalencytosine. On the other hand, the quadrupole coupling constant and thus the z-component of the EFG tensor at -N= nitrogen, is much higher in the derivatives whose substituents are not separated by the CH_2CH_2 chain The difference between the population of the NC bond for pure and substituted cytosine is small - 0.001 for 4N-thioethylcytosine but as great as 0.132 for 4N-pnenylomethylcytosine which is still much less than the difference between the populations of σ and π bonds. Such a situation indicates that the changes in σ -bond population are dominant. In 4N-naphthalencytosine the change in π -electron density is dominant. This implies that -N= in phenylmethylcytosine and naphthalencytosine plays the role of a buffer. In 4N-phenylmethylcytosine and 4N-naphthalencytosine the electron density of a free electron pair at the nitrogen -NHR is significantly delocalised. The electron density on the NH bond in 4N-naphthalencytosine, 4N-phenylmethylcytosine and 4N-thioethylcytosine relative to that in pure cytosine changes by 0.053, 0.038 and 0.005, respectively, while for 4N-phenyloethylcytosine there is no change. Thus, the amine group which acts as π -electron acceptor in the majority of molecular systems, becomes the electron donor in phenylocytosine and

naphthalenecytosine. The aromatic rings which usually compensate changes in electron density in cytosine act as electron acceptors. When the aromatic substituents are separated by the chain $-\text{CH}_2\text{CH}_2$, the density redistribution is reduced which is in agreement with the tendency observed for chlorobenzenes. Results of investigations of cytosine and its derivatives proved that the cytosine derivatives with an aliphatic substituent do not show anticancer effect, but the ones with aromatic substituent do, however, the mechanism of this activity has not been explained. The results reported in this paper suggest that in the search of anticancer drugs from the group of 4N-cytosine derivatives, the choice should be those in which the aromatic substituents are not separated by a chain CH_2CH_2 whose presence induces a significant redistribution of π -electron density. The ^{14}N -NQR frequencies recorded for cytosine derivatives were practically the same at the ambient and liquid nitrogen temperatures which means that no essential redistribution of electron density occurs in this temperature range.

The nitrogen 14 nucleus, because of its widespread occurrence in all types of systems (especially biologically active) is of particular interest in studying electron density distribution, molecular reorientations and intermolecular time dependent interactions. It seems that such studies will acquire more and more importance in the future and will acquire more and more frequent, especially with the availability of double resonance spectrometers and new techniques, such as maximum entropy method.

The examples discussed do not of course exhaust the potential of NQR as a tool for structure and chemical bonding. These are only simple illustrations to the applied aspects of NQR spectroscopy.

NQR is nevertheless not as extensively useful at present as NMR. The best results on light nuclei, such for example as those on ^{27}Al QCC in mineral samples, have been made using NMR. The changes in NMR spectra were considered as a function of the orientation of a single crystal in external magnetic field. The NQR could however directly measure the same QCC data using neither single crystals nor an external magnetic field. NQR measurements possess high spectral resolution, precision, specificity and speed of measurements. The reason for relatively limited practical application of NQR seems to lie in the lack of sufficiently sophisticated equipment.

NQR applications can be divided into four groups:

1. Studies of the electron density distribution in a molecule – changes in orbital populations under substitution, complexation

2. Studies of the molecular motions – reorientations, rotations, hindered rotations
3. Studies of the phase transitions
4. Studies of the impurities and mixed crystals

Bibliography

Advances in Nuclear Quadrupole Resonance vol.1-5 J.A.Smith, (1974-79). Heiden & Son Ltd.: London, New York, Rheine.

Buslaev JA, Kolditz L and Kravchenko EA (1987) Nuclear Quadrupole Resonance in Inorganic Chemistry. VEB Deutsche Verlag der Wissenschaften: Berlin.

Das TP and Hahn EI (1958) *Nuclear Quadrupole Resonance Spectroscopy*. Solid State Physics (suppl. I). Academic Press: New York, London.

Gretschischkin WS (1973) *Yadernye kvadrupolnye vzaimodejstviya v tverdykh telach*. Nauka: Moskva.

Lucken EAC (1969) *Nuclear Qudrupole Coupling Constants*. Academic Press: London and New York.

Safin IA and Osokin D (1977) *Yadernyj kvadrupolnyj rezonans v soedineniach azota*. Nauka: Moskva.

Semin GK, Babushkina TA and Yakobson GG (1975) NQR Group of INEOS AN SSSR, *Nuclear Quadrupole Resonance in Chemistry*. English Edition: John Wiley & Sons.

Townes CH and Dailey BPJ (1948) *Journal of Chemical Physics* **17**: 782.

Townes CH and Dailey BPJ (1955) *Journal of Chemical Physics* **23**:118.

Table 1. The angles between the directions of C-Cl bonds and the crystal axes in 1,3,5-trichlorobenzene according to NQR and X-Ray results

| Chlorine position | Crystal axes | | | | | |
|-------------------|--------------|--------|--------|-------|--------|--------|
| | a | | b | | c | |
| | NQR | X-Ray | NQR | X-Ray | NQR | X-Ray |
| Cl ₁ | 119.1° | 118.8° | 149.5° | 150° | 81.7° | 80.9° |
| Cl ₂ | 64.1° | 65.0° | 31.3° | 30.2° | 73.7° | 74.3° |
| Cl ₃ | 24.8° | 24.0° | 90.4° | 90.5° | 114.8° | 114.0° |

Table 2. ³⁵Cl and ²⁰⁹Bi NQR spectra of BiCl₃

| Isotope | T [K] | Transition frequencies | | | | e ² Qqh ⁻¹ [MHz] | η [%] | Assign-ment |
|-------------------|-------|------------------------|---------|---------|---------|--|-------|-------------|
| | | [MHz] | | | | | | |
| | | 1/2-3/2 | 3/2-5/2 | 5/2-7/2 | 7/2-9/2 | | | |
| ³⁵ Cl | 291 | 15.952(2) | - | - | - | 30.960 | 43.1 | Cl(1) |
| | | 19.173(1) | | | | 38.145 | 17.8 | Cl(2) |
| ²⁰⁹ Bi | 294 | 31.865 | 25.132 | 37.362 | 51.776 | 318.900 | 55.5 | |

Table 3. ^{35}Cl quadrupole resonance frequencies for phosphorus and antimony pentachlorides

| Compound | $\nu^{35}\text{Cl}$ | | | Assignment |
|------------------------------------|---------------------|--------|--------|--------------------|
| | [MHz] | | | |
| $(\text{PCl}_4)^+(\text{PCl}_6)^-$ | 28.395 | 28.711 | 29.027 | $(\text{PCl}_6)^-$ |
| | 30.060 | 30.457 | 30.572 | $(\text{PCl}_6)^-$ |
| | 32.279 | 32.384 | 32.420 | $(\text{PCl}_4)^+$ |
| | 32.602 | | | $(\text{PCl}_4)^+$ |
| PCl_5 | 29.242 | 29.274 | | axial |
| | 33.751 | | | equatorial |
| SbCl_5 | 30.18 | | | equatorial |
| | 27.85 | | | axial |
| $\text{Sb}_2\text{Cl}_{10}$ | 27.76 | | | equatorial |
| | 30.18 | | | axial |
| | 18.76 | | | bridging |

Table 4. ^{35}Cl quadrupole resonance frequencies and asymmetry parameters of some $\text{SnCl}_4\cdot 2\text{L}$ and $\text{SbCl}_5\cdot \text{L}$ complexes

| Complex | $\nu^{35}\text{Cl}$ | | Assignment |
|---|---------------------|------------|------------|
| | [MHz] | η [%] | |
| $\text{SnCl}_4\cdot 2\text{NC}_5\text{H}_5$ | 17.644 | 15.4 | - |
| | 17.760 | 15.4 | - |
| $\text{SnCl}_4\cdot 2\text{OPCl}_3$ | 19.030 | 11.7 | equatorial |
| | 19.794 | 11.1 | equatorial |
| | 21.132 | 2.3 | axial |
| $\text{SbCl}_5\cdot \text{OPCl}_3$ | 24.399 | 11.3 | cis- |
| | 25.821 | 2.5 | trans- |
| | 26.119 | 4.7 | cis- |
| | 27.314 | 4.9 | cis- |
| $\text{SbCl}_5\cdot \text{NCCCl}_3$ | 26.008 | 6.2 | cis- |
| | 26.313 | 10.3 | cis- |
| | 26.409 | 2.2 | trans- |
| | 27.297 | 11.2 | cis- |

Table 5. NQR spectral parameters of some non-transition and transition dimer halogenides

| Compound | $\nu(X_b)$ [MHz] | η_b [%] | $\nu(X_t)$ [MHz] | η_t [%] | ξ [deg] |
|-------------------|------------------|-----------------|------------------|-----------------|----------------|
| GaCl ₃ | 14.667 | 47.3 | 19.084 | 8.9 | 86.0 |
| | | | 20.225 | 3.4 | |
| GaI ₃ | 133.687 | 23.7 | 173.650 | 0.9 | 94.5 |
| | | | 174.589 | 2.8 | |
| AlBr ₃ | 97.945 | - | 113.790 | - | 82.0 |
| | | | 115.450 | - | |
| AlI ₃ | 111.017 | 18.1 | 129.327 | 0 | 93.5 |
| | | | 129.763 | - | |
| InI ₃ | 122.728 | 29.7 | 173.177 | 1.1 | 94.5 |
| | | | 173.633 | - | |
| NbCl ₅ | 13.290 | 58.8 | 7.330 | - | 101.3 |
| NbBr ₅ | 105.850 | 58.8 | 59.500 | - | 101.3 |
| WBr ₅ | 114.580 | 44.9 | 81.660 | - | 98.6 |

Table 6. The chemical names and substituents of the compounds studied

| No | COMPOUND | R ₁ | R ₂ | R ₃ | R ₄ |
|----|---|---|------------------|----------------|-------------------------------|
| 1 | imidazole | -H | -H | -H | -H |
| 2 | 2-nitro, 5-methylimidazole | -H | -NO ₂ | -H | -CH ₃ |
| 3 | 1-(2-hydroxyethyl)- 2-nitro-5methylimidazole (metronidazole) | -CH ₂ CH ₂ OH | -NO ₂ | -H | -CH ₃ |
| | 1-(2-carboxymethyl) ethyl -2-nitro-5-[2-(p-ethoxy- phenyl) ethenyl] imidazole | - CH ₂ CH ₂ OCOCH ₃ | -NO ₂ | -H | - CH=CHPhCH ₃ O |

Table 7. The quadrupole coupling constants and asymmetry parameters for imidazole derivatives

| No | T [K] | NITROGEN NUCLEUS | | | | | |
|----|----------|-----------------------------|--------|-----------------------------|--------|-----------------------------|--------|
| | | -N= | | -NR ₄ | | -NO ₂ | |
| | | $e^2Qq_{zz}h^{-1}$ [MHz] | η | $e^2Qq_{zz}h^{-1}$ [MHz] | η | $e^2Qq_{zz}h^{-1}$ [MHz] | η |
| 1 | 291 | 3.222 | 0.119 | 1.391 | 0.930 | - | - |

| | | | | | | | |
|---|-----|-------|-------|-------|-------|-------|-------|
| | 77 | 3.253 | 0.135 | 1.418 | 0.997 | - | - |
| 2 | 296 | 3.243 | 0.250 | 1.569 | 0.821 | 1.225 | 0.356 |
| | 193 | 3.249 | 0.249 | 1.546 | 0.878 | 1.244 | 0.360 |
| 3 | 296 | 3.299 | 0.150 | 2.467 | 0.317 | 0.936 | 0.381 |
| | 193 | 3.302 | 0.156 | 2.479 | 0.320 | 0.950 | 0.381 |
| 4 | 296 | 3.755 | 0.038 | 2.566 | 0.238 | 0.921 | 0.239 |
| | 193 | 3.779 | 0.039 | 2.565 | 0.238 | 0.931 | 0.230 |

Table 8. Population of the -NH-, -N=, -NO₂ bonds for imidazole and its derivatives

| No | -NH- | | | -N= | | -NO ₂ | | |
|----|----------------|-----------------|-----------------|-------|-----------------|------------------|-----------------|-------|
| | n _a | n _{NC} | n _{NR} | π | n _{NC} | π | n _{NC} | T [K] |
| 1 | 1.330 | 1.120 | 1.330 | 1.640 | 1.260 | - | - | 77 |
| | 1.340 | 1.140 | 1.330 | 1.640 | 1.270 | - | - | 293 |
| 2 | 1.350 | 1.129 | 1.330 | 1.657 | 1.556 | 1.072 | 1.182 | 193 |
| | 1.361 | 1.139 | 1.330 | 1.652 | 1.556 | 1.070 | 1.178 | 296 |
| 3 | 1.672 | 1.250 | 1.368 | 1.449 | 1.390 | 1.042 | 1.128 | 193 |
| | 1.669 | 1.250 | 1.366 | 1.452 | 1.394 | 1.041 | 1.126 | 296 |
| 4 | 1.648 | 1.250 | 1.340 | 1.430 | 1.384 | 1.045 | 1.117 | 193 |
| | 1.648 | 1.250 | 1.340 | 1.430 | 1.384 | 1.044 | 1.116 | 296 |

Nuclear Quadrupole Resonance (NQR) Spectroscopy

Gary P. Wulfsberg

Middle Tennessee State University, Murfreesboro, TN, USA

| | |
|------------------------------|----|
| Method Summary | 1 |
| 1 Introduction | 2 |
| 2 Technical Background | 3 |
| 3 Applications | 6 |
| 4 Abbreviations and Acronyms | 14 |
| 5 Further Reading | 14 |
| 6 References | 14 |

METHOD SUMMARY

Acronyms, Synonyms

- Nuclear Quadrupole Resonance Spectroscopy
- Quadrupole Resonance
- Zero-Field Nuclear Magnetic Resonance Spectroscopy.

Measured physical quantities

- NQR Frequency(ies) (ν) of quadrupolar nucleus ($I \geq 1$)
- temperature dependence of NQR frequency
- linewidths and relaxation times for NQR signals.

Information available

- nuclear quadrupole coupling constant (e^2Qq_{zz}) of the quadrupolar nucleus, which reflects the deviation of the electron distribution around quadrupolar nucleus from spherical symmetry, but includes the asymmetry of the nucleus itself;
- asymmetry parameter ($\eta = e^2Q_{xx} - e^2Q_{yy})/(e^2Qq_{zz})$ of the quadrupolar nucleus, which reflects the deviation of the electron distribution from axial symmetry;
- electric field gradient (EFG, q_{zz}) of the electron distribution around an atom, which measures its deviation from spherical symmetry, and does not include any asymmetry of the nucleus;
- approximate populations of valence orbitals of quadrupolar atom;
- approximate fractional covalent (σ) versus ionic (i) character of a bond, or multiple bond order, of bond(s) to quadrupolar atom; number of electrons transferred to or from quadrupolar atom; partial charge δ of the quadrupolar atom;
- number of chemically and crystallographically distinct quadrupolar nuclei in asymmetric unit of unit cell;
- presence of weak (secondary, noncovalent) bonding interactions to quadrupolar atom.

Information not available, limitations

- Very large frequency ranges may need to be searched (see Table 1, Column E), which may exceed the capabilities of a given NQR spectrometer.
- Unfavorable relaxation times, disorder, and paramagnetism at or near quadrupolar nucleus may cause the spectrum to be unobservable.
- Radio waves used for detection cannot penetrate deep within a metallic sample.

Examples of questions that can be answered

- Is there really a covalent bond of this quadrupolar atom to a nearby atom, even one in a neighboring molecule?
- What is the energy barrier to hindered rotation or fluxional behavior of a functional group bearing a quadrupolar atom?
- Is there a bomb in this suitcase?
- Is there a bomb under the clothing of, or inside the body of this passenger?
- Is there a landmine buried in this field?
- Does this package contain a significant amount of an illicit drug?
- Do we have the right crystalline modification of this compound?
- Is strain building up in this material?

Major advantages

- a nondestructive technique: all of the sample can be recovered
- extremely sensitive to weak (noncovalent, secondary) bonding interactions, which cause easily measured chemical shifts.

Major disadvantages

- Very large chemical shifts are possible, which require long times to scan (hours to days), and may require retuning circuitry or changing radio-frequency coils.

Sample constraints

- Usually the sample must be a microcrystalline solid, without any major disorder.
- The sample size requirements are large: at least about 0.5 g for heavy nuclei with high frequencies (100–1000 MHz, such as $^{79,81}\text{Br}$ and ^{127}I), but as much as 25 g for light nuclei with low frequencies (1–5 MHz, such as ^{14}N).

1 INTRODUCTION

Nuclear quadrupole resonance (NQR) spectroscopy is a method of sensitively characterizing the electronic environment of nuclei with nuclear spins $I \geq 1$. Such nuclei are nonspherical in shape and have electric quadrupole moments; commonly studied nuclei are confined to odd-numbered groups of the periodic table (Table 1). NQR spectra, unlike nuclear magnetic resonance (NMR) spectra (see *Nuclear Magnetic Resonance (NMR) Spectroscopy of Inorganic/Organometallic Molecules*), are measured without external magnetic fields (hence its synonym of zero-field NMR), because the energy levels of quadrupolar nuclei are principally determined not by their magnetic environments, but by their electronic environments. Samples are studied, not in solution, but mainly in the form of microcrystalline solids.

Since more nuclei have spins $I \geq 1$ than have $I = 1/2$ (all but 17 of the naturally occurring elements through uranium have at least one such isotope), and since inorganic chemists commonly are more interested in the electronic rather than the magnetic environment of a nucleus, the technique of NQR became popular soon after its discovery around 1950. Continuous-wave (CW) superregenerative NQR spectrometers (analogous to older NMR spectrometers) were used, which could search fairly wide frequency ranges automatically.

During the 1950s through 1970s many inorganic chemists used the technique to characterize the structure and bonding in polar covalent and covalent molecules and

network solids, coordination compounds, and organometallic compounds. Many types of bonding were studied: ionic, covalent, coordinate covalent, and weaker interactions such as hydrogen bonding and lattice forces. NQR proved much more sensitive to weak bonding interactions than did NMR or infrared (IR) spectroscopy, for example, although NQR required much larger samples.

NQR also offered another way of determining elements of crystal structure, such as the presence of bridging versus terminal atoms, number of crystallographically inequivalent molecules in the unit cell, and so on. However, X-ray crystallography subsequently improved vastly in quickness and ease of use, and supplanted this use of NQR.

NQR has its drawbacks. One fails to observe expected NQR signals much more frequently than expected NMR signals, since NQR relaxation times can be either too long or too short for effective detection of signals, especially using CW-NQR spectrometers, and especially for transition-metal nuclei and nuclei in ionic compounds. The search for an unknown NQR signal can take much longer than the search for an NMR signal: in NMR, one deals with chemical shifts and coupling constants of hertz, while in NQR, the frequency ranges (shifts) one needs to scan for a given nucleus may be many *megahertz*. Thus it is easy to see why NQR is much less frequently used than NMR.

Now pulse-Fourier Transform (pulse-FT) NQR instruments are commercially available, which allow signal averaging and improved sensitivity. They strongly resemble

Table 1 Abundant nuclei most commonly studied by NQR spectroscopy^(a)

| A Group. | B Element | C Isotope | D Abund. | E ν range MHz | F Spin | G High e^2Qq_{zz} MHz | H η | I Substance | J e^2Qq_0 MHz | K for orbital |
|----------|-----------|-----------|----------|-------------------|--------|-------------------------|----------|--|-----------------|---------------|
| 3 | La | 139 | 100 | 6–26 | 7/2 | 121.8 | 0.000 | La ₂ NiO ₄ | | |
| 3 | Lu | 175 | 97 | 17–195 | 7/2 | 691.5 | 0.615 | Lu ₂ (SO ₄) ₃ · 8H ₂ O | | |
| 5 | Nb | 93 | 100 | 1–21 | 9/2 | 117.29 | 0.190 | NbF ₅ | | |
| | Ta | 181 | 100 | 50–240 | 7/2 | 1796.5 | | Ta ₂ Cl ₁₀ | | |
| 7 | Mn | 55 | 100 | 9–24 | 5/2 | 78.92 | 0.061 | C ₅ Cl ₅ Mn(CO) ₃ | | |
| | Re | 187 | 63 | 27–300 | 5/2 | 833.555 | 0.143 | Re(CO) ₅ I | | |
| | Re | 185 | 37 | | 5/2 | | | | | |
| 9 | Co | 59 | 100 | 8–36 | 7/2 | 171.5 | 0.000 | (C ₅ H ₅) ₂ Co(ClO ₄) | | |
| 11 | Cu | 63 | 69 | 8–62 | 3/2 | 117.0 | 0.028 | Cu ₂ (C ₂ H ₃ O ₂) ₄ · 2H ₂ O | | |
| | Cu | 65 | 31 | | 3/2 | | | | | |
| 13 | B | 11 | 81 | 0.7–2.7 | 3/2 | 10.216 | 0.000 | B(CD ₃) ₃ | –11.83 | 2p |
| | B | 10 | 19 | | 3 | | | | –5.390 | 2p |
| | Al | 27 | 100 | 0.1–13 | 5/2 | 45.41 | 0.070 | Al(<i>t</i> -C ₄ H ₉) ₃ | –37.52 | 3p |
| | Ga | 69 | 60 | 7–81 | 3/2 | Ca. 162 | | Ga(CH ₃) ₃ | –125.045 | 4p |
| | Ga | 71 | 40 | | 3/2 | | | | –78.80 | 4p |
| | In | 115 | 96 | 7–212 | 9/2 | 1115.1 | 0.140 | In(CH ₃) ₃ | –899.105 | 5p |
| 15 | N | 14 | 100 | 0.1–6.0 | 1 | 6.333 | 0.788 | (CH ₃) ₂ NCl | –10 ± 4 | 2p |
| | As | 75 | 100 | 15–170 | 3/2 | | | (CH ₃)AsCl ₂ | –400 | 4p |
| | Sb | 121 | 57 | 7–254 | 5/2 | | | | +650 | 5p |
| | | 123 | 43 | | 7/2 | 884.43 | 0.000 | (C ₆ H ₅) ₃ SbCl ₂ | +830 | 5p |
| | Bi | 209 | 100 | 14–178 | 9/2 | 1069.9 | 0.020 | (C ₆ H ₅) ₃ BiCl ₂ | +1500 | 6p |
| 17 | Cl | 35 | 75 | 0–75 | 3/2 | –108.95 | 0.20 | Cl ₂ | +109.746 | 3p |
| | Cl | 37 | 25 | | 3/2 | | | | +86.510 | 3p |
| | Br | 79 | 51 | 0–445 | 3/2 | 765.85 | 0.20 | Br ₂ | –769.762 | 4p |
| | | 81 | 49 | | 3/2 | | | | –643.032 | 4p |
| | I | 127 | 100 | 0–940 | 5/2 | –2156 | 0.175 | I ₂ | +2292.712 | 5p |

^(a)Column headings: A = Group of periodic table; D = Percent abundance; E = NQR frequency(ν) ranges (MHz); G = One of highest observed quadrupole coupling constants (MHz); H = Asymmetry parameter corresponding to value in column G; I = Substance to which data in columns G and H apply; J = Quadrupole coupling constant for one valence electron in isotope in column C; K = Orbital occupied by valence electron in column J.

pulse-FT NMR spectrometers without the magnets, so they are much less expensive than modern NMR spectrometers. Indeed, some pulse-FT NMR spectrometers can be used as pulse-FT NQR spectrometers by disconnecting the magnets and making other adjustments. But pulse-FT NQR spectrometers (the only kind currently available) have some disadvantages as well as advantages as compared to continuous wave NQR (CW-NQR) spectrometers. Because of the large range of chemical shifts found in NQR, single pulses cannot be wide enough to cover the entire frequency range that needs to be scanned, so the circuit must then be retuned (normally manually) and run again in the new frequency range; CW-NQR spectrometer can cover broader frequency ranges without adjustments. Thus pulse-FT NQR spectrometers, which can accumulate spectra far more easily, in the end, may not give spectra any more quickly.

However, only pulse instruments can deal with the aforementioned difficulties associated with broad signals and unfavorable relaxation times. Therefore, some of the problems that inorganic chemists gave up on using CW-NQR to solve after the 1970s could now be solved with FT-NQR, especially using its new pulse sequences and enhanced data acquisition ability. Modern applications of pulse-FT NQR include studies of glasses, nondestructive

characterization of materials, studies of host-guest interactions and probes of host cavity symmetry and size in supramolecular chemistry,¹ and (using the great temperature sensitivity of NQR frequencies and linewidths) the studies of activation energies for hindered rotations and fluxional behavior of NQR-active groups such as *monohapto*-C₅Cl₅.² In certain situations NQR can provide information not easily obtained by other methods. In this review we try to highlight opportunities of this type, particularly for research problems for which one needs sensitive information on weak bonding or even noncovalent interactions involving quadrupolar nuclei.

2 TECHNICAL BACKGROUND

2.1 Direct Uses of NQR Frequencies

Like NMR, NQR spectra^{3,4} are detected by flipping nuclei using MHz-range radio-frequency waves; NQR frequencies can readily be measured to within a few kHz. Since NQR frequencies are *extremely* sensitive to small changes in the electronic environment of quadrupolar nuclei, they are

shifted by their environment over a range of a few or many MHz (Table 1, Column E). Thus virtually every compound has a unique set of NQR frequencies.

NQR frequencies are so sensitive to electronic environments that they are affected by charges in neighboring functional groups, neighboring molecules, and (especially) neighboring ions. Therefore, different polymorphs of compounds have different NQR frequencies, and phase transitions between polymorphs can be detected. Within a given crystalline modification of a compound, NQR spectra include distinct frequencies for each crystallographically distinct atom: as an extreme example, $\text{CCl}_4(\text{s})$ adopts a complex lattice with 16 crystallographically inequivalent chlorine sites. $\text{CCl}_4(\text{s})$ has 16 ^{35}Cl NQR frequencies averaging 40.64 MHz, with a *spectral width* between the highest and lowest frequency of 0.351 MHz. Spectral widths in covalent organochlorine compounds normally are limited to about 0.8 MHz. However, in a study of 11 clathrate compounds in which CCl_4 is the guest, the spectral widths exceeded this amount in three, being as large as 1.3 MHz in one case.⁵ Quadrupolar nuclei are very sensitive both to their electronic environments and to the polarizing effects of lattice ionic charges, so spectral widths can be larger in ionic compounds: we estimate up to at least 1.4 MHz in salts of chlorinated organic anions.⁶ These differences have historically been termed “crystal field effects”,⁷ although they have nothing to do with the crystal field theory in inorganic chemistry.

Consequently, NQR frequencies are useful for detecting and quantifying extremely weak noncovalent (secondary-bonding) interactions between molecules or ions (such as the host-guest interactions in CCl_4 clathrates). These weak secondary interactions will be a main emphasis of this article. However, since mere crystallographic inequivalence produces quite substantial spectral widths, one must use caution in concluding that small frequency shifts are due to what one chooses to call “noncovalent” or “secondary-bonding” interactions. (One might argue that NQR frequencies are too sensitive to their environment for their own good!)

2.2 Quantities Derived from NQR Frequencies

The number of NQR frequencies observed per crystallographically and chemically inequivalent atom depends on the spin I of the nucleus: each inequivalent $I = 3/2$ nucleus gives only one NQR frequency, while each $I = 1$ or $I > 3/2$ nucleus gives two or more frequencies. With two or more NQR frequencies, it is possible to calculate the two intermediate physical properties of interest. One is the *nuclear quadrupole coupling constant* e^2Qq_{zz} (or, removing the effect of the *quadrupole moment* Q of the nucleus, the *electric field gradient EFG* or eq_{zz}) which measures the deviation of the electronic environment from *spherical* (in practice, from a higher-order point group) symmetry. This depends on the *number of unbalanced electrons* around the nucleus (the number of electrons in the z direction minus the average of

the numbers in the x and y directions). (Thus, e^2Qq_{zz} for a chloride ion in an octahedral environment in the NaCl lattice is zero.) The other is the *asymmetry parameter* η , which falls between zero and one, and measures the deviation of the electronic environment from *axial* symmetry (in practice, threefold or higher symmetry), and relates to the difference in the numbers of electrons in the x and in the y directions. For the many spin-3/2 nuclei (Table 1, Column F) calculating these quantities requires additional data from single-crystal or other specialized measurements, or requires certainty that η is close to zero, as is normally found to be the case in covalent compounds in which the quadrupolar atom is a terminal atom, singly bonded to one other atom. Values of the e^2Qq_{zz} and η can also be determined experimentally in appropriate cases using microwave (*see Microwave Rotational Spectroscopy*), EPR (*see Electron Paramagnetic Resonance (EPR) Spectroscopy*), NMR (*see Nuclear Magnetic Resonance (NMR) Spectroscopy of Inorganic/Organometallic Molecules*), and Mössbauer (*see Mössbauer Spectroscopy*) spectroscopy, and using the perturbed angular correlation (PAC) method (*see Perturbed Angular Correlations of γ -rays (PAC) Spectroscopy*).

From atomic spectral or atomic beam measurements it is possible, in favorable cases, to measure the quadrupole coupling constants e^2Qq_0 of atoms in which there is one valence electron, or one hole in the valence-electron shell (Column J of Table 1). From this one can obtain the number of unbalanced electrons, and ultimately, the *populations of the valence orbitals* of the quadrupolar atom and its *partial charge*, δ .

Therefore, there is a more direct connection between valence orbital populations and NQR frequencies than there is with NMR frequencies, and indeed the Gaussian computational program allows for straightforward calculations of the electric field gradient.⁸ However, the *EFG* is especially sensitive to any nonsphericity of the core electrons (or inner lobes of the valence orbitals), which normal molecular-orbital computations tend to neglect or approximate, so that such computations seriously miss producing the experimental *EFG* values. More successful calculations have been obtained by using density functional theory (DFT) and by avoiding the pseudopotential method, which simplifies the core electron wave functions.⁹ These calculations give values of the *EFG* that correlate very well with the experimental ones for nitrogen and halogen atoms in a variety of bonding situations.

Often the Townes–Dailey approximation¹⁰ is used rather successfully. This approximation assumes that contributions to the *EFG* from nonsphericity of core electron and from lattice charge distributions offset each other. Then the *EFG* results from imbalances in valence electron populations. The calculations also show that the errors introduced by the approximations of the Townes–Dailey theory do not exceed 5%. Thus Townes–Dailey calculations generally do well in showing *trends* in quadrupole coupling constants or NQR frequencies.

Using the Townes–Dailey theory, a relationship of the NQR frequency of a single-bonded terminal unhybridized ^{35}Cl atom can be derived to the ionic character, i , of the bond to the chlorine atom, or to the partial charge of the chlorine atom, δ_{Cl} .

$$\begin{aligned} \nu(^{35}\text{Cl}) &= -\frac{1}{2}(1-i)e^2Qq_0 = -\frac{1}{2}(1-i)(109.746 \text{ MHz}) \\ &= 54.873(1 + \delta_{\text{Cl}}) \end{aligned} \quad (1)$$

$$\delta_{\text{Cl}} = -1 + \frac{\nu(^{35}\text{Cl})}{54.873} \quad (2)$$

Hence the chlorine NQR frequency is very sensitive to the ionic character of its single bond. In close agreement with the prediction from equation (1), the NQR frequency of $\text{Cl}_2(\text{s})$ is 54.247 MHz, while NQR frequencies for solid Group I halides are zero, expected both from their virtually complete ionic character and their high solid-state symmetry.

In Gordy's approach¹¹ the ionic character of a single bond to chlorine equals one-half of the difference in electronegativities of the chlorine, 3.16, and the atom to which it is bonded. Thus the NQR frequency of this chlorine atom is a strong function of the Pauling electronegativity, X_{P} , of the atom M bonded to chlorine:

$$\text{Theoretical } \nu(^{35}\text{Cl}) = 27.436 (X_{\text{P}} - 1.16) \quad (3)$$

$$\text{Empirical best fit } \nu(^{35}\text{Cl}) = 24.500 (X_{\text{P}} - 1.07) \quad (4)$$

Figure 1 shows the fit of predicted and observed NQR frequencies for other solid binary chlorides in which the chlorine is terminal and singly bonded; similar results can be obtained for bromine and iodine. For chlorine bonded to carbon ($X_{\text{P}} = 2.55$) these equations predict a frequency of 38.14 or 36.26 MHz, respectively. The observed NQR frequencies of $\text{R}_1\text{R}_2\text{R}_3\text{C}-\text{Cl}$ compounds span a wider range of about 33–42 MHz: they are strongly influenced by the inductive (electron-withdrawing) effects of the R groups and on any other interactions that may be present with those groups.

If the terminal atom is multiply bonded to its neighbor, slightly different equations result. The π bonding results in a reduction of population(s) of the chlorine p_{π} orbitals below 2.00 electrons, to a value closer to the population of the chlorine p_{σ} orbital. Therefore the quadrupole coupling constant and the NQR frequency of the chlorine atom are reduced.

If the atom is doubly bonded, a nonzero asymmetry parameter η also results; if the atom is triply bonded, there is axial symmetry and η returns to zero. For the case of doubly bonding the π bond order can be calculated if η can be determined:

$$\pi = \left(\frac{2}{3}\right) \eta \left(\frac{e^2Qq_{zz}}{e^2Qq_0}\right) \quad (5)$$

In practice double bonding is appreciable for chlorines bonded to aromatic rings ($\eta > 0$), and partial triple

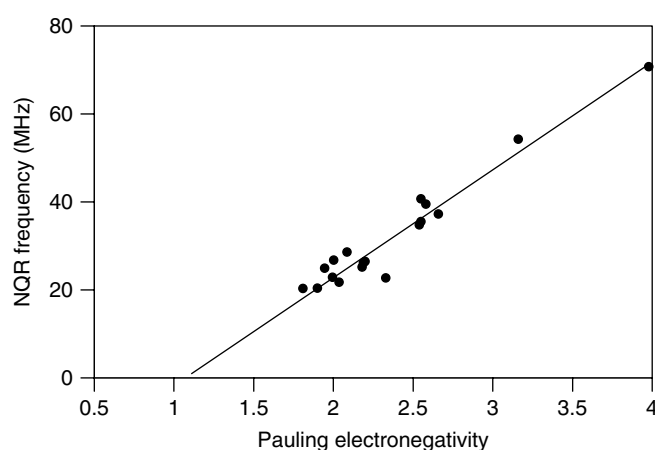


Figure 1 Average ^{35}Cl NQR frequencies (MHz) of terminal singly bonded binary element chlorides, measured in the solid state at 77 K, as a function of the Pauling electronegativity of the element

bonding is quite substantial for the chlorides of early transition metals having vacant d orbitals to which the p_{π} electrons are donated.¹² Thus such chlorides have been deleted from the correlation of Figure 1. For example, the electronegativity of Ti, 1.54, leads us to expect a ^{35}Cl NQR frequency of 10.42 MHz (equation 3) or 11.51 MHz (equation 4). In practice, the average frequency for TiCl_4 is 6.052 MHz. The cyclopentadienide anion, C_5H_5^- , is a much better π -donor than chloride, however, so that when it is substituted for Cl^- the π -donating ability of Cl^- is suppressed. Consequently the average frequencies¹³ grow closer to the predicted values: $(\text{C}_5\text{H}_5)\text{TiCl}_3$, 8.076 MHz, and $(\text{C}_5\text{H}_5)_2\text{TiCl}_2$, 11.971 MHz.

If the quadrupolar atom is bonded to more than one other atom (i.e., it is bridging or even central to the complex), the Townes–Dailey theory can be applied to give a different equation for each geometry at the bridging or central atom; a nonzero η generally results. We will consider in detail only two-coordinate bridging quadrupolar atoms. In this case, the two bonds to the bridge can be equivalent (symmetrical bridging): the NQR frequency then depends sensitively on the interbond angle at the quadrupolar atom.

Or (in the case we will emphasize), one of the two bonds may be a normal covalent bond (with a high covalent bond order) and the other “bond” is a weak (secondary) Lewis base donation of an electron pair to a nearby Lewis acid. Then NQR can be used to estimate the number of electrons that are transferred from the halogen lone pair in the valence p_y orbital to (or polarized toward) the site of Lewis acidity; we can also refer to this quantity as the secondary covalent bond order σ_{B2} . If the asymmetry parameter η is known, σ_{B2} can be calculated from it using an equation analogous to equation (5):

$$\sigma_{\text{B2}} = \left(\frac{2}{3}\right) \eta \left(\frac{e^2Qq_{zz}}{e^2Qq_0}\right) \quad (6)$$

More frequently η is not known. However, it is still possible to proceed if the NQR frequency of the donor atom is known both for the terminal halogen in the free ligand and for the otherwise-equivalent bridged halogen atom in the complexed ligand. For the terminal (one-coordinate) halogen atom we designate its NQR frequency as ν_T and its covalent bond order as σ_T ; for the bridged halogen atom we designate its NQR frequency as ν_B and its primary covalent bond order as σ_{B1} . For ^{35}Cl the approximate Townes–Dailey equation that results is:

$$\frac{(\nu_T - \nu_B)}{54.873} = (\sigma_T - \sigma_{B1}) + \frac{1}{2}\sigma_{B2} \quad (7)$$

To solve this equation for σ_{B2} we need to know the relationship of σ_T and σ_{B1} , that is, whether the primary covalent bond order is altered upon coordination. For halocarbons as ligands there is generally no detectable lengthening of the bond noted by X-ray crystallography, which might justify the conclusion that $\sigma_T \approx \sigma_{B1}$. If so, we have:

$$\sigma_{B2} = \frac{2(\nu_T - \nu_B)}{54.873} \quad (8)$$

In some secondary-bonding situations the primary bond is lengthened and therefore, σ_T and σ_{B1} are presumably not equal. This case will be considered in Section 3.2.

3 APPLICATIONS

There have been several modern developments in pulse-FT NQR spectrometry dealing with important practical applications which are not necessarily considered to be inorganic:

- $^{63,65}\text{Cu}$ and ^{139}La NQR have been extensively used to study high-temperature superconductors while they are in the superconducting state, and the magnetic fields needed for NMR are being excluded.¹⁴
- ^{14}N NQR is used to detect, identify, and quantify amounts of illicit drugs hidden in suitcases, packages, or the body, without having to open the container.
- ^{14}N NQR is used to detect, identify, and quantify amounts of explosives hidden in suitcases, packages, on the body, or in buried landmines, without having to put the sample inside the instrument.¹⁵
- NQR (a proprietary type) is being investigated for use to detect strains that may develop in aerospace composite structures before these structures can fail and lead to crashes.
- ^{14}N and ^{35}Cl NQR are being investigated for uses in the pharmaceutical industry for measuring quantities of medicines in containers without opening them, and for determining whether, during the manufacturing process,

the proper polymorph of the pharmaceutical is being produced.¹⁶ (Different polymorphs of drugs can have different stabilities and bioavailabilities.)

In this article we emphasize modern uses of NQR spectroscopy in inorganic chemistry, particularly those involved with characterizing relatively weak bonding and noncovalent interactions. We divide them according to the bonding situation in which the quadrupolar nucleus is found, beginning with terminal (one-coordinate) atoms, for which Townes–Dailey equations (1) through (5) apply, followed by bridging (two-coordinate) atoms, for which equations (6) through (8) apply, followed by brief mention of some cases of central (three-coordinate or higher) atoms, for which a variety of Townes–Dailey equations can be derived but will not be described.

3.1 Applications Involving Terminally Single-bonded Halogen Complexes and Organometallic Compounds

3.1.1 Relativistic Effects

The s and p orbitals of heavy atoms undergo relativistic contraction: an electron in such an orbital is accelerated to a speed near that of light.¹⁷ The electron increases in mass, and consequently is pulled closer to the nucleus: the electronegativity of the atom therefore increases. This effect reaches a maximum in elements close to gold, which therefore is predicted to show an unusually high electronegativity. The Pauling electronegativity of Au is the highest of any metal, 2.54, and is close to that of iodine, 2.66. Correspondingly, the terminal chlorines of Au_2Cl_6 have the highest ^{35}Cl NQR frequencies found in any metal chlorides, 36.094, and 33.401 MHz¹⁸; these values are similar to those found in I_2Cl_6 , 35.680, and 33.916 MHz. (Much lower NQR frequencies would be predicted using the Allred–Rochow electronegativity of Au, 1.42, which is derived from the nonrelativistic approximations of Slater's rules.¹⁷) The chemistry of gold indeed shows remarkable similarities to that of iodine (e.g., Au forms Au^-). Relativistic effects on EFGs for elements through Np have been calculated.¹⁹

3.1.2 Effects of Nearby Charges in Haloacetate Salts

The properties of the familiar chloroacetate ion, $\text{ClCH}_2\text{COO}^-$, are surprisingly cation dependent: among group 1 chloroacetates in the solid state, thermal decomposition to metal chloride and the polymer poly(glycolide), $(\text{CH}_2\text{CO}_2)_n$,²⁰ does not occur in the lithium salt, but occurs at progressively lower temperatures with larger cations; the cesium salt decomposes at room temperature (Table 2). As noted earlier by Guibé,²¹ the ^{35}Cl NQR frequencies in group 1 chloroacetates decrease for larger cations—for example, by 3.46% from the Li^+ salt to the K^+ salt. Ab initio calculations⁶

Table 2 NQR frequencies and decomposition temperatures of group 1 chloroacetates and hexachlorostannates

| Chloroacetates M ⁺ ClCH ₂ CO ₂ ⁻ Layer lattice type | | | Hexachlorostannates (M ⁺) ₂ SnCl ₆ ²⁻ Cubic antiferroite lattice | | |
|---|---|---|---|--|---|
| Cation | NQR ν MHz at 77 K ^(a) | Decomp. Temperature (K) ^(b) | Cation | NQR ν MHz at 298 K ^(c) | Decomp. Temperature (K) ^(d) |
| Li ⁺ | 35.254 | 484 | Li ⁺ | | 415 |
| Na ⁺ | 34.794 | 471 | Na ⁺ | | 457 |
| K ⁺ | 34.11 | 430 | K ⁺ | 15.064 | 729 |
| Rb ⁺ | 33.82 | 393 | Rb ⁺ | 15.60 | 760 |
| Cs ⁺ | | <298 | Cs ⁺ | 16.05 | 785 |
| Me ₄ N ⁺ | | | Me ₄ N ⁺ | 16.663 | |
| | | | Et ₃ NMe ⁺ | 16.844 | |

^(a)Source: Ref. 21.

^(b)Source: Ref. 20.

^(c)Sources: T. B. Brill, Z. Z. Hugus, Jr., and A. F. Schreiner, *J. Phys. Chem.*, 1970, **74**, 2999–3002; D. Borchers and A. Weiss, *Ber. Bunsen-Ges. Phys. Chem.*, 1989, **93**, 559–568.

^(d)Source: T. Janiak, I. Nikel, and J. Blazejowski, *J. Therm. Anal.*, 1990, **36**, 2205–2210.

on symmetrically chelated ClCH₂COO-M systems predict a 3.24% drop in electric field gradients (hence NQR frequencies) from the Li⁺ salt to the K⁺ salt. These calculations and the NQR data suggest that the Cl atom in the chloroacetate ion carries substantially more negative charge in salts of larger, less polarizing cations, and hence, is more readily lost as chloride ion. It should be noted that haloacetate salts typically have layer structures, in which the nearest neighbors of the halogen ends of the anions include no metal cations to attract neighboring layers of anions close together.

3.1.3 Effects of Nearby Charges in Halometallate Salts

In contrast, the thermal stability and NQR frequencies increase in hexahalometallate salts of larger group 1 cations (Table 2).²² The trend in stability limits the usefulness of hexahalometallate ions as weakly coordinating anions, since they are easily broken down into MX₄, and so on, and group I MX by typical small or more highly charged cations. Hexahalometallate salts have typical ionic structures, in which anions and cations alternate, and halogen atoms have group 1 cations and chlorines of neighboring anions as neighbors. Due to the large numbers of electrons, the theoretical analyses of these trends have involved point-sphere and soft-sphere²³ along with MS-X α ²⁴ calculations. The latter two types of calculations successfully give the trend of increasing EFGs with increasing cation radius, and indicate that the gradient due to the lattice is responsible (the lattice gradient partially opposes the EFG due to the Sn–Cl bond). There is a good correlation of ³⁵Cl NQR frequencies with interionic chlorine–chlorine distances and with Born repulsive potentials $e^{-r/\rho}$ (r is the Cl–Cl interionic distance) in hexachlorostannates.²⁵ The calculations are consistent with the changes in the lattice EFGs due to changing polarization of the chlorine p_{x,y} orbitals as they are drawn into closer contact with chlorine atoms in adjacent ions in salts of smaller group

1 cations. The calculations tend to refute another possible explanation: that smaller cations may polarize the Sn–Cl σ bond more toward chlorine.

3.1.4 Effects of Nearby Charges in Organosilicon Compounds

The electronegativity of silicon is well below that of carbon; consequently organosilyl chlorides R₃SiCl have lower ³⁵Cl NQR frequencies (16–20 MHz) than corresponding organic halides R₃CCl (33–42 MHz). We might expect the same trend if a –CH₂– group were to be inserted in the element–chlorine bond. But the opposite is, in fact, observed:²⁶ (CH₃)₃SiCH₂Cl (34.320 MHz) > (CH₃)₃CCH₂Cl (33.015 MHz); H₃SiCH₂Cl (34.3 MHz) > H₃CCH₂Cl (32.646 and 32.759 MHz); Cl₃SiCH₂Cl (36.786 MHz) > Cl₃CCH₂Cl (36.40 MHz). Computations suggest that the chlorine 3p_z orbital population in (CH₃)₃CCH₂Cl is anomalously higher (0.960 e⁻) than the chlorine 3p_z population in (CH₃)₃SiCH₂Cl (0.948 e⁻), while the corresponding chlorine 3p_{x,y} populations are virtually identical. It was concluded²⁷ that the direct cause of the anomalous frequency raising is due to the polarizing effect of the nearby partially positive (CH₃)₃Si (and H₃Si) groups, which polarize the CH₂–Cl bond electrons toward CH₂. Measurements of η for some compounds of this type give values near zero. This and the calculations are inconsistent with earlier suggestions that this ‘‘alpha effect’’²⁸ is due to electron donation from the Cl 3p_x orbital to a vacant Si 3d orbital, creating some Si=Cl double bond character.

3.1.5 Cis and Trans Influences in Substituted Halometallate Anions

Ligands in octahedral complexes alter the bonding to ligands that are trans- to them in ways that are different

Table 3 NQR data illustrating *cis* and *trans* influences in halo complexes

| a. Halogens <i>trans</i> to the Substituent (Distances, NQR Frequencies, Charges) | | | | | | |
|--|---|---|---|--|---|---|
| Halo Anion | $d(\text{M}-\text{Cl})$, pm <i>trans</i> -Cl | $d(\text{M}-\text{Br})$, pm <i>trans</i> -Br | NQR ν <i>trans</i> -Cl | NQR ν <i>trans</i> -Br | Charge per <i>trans</i> -Cl | Charge per <i>trans</i> -Br |
| OsX ₆ ²⁻ | 240.0 | | 16.84 | 111.80 | -0.57 | -0.53 |
| Os(NO)X ₅ ²⁻ | 238.6 | 252.1 | 14.10 | 91.08 | | |
| OsNX ₅ ²⁻ | 260.5 | | 7.00 | 44.95 | -0.87 | -0.86 |
| OsNX ₄ ⁻ | | | | | | |
| SnX ₆ ²⁻ | 242.2 | 260.5 | 16.68 | 115.07 | -0.70 | -0.64 |
| Sn(Alk)X ₅ ²⁻ | 241.0 | 256.6 | 18.04 | 130.79 | -0.67 | -0.58 |
| b. Halogens <i>cis</i> to the Substituent (Distances, NQR Frequencies, Charges) | | | | | | |
| Halo Anion | $d(\text{M}-\text{Cl})$, pm <i>cis</i> -Cl ₄ | $d(\text{M}-\text{Br})$, pm <i>cis</i> -Br ₄ | NQR ν <i>cis</i> -Cl ₄ | NQR ν <i>cis</i> -Br ₄ | Charge per <i>cis</i> -Cl ₄ | Charge per <i>cis</i> -Br ₄ |
| OsX ₆ ²⁻ | 240.0 | | 16.84 | 111.80 | -0.57 | -0.53 |
| Os(NO)X ₅ ²⁻ | 238.0 | 251.9 | 18.15 | 122.10 | | |
| OsNX ₅ ²⁻ | 236.2 | | 20.40 | 140.50 | -0.62 | -0.56 |
| OsNX ₄ ⁻ | 231.0 | 245.7 | 22.26 | 149.50 | -0.59 | -0.53 |
| SnX ₆ ²⁻ | 242.2 | 260.5 | 16.68 | 115.07 | -0.70 | -0.64 |
| Sn(Alk)X ₅ ²⁻ | 251.6 | 269.9 | 12.30 | 80.55 | -0.77 | -0.73 |
| c. Iodides <i>cis</i> and <i>trans</i> to the Substituent (Distances, NQR Quadrupole Coupling Constants) | | | | | | |
| | $d(\text{M}-\text{I})$, pm <i>cis</i> -I ₄ | $d(\text{M}-\text{I})$, pm <i>trans</i> -I | NQR $e^2 Qq_{zz}$ <i>cis</i> -I ₄ | NQR $e^2 Qq_{zz}$ <i>trans</i> -I | | |
| OsX ₆ ²⁻ | | | 942.33 | 942.33 | | |
| Os(NO)X ₅ ²⁻ | 271.9 | 274.0 | 1033.50 | 782.20 | | |
| OsNX ₅ ²⁻ | | | | | | |
| OsNX ₄ ⁻ | | | 1366.50 | | | |

Source: Ref. 29.

from the effects on ligands that are *cis*- to them.²⁹ This effect shows up through changes in bond lengths, but even more sensitively through changes in NQR frequencies. Alkyl groups are more strongly electron donating than halo groups due to electronegativity effects, while nitrido ions ($\equiv\text{N}^{3-}$) donate electrons not only via σ bonds, but also via two π bonds, so are also more strongly electron donating than halo groups. The nitrosyl ligand ($\text{N}\equiv\text{O}$) falls between nitrido and halo ligands in this respect.

The effects on halo groups depend, however, on whether the central metal ion of the complex is from the d block or the p block. In complexes of the type $[\text{OsLX}_5]^{2-}$, when L is changed from being another X⁻ to being NO and then to being N³⁻, the effects on bond lengths and especially NQR frequencies are dramatically different for the four halogens *cis* to L as compared to the unique halogen that is *trans* to L. Data are shown in Table 3 for osmium chloro and bromo complexes of these ligands (it must be noted that the oxidation state of Os also changes during these substitutions). The chloro- or bromo-ligand *trans* to the new nitrido experiences an 8.5% increase in bond length, a 60% decrease in NQR frequency, and a 53% increase in partial charge δ (as computed from NQR frequencies). The effects on the four *cis* ligands are much more modest: a 1.6% decrease in bond length, a 21–26% increase in NQR frequency, and a 6–9% increase in δ . We note that these *cis* and

trans effects manifest themselves both in NQR and in X-ray crystallographic data, but more dramatically in the NQR data.

Table 3 also shows data for $[\text{SnLX}_5]^{2-}$ complexes, in which L is changed from being another X⁻ to being a much more electron-donating alkyl group (ethyl or butyl). The effects in these p-block complexes are opposite to those seen above for the d-block element Os: when the alkyl ligand is introduced, the *trans*-halogen atom experiences a 0.5–1.5% decrease in bond length, an 8–14% increase in NQR frequency, and a 4–9% decrease in δ . Clearly the *trans* bond is strengthened in tin complexes but weakened in osmium complexes. In the tin complexes the *cis* ligands experience the largest, not the smallest effects: a 4% increase in bond length, a 27–30% decrease in NQR frequency, and a 10–14% increase in δ .

3.1.6 Trihalide Ions

Bromine and iodine atoms can be at the center of linear (two-coordinate) complexes when in the familiar trihalide ions, Br₃⁻ and I₃⁻. NQR data are then available on all atoms in the complex,^{30,31} and can be analyzed to show the charge distribution within the ion using equations corresponding to equation (2) and a related equation for the central halogen atom. When these simple Townes–Dailey equations presume

neither the involvement of halogen s nor halogen d orbitals, it is found that the totals of the three charges in all cases add up to sums (in practice, from -0.94 to $-1.06 e^-$) close to the actual -1 charge on the trihalide ion. Although this could be due to fortuitous cancellation of the opposing effects of s and d hybridization, this seems unlikely since the conclusion holds for all 13 salts studied. In all cases the central halogen atom is computed to have a small *positive* partial charge of $+0.04$ – $+0.08$, while the terminal halogen charges average close to -0.50 . This is consistent with three-centered, four-electron bonding, with the highest occupied molecular orbital being localized on the two outer (terminal) halogens.

However, the negative charge is not always equal on the two terminal halogen atoms. With very large cations (tetramethylammonium through tetrabutylammonium), each terminal bromine or iodine atom carries the same, or nearly the same charge of $-0.50 e^-$ each. But with the smaller Tl^+ , Cs^+ , Rb^+ , and NH_4^+ cations, one halogen atom carries most of the negative charge. For the extreme case, NH_4Br_3 , one bromine atom has only a -0.18 charge while the opposite bromine atom bears a large -0.87 charge. The bond distances are all long, since the covalent bond orders are less than one: in CsBr_3 the shorter Br–Br bond distance is 244 pm and the longer 270 pm, as compared to the sum of Br covalent radii, 228 pm. Clearly, in such a case the two Br–Br bonds are unequal in covalent bond order: in this case it seems to be appropriate to call the bond to the second Br atom a *secondary bond*, and one might represent the bonding as $\text{Br}-\text{Br}^{\cdots}\text{Br}^-$.

3.2 Applications Involving Secondary Bonding of Halogens to Metal Ions

Weak (“noncovalent”) interactions between molecules are currently of great interest in chemistry, not only in biochemistry (e.g., the study of enzyme–substrate bonding) but in the study of—host–guest interactions and crystal engineering, for example. (The very important phenomenon of hydrogen bonding falls in this category, but will not be considered here.) In the chemistry of halocarbons, metal halides, and even the halogens themselves, such bonding (to metal atoms or ions, or even other molecules of the same type) was originally overlooked, but is increasingly being found to be of interest. The earliest focus on it was perhaps in the review of Allcock, who termed such interactions *secondary bonding*.³²

Secondary bonds are characterized crystallographically by bond lengths that are longer than the sums of covalent radii of the atoms involved, but are shorter than the sums of van der Waals radii. However, van der Waals radii are difficult to determine, since one must first be assured that there is, in fact, no bonding in the direction in which the nonbonded distances are measured.

For example, solid halocarbons commonly pack with halogen–halogen distances that are less than the sums of their van der Waals radii. This raises questions as to whether the van der Waals radii are incorrect, or differ in different

directions around an organohalogen atom, or whether the radii are correct, and the halocarbon molecules are in fact bonding to each other via *halophilic* interactions.³³

Furthermore, secondary bond distances vary widely, even among chemically equivalent bonds in the same complex (e.g., from 264.0 pm to 292.6 pm for $\text{Ag}^{\cdots}\text{Cl}$ contacts in $\text{Ag}[\text{CB}_{11}\text{H}_6\text{Cl}_6]^{34}$). One wonders whether these differences signify any difference in secondary bond strength or bond order, or whether secondary bonding involves such a shallow potential well that the differences merely represent variations in what is needed to achieve optimal solid-state packing.

Hence confirmation by another method is very helpful in determining whether a long metal–donor atom contact actually signifies secondary bonding and involves coordinate covalent bond formation. Most spectroscopic methods cannot reliably detect or interpret such subtle bonding interactions, but halogen NQR spectroscopy offers great promise here.

Even in the solid halogens themselves, halophilic secondary interactions (donation from a lone pair of electrons on one X_2 molecule to the empty σ^* orbital of another) occur between diatomic molecules in the same layers, giving interatomic distances much shorter within layers than between layers, and a lengthened σ bond in the case of I_2 . This destroys the axial symmetry of the X_2 molecule, so that they have nonzero asymmetry parameters (Table 1, Column H): $\eta = 0.20$ for Cl_2 and for Br_2 ; $\eta = 0.175$ for I_2 .

Secondary bonding of halogens in one molecule to metal or metalloid atoms in a neighboring molecule is a common feature in the chemistry of the halides of the heavier elements of the p- and late d blocks. With such weak interactions, the angle between the shorter primary bond in the molecule and the secondary bond to the metal center in the next molecule is normally in the range of 90° – 109° . If there is one secondary interaction per halogen atom, and if the bond angle is taken as 90° , as discussed in Section 2.2 the situation from the halogen atom’s point of view is similar to that in a double bond to the halogen, which involves a stronger (primary) σ bond using the p_z orbital and a weaker (secondary) π bond involving the p_y orbital. The consequence of such bonding is also similar: there is a nonzero asymmetry parameter, and a lowering of the quadrupole coupling constant and NQR frequency of the halogen atom (as suggested by equation (8)).

An analysis was made of 15 such cases of secondary bridging halogen atoms, primarily among adducts of HgI_2 and SbCl_3 .³⁵ Values of η for these adducts ranged from 0.057 in SbCl_3 to 0.18 in BiCl_3 and AsI_3 ; the resulting secondary bond orders σ_{B2} computed using equation (6) ranged from 0.041 in SbCl_3 to 0.071 in AsI_3 . For these adducts the Sb–halogen and Hg–halogen bonds do lengthen slightly upon coordination, so that the approximation of equation (8) is not justified. For seven of these adducts for which η , ν_{T} , and ν_{B} were all known, it was found that typically, about one-third of the electronic effect of secondary bonding is compensated by an alteration of the primary bonding. This gives a moderate alteration of

equation (8).

$$\sigma_{B2} = \frac{2.4(\nu_T - \nu_B)}{54.873} \quad (9)$$

These calculations, of course, are subject to the usual limitations of Townes–Dailey theory, as well as the assumption that the bond angle is effectively 90° . So they are most likely useful to show, not absolute values of σ_{B2} , but periodic trends in those values.

3.2.1 Halocarbons as Ligands

For decades inorganic chemists assumed that chlorocarbons could safely be used as noncoordinating solvents for reactions of metal ions and complexes, but this view is no longer tenable,³⁶ particularly since the work of Strauss and others on Ag^I complexes of dichloromethane and related halocarbons.³⁷ As an example, they prepared the complex $[\text{Ag}(1,2\text{-C}_2\text{H}_4\text{Cl}_2)(\text{OTeF}_5)]_2$, with chelating chlorocarbons ligands having $\text{Ag}\cdots\text{Cl}$ secondary bond distances of 262.4–300.0 pm, longer than the sums of Ag and Cl covalent radii, 251 pm, but well within the sums of van der Waals radii, 340–350 pm. In this complex the ^{35}Cl NQR frequency of 1,2- $\text{C}_2\text{H}_4\text{Cl}_2$, 34.361 MHz, is replaced by four frequencies between 31.700 and 32.036 MHz. The average $(\nu_T - \nu_B)$ is 2.513 MHz, so that σ_{B2} is 0.19 according to equation (8) or 0.22 according to equation (9). If these numbers are not too far off due to the approximations in the theory, the secondary bond order is about 20% that of a full covalent bond (as in Cl_2); qualitatively this seems plausible since the $\text{Ag}\cdots\text{Cl}$ distance is not so much longer than that expected for a covalent Ag–Cl bond. No value of η was obtained for these complexes.

The asymmetry parameter was measured for the intramolecularly coordinated organochlorine atom in the compound $\text{ClCH}_2\text{CH}_2\text{CH}_2\text{SnCl}_3$,³⁸ which has a five-coordinate tin atom with the organochlorine atom in an axial position, showing an $\text{Sn}\cdots\text{Cl}$ distance of 327.9 pm, intermediate between the 239-pm sum of covalent radii and the 400-pm sum of van der Waals radii. The ^{35}Cl NQR frequency for the organochlorine is 31.750 MHz, considerably below the value typical for longer-chain $\text{Cl}(\text{CH}_2)_n\text{X}$ compounds with $n \geq 3$, 33.1 MHz. The application of equations (8) and (9) gives values for σ_{B2} between 0.049 and 0.059. The value measured for η for this chlorine was 0.087 ± 0.020 , which when used with equation (6) gives us $\sigma_{B2} = 0.034 \pm 0.008$, in rough agreement with the values obtained using equations (8) and (9).

Iodocarbons are expected to be softer bases than chlorocarbons, so should complex more strongly to the soft Ag^+ cation; Powell and others have found the synthesis of iodocarbon complexes of Ag^+ to be more facile and commonly achieved than the syntheses of chlorocarbon complexes; the iodocarbon ligands in these complexes tend to be bridging

rather than chelating. For example, in $[\text{Ag}(\text{I}_2\text{CH}_2)_2](\text{PF}_6)$ the average $\text{Ag}\cdots\text{I}$ distance is 285.9 pm, only 0.9 pm longer than the sum of covalent radii, while the C–I bond lengths in such complexes is 211 pm, very slightly longer than the normal C–I bond length, 210 pm. The average C–I–Ag bond angle is 101.5° . For purposes of comparison, in diphenyliodonium salts (in which iodine is symmetrically bridging) the C–I bond lengths are 207–210 pm, and the C–I–C bond angles are 91.8° – 93.2° .³⁹

For $[\text{Ag}(\text{I}_2\text{CH}_2)_2](\text{PF}_6)$ the average e^2Qq_{zz} was 1744 MHz, below the 1897 MHz found in the free ligand, and η for iodine in the silver complex was quite substantial, 0.32. For diphenyliodonium salts e^2Qq_{zz} values range from 1944 to 1970 MHz, above the 1822 MHz average for $\text{C}_6\text{H}_5\text{I}$, and η for iodine in the iodonium salts is also quite substantial, 0.369–0.395.⁴⁰ (The values of η in these two free ligands are much smaller, 0.027 and 0.069, respectively.)

If one assumes that the $\text{Ag}\cdots\text{I}$ bond in $[\text{Ag}(\text{I}_2\text{CH}_2)_2](\text{PF}_6)$ is secondary, with no sp hybridization, substitution of the observed η in equation (6) gives a value for σ_{B2} of 0.162; this corresponds to the donation of the slight δ found in neutral CH_2I_2 , $0.15 e^-$, to Ag^+ to give a neutral iodine atom in the complex. However, use of the quadrupole coupling constants of the free and complexed ligand in equations analogous to equations (8) or (9) give significantly different σ_{B2} values of 0.067 and 0.080.

Because the $\text{Ag}\cdots\text{I}$ distance is so close to the sum of covalent radii, one may alternately assume that the $\text{Ag}\cdots\text{I}$ bond is a full covalent bond, not a secondary bond. If we then call the C–I–Ag bridging interaction ‘‘symmetrical’’, the covalent Ag–I bond order can be computed from the equation

$$\sigma_{B2} = \left(1 + \frac{\eta}{3}\right) \left(\frac{e^2Qq_{zz}}{e^2Qq_0}\right) \quad (10)$$

and the value of σ_{B2} is computed to be 0.84, which is virtually identical to the C–I covalent bond order in the free CH_2I_2 ligand, 0.85. This then puts a large δ of +0.68 on the iodine atom, which is broadly comparable to the δ values found in iodonium ions (+0.78 – +0.81).⁴¹ (However, contributions to EFG and η from the ionic lattice forces have not been taken into account; these could be significant.) With the assumption that the iodine atom in this complex undergoes sp hybridization that is set by the bond angle θ , the Townes–Dailey theory predicts:

$$\eta = -3 \cos \theta \quad (11)$$

From the observed asymmetry parameter $\eta = 0.32$, one calculates an interbond angle $\theta = 96^\circ$, which is in the vicinity but not identical to the observed internuclear angle of 101.5° . It is unfortunate that the atoms involved are so heavy, as more detailed molecular-orbital calculations would help clarify whether the Ag–I interaction is secondary, fully covalent, or somewhere in between.

3.2.2 Chloroacetates and Chlorophenolates as Cl-Donor Ligands

Weak $\text{Cl}\cdots\text{M}$ secondary bonding is likely to be stabilized if the secondary bond completes the formation of a chelate ring, as in the case of $\text{ClCH}_2\text{CH}_2\text{CH}_2\text{SnCl}_3$ discussed previously. The crystal structure of calcium chloroacetate,⁴² $\text{Ca}(\text{ClCH}_2\text{CO}_2)_2\cdot\text{H}_2\text{O}$, involves one of the two chlorines in a chelate ring with a $\text{Cl}\cdots\text{Ca}^{2+}$ contact of 320.6 pm, which is long compared to the $\text{Cl}\cdots\text{Ca}^{2+}$ distance of 274.1 pm in $\text{CaCl}_2\cdot 4\text{H}_2\text{O}$ (the van der Waals radius of Ca is unavailable for computing that sum). Because of the large difference in electronegativities and hard-soft properties, the $\text{Cl}\cdots\text{Ca}^{2+}$ secondary interaction is not expected to be coordinate covalent, but is more likely to be of an ion-dipole type. The crystal structure of dimeric silver chloroacetate,⁴³ $\text{Ag}_2(\text{ClCH}_2\text{CO}_2)_2$, shows interdimer coordination of all chlorines to silver at a distance of 290.3 pm, which exceeds the sum of Ag and Cl covalent radii, 251 pm, but is well under the 340–350 pm sum of van der Waals radii; covalent secondary bonding of soft Ag and Cl is considerably more likely here. The ³⁵Cl NQR spectrum²¹ of $\text{Ca}(\text{ClCH}_2\text{CO}_2)_2\cdot\text{H}_2\text{O}$ shows no significant difference between the free and coordinated chlorines: 34.49 and 34.77 MHz. The spectrum of $\text{Ag}_2(\text{ClCH}_2\text{CO}_2)_2$ shows four closely spaced NQR frequencies⁶ averaging 33.671 MHz, which is much lower than found in covalent chloroacetates, but is in the range found for some ionic chloroacetates. Since no reference NQR frequency for a noncoordinated Cl in silver chloroacetate is available, a measurement of η would be useful.

The 2,6-dichlorophenoxide ion can readily form chelate complexes with a number of metal ions, in which coordination is through the oxygen and the 2-chlorine atoms, while the 6-chlorine remains noncoordinated (and thus provides the reference NQR frequency ν_T for a terminal atom). There is some π -bond character to the Cl-aromatic C bond (η values of several percent are found). In principle these alter the usefulness of equations (8) and (9)—in practice, insignificantly so—but the usefulness of equation (6) is significantly compromised by this π bonding.

We first consider complexes of some d^{10} metal ions. Substituted phenyl mercury chlorophenolates gave frequency differences ($\nu_T - \nu_B$) between the 2- and 6-chlorines in the range 0.88–1.25 MHz,^{44,45} which is barely outside of the 0.8-MHz spectral width expected for molecular compounds. The crystal structure of phenylmercury 2-chloro-4-bromophenolate shows a $\text{Cl}\cdots\text{Hg}$ intramolecular bond distance of 303 pm, which is well over the sum of covalent radii, 247 pm, but which is still under the sum of van der Waals radii, 330 pm. The d^{10} ions Ag^+ and Cu^+ gave larger frequency differences of 1.675 MHz and 1.88–2.05 MHz in the compounds $(\text{Ph}_3\text{P})_2\text{Ag}(\text{OC}_6\text{H}_3\text{Cl}_2-2,6)$ and $(\text{Ph}_3\text{P})_2\text{Cu}(\text{OC}_6\text{H}_3\text{Cl}_2-2,6)$, respectively, and 1.50 MHz in $(\text{Ph}_3\text{P})_2\text{Ag}(\text{OC}_6\text{H}_2\text{Cl}_3-2,4,6)$.⁴⁶ The crystal structure of the latter compound showed a $\text{Cl}\cdots\text{Ag}$ intramolecular bond distance of 316 pm, which is 65 pm over the sum of

covalent radii, 251 pm. A very acute O–Ag–Cl bond angle of 64.5° is found, which was attributed to strain in the nonplanar chelate ring. Finally, NQR data were obtained for two Zn^{II} 2,6-dichlorophenolates,⁴⁷ one containing two pyridine (py) ligands and the other containing one tetramethylethylenediamine (TMED) ligand. The frequency differences averaged 1.191 MHz and 1.116 MHz, respectively, and thus were similar to those found in Hg^{II} derivatives.

The study was then extended leftward in the periodic table to incorporate the 2,6-dichloro-, 2,4,6-trichloro-, and 4-bromo-2,6-dichlorophenolates of the d^7 through d^9 ions Co^{2+} , Ni^{2+} , and Cu^{2+} , with (mainly) the coligands py, TMED, and N-methylimidazole.^{47–49} Crystal structures of several complexes of these metals and ligands (generally involving 2,4,6-trichlorophenolato groups) are also available. Figure 2 shows that there is a good (though nonlinear) correlation of the NQR frequency differences between the 2-chlorine and the 6-chlorine, and the excess $\text{M}\cdots\text{Cl}$ bond distance (the observed $\text{M}\cdots\text{Cl}$ distance minus the normal single $\text{M}\cdots\text{Cl}$ bond distance). (It should be noted that this correlation is for chlorophenolates, and does *not* apply to silver-chlorocarbon complexes.)

Finally, it was determined that the NQR frequency difference depended strongly on the identity (d^n electron configuration) of the metal ion, as would be expected from the (inorganic) crystal field theory. With complexes of M^{II} 2,6-dichlorophenolates and common coligands (TMED or two py), if the 2-chlorine is coordinated to the metal and is acting as a classical ligand, one has octahedral complexes; if the chlorines are not coordinated, one has tetrahedral complexes. The octahedral site stabilization energy (OSSE) (energy preference for octahedral over tetrahedral coordination) depends on the

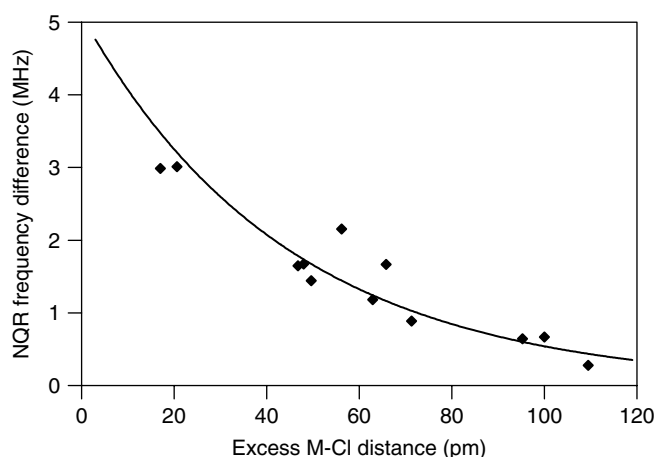


Figure 2 Average ³⁵Cl NQR frequency difference of coordinated ortho-chlorine and noncoordinated (free) ortho-chlorine atoms in 2,6-dichlorophenolato(*O,Cl*) complexes of metals, as a function of the excess M–Cl distance, defined as the average observed M–Cl distance minus the normal M–Cl single bond distance in octahedral complexes, from A. G. Orpen, L. Branner, F. H. Allen, O. Kennard, D. G. Watson, and R. Taylor, *J. Chem. Soc., Dalton Trans.* 1989, S1–S83

Table 4 Effects of OSSE on average ^{35}Cl NQR frequency differences of coordinated and free *ortho* chlorines 2,6-dichlorophenolato(*O,Cl*) complexes of late transition metals (as compared to zinc complexes)

| Complex Type ^(a) | M = Co vs. Zn ^(b) | M = Ni vs. Zn ^(b) | M = Cu vs. Zn ^(b) |
|---------------------------------------|------------------------------|------------------------------|------------------------------|
| OSSE (Δ_{oct}) | 0.267 Δ_{oct} | 0.845 Δ_{oct} | 0.422 Δ_{oct} |
| M(TMED)(OPhH) ₂ | 0.559 MHz | 1.450 MHz | 0.118 MHz |
| Mpy ₂ (OPhH) ₂ | 0.226 MHz | 1.577 MHz | 0.132 MHz |
| M(TMED)(OPhCl) ₂ | 0.373 MHz | 1.704 MHz | -0.340 MHz |
| Mpy ₂ (OPhCl) ₂ | 0.554 MHz | 1.713 MHz | 1.590 MHz |
| Mean | 0.428 MHz | 1.611 MHz | 0.375 MHz |
| Standard deviation | ±0.160 MHz | ±0.124 MHz | ±0.839 MHz |

^(a)Ligand abbreviations: TMED = tetramethylethylenediamine; py = pyridine; OPhH = 2,6-dichlorophenolato(*O,Cl*); OPhCl = 2,4,6-trichlorophenolato(*O,Cl*).

^(b)NQR frequencies shown are the average differences of the 2- and 6-chlorine NQR frequencies in a given metal complex minus the corresponding average difference in the zinc complex.

Sources: Refs. 47–49.

d^n electron configuration, and is zero for the d^{10} ion Zn^{2+} . As indicated in the first row of Table 4, the d^7 and d^9 ions Co^{2+} and Cu^{2+} ions have intermediate OSSE (for weak-field ligands such as in these complexes), and the largest stabilization energy is expected for the d^8 Ni^{2+} ion. As shown in the remainder of Table 4, nickel chlorophenolates indeed give significantly the largest frequency differences between free and coordinated *ortho* chlorines of any of these metals (in Table 4, these are compared to the frequency differences of the zinc chlorophenolates). It may be noted that there is a great deal of variability for the Cu^{II} complexes: the chlorines in these octahedral complexes occupy sites showing quite variable Jahn-Teller elongation.

Another example not involving 4th-period d-block ions or chlorophenolates has been studied. The Schiff base formed from 2-chloroaniline and 2,6-dichlorobenzaldehyde undergoes oxidative addition to $\text{Mo}(\text{CO})_6$ to give a d^4 molybdenum tricarbonyl complex with a $\text{Mo}\cdots\text{Cl}(\text{aniline})$ distance of 262.4 pm, only a little longer than the single inorganic $\text{Cl}-\text{Mo}$ bond distance of 247.3 pm in the same compound.⁵⁰ The ^{35}Cl NQR frequency of the complexed Schiff base is 3.685 MHz lower than the free Schiff base. Applying equations (8) and (9) allows us to estimate $\sigma_{\text{B}2} = 0.134\text{--}0.161$. This large value can be justified by noting that Period 5 metal ions give larger crystal field stabilization energies than do Period 4 metal ions, especially when strong-field ligands such as CO are present.

3.2.3 Weakly Coordinating Anions

Chemists working in catalysis need weakly coordinating anions⁵¹ as counterions to serve as good leaving groups from complexes of very reactive cations such as silylium ions, R_3Si^+ , porphyrinatometal cations, (porphyrinato) Fe^+ , and various catalytically active transition-metal organometallic cations, most importantly the zirconocene catalysts that

are used in the industrial polymerization of alkenes.⁵² Almost all anions will bond to such cations in preference to the neutral substrates (e.g., alkenes) required for the catalytic process involved. Therefore, one seeks very weakly coordinating anions that would be bound to the reactive cation only by very weak secondary bonding or even only by weak (since long-range) electrostatic (ion–ion or ion-induced dipole) interactions.

In order to be weakly attracted electrostatically to the cation, a weakly coordinating anion should have a low charge and a large size over which the charge can be dispersed: it should be as nonbasic¹⁷ as possible. The weakly basic and poorly coordinating properties of anions such as methanesulfonate (CH_3SO_3^-), tetraphenylborate, $[\text{B}(\text{C}_6\text{H}_5)_4]^-$, and 1-carba-*closo*-dodecaborate, $(\text{CB}_{11}\text{H}_{12})^-$ can be further reduced by extensively substituting them with very electronegative atoms such as halogens, to give anions such as CF_3SO_3^- and $[\text{B}(\text{C}_6\text{F}_5)_4]^-$.

However, such fluorine atoms are hard bases, and have been shown to coordinate to the (presumably) hard zirconium cation.⁵³ It is worth investigating whether the secondary bonding would be weaker if the fluorine atoms on typical nonbasic anions were replaced with softer chlorine, bromine, or iodine atoms. Perhaps, in this light, it may be significant that zirconocene catalysis is especially efficient when the anion is $(\text{CB}_{11}\text{H}_6\text{X}_6)^-$ ($\text{X} = \text{Cl}, \text{Br}, \text{or I}$).

Since the oxygen atoms of carboxylate anions or even sulfonate ions are hard bases, they coordinate readily to zirconium, as indicated by the infrared spectra of zirconocene and hafnocene bis(chloroacetates) and by X-ray crystallography for titanocene bis(trifluoromethanesulfonate).⁵⁴ Thus we envision the design of a large, low-charged, nonbasic anion that might be very weakly coordinating to hard acids such as the zirconocene cation having *no* hard-base atoms on its surface, yet having electronegative atoms (hence Cl, Br, or I). Oxygen atoms would either have to be absent from this anion, or would have to be confined to its interior. An example of the former

might be a C_{60}^- anion which had been thoroughly chlorinated, so that no double bonds were available to coordinate to Zr; an example of the latter might be the perchloro analogue of the well-known weakly coordinating anion $[Al(O-tert-C_4F_9)]^-$, in which the oxygen atoms are inaccessible.

We might be able to use chlorine NQR to identify whether such an anion showed secondary bonding interactions with catalyst cations, or whether it interacted with them only by long-range (and therefore weak) interionic attractions. Such an anion probably *would* show secondary interactions with soft cations such as Ag^+ , which would result in low halogen NQR frequencies for the coordinated chlorines (and, if measurable, high asymmetry parameters). However, we would hope for no such results for hard-acid cations that are similar in charge and size to Ag^+ (e.g., Na^+ or K^+).

However, there *would* be significant ‘‘crystal field effects’’ from nearby ions. As we discussed earlier, these are significant, and differ in how they depend on cation size. If our salts adopted typical ionic lattices as found in the hexahalometallate salts discussed earlier, we might again see *increases* in NQR frequencies with increasing group 1 cation radius. Since we hope that our anion would be less polarizable (and less easy to dismember) than $SnCl_6^{2-}$, we would then look for *smaller* increases with increasing cation size. On the other hand, the zirconocene cation itself is only open to coordinate anions on one side, so that its salts might adopt layer type lattices (or even be present as discrete ion pairs). In this case we might see *decreases* in NQR frequencies with increasing cation size, but they would hopefully be less than is the case in chloroacetates. And in such a case, the chlorines on one side of the large perchlorinated anion would not be close to a cation at all, so their NQR frequencies might be independent of cation size. Regardless of whether the salts adopted typical ionic lattices or layer lattices, we would look for an anion in which the effect of the hard-acid cation on the NQR frequency was notably small.

3.3 Applications Involving Multivalent Central Atoms

The Townes–Dailey approach to interpreting NQR spectra of atoms at the center of polyatomic ions or complexes depends in its details on the geometry and bond angles of the central atom, so no attempt will be given here to summarize the equations; we will only mention a few examples to illustrate the availability and use of the data.

High-temperature superconductors are based on copper, which has NQR-active nuclei, and NQR spectra can be obtained on these superconductors while they are in the superconducting state, which excludes magnetic fields. For the classic superconductor $YBa_2Cu_3O_{6.9}$, two ^{63}Cu NQR signals can be obtained. The square-planar-coordinated Cu(1) gives an NQR signal at 22.05 MHz, for which $e^2Qq_{zz} = 38.9$ MHz and $\eta = 0.95$; the square-pyramidal-coordinated Cu(2) gives an NQR signal at 31.5 MHz, for which $e^2Qq_{zz} = 63.08$ MHz and $\eta = 0.04$.^{14,55} Data have also been obtained using the

medium-abundance isotope ^{133}Ba , as well as ^{139}La in the La_2CuO_4 -related superconductors. We also mention a review of Cu NQR spectroscopy in Cu^I complexes.⁵⁶

There have been reviews of NQR spectroscopic studies of central-atom nuclei in complexes^{57,58} and in organometallic compounds.⁵⁹ The interpretation of the e^2Qq_{zz} and η values of these nuclei depends on the coordination number of the atom, the bond angles, the covalency of the bonds to the central atom, and lattice effects, so it is not practical to summarize the field. We illustrate with a ^{59}Co NQR and NMR spectroscopy study⁶⁰ of a series of cobaloxime (bis-dimethylglyoximate)cobalt(III), $[XCo(dmg)_2L]$ complexes, in which *dmg* is the dimethylglyoximate monoanion, L is a Lewis base such as methanol, pyridine, trimethylamine, halide ion, and triphenylphosphine, and X is an anion such as CH_3^- , $CHCl_2^-$, Cl^- , and Br^- . (These complexes are of interest as bioinorganic models for Vitamin B₁₂ (cobalamin).) A ‘‘partial field gradient’’ model was developed for the bonding, composed of contributions from the equatorial (dimethylglyoximate) and the axial (X and L) ligands. It proved to be less appropriate to derive fixed partial field gradients for each ligand, than to assume that the sums of all partial field gradients were constant in this set of complexes (changing the axial ligand also changed the partial field gradient due to the equatorial bis(dimethylglyoximate) ligand). Then it was possible to order the axial ligands in terms of the ratios of the axial and equatorial partial field gradients: for example, methanol > trimethylamine > pyridine > triphenylphosphine.

Studies have also been made of complexes from the point of view of the nitrogen atom in the ligand. Because of the low NQR frequencies of ^{14}N , these have often been done using NMR–NQR double resonance techniques. Again we cite only one example, a series of studies of pyridine (C_5H_5N) ligands coordinated to different diamagnetic metal⁶¹ (and even nonmetal)⁶² atoms. Through another adaptation of the Townes–Dailey method, the electron populations of the σ -donating orbital of the pyridine nitrogen atom were deduced, and showed reasonable trends: free pyridine ($2.00 e^-$) > $Cdpy_2Cl_2$ ($1.87 e^-$) > $Znpy_2Cl_2$ ($1.79 e^-$) > $py \cdot I_2$ ($1.74 e^-$) > $Fepy(CO)_4$ ($1.72 e^-$) > $[Ipy_2]ClO_4$ ($1.64 e^-$) > $[pyH]NO_3$ ($1.38 e^-$). In this series, the coordinate covalent bond order would then proceed in the other direction, from 0.00 in free pyridine to 0.62 in the $[pyH]^+$ cation.

The usefulness of NQR spectroscopy is thus not confined to the study of weak secondary bonds, but can be applied to ordinary covalent or coordinate covalent bonding as well. Hopefully with the advent of modern pulse-FT NQR methods, easier structural determination by X-ray crystallography, and more powerful computational methods to handle the many bonds in complex ions, NQR can resume its contribution in this area of inorganic chemistry as well.

4 ABBREVIATIONS AND ACRONYMS

CW = continuous-wave; CW-NQR = continuous wave NQR; DFT = density functional theory; EFG = electric field gradient; IR = infrared; NMR = nuclear magnetic resonance; NQR = nuclear quadrupole resonance; OSSE = octahedral site stabilization energy; PAC = perturbed angular correlation; pulse-FT = pulse-fourier transform; TMED = tetramethylethylenediamine.

5 FURTHER READING

- I. P. Biryukov, M. G. Voronkov and I. A. Safin, 'Tables of Nuclear Quadrupole Resonance Frequencies', Israel Program for Scientific Translation, Jerusalem, 1969, Includes frequencies measured at different temperatures (commonly 77 K, 195 K, and 273 K or 298 K): temperature effects in NQR are quite substantial and have not been reviewed here.
- T. B. Brill, *Adv. Nucl. Quadrupole Reson.*, 1977, **3**, 131. Good compilation of principles and data.
- Yu. A. Buslaev, E. A. Kravchenko and L. Kolditz, Special issue of *Coord. Chem. Rev.*, 1987, **82**, 1.
- H. Chihara and N. Nakamura, in 'Landolt-Börnstein Numerical Data and Functional Relationships in Science and Technology', 'New Series: Group III, Crystal and Solid State Physics, Vols. 20a, 20b, 20c, 31a, 31b, and 39', eds. K.-H. Hellwege and A. M. Hellwege, Springer-Verlag, Berlin, 1989, 1993, 1997, Critical compilations of NQR frequencies, quadrupole coupling constants, and asymmetry parameters.
- T. P. Das and E. L. Hahn, 'Nuclear Quadrupole Resonance Spectroscopy' (Supplement 1 in the series *Solid State Physics*) Academic Press, New York, 1958, The classic early work on NQR theory.
- K. B. Dillon, Annual chapters in *Spectrosc. Prop. Inorg. Organomet. Compd.*
- Fortschr. Chem. Forsch. Top. Curr. Chem.*, 1972, **30**, 1. Special issue on NQR spectroscopy, with useful article on crystal field effects in NQR.
- E. A. C. Lucken, 'Nuclear Quadrupole Coupling Constants', Academic Press, London, 1969, A good summary of NQR theory and applications to different bonding situations, with selected NQR data.
- 'Nuclear Quadrupole Resonance Spectra Database', Japan Association for International Chemical Information, Tokyo. Updated twice yearly.
- G. K. Semin, T. A. Babushkina and G. G. Yakobson, 'Nuclear Quadrupole Resonance in Chemistry', John Wiley & Sons, New York, 1975, A good catalog of NQR frequencies, e^2Qq_{zz} values, and η values as well as a summary of NQR theory and applications.

6 REFERENCES

1. E. A. C. Lucken, F. Grandjean and G. J. Long, *Compr. Supramol. Chem.*, 1996, **8**, 225.
2. N. Weiden, A. Weiss, G. Wulfsberg, W. Ilsley, K. Benner and W. Wourster, *Z. Naturforsch., A: Phys. Sci.*, 1990, **45a**, 503.
3. E. A. C. Lucken, 'Nuclear Quadrupole Coupling Constants', Academic Press, London, 1969, Chap. 7.
4. G. K. Semin, T. A. Babushkina and G. G. Yakobson, 'Nuclear Quadrupole Resonance in Chemistry', John Wiley & Sons, New York, 1975.
5. L. Pang, E. A. C. Lucken and G. Bernardinelli, *J. Am. Chem. Soc.*, 1990, **112**, 8754.
6. G. Wulfsberg, M. Cochran, J. Wilcox, T. Koritsanszky, D. J. Jackson and J. C. Howard, *Inorg. Chem.*, 2004, **43**, 2031.
7. A. Weiss, *Top. Curr. Chem.*, 1972, **30**, 1.
8. O. Kh. Poleshchuk, J. N. Latošinska and B. Nogaj, *Z. Naturforsch., A: Phys. Sci.*, 2000, **55a**, 271.
9. J. N. Latošinska, *Int. J. Quantum Chem.*, 2003, **91**, 284.
10. C. H. Townes and B. P. Dailey, *J. Chem. Phys.*, 1949, **17**, 782.
11. W. Gordy, *J. Chem. Phys.*, 1951, **19**, 792.
12. D. Nakamura, R. Ikeda and M. Kubo, *Coord. Chem. Rev.*, 1975, **17**, 281.
13. E. V. Bryukhova, G. K. Semin, I. M. Alimov, A. N. Nesmeyanov, O. V. Nogina, V. A. Dubovitsky and S. I. Kuznetsov, *J. Organomet. Chem.*, 1974, **81**, 195.
14. D. Brinkmann, *Z. Naturforsch., A: Phys. Sci.*, 1990, **45a**, 393.
15. J. B. Miller and G. A. Barrall, *Am. Sci.*, 2005, **93**, 50.
16. E. Balchin, D. J. Malcolme-Lawes, I. J. F. Poplett, M. D. Rowe, J. A. S. Smith, G. E. S. Pearce and S. A. C. Wren, *Anal. Chem.*, 2005, **77**, 3925.
17. G. Wulfsberg, 'Inorganic Chemistry', University Science Books, Sausalito, 2000.
18. R. Lenk and E. A. C. Lucken, *Chem. Phys. Lett.*, 1973, **21**, 552.
19. P. Pyykkö and M. Seth, *Theor. Chem. Acc.*, 1997, **96**, 92.
20. M. Epple and O. Herzberg, *J. Mater. Chem.*, 1997, **7**, 1037.
21. S. David, L. Guibé and M. Gourdji, *New J. Chem.*, 1995, **19**, 37.
22. Yu. A. Buslaev, E. A. Kravchenko and L. Kolditz, *Coord. Chem. Rev.*, 1987, **82**, 1 (specifically, pages 53–62).
23. D. H. Current, *J. Magn. Reson.*, 1975, **20**, 259.
24. D. Borchers, P. C. Schmidt and A. Weiss, *Z. Naturforsch., A: Phys. Sci.*, 1988, **43**, 643.
25. T. B. Brill, R. C. Gearhart and W. A. Welsh, *J. Magn. Reson.*, 1974, **13**, 27.
26. M. G. Voronkov, V. P. Feshin, V. F. Mironov, S. A. Mikhailyants and T. K. Gar, *J. Gen. Chem. USSR*, 1971, **41**, 2237.
27. V. P. Feshin, *Main Group Met. Chem.*, 1997, **20**, 669.
28. V. P. Feshin, L. S. Romanenko and M. G. Voronkov, *Russ. Chem. Rev. (Engl. Transl.)*, 1981, **50**, 248.

29. E. A. Kravchenko and M. Yu. Burtzev, *Z. Naturforsch., A: Phys. Sci.*, 1992, **47a**, 134.
30. A. Sasane, D. Nakamura and M. Kubo, *J. Phys. Chem.*, 1967, **71**, 3249.
31. H. Harada, D. Nakamura and M. Kubo, *J. Magn. Reson.*, 1974, **13**, 56.
32. N. W. Alcock, *Adv. Inorg. Chem. Radiochem.*, 1972, **15**, 1.
33. G. R. Desiraju and R. Parthasarathy, *J. Am. Chem. Soc.*, 1989, **111**, 8725.
34. Z. Xie, B.-M. Wu, T. C. W. Mak, J. Manning and C. A. Reed, *J. Chem. Soc., Dalton Trans.*, 1997, 1213.
35. G. Wulfsberg and A. Weiss, *Ber. Bunsen-Ges. Phys. Chem.*, 1980, **84**, 474.
36. R. J. Kulawiec and R. H. Crabtree, *Coord. Chem. Rev.*, 1990, **99**, 89.
37. M. R. Colman, T. D. Newbound, L. J. Marshall, M. D. Noirot, M. M. Miller, G. P. Wulfsberg, J. S. Frye, O. P. Anderson and S. H. Strauss, *J. Am. Chem. Soc.*, 1990, **112**, 2349.
38. V. P. Feshin, G. V. Dolgushin, M. G. Voronkov, Ju. E. Sapozhnikov, Ja. B. Jasman and V. I. Shirjaev, *J. Organomet. Chem.*, 1985, **295**, 15.
39. N. W. Alcock and R. M. Countryman, *J. Chem. Soc., Dalton Trans.*, 1977, 217.
40. G. K. Semin, T. L. Khotsyanova, S. I. Gushin and S. A. Petukhov, *Chem. Phys. Lett.*, 1985, **114**, 147.
41. H. Ikezawa, M. Takahashi, M. Takeda and Y. Ito, *Bull. Chem. Soc. Jpn.*, 1993, **66**, 1959.
42. A. Karipides and K. Peiffer, *Inorg. Chem.*, 1988, **27**, 3255.
43. M. Epple and H. Kirschnick, *Chem. Ber. Recl.*, 1997, **130**, 291.
44. D. N. Kravtsov, A. P. Zhukov, B. A. Faingor, El. M. Rokhlina, G. K. Semin and A. N. Nesmeyanov, *Bull. Acad. Sci. USSR, Div. Chem. Sci.*, 1968, 1611.
45. G. Wulfsberg, R. J. C. Brown, J. Graves, D. Essig, T. Bonner and M. Lorber, *Inorg. Chem.*, 1978, **17**, 3426.
46. G. Wulfsberg, D. Jackson, W. Ilsley, S.-Q. Dou, A. Weiss and J. Gagliardi, Jr, *Z. Naturforsch., A: Phys. Sci.*, 1992, **47a**, 75.
47. M. F. Richardson, G. Wulfsberg, R. Marlow, S. Zaghoni, D. McCorkle, K. Shadid, J. Gagliardi, Jr and B. Farris, *Inorg. Chem.*, 1993, **32**, 1913.
48. R. Meyer, J. Gagliardi, Jr and G. Wulfsberg, *J. Mol. Struct.*, 1983, **111**, 311.
49. G. Wulfsberg, J. Yanisch, R. Meyer, J. Bowers and M. Essig, *Inorg. Chem.*, 1984, **23**, 715.
50. R. Harrison, A. M. Arif, G. Wulfsberg, R. Lang, T. Ju, G. Kiss, C. D. Hoff and T. G. Richmond, *J. Chem. Soc., Chem. Commun.*, 1992, 1374.
51. S. H. Strauss, *Chem. Rev.*, 1993, **93**, 927.
52. R. F. Jordan, *Adv. Organomet. Chem.*, 1991, **32**, 325.
53. Y. Sun, R. Ev. H. Spence, W. E. Peirs, M. Parvez and G. P. A. Yap, *J. Am. Chem. Soc.*, 1997, **119**, 5132.
54. U. Thewalt and H.-P. Klein, *Z. Kristallogr.*, 1980, **153**, 307.
55. D. Brinkmann, *Physica C*, 1988, **153–155**, 75.
56. E. A. C. Lucken, *Z. Naturforsch., A: Phys. Sci.*, 1994, **49a**, 155.
57. L. Ramakrishnan, S. Soundararajan, V. S. S. Sastry and J. Ramakrishna, *Coord. Chem. Rev.*, 1977, **22**, 123.
58. T. L. Brown, *J. Mol. Struct.*, 1980, **58**, 293.
59. T. B. Brill, *Adv. Nucl. Quadrupole Reson.*, 1977, **3**, 131.
60. R. A. LaRossa and T. L. Brown, *J. Am. Chem. Soc.*, 1974, **96**, 2072.
61. Y.-N. Hsieh, G. V. Rubenacker, C. P. Cheng and T. L. Brown, *J. Am. Chem. Soc.*, 1977, **99**, 1384.
62. G. V. Rubenacker and T. L. Brown, *Inorg. Chem.*, 1980, **19**, 398.

NUCLEAR QUADRUPOLE RESONANCE (PAPER II)*Allen N. Garroway, Naval Research Laboratory¹*

INTRODUCTION: NUCLEAR QUADRUPOLE RESONANCE AT THE NAVAL RESEARCH LABORATORY

The Polymer Diagnostics Section (Code 6122) of the U.S. Naval Research Laboratory (NRL) has expertise in solid state nuclear magnetic resonance (NMR), magnetic resonance imaging (MRI), and nuclear quadrupole resonance (NQR). In 1983, NRL established an interagency agreement with the Federal Aviation Administration (FAA) to advise the FAA on NMR methods to detect explosives. We were aware of earlier work [1] on the use of NQR for explosives detection, and in 1987 we initiated a research program at NRL to explore NQR, with initial support of the FAA and Technical Support Working Group (Department of Defense). NQR explosives detection technologies, including methods applicable for landmine detection, have been developed and patented by NRL and have been licensed by the U.S. Navy to Quantum Magnetics (San Diego, Calif.), a subsidiary of InVision Technologies Inc.

PHYSICAL PRINCIPLES**Limitations of Conventional Detection Methods²**

The basic technology for both military and humanitarian mine detection is still the electromagnetic metal detector, a direct descen-

¹This work was prepared by a U.S. government employee as part of his official duties.

²This section is adapted from Garroway et al. [1].

dant of those used in World War II. Finding a metal-encased antitank mine (5–10 kg of explosive) buried 10 cm underground is trivial for such a device, but finding a “low-metal” antipersonnel mine (50–100 g of explosive, and perhaps 0.5 g of metal for the firing pin) below the surface is highly challenging. The electromagnetic return signal from the antipersonnel mine is much weaker, and so the operator must turn up the detector gain. At higher sensitivity, however, much more of the other metal detritus, such as nails and shell fragments, becomes visible to the detector. The operator is compelled to operate at very high sensitivity and to flag any alarm as a potential landmine. Unfortunately, the next step is the most difficult: One must then separate the landmines from the false alarms arising from this benign background of signals. Currently, that “resolution of false alarms” is still done by mechanical probing: The deminer or combat engineer performs very delicate archeology with a pointed stick to classify the source of the electromagnetic signal—a landmine, perhaps rigged with an antihandling device, or just a rusty nail. In that sense, finding landmines is easy; however, separating them from the clutter is tough—and extremely hazardous.

Why NQR? What is desired is a detector based on a signal that is specific to the landmine. Certainly a unique signature of the explosive would provide a way to reduce this clutter problem. Such arguments lead to chemical detection of the explosives in landmines. While dogs are being used to find landmines, their method of detection is still a subject of controversy and their efficiency is not high. The vapor pressure of the military explosives used in landmines is quite low, and commercially manufactured mines hermetically seal the explosives in a polymeric case. Further, as explosive vapors and particles are quite sticky, the transport of explosive from the main charge, through the case, and then through the ground is slow and inefficient. Vapor sensors have been explored for landmine detection, and there is a recent indication that, under some field conditions, exquisitely sensitive vapor detectors can detect the plume from a landmine [2].

But there is another method—NQR—that is specific to the chemistry of an explosive, regardless of how it is packaged.

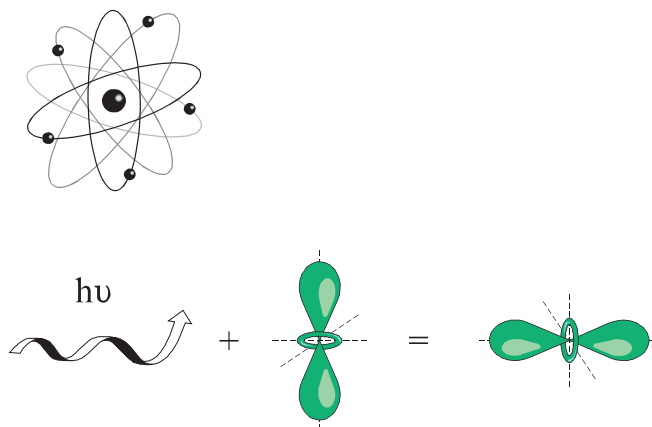
BASICS OF NQR

NQR [3] is a magnetic resonance phenomenon related to NMR and its offspring, MRI. In NMR and MRI, a large static magnetic field (0.05–20.00 T, 0.5–200.0 kG) orients the nuclei so that slightly more are in the low energy state (aligned parallel to the static field) than are in the higher state (opposed to the field). This population difference corresponds to a weak diamagnetism of the nuclear spins, with a classical magnetization vector aligned along the static magnetic field. The magnetic field corresponding to this nuclear diamagnetism can be observed by applying a resonant radio frequency (RF) pulse (at the Larmor frequency and at right angles to the static field), causing the magnetization to rotate away from the axis of the static magnetic field. The magnetization then precesses freely in the static field, at the Larmor frequency, and this time-dependent flux induces a weak voltage in an RF pickup coil perpendicular to the static field. This induced signal is the NMR signal.

Comparison to Nuclear Magnetic Resonance

NQR is similar to NMR but has some important distinctions. In NQR, the splitting of the nuclear spin states is determined by the electrostatic interaction of the nuclear charge density, $\rho(r)$, with the external electric potential, $V(r)$, of the surrounding electron cloud (see Figure K.1). A moment expansion of this electrostatic interaction shows that the important coupling is between the nuclear quadrupole moment, indicated schematically in Figure K.1, and the second derivative of the electric potential (equivalently, the gradient of the electric field). *This is a key result.* The quadrupole moment, nonzero only for nuclei with spin quantum number I greater than or equal to 1, is a nuclear physics parameter describing the distribution of charge in the nucleus. (For landmine applications, the primary nucleus of interest is ^{14}N , with I equal to 1.) The second term, the coupling to the electric field gradient of the valence electrons is largely based on chemistry, although the local crystal packing also plays a role.

Contrast the chemical specificity of NQR with that of NMR. While NMR provides highly detailed information about chemical structure, the range of “chemical shifts” is generally small. Hydrogens in any

NQR

NOTE: Applying a pulse of the correct frequency ν flips the nuclear spin and induces an NQR signal in a pickup coil.

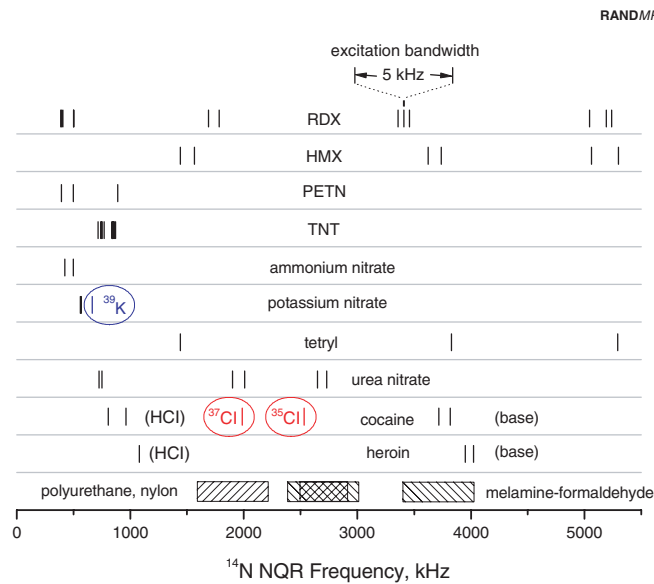
Figure K.1—A Quadrupolar Nucleus Slightly Aligned by the Electrostatic Interaction with the Valence Electrons

arbitrary organic structure differ by a range of about 10 ppm away from their nominal NMR frequency, e.g., a 6-kHz range of frequencies in a 600-MHz NMR spectrometer. However, for ^{14}N NQR, the NQR frequencies can range from *zero to 6 MHz*, depending on the symmetry of the molecule. Indeed, one of the difficulties of NQR is that it can be *too sensitive* to the chemistry of the compound of interest.

There are also some significant subtleties in NQR compared with NMR: For NQR the nuclear spin is greater than or equal to 1, and the spins are quantized along the principal axis system of the electric field gradient, rather than for the NMR or MRI case that (commonly) involves spin-1/2 nuclei quantized along the static magnetic field. For the present purpose, these distinctions are best overlooked, and, in a rough sense, it suffices to regard NQR as NMR without the magnet.

NQR as a Detector

One significant advantage of NQR is the absence of a magnet: Even if the NMR approach were thought to give some advantage to detecting explosives, projecting a large static magnetic field into the ground is difficult. But the main advantage is that NQR provides a highly specific and arguably unique frequency signature for the material of interest. Figure K.2 shows the NQR frequencies for a number of common explosives, as well as for some narcotics and other materials. Although the chemical structure of RDX (Figure K.3) indicates that the three ring nitrogens are chemically equivalent and hence would be expected to have identical NQR frequencies, in fact the crystal packing is sufficient to remove this degeneracy, and indeed the chemically equivalent ring nitrogens are separated by the order



NOTE: Unless otherwise indicated, the frequencies are for ¹⁴N. Also shown are estimates for the general frequency bands expected for some commercial polymers.

Figure K.2—Representative NQR Frequencies for Some Explosives and Narcotics

RANDMR1608-K.3

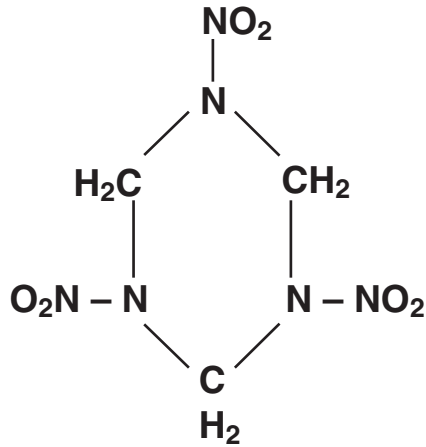


Figure K.3—Chemical Structure of RDX

of 100 kHz from one another (see Figure K.2). This demonstrates the specificity of NQR: Even such small effects from crystal packing are sufficient to resolve the NQR lines from nominally equivalent nitrogens. Because the bandwidth of excitation is only about 5 kHz for commercial NQR detectors, NQR lines more than 5 kHz away from the carrier will not be excited.

For landmine detection, TNT, RDX, and, to a lesser extent, tetryl are the most important explosives. The basic detection concept is particularly simple: Apply a pulse or series of RF pulses resonant at the appropriate NQR frequency of the explosives of interest, and look for the presence (or absence) of a return signal.

As discussed below, the intrinsic signal-to-noise ratio (SNR) (of the NQR signal to the random thermal noise, primarily Johnson noise from the detector coil) is inherently low, and much effort goes into designing effective RF pulse sequences and detector coil geometries that maximize the SNR per unit time. To the degree that the noise is completely random, the improvement in SNR increases with the square root of scan time. A major complication in landmine detection is that radio frequency interference (RFI) from far field sources,

such as AM radio transmitters, and near field sources, such as automobile ignitions and computers, creates substantial coherent noise that can be within the frequency regime of interest. Note (Figure K.2) that TNT frequencies are below 1 MHz, right in the AM band. Much effort has been devoted to reducing this problem—by coil design and by monitoring the RFI with a separate antenna and then subtracting the unwanted RFI signal. Nonetheless, the inherently weak NQR signals and the possible contamination by RFI dictate that *for present technology* it is not expected that the NQR detector will be satisfactory as a *primary* sensor for landmine detection in military applications. However, the exquisite selectivity suggests NQR is tailor-made as a *confirmation* sensor: e.g., when a primary sensor, such as an electromagnetic induction coil or ground-penetrating radar, indicates an anomaly, the NQR detector can be used as a confirmation tool to distinguish false alarms from landmines, without the need to mechanically probe the ground.

STATE OF DEVELOPMENT

In the United States there are presently two programs to develop prototype NQR landmine detectors, both executed by Quantum Magnetics (QM). The U.S. Army Mine Countermeasure Division at Fort Belvoir, Va., sponsors development of a vehicle-mounted prototype NQR detector, designed initially as a confirmation sensor to clear mines from roadways. Under support from the Office of Naval Research and the U.S. Marine Corps, QM is also developing a prototype handheld landmine confirmation detector for the U.S. Marine Corps Systems Command, Quantico, Va.

CURRENT CAPABILITIES

The prototype developments, above, represent the current capabilities. Both are for military applications, and development of an NQR detector for humanitarian purposes would use the basic technology but would take a somewhat different path—see below.

It is premature to report receiver operating characteristic curves.

KNOWN LIMITATIONS

Not all explosives exhibit an NQR signal. In particular, some landmines, such as the PFM-1, employ liquid explosives that are not expected to be detectable [4]. Of course, NQR requires that the RF field must penetrate to the explosive, and so no NQR signal is obtained from a metal-encased mine. However, metal mines are easily found by metal detectors, and indeed the NQR detector acts as a crude metal detector itself. If the RF flux is excluded from a conducting volume, the effective inductance of the NQR detector coil is reduced and the presence of the metal case is indicated by an inability to resonantly tune the coil within the range of the variable tuning capacitor.

Both the NQR frequency and the relevant NQR relaxation times T_1 and T_2 are functions of temperature. The relaxation time T_1 determines how rapidly the pulse sequence can be repeated, and T_2 restricts the maximum length of the “spin echo” sequence used for TNT and tetryl detection. Roughly speaking, an acquisition of length T_2 can be obtained every T_1 . Because the exact temperature of the mine is not known, one uses pulse sequence parameters that are broadly effective over a band of temperature. With some improvements, it is expected that estimating the approximate mine temperature to within 10–20°C should be adequate.

Detectability of RDX and tetryl is rather good by NQR, but for TNT the NQR relaxation times are less favorable, and the possible presence [5] of two crystalline polymorphs (monoclinic and orthorhombic) lead to weaker TNT signals. Finding small (50 g) antipersonnel TNT mines by NQR will be difficult, but is not ruled out. RDX and tetryl mines are much easier to find.

Most NQR detector coils use variants of a simple circular surface coil, for which the magnetic field intensity drops by about a factor of three at a distance of one coil radius along the coil axis. Beyond that distance, the field drops off more rapidly with distance, and so the detector coil radius determines the *approximate* useful depth of interrogation. A larger coil is an alternative, but more RF power is required for the transmitter, and because the “filling factor” (the volume fraction of the explosive divided by the effective volume irradiated by the coil) is reduced, the overall SNR can be reduced. Corre-

spondingly, a significant increase in the “standoff distance” of the coil above the ground will also reduce the SNR of the mine.

In general, soil characteristics do not play a significant role in NQR detection. At these NQR frequencies (1–5 MHz), the RF field is not significantly attenuated, even for rather wet soils. The decrease in the effective Q of the detector coil corresponding to this RF loss results in a rather insignificant deterioration in SNR.

POTENTIAL FOR IMPROVEMENT

Compared with combat engineering applications, there are some advantages to NQR for humanitarian demining. It is anticipated that increased scan time can be tolerated for humanitarian applications, especially if NQR is used as a confirmatory tool. For example, for TNT with a nominal T_1 relaxation time of 6 seconds at 20°C, two data acquisitions can be taken with a 6-second scan (using a delay of T_1 between acquisitions), but 51 acquisitions can be obtained in a 5-minute scan, giving an improvement of 5x in SNR. In other words, a 50-g mine would give the same SNR or detectability in 5 minutes as a 250-g mine in 6 seconds—an easy task for NQR. And, a 5-minute NQR scan sounds more appealing than digging by hand for 5 minutes.

Improvements in technology, especially the RF transmitter, and advanced NQR techniques such as “stochastic NQR” [6], should reduce the weight and the power requirements of the present military prototype detector and will be advantageous for humanitarian applications.

Other approaches that may be viable for humanitarian demining include combined NQR-NMR methods. For these a weak polarizing magnetic field is used, on the order of 10–100 G. Variants allow a cross relaxation between the nitrogen transitions and hydrogen NMR transitions, to either decrease the nitrogen T_1 relaxation time or to detect the nitrogen NQR transition as a perturbation on the much stronger proton NMR signal. These techniques have been explored to some extent in the laboratory for the past 50 years, and certain variants may be appropriate to humanitarian demining. See Nolte et al. [7] for a recent application, albeit one more suited to the laboratory.

Even with improvements, it is anticipated that NQR would still be integrated with some other detection method, such as electromagnetic metal detection.

R&D PROGRAM TO REALIZE THE POTENTIAL

As indicated, NQR landmine detection for military applications is still in the prototype stage, and substantial improvement in the technology is expected as experience is gained. Extension to humanitarian demining can build on this experience, but significant effort should be devoted to adapt NQR to humanitarian demining.

The current five-year program to develop a prototype handheld NQR detector represents a projected investment of about \$15 million for engineering and some science and technology (S&T). Further S&T work is necessary for the humanitarian approaches, perhaps \$3 million worth. A program funded at about \$1 million per year for research and development and \$5 million per year for engineering development over a three-year period should make real progress toward an NQR detector specialized for humanitarian applications.

In the near term, the military version of the handheld NQR detector should be available in about four years. One might use those detectors for humanitarian purposes, assuming that there is no difficulty in the “dual use” of this technology. However, this appears to be at best a short-term solution because humanitarian demining requirements are different than those of the combat engineer.

REFERENCES

1. A. N. Garroway, M. L. Buess, J. B. Miller, B. H. Suits, A. D. Hibbs, G. A. Barrall, R. Matthews, and L. J. Burnett, “Remote Sensing by Nuclear Quadrupole Resonance (NQR),” *IEEE Transactions on Geoscience and Remote Sensing*, No. 39, 2001, pp. 1108–1118.
2. C. Cumming, C. Aker, M. Fisher, M. Fox, M. la Grone, D. Reust, M. Rockley, T. Swager, E. Towers, and V. Williams, “Using Novel Fluorescent Polymers as Sensory Materials for Above-Ground Sensing of Chemical Signature Compounds Emanating from Buried Landmines,” *IEEE Transactions on Geoscience and Remote Sensing*, No. 39, 2001, pp. 1119–1128.

3. J. A. S. Smith, "Nuclear Quadrupole Resonance Spectroscopy, General Principles," *J. Chemical Education*, No. 48, 1971, pp. 39–49; Y. K. Lee, "Spin-1 Nuclear Quadrupole Resonance Theory with Comparisons to Nuclear Magnetic Resonance," *Concepts in Magnetic Resonance*, No. 14, 2002, pp. 155–171.
4. *Jane's Mines and Mine Clearance*, 2001–2002.
5. G. R. Miller and A. N. Garroway, *A Review of the Crystal Structures of Common Explosives Part I: RDX, HMX, TNT, PETN, and Tetryl*, NRL Memorandum Report NRL/MR/6120-01-8585, October 15, 2001.
6. A. N. Garroway, J. B. Miller, D. B. Zax, and M-Y. Liao, "A Means for Detecting Explosives and Narcotics by Stochastic Nuclear Quadrupole Resonance (NQR)," U.S. Patent 5,608,321, March 4, 1997.
7. M. Nolte, A. Privalov, J. Altmann, V. Anferov, and F. Fujara, "¹H–¹⁴N Cross-Relaxation in Trinitrotoluene: A Step Toward Improved Landmine Detection," *J. Phys. D: Appl. Phys.*, No. 35, 2002, pp. 939–942.

Nuclear Quadrupole Resonance Spectroscopy

General principles

Nuclear quadrupole resonance spectroscopy is a branch of magnetic resonance spectroscopy and is concerned with the absorption of radio waves by matter in zero magnetic field. A unique feature of this kind of spectroscopy is the remarkably simple instrument that can be used to detect some signals, a circuit that can be constructed by anyone with some experience of radio techniques at a cost comparable to that of the cheapest transistor radio. We will return to the subject of instrumentation, however, in the second of this series of articles; the first deals with the basic principles of nuclear quadrupole resonance spectroscopy in solids, and subsequent parts will summarize some recent applications to chemistry (see Editor's Note).

General Principles

In order to understand the origin of nuclear quadrupole resonance, we need to consider in some detail the electrical interactions between the nuclei and electrons which form part of an atom or molecule. Starting at the simplest level, we may visualize the molecule as a charge cloud extending over several angstroms, in which are embedded the nuclei with their own considerably smaller charge distributions, about 10^{-4} Å in size. We then ask what symmetry is the nuclear charge distribution likely to have. Since all the nuclei giving rise to nuclear quadrupole resonance have a magnetic moment which we explain in terms of nuclear angular momentum, we expect all quadrupolar nuclei in our laboratory frame of reference to have one axis of cylindrical symmetry, the "spin" axis, or the axis with respect to which the angular momentum is defined. Such a charge distribution is represented in general *not* by a sphere but by an ellipsoid of revolution which we may derive from a sphere by compression or extension along a given direction (Fig. 1). Compression gives an oblate spheroid, and extension a prolate spheroid; the "quadrupole moment" Q of such a charge distribution may be defined as

$$eQ = \int \rho_n (3z_n^2 - r_n^2) d\tau_n \quad (1)$$

where ρ_n is the nuclear charge density in a volume element $d\tau_n$; $-e$ is the charge on the electron; and the integral extends over the nuclear volume. For a sphere,

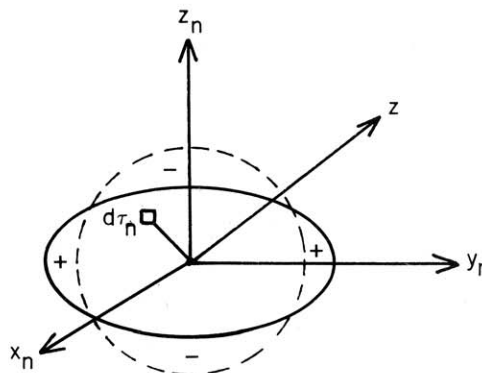


Figure 1. Nuclear electric quadrupole moment.

this integral will be zero, since the average value of z^2 equals that of $r^2/3$, but for a prolate spheroid the integral is finite and positive, and negative for an oblate spheroid; because of the presence of the fundamental unit of charge on both sides of eqn. (1), Q itself has the dimensions of r^2 , viz., cm^2 , and is of the order of the nuclear *area*, viz., 10^{-24} cm^2 . Nuclear quadrupole moments will therefore be expressed in units of 10^{-24} cm^2 and can be either positive or negative.

To return to Figure 1, we note that compression of the original sphere has removed positive charge from two regions, marked $-$, and transferred it to two other regions, marked $+$. From a spherical charge distribution, the compression has given two antiparallel electric dipoles. In an electric field, each of these experiences a torque tending to align them along the field; since the two turning torques are equal and opposite, there is no net effect. However, in an electric field *gradient* which we assume to be axially-symmetric about Oz in Figure 1, the torques on the two dipoles are *not* equal and a net turning torque exists which is clearly proportional both to the electric field gradient and to the extent to which the nuclear charge distribution departs from spherical symmetry, that is to eQ . Calling the electric field gradient in the Oz direction $(\partial E/\partial z) = -eq$, the net turning torque is proportional in magnitude to $|e^2qQ|$. Since all quadrupolar nuclei also have angular momentum, the situation may be compared to the precessional model for a nuclear magnet in an applied magnetic field, a model useful in discussing nuclear magnetic resonance; the field tries to turn the magnet into parallelism, and the magnet responds in some respects as would a gyroscope by precessing about the direction of the magnetic field with a precessional frequency ω (in radians sec^{-1}) of $\gamma_n H$ (γ_n is a constant known as the nuclear gyromagnetic ratio). This equation comes from Larmor's theorem. By analogy, the nuclear quadrupole responds to the torque by precessing about the direction of the maximum electric field gra-

EDITOR'S NOTE: Professor Smith's review of Nuclear Quadrupole Resonance spectroscopy will appear in four installments, of which this is the first. Subsequent sections will appear in the "Topics in Chemical Instrumentation" column in the A-pages of THIS JOURNAL for February, March, and April, 1971. Reprints will be prepared for the series as a whole, and will be available in limited quantity from the author and from G. W. Ewing, Department of Chemistry, Seton Hall University, South Orange, N. J. 07079.

dient with a frequency which should be proportional to $|e^2qQ/h|$ (where $h =$ Planck's constant). However, there is an important difference from the magnetic case which arises essentially because we have used different coordinate systems to define q and Q ; in the quadrupolar case, the precessional frequency varies with orientation, whereas in the magnetic case, the frequency is the same for all orientations. The model of quadrupolar precession approaches the quantum-mechanical one only in the limit of high quantum numbers. If, however, we imagine that the nuclear spin axis can be "set" at one or more fixed orientations, conveniently defined by I_z , the component of the nuclear angular momentum along Oz , then at one of these positions there will be *one* precessional frequency; this precession of the nucleus carries with it, of course, the nuclear angular momentum and hence the nuclear magnetic moment, thereby producing a small *magnetic* field at right angles to Oz rotating in phase with the nuclear quadrupole at the same frequency. Now a linearly oscillating field

$$H = 2H_1 \cos \omega t \quad (2)$$

can be resolved into two rotating fields

$$\left. \begin{aligned} H(\text{cw}) &= H_1 \cos \omega t + iH_1 \sin \omega t \\ H(\text{ccw}) &= H_1 \cos \omega t - iH_1 \sin \omega t \end{aligned} \right\} \quad (3)$$

where

$$H = H(\text{cw}) + H(\text{ccw})$$

so that $H(\text{cw})$ rotates clockwise, $H(\text{ccw})$ rotates counterclockwise; such a field is obtained by enclosing the sample in a small induction coil through which we send alternating current. That component of eqn. (3) which rotates *in phase* with the precessing nucleus can exchange energy with it—in classical terms, we have a resonance process occurring at a specific frequency, which we label ν_Q (in Hz) or ω_Q (in radians sec^{-1}), the nuclear quadrupole resonance frequency. Now Q for ^{35}Cl is close to $-0.0802 \times 10^{-24} \text{ cm}^2$ (see the table), and in HCl this nucleus finds itself in an electric field gradient (eq) of $+0.96 \times 10^{24} \text{ e cm}^{-3}$ from the adjacent proton (using $r_e = 1.278 \text{ \AA}$) and $+23.41 \times 10^{24}$ from the electrons, giving a net value of $+24.37 \times 10^{24}$; the product e^2qQ/h is then -67.85 MHz , corresponding to transition frequencies in the radio frequency region. In fact, for *all* quadrupolar nuclei in the periodic table, the range of possible frequencies is from a few kHz to several thousand MHz so that the induction coil which generates the exciting magnetic field will be part of a *radio frequency* spectrometer. The observed frequencies, which we compare with the classical precessional frequencies of an electric quadrupole, are governed by *electric* effects with the atom or molecule, but the mechanism whereby they are observed involves the *magnetic* moment of the nucleus, that is they are *magnetic dipole* transitions in origin.

The reader will appreciate that the previous paragraphs have been concerned with a highly simplified description of nuclear quadrupole resonance in terms of classical mechanics, and for a fuller account of the classical equations of motion and their solutions he is referred to an interesting article by Raich and Good (1). The quantitative expressions for the nuclear quadrupole resonance frequencies and their relative intensities are usually derived by the methods of quantum me-

chanics, and we next discuss the results of such calculations. In order to do this, we need more precise definitions of both the nuclear quadrupole moment and the electric field gradient. Mathematically, we will proceed by first deriving the full expression for the energy of a nuclear electric quadrupole in an electrostatic environment, and then presenting the solutions of these equations. For the intermediate stages, in which the quantum-mechanical operator is first derived and the eigenvectors and eigenvalues obtained, the reader is referred to the excellent introductory account by Slichter (2).

Consider a quadrupolar nucleus which is part of an atom or molecule and a volume element in that charge distribution $d\tau_n = dx dy dz$ of charge density ρ_n distant r_n from our origin at O (midway between the two foci of the ellipse, see Figure 1). The nuclear charge is imagined to be under the influence of the electronic charge distribution of the atom or molecule, which produces a *potential* at $d\tau_n$ of V . The potential energy of this nuclear charge element in its electrostatic environment is then

$$-\rho_n d\tau_n \cdot V$$

and for the complete nucleus

$$\text{Potential energy} = -\int \rho_n V \cdot d\tau_n \quad (4)$$

Now V varies over the nuclear volume, but we may express this variation in terms of the values of V and its first and higher differentials at the origin by means of a Taylor expansion, i.e.

$$V = V_0 + \left\{ x_n \left(\frac{\partial V}{\partial x} \right)_0 + y_n \left(\frac{\partial V}{\partial y} \right)_0 + z_n \left(\frac{\partial V}{\partial z} \right)_0 \right\} + \frac{1}{2} \left\{ x_n^2 \left(\frac{\partial^2 V}{\partial x^2} \right)_0 + x_n y_n \left(\frac{\partial^2 V}{\partial x_n \partial y_n} \right)_0 + \dots \right\} \quad (5)$$

where V_0 , $(\partial V/\partial x)_0$, etc. are to be evaluated at the origin O and (x, y, z) are coordinates in the nuclear frame of reference (labeled $x_n y_n z_n$ in Figure 1). Since we are interested in effects which *vary* with nuclear orientation, the first term involving V_0 will not be relevant to what follows and may therefore be omitted. The second term involves first differentials of V , i.e., electric fields, since

$$\mathbf{E} = -\text{grad } V$$

or

$$\frac{\partial V}{\partial x} = -E_x, \quad \frac{\partial V}{\partial y} = -E_y, \quad \frac{\partial V}{\partial z} = -E_z$$

so that one term, viz., $\rho_n x_n (\partial V/\partial x)_0$, represents the contribution of the electric moment of the volume element x_n with respect to the origin at O . When the integration of eqn. (4) is therefore performed, the second term will represent the interaction of the electrostatic dipole moment of the nucleus in the electric field of its environment; now there is good evidence, both experimental and theoretical, that nuclear electric dipole moments are zero, and since the induced moment is also taken as zero, we may also omit the second term in eqn. (5). The third part is the electric quadrupole term, to which we now turn our attention (neglecting higher terms, which *may* however be important in certain cases).

The full expression for the quadrupole potential energy will be

$$\text{Potential energy} = - \int \frac{1}{2} \left\{ \rho_n x_n^2 \left(\frac{\partial^2 V}{\partial x^2} \right)_0 + y_n^2 \left(\frac{\partial^2 V}{\partial y^2} \right)_0 + z_n^2 \left(\frac{\partial^2 V}{\partial z^2} \right)_0 + 2x_n y_n \left(\frac{\partial^2 V}{\partial x \partial y} \right)_0 + 2z_n x_n \left(\frac{\partial^2 V}{\partial z \partial x} \right)_0 + 2y_n z_n \left(\frac{\partial^2 V}{\partial y \partial z} \right)_0 \right\} d\tau_n \quad (6)$$

in which we have nine terms involving the nuclear coordinates and nine involving second derivatives of the electronic charge distribution. Such quantities, strictly speaking, are *tensors* and should be manipulated by the methods of tensor algebra: we will make the assumption, which is discussed in the monograph by Nye (3), that it will always be possible to select a *new* coordinate system (x, y, z) in which only the simple derivatives $\partial^2 V / \partial x^2$, etc., are non-zero; these will now be called the principal components of the second derivatives, and eqn. (6) becomes

$$\text{Potential energy} = - \int \frac{1}{2} \left\{ \rho_n x_n^2 \left(\frac{\partial^2 V}{\partial x^2} \right)_0 + \rho_n y_n^2 \left(\frac{\partial^2 V}{\partial y^2} \right)_0 + \rho_n z_n^2 \left(\frac{\partial^2 V}{\partial z^2} \right)_0 \right\} d\tau_n \quad (7)$$

The remaining terms in eqn. (7) are related to the *nuclear* charge distribution and hence to its quadrupole moment. The condition for a nucleus to possess an electric quadrupole moment is that $I \geq 1$, where I is the nuclear spin quantum number. Many common nuclei fulfil this condition, i.e., ^{14}N ($I = 1$), ^{35}Cl and ^{37}Cl ($I = 3/2$), ^{59}Co ($I = 7/2$); the proton, ^1H , has $I = 1/2$, but its common isotope ^2H is eligible, since $I = 1$. Similarly, we have ^{17}O ($I = 5/2$) and ^{33}S ($I = 3/2$), the common isotopes being non-magnetic ($I = 0$). Other isotopes, like ^{57}Fe , are inaccessible in their nuclear ground states, since $I = 1/2$, but have a nuclear quadrupole moment in one or more of their nuclear excited states, and so can be studied by Mössbauer spectroscopy.

Equation (7) may be simplified even further by the methods of quantum mechanics, as is described by Slichter (2). One convention that is thereby introduced is to redefine the nuclear quadrupole moment in eqn. (1) such that the integration is carried out in the state in which the maximum component of the nuclear magnetic moment lies along the z axis (that is, $I_z = I$). The quantities in round brackets in eqn. (7) become the expectation or average values of the principal components of the electric field gradient over the ground-state wave-function of the molecule—like the dipole moment, therefore, the electric field gradient is a ground-state property. If we neglect the effects of the very small electronic charge distribution *within* the nucleus, we may use Laplace's equation and write

$$\frac{\partial^2 V}{\partial x^2} + \frac{\partial^2 V}{\partial y^2} + \frac{\partial^2 V}{\partial z^2} = 0 \quad (8)$$

in which case we need only *two* quantities to define the electric field gradient (in addition, of course, to their direction cosines with respect to the principal coordinates); these we select to be the *maximum* principal component, which is by convention taken to be $\partial^2 V / \partial z^2$ or V_{zz} ($|V_{zz}| > |V_{yy}| > |V_{xx}|$), and we then define the parameters

$$eq = \frac{\partial^2 V}{\partial z^2} (= V_{zz}) \quad (9)$$

and

$$\eta = \frac{\partial^2 V}{\partial x^2} - \frac{\partial^2 V}{\partial y^2} / \frac{\partial^2 V}{\partial z^2} = \frac{V_{xx} - V_{yy}}{V_{zz}} \quad (10)$$

q will be called the electric field gradient (strictly speaking, this quantity is $-eq$) and can be either positive or negative. η is called the asymmetry parameter and is a *positive* number; it measures the departure of the electronic charge distribution at the nucleus from cylindrical symmetry. q , the maximum principal component, will be zero only at sites of very high symmetry, e.g., tetrahedral and octahedral; thus the quadrupole interaction at the ^{33}S nucleus in gaseous SF_6 and at the ^{35}Cl nucleus in crystalline NaCl will be zero. η will also be determined to some extent by symmetry considerations. For example, in studying ^{35}Cl nuclear quadrupole resonance, one is principally (but not always) concerned with an atom which is attached to only one other; in HCl and CH_3Cl (at least, in the gas), we have axes of infinite and three-fold symmetry, respectively, so that in both molecules $V_{xx} = V_{yy}$ and η is zero. In $\text{C}_6\text{H}_5\text{Cl}$, however, the C-Cl bond is on an axis of at most 2-fold symmetry, so that we must expect η to be non-zero. There is, in addition, the possibility of conjugation of $3p$ electrons on Cl with the π -electron system of the ring; the interaction will be strongest for those $3p$ electrons whose lobes are perpendicular to the plane of the benzene ring, and this will introduce an additional asymmetry and a further contribution to η .

Having therefore defined the principal parameters, we may now turn to the solution of the full quantum-mechanical equations for the potential energy. The detailed derivation of these solutions is given by Das and Hahn (4) in their monograph; we present here the conclusions in the form of the energy levels of the system, which we classify as in the precessional model according to the projection I_z of the nuclear spin angular momentum in the direction of the maximum principal component of the electric field gradient which defines V_{zz} . The quantum number we therefore use is that appropriate to the *operator* I_z , viz., m , the nuclear magnetic quantum number, which also is used to specify the magnetic levels in the applied field in nuclear magnetic resonance. This is *not* a complete description of the system, for it deals only with the longitudinal components of nuclear magnetization, or those which are parallel to the z -axis, and neglects the transverse components. These are important in *relaxation* processes, and will be reconsidered in the second article in this series. It turns out that for a nuclear spin of I , there will be $2I$ levels, and the way in which these are arranged depends on whether I is half-integral or integral.

Half-Integral Spins

For I *half-integral*, viz., ^{35}Cl and ^{37}Cl ($I = 3/2$), or ^{127}I ($I = 5/2$), the levels occur in pairs, leaving a degeneracy in m which is not removed even when η is finite. Considering first the case of zero η , we show in Figure 2 the order of the levels for the cases $I = 3/2, 5/2$, and $7/2$ and by their side the appropriate equations giving the magnitude of the frequencies. The selection rule for magnetic dipole transitions is $\Delta m = \pm 1$, so that for $I = 3/2$ we observe just one transition at a frequency

$$\nu = \left(\frac{e^2 q Q}{h} \right) \frac{1}{2} \quad (11)$$

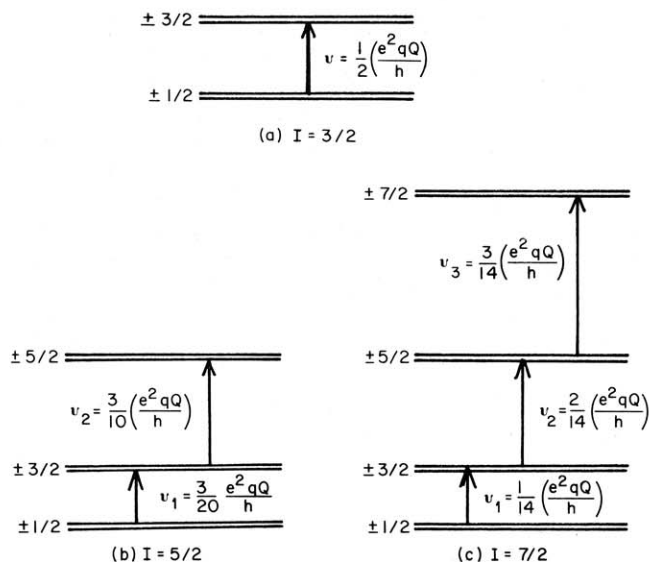


Figure 2. Quadrupole energy levels and transitions for (a) $I = 3/2$, (b) $I = 5/2$, (c) $I = 7/2$ ($\eta = 0$).

The quantity in parentheses is often referred to as the quadrupole coupling constant and quoted in units of MHz. For eqn. (11) it is the modulus that should be taken, but it will be convenient to omit this sign in subsequent equations. It can of course be either positive or negative according to the product of the signs of q and Q , but this is *not* determined from the spectrum, since a change in sign of (e^2qQ/h) merely inverts the order of the levels and does not change the frequency. For ^{35}Cl and ^{37}Cl , therefore, the quadrupole coupling constant is just twice the observed frequency, and in molecules like HCl or CH_3Cl there is good evidence from experimental methods that do give signs (e.g., microwave spectroscopy) that it is negative. For $I = 5/2$ (e.g., ^{121}Sb , ^{127}I), we observe *two* frequencies

$$\begin{aligned} \nu_1 &= \frac{3}{20} \left(\frac{e^2qQ}{h} \right) \\ \nu_2 &= \frac{3}{10} \left(\frac{e^2qQ}{h} \right) \end{aligned} \quad (12)$$

which are in an harmonic ratio when $\eta = 0$; thus in SiI_4 at 77°K , ^{127}I quadrupole transitions are observed at 198.736, 199.999 and 397.430, 399.993 MHz, appropriate to nearly zero η and quadrupole coupling constants of 1324.77 and 1333.31 MHz, almost certainly negative. The reason for *two* constants rather than just *one* presumably lies in the lower point symmetry of the molecule in the crystal compared to the vapor.

For $I = 7/2$ (e.g., ^{59}Co), we observe *three* frequencies

$$\begin{aligned} \nu_1 &= \frac{1}{14} \left(\frac{e^2qQ}{h} \right) \\ \nu_2 &= \frac{2}{14} \left(\frac{e^2qQ}{h} \right) \\ \nu_3 &= \frac{3}{14} \left(\frac{e^2qQ}{h} \right) \end{aligned} \quad (13)$$

again in an harmonic ratio; thus in cobalticinium perchlorate, $[\text{Co}(\text{C}_5\text{H}_5)_2]^+\text{ClO}_4^-$, three groups of frequencies are found near 12, 24, and 36 MHz, giving a quadrupole coupling constant of 170 MHz (probably positive, corresponding to positive q), and a near-zero η , as would be expected for the sandwich structure of the cation.

When η is non-zero, the energy-level diagram for $I = 3/2$ is unchanged in appearance, but the energies now contain a term in η , so that again *one* transition frequency is observed given by the equation

$$\nu = \left(\frac{e^2qQ}{h} \right) \frac{1}{2} \left(1 + \frac{\eta^2}{3} \right)^{1/2} \quad (14)$$

The quadrupole coupling constant cannot therefore be derived unless η is known, since neither (e^2qQ/h) nor η is separately derived; in practice, if $\eta < 0.1$, as is often the case in ^{35}Cl quadrupole resonance, the error in setting twice the frequency equal to the quadrupole coupling constant is small. In order to derive η for $I = 3/2$, separate experiments are necessary in weak magnetic fields, and these will be described shortly.

For $I = 5/2, 7/2$, etc., with non-zero η , closed solutions to the quantum mechanical equations do not exist, except in the limiting cases of low η . For $I = 5/2$, and low η (say < 0.25)

$$\begin{aligned} \nu_1 &= \frac{3}{20} \left(\frac{e^2qQ}{h} \right) (1 + 0.09259\eta^2 - 0.63403\eta^4) \\ \nu_2 &= \frac{3}{10} \left(\frac{e^2qQ}{h} \right) (1 - 0.20370\eta^2 + 0.16215\eta^4) \end{aligned} \quad (15)$$

for $I = 7/2$

$$\begin{aligned} \nu_1 &= \frac{1}{14} \left(\frac{e^2qQ}{h} \right) (1 + 3.63333\eta^2 - 7.26070\eta^4) \\ \nu_2 &= \frac{2}{14} \left(\frac{e^2qQ}{h} \right) (1 - 0.56667\eta^2 + 1.85952\eta^4) \\ \nu_3 &= \frac{3}{14} \left(\frac{e^2qQ}{h} \right) (1 - 0.1001\eta^2 - 0.01804\eta^4) \end{aligned} \quad (16)$$

The important conclusions from these equations are firstly that the harmonic ratio of the frequencies in eqns. (12) and (13) is no longer observed and secondly that from the observed frequencies both η and (e^2qQ/h) can be separately derived provided the theoretical equations can be fitted to the observed frequencies. In practice, this is done by using tabulations of frequency ratios calculated for various values of η ; such tables have been prepared for example by Cohen (5) for $I = 5/2, 7/2$, and $9/2$. As an interesting example of the solution of such a problem we may quote the ^{127}I quadrupole resonance frequencies of 212.6 and 340.1 MHz in BI_3 (the temperature at which this measurement was carried out was not specified); these are clearly not in an harmonic ratio, so that η must be non-zero, as would be expected if there were considerable "back-donation" from orbitals of π symmetry on I to the unfilled $2p_\pi$ orbital on B. Equation (16) is fitted by the values $(e^2qQ/h) = 1176$ MHz and $\eta = 0.456$ (or 45.6%).

Before concluding this discussion of quadrupole frequencies of nuclei with half-integral spin, we refer briefly to two methods of measuring η for nuclei of $I = 3/2$ (e.g., ^{35}Cl , ^{37}Cl , ^{75}As , ^{79}Br , ^{81}Br). In the first, of higher accuracy, a single crystal is required, often at least 1 cm^3 in volume, which is placed in a uniform but weak magnetic field H of precisely known orientation with respect to the crystal axes; by weak, we mean that the interaction of the nuclear magnetic moment with the magnetic field produces splittings or shifts of magnitude much smaller than the pure quadrupole resonance frequency. One effect of the magnetic field is to remove the $\pm m$ degeneracy noted in Figure 2, so that four lines now appear, corresponding to the selection rule $\Delta m =$

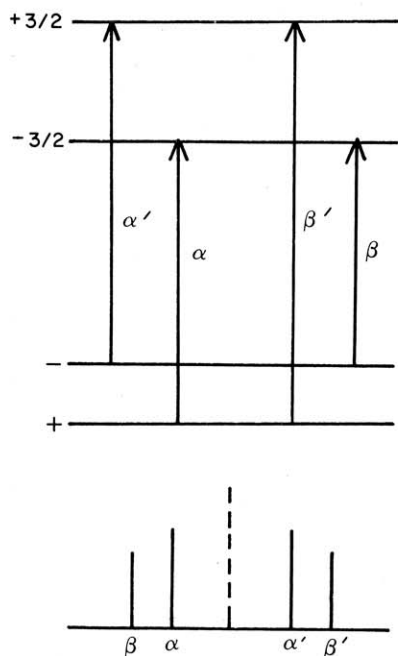


Figure 3. Energy levels and transitions for $I = 3/2$ in a weak magnetic field.

± 1 , as we show in Figure 3. The quadruplet is symmetrical about the original quadrupole resonance frequency in zero field, and the inner pair is conveniently referred to as the α doublet and the outer the β doublet. Both the positions and intensities of these doublets vary with orientation of the crystal in the applied magnetic field. For example, when H is perpendicular to V_{zz} , the splitting between the α and β doublets is calculated to be

$$\nu_{\alpha} - \nu_{\beta} = \frac{gH_0\eta}{h} \left[1 + \frac{\eta}{6} (\cos 2\phi - \eta) \right] \quad (17)$$

where ϕ is the azimuthal angle with respect to the direction of V_{xx} and g is the nuclear g -factor (a known constant for each nucleus); the dependence on ϕ can be neglected when $\eta < 0.25$, so that $\nu_{\alpha} - \nu_{\beta}$ is directly proportional to η via known constants. Hence η can be calculated to considerable accuracy provided the direction of V_{zz} (and possibly V_{xx}) can be located; in this technique, known as the field-frequency method (6), fields of up to 500 gauss are used, and can be measured by a Hall-effect probe or a proton magnetometer. In another and earlier variation, the method of zero-splitting locus (7), the investigator looks for the locus of zero-splitting of the α doublet; the geometrical shape of this locus can be shown to be related to η and its orientation to the directions of V_{zz} and V_{xx} . In this method, homogeneous fields of up to 100 gauss are used for ^{35}Cl work, but considerable care is needed in determining the orientation of the crystal with respect to the magnetic field.

In the second kind of technique (8), of lower accuracy, a polycrystalline sample is placed in a small magnetic field H (about 50 to 100 gauss) which is parallel to the rf field H_1 , i.e., parallel to the axis of the rf coil. Since the positions of the α and β doublets referred to in the previous paragraph depend on the orientation of the crystallites with respect to the static magnetic field, at first sight one might expect a uniform broadening of the line and in large fields a disappearance into the noise of the spectrometer. In practice, in fields

of the order of 30–60 gauss, strong signals still show some fine structure, and this arises essentially because those crystallites which find themselves oriented with the maximum principal component of the electric field gradient (along z) perpendicular to H give rise to transitions of maximum intensity, and that only the inner or outer transitions of the two doublets are allowed according as to whether H is parallel to V_{xx} or V_{yy} , respectively. From the shape of the observed fine structure and its dependence on H , a value for η can be estimated. The errors are greater than those of the best single crystal measurements, and the directions of V_{xx} and/or V_{yy} are not, of course, found. Strong signals are needed in the first place, and in addition the method implies some assumptions about line shapes in nuclear quadrupole resonance which may not be correct.

Integral Spins

For integral spins, of which the most studied at the present time is ^{14}N ($I = 1$) and to which we devote all our attention, the value of η can once again be determined from the spectrum of the powder (single crystal studies are needed to locate the directions of the principal components). Figure 4 shows the behavior of the

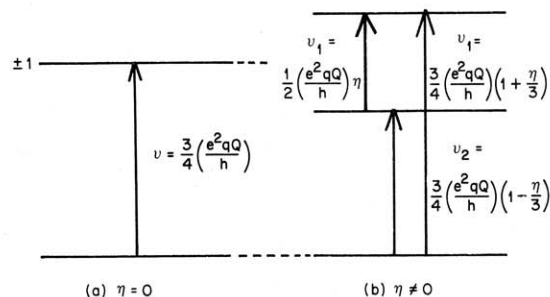
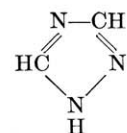


Figure 4. Quadrupole energy levels and transitions for $I = 1$: (a) $\eta = 0$ (b) $\eta \neq 0$.

energy levels and transition frequencies for $\eta = 0$ and finite η ; in the latter case, we can observe three transitions at frequencies of

$$\begin{aligned} \nu_1 &= \left(\frac{e^2qQ}{h} \right) \frac{1}{2} \eta \\ \nu_2 &= \frac{3}{4} \left(\frac{e^2qQ}{h} \right) \left(1 - \frac{\eta}{3} \right) \\ \nu_3 &= \frac{3}{4} \left(\frac{e^2qQ}{h} \right) \left(1 + \frac{\eta}{3} \right) \end{aligned} \quad (18)$$

When $\eta \rightarrow 0$, these frequencies go to just one at $3/4$ (e^2qQ/h). In 1,2,4-triazole



we find three frequencies for N' at 3.8759, 2.4692, and 1.4070 MHz at 77°K, which from eqn. (18) lead to a quadrupole coupling constant of 4.2301 MHz (almost certainly negative) and $\eta = 0.6651$. It is however fairly rare to observe ν_1 , since quite high values of η are needed to bring this frequency into a sensitive range. In most ^{14}N work, only ν_2 and ν_3 are observed, but this is sufficient information to enable both η and the quadrupole coupling constant to be separately deduced.

In concluding this section, we should mention that quadrupole coupling constants can also be derived by studying the quadrupole splitting of the nuclear magnetic resonance spectra of solids or of suitable solutions in liquid crystal media; in fact, for ^2H , with its very low quadrupole moment ($0.0027965 \times 10^{-24} \text{ cm}^2$) and hence low quadrupole coupling constants (viz., 56 kHz in CD_3CO_2^-), such methods are the only direct ones that have been used in condensed states. Such techniques, however, are outside the scope of these articles, and the interested reader is referred to other reviews in the literature (9).

Theoretical Interpretation of Quadrupole Coupling Constants

In this section we attempt to answer the question: What is the significance of the quadrupole coupling constant in theoretical chemistry?

Consider a set of Cartesian axes embedded in a molecule, with the origin located at the quadrupolar nucleus whose quadrupole coupling constant we are studying (Fig. 5). A volume element $d\tau$ of the molecular

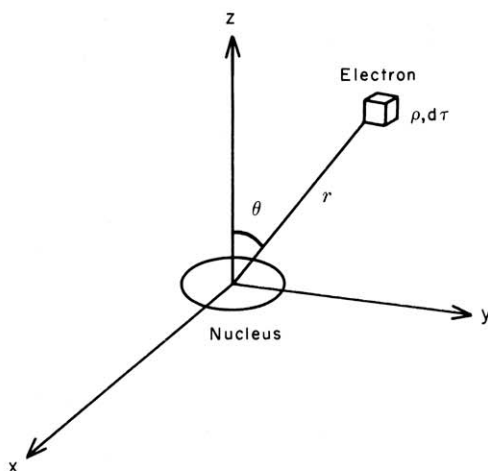


Figure 5. Cartesian axes in a molecular electronic charge distribution.

charge density ρ (including sign),¹ produces at the origin an electrostatic potential of

$$V = \frac{\rho d\tau}{r} \quad (19)$$

Hence

$$\frac{dV}{dz} = -\rho \left(\frac{z}{r^3} \right) d\tau = -\rho \left(\frac{\cos \theta}{r^2} \right) d\tau \quad (20)$$

since

$$dr/dz = z/r = \cos \theta$$

and

$$\frac{d^2V}{dz^2} = \rho \left(\frac{3 \cos^2 \theta - 1}{r^3} \right) d\tau \quad (21)$$

Similarly one may prove that

$$\frac{d^2V}{dx^2} = \rho \left(\frac{3 \sin^2 \theta \cos^2 \phi - 1}{r^3} \right) d\tau$$

and

$$\frac{d^2V}{dy^2} = \rho \left(\frac{3 \sin^2 \theta \sin^2 \phi - 1}{r^3} \right) d\tau \quad (22)$$

so that eqns. (21) and (22) satisfy eqn. (8).

To derive the *total* electric field gradient at the origin, we must integrate over the right-hand side of eqn. (21) to derive

$$V_{zz} = \int \rho \left(\frac{3 \cos^2 \theta - 1}{r^3} \right) d\tau \quad (23)$$

In quantum mechanical terms, we may use the Bohr probability criterion to replace $\rho d\tau$ by $\psi^* \psi d\tau$, at the same time separating out from the right-hand side of eqn. (23) the contribution of the other nuclei, which effectively behave as point charges. If we multiply both parts of the equation by the electronic charge e (*unsigned*) and distinguish between the two contributions by their different sign, we have

$$eq = V_{zz} = -e \int \psi^* \left(\frac{3 \cos^2 \theta - 1}{r^3} \right) \psi d\tau + \sum_i Z_i e \left(\frac{3 \cos^2 \theta_i - 1}{R_i^3} \right) \quad (24)$$

$Z_i e$ is the total charge on any other nuclei in the molecule distant R_i from the one under consideration. The nuclear term thus depends only on the geometry of the molecule, from which it can be calculated directly; in more refined calculations, it may be necessary to average this factor over the vibrational modes of the molecule. The factor which is related to the *electronic* structure of the molecule is the first, so that part of the answer to our question is that the term q in the quadrupole coupling constant measures at a fixed point within an atom or molecule the average value of the function $(3 \cos^2 \theta - 1)/r^3$ over the molecular charge distribution (and over the ground vibrational state). Knowing atomic or molecular wave functions, we should therefore be able to calculate quadrupole constants *providing that* the nuclear quadrupole moment Q is known, and in these circumstances the parameter is then a test of such wave functions. Like the dipole moment or molecular quadrupole moment, therefore, q depends on the ground state wave function of the molecule. In practice, its calculation is beset by many difficulties which arise from our lack of knowledge of reliable atomic or molecular wave functions, and in order to proceed further, it is convenient to consider atoms and molecules separately.

Quadrupole Coupling Constants in Atoms

Although no nuclear quadrupole resonance measurements have been performed on atoms, accurate values for the quadrupole coupling constants have been obtained from the nuclear hyperfine structure in atomic spectra (10) or atomic beams (10, 11), and it is essential to consider the significance of these results before we proceed to the study of molecules.

We may first turn our attention to hydrogen and hydrogen-like atomic orbitals. From eqn. (24), we require the value of $(3 \cos^2 \theta - 1)/r^3$ at the nucleus averaged over the orbital. Now s orbitals have full spherical symmetry, so that the average value of $(3 \cos^2 \theta - 1)$ will be zero ($\langle \cos^2 \theta \rangle = 1/3$); s electrons therefore have zero electric field gradient. For p orbitals, we consider $2p_z$ (z being the axis used to define

¹ Note the difference between this symbol and that in eqns. (4), (6), and (7) where ρ_n refers to the nuclear charge density.

θ), whose normalized wave function (omitting electron spin) is

$$\psi(2p_z) = \frac{1}{4\sqrt{2\pi}} \left(\frac{Z}{a_0}\right)^{5/2} r \cdot \exp\left(-\frac{Zr}{2a_0}\right) \cos \theta$$

Hence from eqn. (24) the integral we need to solve is

$$\frac{d^2V}{dz^2} = V_{zz} = -\frac{e}{32\pi} \left(\frac{Z}{a_0}\right)^5 \iiint \left(\frac{3 \cos^2 \theta - 1}{r^3}\right) r^2 \times \exp\left(-\frac{Zr}{a_0}\right) \cos^2 \theta d\tau \quad (25)$$

The volume element $d\tau$ in Cartesian coordinates is related to that in spherical polar coordinates by the relation

$$d\tau = dx dy dz = r^2 \sin \theta dr d\theta d\phi \quad (26)$$

Inserting eqn. (26) into eqn. (25) and separating the triple integral into its component parts gives

$$V_{zz} = -\frac{e}{32\pi} \left(\frac{Z}{a_0}\right)^5 \int_0^\infty r \exp\left(-\frac{Zr}{a_0}\right) dr \int_0^\pi \cos^2 \theta (3 \sin^2 \theta - 1) \times \sin \theta d\theta \int_0^{2\pi} d\phi \quad (27)$$

The first integral is $(Z/a_0)^{-2}$; the second $8/15$; and the third is just 2π . Hence

$$\begin{aligned} V_{zz} &= -\frac{e}{32\pi} \cdot \left(\frac{Z}{a_0}\right)^5 \cdot \left(\frac{Z}{a_0}\right)^{-2} \cdot \frac{8}{15} \cdot 2\pi \\ &= -\frac{4e}{15} \left(\frac{Z}{2a_0}\right)^3 \end{aligned} \quad (28)$$

A similar calculation using the normalized forms for $2p_x$ and $2p_y$ and calculating the electric field gradient along Oz gives

$$V_{zz}(2p_x) = V_{zz}(2p_y) = -\frac{1}{2} V_{zz}(2p_z) \quad (29)$$

These equations enable us to draw several conclusions. Firstly, the electric field gradient of one electron in a p orbital depends on Z^3 , so that quadrupole resonance frequencies are likely to be higher for nuclei of high atomic number. Secondly, because of the inverse dependence on r^3 , electron density nearest to the nucleus is most likely to be effective; for this reason, the value of V_{zz} for d orbitals is considerably less than for p orbitals of the same principal quantum number. Thirdly, from eqns. (28) and (29), the electric field gradient of a filled p shell is zero; in general, closed-shell atoms or ions in the gaseous phase will not have an electric field gradient at the nucleus and will therefore give no information on the nuclear quadrupole moment. The same will be true for all atoms in states of S symmetry; for example, the ground state of the nitrogen atom is 4S , so that any information on the ^{14}N nuclear quadrupole moment must either be derived from excited states of the atom or from the coupling constants in molecules.

The critical stage of the calculation has now been reached. Experimentally, we measure the quantity (e^2qQ/h) , which contains the product of q and Q ; having a reliable theoretical value of q for an atom then enables us to derive Q for the nucleus of that atom; we may then use this value to derive q in compounds of the atom and compare with values calculated from trial wave functions. This would be the ideal procedure, but the critical question, which unfortunately is still un-

answered for the majority of nuclei, is: how reliable are our estimates of q in atoms? One might expect the most reliable estimates to come from the use of analytical Hartree-Fock atomic wave functions. Such wave functions have been shown to give reasonable estimates of electric field gradients in atoms (12), but the question of accuracy has *not* been resolved, partly because of well-known deficiencies in Hartree-Fock wave functions, particularly the failure to allow for electron correlation. Very recently, Lyons, Pu, and Das (13) and other workers have attempted to allow for such effects by the use of Brueckner-Goldstone perturbation theory. We discuss these problems further in the next paragraphs.

Alternatively, one could turn to other properties of the atom which depend on $\langle 1/r^3 \rangle$, and use the "measured" value of this quantity in equations similar to those of eqn. (28) and (29) derived generally for atoms with one or more valence electrons. For open-shell atoms, the function $(3 \cos^2 \theta - 1)/r^3$ is identical with that in one term in the expression for the dipolar interaction between a nuclear and electron spin, the origin of hyperfine coupling in atoms. From *measured* hyperfine couplings, we can therefore derive average values of $(3 \cos^2 \theta - 1)/r^3$. Unfortunately the equations relating the two quantities also contain approximations and assumptions, so that the "measured" values of q are also of uncertain reliability. However, the majority of nuclear quadrupole moments quoted in the literature have been obtained in this way, and Ramsey (11) has given a critical discussion of their reliability.

Unfortunately, there is still one more factor which makes matters even more complex, and this is the existence of inner shell shielding. As Sternheimer (14) was the first to recognize, the closed inner shells of the atom cannot be regarded as spherically-symmetrical charge distributions unresponsive to the electrical distortions imposed on them by the nucleus or the valence electrons, as we have assumed in the previous paragraph. If we have one valence electron in a p orbital, as we have seen we may *expect* an electric field gradient at the nucleus which we may call V_{zz}° ; if, however, the inner shells are simultaneously distorted by this valency electron, they will produce an *additional* electric field gradient at the nucleus, which we set equal to $-\gamma V_{zz}^\circ$. Hence the total electrical field gradient experienced by the nucleus is

$$V_{zz}^\circ - \gamma V_{zz}^\circ$$

or

$$V_{zz}^\circ (1 - \gamma) \quad (30)$$

γ is a constant and is known as the Sternheimer polarization factor of the atom. In his early papers (14), Sternheimer showed that the mechanism we have been discussing here produces an entirely equal contribution to one in which the quadrupole moment of the nucleus is allowed to polarize the inner shells, and the resulting quadrupolar distortion of their charge distribution then allowed to interact with the electric field gradient of the p electron. While the former model may be more readily used in calculations for atoms, the latter enables us to give a better conceptual description of the process. Consider a spherical shell of charge surrounding a quadrupolar nucleus (Fig. 6); the lines of force emanating from the nuclear quadrupole will tend to pro-

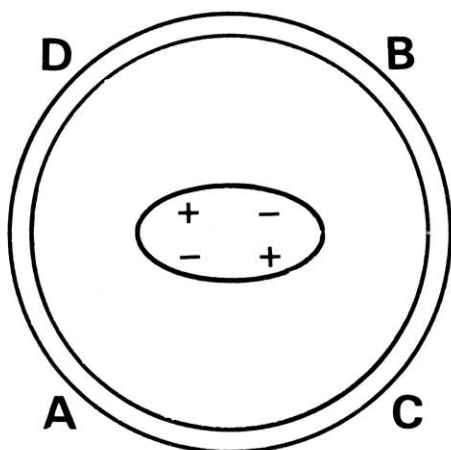


Figure 6. Sternheimer polarization of electron shell.

duce *two* rather different kinds of distortion in the closed shell. In the first, the inner shell suffers a *radial* distortion by a repulsion of charge at A,B and attraction at C,D; if $Q > 0$, from the point of view of a *distant* (i.e., valence) electron, the quadrupole interaction with the nucleus is reinforced, corresponding to antishielding (i.e., γ is $-ve$). In the second, the inner shell suffers an *angular* distortion in that charge at A and B tends to move towards C and D; if $Q > 0$, this effect reduces the quadrupolar interaction, corresponding to shielding (i.e., $\gamma > 0$ but less than one). By means of the angular distortions, for example, an *s* orbital in the inner shell acquires a little of the appearance of a *d* orbital, i.e., $ns \rightarrow d$; on the other hand, a *p* orbital in the inner shell acquires "*p*-character" by virtue of the radial distortion (viz., $np \rightarrow p$) and "*f*-character" by virtue of the angular distortion (viz., $np \rightarrow f$). These distortions are known as "excitations," and each occupied orbital in the atom will contribute by means of these excitations to the total electric field gradient, the actual value of γ being a summed average over the electron distribution in each occupied orbital. It will be clear that for atoms other than H equations like eqn. (28) will need to be multiplied by the factor $1 - \gamma$ before a reliable estimate of the true electric field gradient is obtained. In atoms, it is more usual to use the symbol R_Q or R for γ . Now $1 - R_Q$ can be calculated from atomic wave functions, although the majority of calculations hitherto involve approximations. Fortunately, in most open-shell atoms, $1 - R_Q$ is not large, e.g., in Cl, $1 - R_Q$ is estimated to be 0.888 and in B, 0.857, corresponding to shielding. Recently, some attempt has been made to take many-body interactions into account in such calculations by the use of Brueckner-Goldstone perturbation theory (see, e.g., ref. (13)): for example, such a calculation for ${}^7\text{Li}({}^2P_{3/2})$ has yielded a value for $(1 - R_Q)$ of 0.8300, compared to a one-electron value of 0.8844; the new quadrupole moment of ${}^7\text{Li}$ is then calculated to be $-(3.9 \pm 2.6) \times 10^{-26} \text{ cm}^2$ (the main uncertainty being probably in the experimental value of the quadrupole coupling constant!) in reasonable agreement with a value of -4.4×10^{-26} from molecular beam measurements on LiH. Unfortunately, such calculations have been performed for very few atoms, so that estimates of the polarization factor still represent yet another source of uncertainty in the derivation of nuclear quadrupole moments from atomic spectra.

When the distortions are produced by charges wholly

external to the atom or ion, as in calculations of electric field gradients in ionic crystals, the factor γ used in such circumstances can be very large; for example, values for a large negative ion like O^{2-} range from -10 to -430 ! The reliability of the polarization factors is then a *major* factor in the calculation, to which we return in the subsequent articles.

Quadrupole Coupling Constants in Molecules

At the present time, we have the somewhat paradoxical situation that whereas for atoms we have in general good experimental data and rather poorer theoretical calculations, for diatomic molecules the reverse is often true. One basis for this rather sweeping generalization is that the "best" experimental data for the theoretical chemist comes from measurements on gases, since his calculations can then ignore solid state effects which are bound to arise in nuclear quadrupole resonance spectroscopy (and to which we return later), and the most accurate measurements in gases tend to be for atoms. Another is the remarkable success of molecular orbital calculations based on self-consistent field methods and using highly extended basis sets of atomic orbitals in predicting molecular properties, particularly for diatomic molecules. For example, such a calculation of the ${}^{35}\text{Cl}$ quadrupole coupling constant in HCl by Cade (15) has given the value -67.9 MHz , compared with an experimental value (from microwave spectra in the gas) of -67.5 MHz . Even more accurate predictions of deuterium quadrupole constants can be made; such a calculation for HD (16), the coupling constant of which has been measured as $227 \pm 4 \text{ kHz}$ by molecular beam techniques (11), has enabled some of the first really reliable estimates of a nuclear quadrupole moment to be made, namely, $0.0027965 \times 10^{-24} \text{ cm}^2$ for ${}^2\text{H}$. It is somewhat ironic that this should come from calculations on a molecule rather than on an atom!

In view of the present rather gloomy picture of calculations of the quadrupole coupling constants of atoms, one might ask why it is that calculations for molecules are apparently more successful. For HD, the simple answer is that present molecular wave functions are so good—and of course there is no inner shell polarization. Otherwise the best results have been obtained for diatomic hydrides of first and second-row elements and homonuclear diatomic molecules of the first row elements and some of their simpler polyatomic species; the present most reliable values of the quadrupole moment of ${}^{14}\text{N}$ ($+0.015$ and $+0.0166 \times 10^{-24}$) have come by combining theoretical calculations and experimental results for molecular N_2 and the molecules HCN, FCN, ClCN and CH_2CN . Calculations of the ${}^{17}\text{O}$ quadrupole coupling constant in H_2O or ${}^{14}\text{N}$ in NH_3 are extremely encouraging but not at present so reliable, although the ${}^2\text{H}$ quadrupole coupling constants of the deuterated molecule are often well-reproduced. But what about the Sternheimer polarization factor for the heavier atoms? In self-consistent-field calculations of the kind we are discussing, the basis set includes *all* orbitals of the two atoms, so that what we call the "core" orbitals are already heavily-distorted in the final electron distribution. There is therefore some reason for supposing that polarization effects have been taken into account, and that the Sternheimer effect can be ignored. The test will come when we have calcula-

tions of a similar caliber for a set of molecules with a common quadrupolar nucleus, e.g., the series H-Cl, F-Cl, Cl-Cl, which could give us three independent estimates of the ^{35}Cl nuclear quadrupole moment. In this connection, the value of ^{17}O quadrupole coupling constants cannot be overestimated. In the meanwhile, the increasing interest of theoretical chemists in quadrupole coupling constants as an important parameter to be derived from their calculations is certain in the future to exert a considerable and beneficial influence on the subject.

We conclude this section with a list (see Table 1) of the "best-available" values of the quadrupole moments of nuclei discussed in these articles.

Table 1. Some Nuclear Quadrupole Moments and Quadrupole Moment Ratios

| Nucleus | Natural abundance (%) | Nuclear spin quantum no. (I) | Estimated nuclear quadrupole moment ^a Q ($\times 10^{24}$ cm ²) | Isotopic ^b ratio |
|-------------------|-----------------------|----------------------------------|---|-----------------------------|
| ^2H | 1.56×10^{-2} | 1 | +0.0027965 | }0.019 |
| ^6Li | 7.43 | 1 | -0.000741 | |
| ^7Li | 92.57 | $3/2$ | -0.039 | |
| ^9Be | 100 | $3/2$ | +0.029 | }2.084 |
| ^{10}B | 18.83 | 3 | +0.074 | |
| ^{11}B | 81.17 | $3/2$ | +0.036 | |
| ^{14}N | 99.635 | 1 | +0.0166 | }1.26878 |
| ^{17}O | 3.7×10^{-2} | $5/2$ | -0.0301 | |
| ^{27}Al | 100 | $5/2$ | +0.151 | |
| ^{35}Cl | 75.4 | $3/2$ | -0.0802 | }1.0806 |
| ^{37}Cl | 24.6 | $3/2$ | -0.0632 | |
| ^{55}Mn | 100 | $5/2$ | +0.355 | |
| ^{59}Co | 100 | $7/2$ | +0.40440 | }1.19707 |
| ^{63}Cu | 69.09 | $3/2$ | -0.163 | |
| ^{65}Cu | 30.91 | $3/2$ | -0.153 | |
| ^{75}As | 100 | $3/2$ | +0.32 | }0.986365 |
| ^{79}Br | 50.57 | $3/2$ | +0.332 | |
| ^{81}Br | 49.43 | $3/2$ | +0.282 | |
| ^{113}In | 4.16 | $9/2$ | +1.145 | }0.78447 |
| ^{115}In | 95.84 | $9/2$ | +1.165 | |
| ^{121}Sb | 57.25 | $5/2$ | -0.5310 | |
| ^{123}Sb | 42.75 | $7/2$ | -0.6810 | }1.534 |
| ^{127}I | 100 | $5/2$ | -0.785 | |
| ^{135}Ba | 6.59 | $3/2$ | +0.182 | |
| ^{137}Ba | 11.32 | $3/2$ | +0.283 | }1.056 |
| ^{185}Re | 37.07 | $5/2$ | +2.8 | |
| ^{187}Re | 62.93 | $5/2$ | +2.6 | |
| ^{197}Au | 100 | $3/2$ | +0.606 | } |
| ^{209}Bi | 100 | $9/2$ | -0.4 | |

^a No Sternheimer polarization factor has been applied, except for ^2H and possibly for ^7Li and ^{14}N .

^b This ratio is usually known to a considerably higher accuracy than the individual nuclear quadrupole moments.

Approximate Methods of Deriving Quadrupole Coupling Constants in Molecules

Wavefunctions expressed in terms of extended basis sets such as we have been discussing in the previous section, simply do not exist at the present time for the vast majority of polyatomic molecules. It is natural, therefore, that chemists should turn to more approximate methods of predicting quadrupole coupling constants in terms of such familiar parameters as orbital populations, bond hybridization, and ionic character. While the success of these methods has been rather limited, they are used in many discussions of quadrupole coupling constants, and they will therefore be briefly discussed in this section.

We start from eqn. (24) and imagine to begin with that our molecule will be described by a set of N doubly-occupied orthogonal molecular orbitals, each of

which will be written as a linear combination of n orthogonal atomic orbitals, ϕ_i . The j th member of this set we write as

$$\begin{aligned} \Phi_j &= C_{1j}\phi_1 + C_{2j}\phi_2 + C_{3j}\phi_3 + \dots + C_{nj}\phi_n \\ &= \sum_i^n C_{ij}\phi_i \end{aligned} \quad (31)$$

and in general inner-shell orbitals are *not* included.

When this equation is substituted into eqn. (24), and the first term summed over all *occupied* orbitals, it is clear that three different kinds of basic integral will arise. To clarify this differentiation, let us imagine that we are interested in the quadrupole coupling constant of the nucleus of atom 1, so that $[(3 \cos^2 \theta - 1)/r^3]_1$ is to be evaluated at nucleus 1 (hence the subscript). The first kind of integral will be of the form

$$C_{2j}C_{3j} \int \phi_2^* \left(\frac{3 \cos^2 \theta - 1}{r^3} \right)_1 \phi_3 d\tau$$

and is a *three-center* integral, since atoms 1, 2, 3 are involved. The *two-center* integrals will therefore be of the form

$$C_{1j}C_{2j} \int \phi_1^* \left(\frac{3 \cos^2 \theta - 1}{r^3} \right)_1 \phi_2 d\tau$$

and the *one-center* integrals (generally the easiest to evaluate)

$$C_{1j}^2 \int \phi_1^* \left(\frac{3 \cos^2 \theta - 1}{r^3} \right)_1 \phi_1 d\tau$$

Note that the quadrupole coupling operator is a *one-electron operator*. Now the two most used approximate methods in the literature differ in the way in which these various integrals are treated. In the method used by Cotton and Harris (17), all three-center integrals are neglected, *some* of the two-center integrals are allowed to cancel the nuclear term [the second in eqn. (24)], the remainder are approximated by a relationship involving the overlap integral S_{ik} , and finally the Sternheimer polarization factor is assumed to vary negligibly from molecule to molecule. The equation they derive is that the quadrupole coupling constant in the free molecule $(e^2qQ/h)_{\text{mol}}$ is equal to

$$\sum_i^n f_i \cdot \left(\frac{e^2q_iQ}{h} \right)_{\text{atom}} \quad (32)$$

where $(e^2q_iQ/h)_{\text{atom}}$ contains the term $q_i = \int \phi_i^* ((3 \cos^2 \theta - 1)/r^3) \phi_i d\tau$ in the atom and

$$f_i = \sum_j^N \left\{ C_{ij}^2 + C_{ij} \sum_{k>i} C_{kj} S_{ik} \right\} \quad (33)$$

being an expression for the occupation (including overlap) of orbital ϕ_i . If overlap is neglected, f_i becomes simply

$$\sum_j^N C_{ij}^2$$

the orbital population of ϕ_i . It should be stressed however that many of the approximations involved in deriving these equations are drastic ones. For complexes of the type MCl_n^{m-} (e.g., PtCl_4^{2-} , PtCl_6^{2-}), for which the theory was originally designed, it has the con-

venient feature that it requires precisely those quantities that are derived in present molecular orbital calculations, e.g., the eigenfunctions and overlap integrals, but the value of such predictions of the quadrupole coupling constant will also depend on the approximations made in deriving these eigenfunctions.

The second theory, much older, and one which has shaped the subject for over twenty years, is that due to Townes and Dailey (18). They use what is essentially a localized-orbital approach, so that for a terminal nucleus, like ^{35}Cl in R-Cl, we consider only orbitals on Cl and the atom to which it is bonded. Three-center integrals are therefore zero, all two center integrals are set against the nuclear contribution of the bonded atom, and the Sternheimer polarization factor is again assumed to vary negligibly from molecule to molecule (although a small correction is sometimes applied when the Cl atom is believed to carry a small positive charge). Everything therefore depends on *how* the Cl $3p$ orbitals are occupied, i.e., on the $3p$ orbital populations, a conclusion which is consistent with the equations of Cotton and Harris when overlap is neglected. If moreover the direction of the principal axes are known, and the same axial system can be used to specify the p orbitals, a particularly simple situation arises. In R-Cl, for example, q_{zz} lies along the chlorine bond—or very nearly so—and we therefore take this as the z direction of our coordinate system. Taking the chlorine bonding orbital ψ_1 as a $3s$ - $3p$ hybrid of s character α

$$\psi_1 = \alpha\psi(3s) + (1 - \alpha^2)^{1/2}\psi(3p_z) \quad (34)$$

of population b , the non-bonding orbital

$$\psi_2 = (1 - \alpha^2)^{1/2}\psi(3s) - \alpha\psi(3p_z) \quad (35)$$

of population n , and the π orbitals

$$\psi_3 = \psi(3p_x) \quad (36)$$

$$\psi_4 = \psi(3p_y)$$

of populations p_x and p_y , we can set up the following table of one-center contributions neglecting *overlap* contributions and using eqn. (29)

| Orbital | Electric field gradient along z | Orbital population | Total contribution to electric field gradient |
|----------|-----------------------------------|--------------------|---|
| ψ_1 | $(1 - \alpha^2)q_0$ | b | $b(1 - \alpha^2)q_0$ |
| ψ_2 | α^2q_0 | n | $n\alpha^2q_0$ |
| ψ_3 | $-1/2q_0$ | p_x | $-\frac{p_x}{2}q_0$ |
| ψ_4 | $-1/2q_0$ | p_y | $-\frac{p_y}{2}q_0$ |

q_0 is the value of the integral

$$\int \psi^* [(3 \cos^2 \theta - 1)/r^3] \psi d\tau$$

for a $3 p_z$ orbital. The total electric field gradient is therefore

$$q = -q_0[(-b + b\alpha^2 - n\alpha^2) + 1/2(p_x + p_y)] \quad (37)$$

If we perform a similar calculation for atomic chlorine (in which the orbital populations are either 1 or 2), we find that q in the atom is equal to $-q_0$; hence multiplying both sides of eqn. (37) by (e^2Q/h) , we finally derive

$$\frac{(e^2qQ/h)_{\text{mol}}}{(e^2qQ/h)_{\text{atom}}} = \frac{(e^2qQ/h)_{\text{mol}}}{-109.7} = - \left\{ b(1 - \alpha^2) + n\alpha^2 \right\} + 1/2(p_x + p_y) \quad (38)$$

where $(e^2qQ/h)_{\text{atom}}$ is measured as -109.7 MHz. It is

now a straightforward procedure to apply eqn. (38) to various molecules containing M-Cl bonds. Thus in molecular chlorine, $b = 1$ (neglecting overlap), $n = 2$, and $p_x = p_y = 2$, so that the ratio comes to $(1 - \alpha^2)$. Since the quadrupole coupling constant in solid chlorine (108.9 MHz) is almost the same as in the atom, this appears to predict that $\alpha \sim 0$, which is not unreasonable; unfortunately this simple picture also neglects the possibility of d orbital participation in the bonding. In R-Cl, with no π bonding, $p_x = p_y = 2$, and if we make $n = 2$

$$\frac{(e^2qQ/h)_{\text{mol}}}{(e^2qQ/h)_{\text{atom}}} = (1 - \alpha^2)(2 - b) \quad (39)$$

b will vary according to the relative electronegativity of the bonding atom with respect to that of Cl; thus on a valence bond picture, it can be related to the ionic character by expressing the wavefunction of the bonding orbital as

$$\psi_b = (1 - i)^{1/2}\psi(\text{R-Cl}) + i^{1/2}\psi(\text{R}^+\text{Cl}^-)$$

assuming only $\psi(\text{R}^+\text{Cl}^-)$ to make a significant contribution; since in R^+Cl^- the chlorine ion has spherical symmetry, its contribution to the electric field gradient (and hence its quadrupole coupling constant) will be zero, so that $(2 - b)$ can be replaced by the factor $(1 - i)$ and the ratio in eqn. (39) becomes simply

$$(1 - \alpha^2)(1 - i) \quad (40)$$

When both $3p_x$ and $3p_y$ participate equally in π bonding to R, the populations p_x and p_y remain equal but fall below 2; calling them $2 - \pi$ (π being the π -character of the bond), on a valence bond picture we may use the revised table of contributions to give

$$\frac{(e^2qQ/h)_{\text{mol}}}{(e^2qQ/h)_{\text{atom}}} = (1 - \alpha^2)(1 - i) - \pi \quad (41)$$

neglecting the product $\pi\alpha^2$. When only *one* of the $3p$ orbitals, say $3p_x$, participates in the π bonding (as expected in chlorobenzene), the bond to chlorine ceases to be axially symmetric and a similar analysis of the field gradients V_{xx} and V_{yy} shows that $V_{xx} > V_{yy}$ and that

$$\eta = \frac{3}{2} \pi \frac{(e^2qQ/h)_{\text{atom}}}{(e^2qQ/h)_{\text{mol}}} \quad (42)$$

Even if we exclude d orbital participation in the bonding, these equations contain two experimental quantities (e^2qQ/h and η) and at least *three* parameters (α , i , π), with an additional factor if polarization effects are to be allowed for. Some other experimental datum at least is required, and perhaps this feature more than any other has been a serious defect in the Townes-Dailey theory. Nevertheless, it has found widespread application in the interpretation of nuclear quadrupole coupling constants, some of which will be considered in the subsequent articles in this series. For an account of the Townes-Dailey theory, the interested reader is referred to a recent book by Lucken (19).

Literature Cited

- (1) RAICH, J. C., AND GOOD, R. H., JR., *Amer. J. Phys.*, **30**, 356 (1963).
- (2) SLICHTER, C. P., "Principles of Nuclear Magnetism," Harper and Row, New York, 1963; Chap. 6.
- (3) NYE, J. F., "Physical Properties of Crystals," Oxford Univ. Press, Oxford, 1957; Chap. 1.
- (4) DAS, T. P., AND HAHN, E. L., "Nuclear Quadrupole Resonance Spectroscopy," Academic Press, New York and London, 1958.
- (5) COHEN, M. H., *Phys. Rev.*, **96**, 1278 (1954).
- (6) REHN, V., *J. Chem. Phys.*, **38**, 749 (1963).

CHAPTER 2

NUCLEAR QUADRUPOLE RESONANCE SPECTROSCOPY

Bryan H. Suits

Physics Department, Michigan Technological University, Houghton, MI, USA

2.1 INTRODUCTION

Nuclear quadrupole resonance (NQR) uses radio-frequency (RF) magnetic fields to induce and detect transitions between sublevels of a nuclear ground state, a description that also applies to nuclear magnetic resonance (NMR). NMR refers to the situation where the sublevel energy splitting is predominantly due to a nuclear interaction with an applied static magnetic field, while NQR refers to the case where the predominant splitting is due to an interaction with electric field gradients within the material. So-called “pure NQR” refers to the common case when there is no static magnetic field at all.

The beginning of NQR in solids dates back to the beginnings of NMR in the late 1940s and early 1950s [1]. The first NQR measurements reported for a solid were by Dehmelt and Kruger using signals from ^{35}Cl in trans-dichloroethylene [2]. An excellent early summary of NQR theory and technique can be found in the 1958 book by Das and Hahn [3]. Several more recent summaries can be found listed at the end of this chapter. Due to practical limitations, discussed below, NQR has not grown to be nearly as common as NMR, and is usually considered a tool for the specialist.

As is the case for NMR spectroscopy, the primary goal for NQR spectroscopy is to determine nuclear transition frequencies (i.e., energies) and/or relaxation times and then to relate those to a property of a material being studied. That property may simply be the sample temperature, for use as an NQR thermometer [4, 5], or even whether or not a sample is present when NQR is used for materials detection [6]. On the other hand, NQR is also used to obtain detailed information on crystal symmetries and bonding, on changes in lattice constants with pressure, about phase transitions in solids, and other properties of materials of interest to solid state physicists and chemists.

As will be seen in more detail below, in order to use NQR spectroscopy one must have available an isotope with a nuclear spin $I > \frac{1}{2}$, which has a reasonably high isotopic abundance, and which is at a site in a solid that has symmetry lower than tetragonal. The most common NMR isotopes, ^1H , ^{13}C , and ^{15}N cannot be used since they have a nuclear spin $\frac{1}{2}$. Of course, ^{12}C and ^{16}O cannot be used either as they have nuclear spin 0. Table 2.1 shows a selection of potential nuclei including those most commonly used for NQR, as well as a few others of possible interest.

2.2 BASIC THEORY

2.2.1 The Nuclear Electric Quadrupole Interaction

Since a nuclear wavefunction has a definite state of parity, a multipole expansion of the fields due to the nucleus yields electric 2^n -poles, where n is even (monopole, quadrupole, etc.) and magnetic 2^n -poles, where n is odd (dipoles, octupoles, etc.). In general these multipole moments become weaker very rapidly with increasing n . In a molecule or in a solid, the nucleus will be at an equilibrium position where the electric field is zero, and so in the absence of a magnetic field the first non-zero interaction is with the electric quadrupole moment of the nucleus. Higher moments, if they exist, are generally much too weak to affect NQR measurements [7–9].

A non-zero electric quadrupole moment arises for nuclei that are classically described as prolate (“stretched”) or oblate (“squashed”) spheroids. The nuclear charge distribution has axial symmetry and the axis of symmetry coincides with the direction of the nuclear angular momentum and the nuclear magnetic dipole moment. In general, an electric quadrupole moment is described by a 3×3 symmetric, traceless tensor \mathbf{Q} . For a nucleus such a tensor can be determined using a single value that describes how prolate or oblate the nucleus is, plus a description of the orientation of the nucleus. Since the charge distribution for a nucleus with spin 0 or $\frac{1}{2}$ is spherical, such nuclei will have no electric quadrupole moment.

If the charge distribution within the nucleus is known, the amount by which the sphere is prolate or oblate is determined by the (scalar) nuclear quadrupole moment Q , which can be calculated using

$$eQ = \int \rho (3z^2 - r^2) d\tau \quad (2.1)$$

where the z -axis is along the direction of axial symmetry, e is the magnitude of the charge on an electron, and ρ is the nuclear charge density as a function of position. While such computations may be done by a nuclear physicist to check a new model for the nucleus, the NQR spectroscopist uses values determined experimentally. Values of Q are conveniently expressed in units of $10^{-24} \text{ cm}^2 = 1 \text{ barn}$.

Table 2.1 Selected quadrupolar nuclei.

| Nucleus | Natural Isotopic Abundance % | Spin I | $\gamma/2\pi$ (kHz/G) | Q (10^{-24} cm ²) |
|-------------------|------------------------------|----------|-----------------------|------------------------------------|
| ² H | 0.015 | 1 | 0.654 | +0.00286 |
| ⁶ Li | 7.4 | 1 | 0.626 | -0.0008 |
| ⁷ Li | 92.6 | 3/2 | 1.655 | -0.040 |
| ¹⁰ B | 19.6 | 3 | 0.458 | +0.085 |
| ¹¹ B | 80.4 | 3/2 | 1.366 | +0.041 |
| ¹⁴ N | 99.6 | 1 | 0.308 | +0.019 |
| ¹⁷ O | 0.048 | 5/2 | -0.577 | -0.26 |
| ²³ Na | 100 | 3/2 | 1.126 | +0.10 |
| ²⁷ Al | 100 | 5/2 | 1.109 | +0.14 |
| ³⁵ Cl | 75.5 | 3/2 | 0.417 | -0.082 |
| ³⁷ Cl | 24.5 | 3/2 | 0.347 | -0.064 |
| ⁵⁰ V | 0.25 | 6 | 0.425 | +0.21 |
| ⁵¹ V | 99.8 | 7/2 | 1.119 | -0.05 |
| ⁵⁵ Mn | 100 | 5/2 | 1.050 | +0.33 |
| ⁵⁹ Co | 100 | 7/2 | 1.005 | +0.40 |
| ⁶³ Cu | 69.1 | 3/2 | 1.128 | -0.21 |
| ⁶⁵ Cu | 30.9 | 3/2 | 1.209 | -0.195 |
| ⁶⁹ Ga | 60.4 | 3/2 | 1.022 | +0.17 |
| ⁷¹ Ga | 39.6 | 3/2 | 1.298 | +0.10 |
| ⁷⁵ As | 100 | 3/2 | 0.729 | +0.31 |
| ⁷⁹ Br | 50.5 | 3/2 | 1.067 | +0.33 |
| ⁸¹ Br | 49.5 | 3/2 | 1.150 | +0.28 |
| ⁸⁵ Rb | 72 | 5/2 | 0.411 | +0.23 |
| ⁸⁷ Rb | 28 | 3/2 | 1.393 | +0.13 |
| ⁹³ Nb | 100 | 9/2 | 1.041 | -0.32 |
| ¹¹³ In | 4.3 | 9/2 | 0.931 | +0.8 |
| ¹¹⁵ In | 95.7 | 9/2 | 0.933 | +0.8 |
| ¹²¹ Sb | 57.3 | 5/2 | 1.019 | -0.4 |
| ¹²³ Sb | 42.7 | 7/2 | 0.552 | -0.5 |
| ¹²⁷ I | 100 | 5/2 | 0.852 | -0.7 |
| ¹³⁸ La | 0.1 | 5 | 0.564 | +0.4 |
| ¹³⁹ La | 99.9 | 7/2 | 0.606 | +0.2 |
| ¹⁸¹ Ta | 99.99 | 7/2 | 0.510 | +3.3 |
| ¹⁹⁷ Au | 100 | 3/2 | 0.073 | +0.55 |
| ²⁰⁹ Bi | 100 | 9/2 | 0.684 | -0.4 |
| ²³⁵ U | 0.72 | 7/2 | -0.076 | +5 |

While the electric field at the nucleus is zero, the electric field gradients (spatial derivatives of that field) may not be. Figure 2.1 is a schematic showing two orientations of a prolate nucleus ($Q > 0$) at a point where the electric field is zero in the vicinity of four fixed point charges. The configuration shown on the left will have a lower energy than that shown on the right since the positive charge of the nucleus is, on the whole, closer to the negative charges. When quantum mechanics is applied, this orientation dependence gives rise to a small splitting of the nuclear ground state.

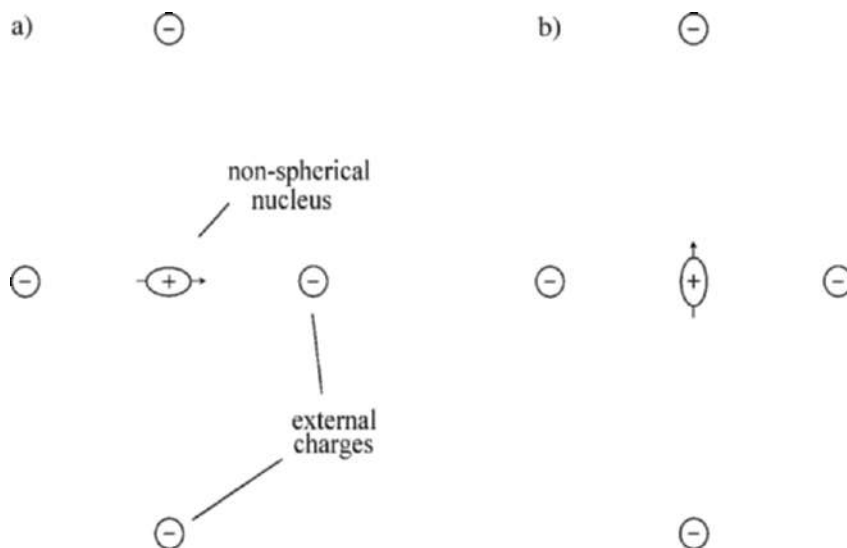


Figure 2.1 Two configurations of a non-spherical nucleus near charges external to the nucleus. The configuration at (a) has a lower energy than that shown at (b).

The electric field gradient at the nucleus due to charges external to the nucleus, ∇E , is conveniently described using spatial derivatives of the corresponding electrostatic potential, V , evaluated at the nucleus. Taking the nucleus to be at the origin of the coordinate system, the desired derivatives are

$$V_{jk} = \left. \frac{\partial^2 V}{\partial r_j \partial r_k} \right|_0 \quad (2.2)$$

where $\{r_i\} = \{x, y, z\}$. Since $V_{jk} = V_{kj}$ and, using Laplace's equation,

$$\sum_{i=x,y,z} V_{ii} = 0, \quad (2.3)$$

the field gradient can be described by a real, symmetric, traceless 3×3 tensor. Such a tensor can always be made diagonal by choosing an appropriate set of coordinate axes known as *principal axes*. Once this is done, it is conventional to define

$$eq = V_{zz} \quad (2.4)$$

$$\eta = \frac{V_{yy} - V_{xx}}{V_{yy} + V_{xx}} = \frac{V_{xx} - V_{yy}}{V_{zz}} \quad (2.5)$$

where η is known as the *asymmetry parameter*. It is convenient to choose the principal axes such that

$$|V_{xx}| \leq |V_{yy}| \leq |V_{zz}| \quad (2.6)$$

giving $0 \leq \eta \leq 1$. Since the principal axes are determined by the environment surrounding the nucleus, those axes are sometimes also referred to as forming a “molecular” or “crystal” coordinate system. For axial symmetry $V_{xx} = V_{yy} = -V_{zz}/2$ and $\eta = 0$.

Classically, the *interaction energy* is given by the tensor scalar product

$$E_Q = \frac{1}{6} \sum_{i,j=x,y,z} V_{ij} Q_{ij}, \quad (2.7)$$

where the two tensors must be expressed in the same coordinate system. Coordinate transformations can be accomplished using well-known relations for 3×3 symmetric tensors.

Since the nuclear state can be described by specifying the nuclear angular momentum, the entire interaction can be written, with appropriate scale factors including the scalar quadrupole moment, in terms of the angular momentum. When written using quantum mechanical operators, the Hamiltonian \mathcal{H}_Q for a nucleus of spin I expressed in the principal axis coordinate system is

$$\mathcal{H}_Q = \frac{e^2 q Q}{4I(2I-1)} \left[3I_z^2 - I^2 + \eta(I_x^2 - I_y^2) \right]$$

where all I 's in the denominator are scalar values while all I 's in the square brackets are operators. The interested reader can find a detailed derivation of this result in Slichter's book [10]. In terms of the usual angular momentum raising and lowering operators, $I_{\pm} = I_x \pm iI_y$, the Hamiltonian can also be written

$$\mathcal{H}_Q = \frac{e^2 q Q}{4I(2I-1)} \left[3I_z^2 - I^2 + \eta \cdot \frac{I_+^2 - I_-^2}{2} \right]. \quad (2.8)$$

To represent the Hamiltonian in other coordinate systems, the appropriate angular momentum rotation operators are applied. Other forms for the operators, such as irreducible tensor operators, are also sometimes employed (see [11] for example).

One of the goals of an NQR measurement will be to determine the quadrupole coupling constant $e^2 q Q$ and the asymmetry parameter η , which contain information about the environment surrounding the nucleus.

2.2.2 Energy Levels and Transition Frequencies

In the case of axial symmetry, $\eta = 0$, the pure quadrupole Hamiltonian is easily diagonalized using eigenfunctions of the operator I_z with quantum number $m = -I, -I + 1, \dots, I - 1, I$. The resulting $2I + 1$ energy levels are given by

$$E_m = \frac{e^2 q Q}{4I(2I-1)} (3m^2 - I(I+1)). \quad (2.9)$$

In this case m is a good quantum number and the usual magnetic dipole transition rules apply, $\Delta m = 0, \pm 1$. Defining

$$\nu_Q = \frac{3e^2 q Q}{4I(2I-1)h}, \quad (2.10)$$

where h is Plank's constant, the allowed transition frequencies are given by

$$\nu_{m,m\pm 1} = \nu_Q |(2m \pm 1)|; |m|, |m \pm 1| \leq I. \quad (2.11)$$

For the more general case of arbitrary η , closed form solutions are known only for $I = 1$ and $I = 3/2$. Due to the symmetry of the Hamiltonian, all the energy levels are doubly degenerate for half-integer spin nuclei. For integer spin nuclei, of which there are very few in practice, there are an odd number of levels and the degeneracy is broken. Furthermore, since the eigenfunctions of I_z are not, in general, energy eigenfunctions, additional transitions are often allowed.

2.2.2.1 Integer Spins

There are only four known stable nuclei with integer spin: ^2H , ^6Li , and ^{14}N , all with $I = 1$, and ^{10}B with $I = 3$. In addition there are some very long-lived radioactive isotopes, such as ^{50}V , with $I = 6$ and ^{138}La with $I = 5$. Most of the NQR work done using integer spin nuclei is for $\sim 100\%$ naturally abundant ^{14}N . Deuterium (^2H) and ^6Li have very small electric quadrupole moments, making direct observation with NQR difficult. There has been some work using ^{10}B but due to its lower natural abundance compared to ^{11}B ($I = 3/2$) the latter is preferred. The long-lived radioactive isotopes also have a very low natural abundance making them quite difficult to use.

For spin 1, the three energy levels are

$$E_0 = -\frac{2}{3} h \nu_Q, \quad E_{\pm} = \frac{(1 \pm \eta)}{3} h \nu_Q, \quad (2.12)$$

and all three possible transition frequencies

$$\nu_0 = \frac{2}{3} \eta \nu_Q, \quad \nu_{\pm} = \left(1 \pm \frac{\eta}{3}\right) \nu_Q, \quad (2.13)$$

are allowed.

For spin 3 an exact solution is not known. Butler and Brown [12] provide a graphical representation showing 18 allowed transitions, arising from the 7 energy levels, as a function of η . Five of those 18 are forbidden when $\eta = 0$ and are somewhat inappropriately referred to as “multiple quantum transitions.” They are allowed single quantum transitions, though some are quite weak, and can be useful to help unravel the wonderfully complicated ^{10}B NQR spectra [13].

2.2.2.2 Spin 3/2

Much of the NQR work in the literature is for spin 3/2 nuclei, which have two doubly degenerate energy levels,

$$E_{\pm 3/2} = h\nu_Q \left(1 + \frac{\eta^2}{3}\right)^{1/2}, \quad E_{\pm 1/2} = -h\nu_Q \left(1 + \frac{\eta^2}{3}\right)^{1/2} \quad (2.14)$$

and hence only one (non-zero frequency) transition,

$$\nu = 2\nu_Q \left(1 + \frac{\eta^2}{3}\right)^{1/2}. \quad (2.15)$$

The fact that there is only one frequency means that one cannot determine the two values ν_Q and η with a simple pure NQR measurement. The application of a small magnetic field, discussed below, is often used to separately determine the two values. For many compounds studied using spin 3/2 NQR, η has not been separately determined. Often such data are interpreted using the assumption $\eta = 0$, which can yield a maximum error of about 16% in the determination of ν_Q .

2.2.2.3 Other Half-Integer Spins

Exact solutions are not known for $I > 3/2$. Tabulated results can be used [14], or it is now quite easy to diagonalize the Hamiltonian numerically. Expansions valid for smaller values of η are also available [15, 16]. Results of numerical computations for half-integer spins 5/2, 7/2, and 9/2 are shown in Figure 2.2. As is customary, the levels are labeled according to the largest component of the wavefunction, though m is only a good quantum number when $\eta = 0$. In addition, when $\eta \neq 0$ virtually all possible transitions are allowed though many are extremely weak. This is similar to what occurs for ^{10}B , mentioned above. The dotted lines in Figure 2.2 indicate some of these weaker transitions, which are not allowed at all when $\eta = 0$ but which may be usable for large η . Those weaker transitions are rarely used in practice but can be helpful when disentangling spectra observed for samples with multiple sites having large η (for example, see [17]).

When $\eta = 1$ it is possible, with some effort, to obtain exact solutions for half-integer spins up to $I = 9/2$. The resulting energy levels for these I are

$$\begin{aligned}
 I = 5/2: & \quad 0, \pm\sqrt{112/9} \\
 I = 7/2: & \quad \pm 2 \left[7 \pm 4\sqrt{7/3} \right]^{1/2} \\
 I = 9/2: & \quad 0, \pm 2 \left[22 \pm \sqrt{748/3} \right]^{1/2}
 \end{aligned} \tag{2.16}$$

in units of $h\nu_Q$.

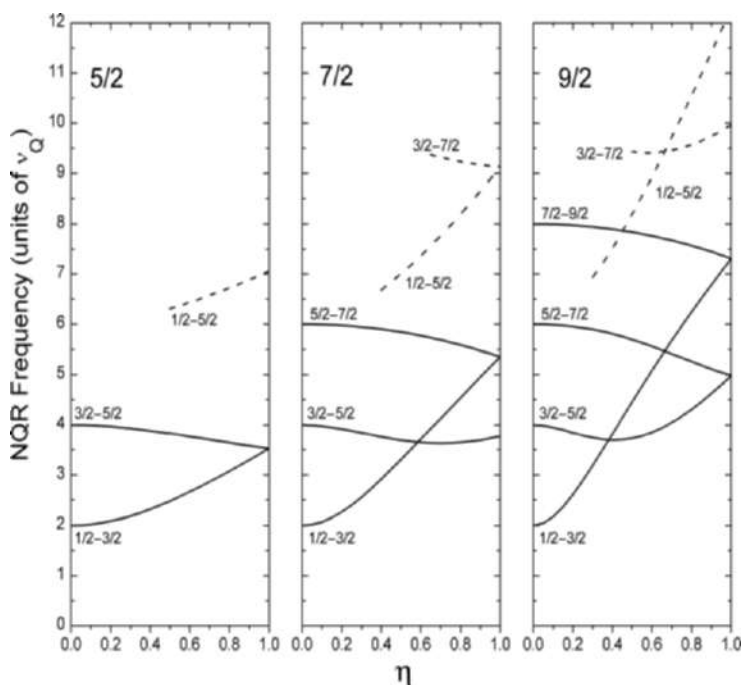


Figure 2.2 NQR transition frequencies for spins $5/2$, $7/2$, and $9/2$. The dashed lines are weaker transitions, which are forbidden when $\eta = 0$.

2.2.3 Excitation and Detection

In a typical NQR measurement transitions are induced between energy levels via the coupling between the nuclear magnetic dipole moment and a resonant time-dependent magnetic field, as is done for NMR. One could also imagine applying a time-dependent electric field gradient, however the required field strengths are much too large to be practical in the laboratory. The required time-dependent electric field gradients can be generated

indirectly by applying acoustic energy, a method important for the spectroscopic technique known as nuclear acoustic resonance (NAR) [18]. Due to practical considerations, NAR has proven to have limited utility.

To couple to the nuclear magnetic moment, the sample is placed within the RF magnetic field produced by an inductor which is carrying an alternating current (AC) of angular frequency, $\omega_r = 2\pi\nu_r$. Most commonly this is done by placing the sample within a solenoid that is part of a tuned circuit. If the AC magnetic field produced is uniform with magnitude, B_1 , and is in the x' -direction in a laboratory reference frame, the *interaction Hamiltonian* is

$$\mathcal{H}_1 = \gamma B_1 I_{x'} \cos(\omega_r t + \phi)$$

where γ is the gyromagnetic (or magnetogyric) ratio for the nucleus, $I_{x'}$ is the angular momentum operator for the component along the x' -direction, and ϕ is a phase factor.

For convenience, the energy eigenfunctions in the absence of the AC field, ψ_n , with energy $E_n = \hbar\omega_n$, can be expressed in terms of the eigenfunctions of I_z , u_m , where z corresponds to the z -direction of the principal axes system. That is,

$$\psi_n = \sum_{m=-I}^I b_{n,m} u_m. \quad (2.17)$$

Then in turn, the total time-dependent wavefunction can be written

$$\Psi(t) = \sum_n a_n(t) \psi_n \exp(-i\omega_n t), \quad (2.18)$$

where the complex coefficients $a_n(t)$ are to be determined. As written, those coefficients will be time-independent when the AC magnetic field is off. Since the AC magnetic field yields a relatively weak interaction \mathcal{H}_1 , compared to that of the static electric quadrupole field \mathcal{H}_Q , the coefficients a_n will vary relatively slowly with time. Placing the total wavefunction into Schrödinger's time-dependent wave equation,

$$-\frac{\hbar}{i} \frac{\partial \Psi}{\partial t} = (\mathcal{H}_Q + \mathcal{H}_1) \Psi, \quad (2.19)$$

and using the orthogonality of the eigenfunctions, the coupled equations for the coefficients, $a_n(t)$, are obtained,

$$\frac{\partial a_j}{\partial t} = \frac{i\gamma B_1}{2} \sum_k a_k \langle \psi_j | I_{x'} | \psi_k \rangle \left\{ e^{-i(\omega_k - \omega_j - \omega_r)t + i\phi} + e^{-i(\omega_k - \omega_j + \omega_r)t - i\phi} \right\}, \quad (2.20)$$

where $\langle \psi_j | I_{x'} | \psi_k \rangle$ is a constant. Expressing $I_{x'}$ in the principal axes system as

$$I_{x'} = c_x I_x + c_y I_y + c_z I_z \quad (2.21)$$

where the c_i are a shorthand notation for the directional cosines, then

$$\begin{aligned}
\langle \Psi_j | I_{x'} | \Psi_k \rangle = & \sum_m \left\{ m c_z b_{j,m}^* b_{k,m} \right. \\
& + (c_x - i c_y) (I(I+1) - m(m+1))^{1/2} \frac{b_{j,m+1}^* b_{k,m}}{2} \\
& \left. + (c_x + i c_y) (I(I+1) - m(m+1))^{1/2} \frac{b_{j,m-1}^* b_{k,m}}{2} \right\}. \tag{2.22}
\end{aligned}$$

Thus far there has been no approximation.

For simplicity, assume that just two states, labeled 1 and 2, with $E_2 > E_1$, are involved. The “slowly varying” part of the solution desired occurs when the time dependence in one of the exponentials becomes small. That will occur when the frequencies in one of the exponentials nearly cancel. The other exponentials will produce rapidly oscillating terms which will tend to average to zero. Keeping only the slowly varying terms, defining $\Omega = \gamma B_1 \langle \Psi_1 | I_{x'} | \Psi_2 \rangle e^{i\phi}$ and $\Delta\omega = \omega_r - (\omega_2 - \omega_1)$, the two coupled equations that result are

$$\begin{aligned}
\frac{\partial a_1}{\partial t} &= \frac{i\Omega}{2} a_2 e^{-i\Delta\omega t} \\
\frac{\partial a_2}{\partial t} &= \frac{i\Omega^*}{2} a_1 e^{+i\Delta\omega t}
\end{aligned} \tag{2.23}$$

which have solution

$$\begin{aligned}
a_1(t) &= e^{+i\Delta\omega t/2} \left[a_1(0) \cos\left(\frac{\omega_{\text{eff}} t}{2}\right) + i \frac{\Omega a_2(0) - \Delta\omega a_1(0)}{\omega_{\text{eff}}} \sin\left(\frac{\omega_{\text{eff}} t}{2}\right) \right] \\
a_2(t) &= e^{-i\Delta\omega t/2} \left[a_2(0) \cos\left(\frac{\omega_{\text{eff}} t}{2}\right) + i \frac{\Omega^* a_1(0) + \Delta\omega a_2(0)}{\omega_{\text{eff}}} \sin\left(\frac{\omega_{\text{eff}} t}{2}\right) \right]
\end{aligned} \tag{2.24}$$

where $a_1(0)$ and $a_2(0)$ are initial values at $t = 0$, and $\omega_{\text{eff}} = \sqrt{|\Omega|^2 + (\Delta\omega)^2}$.

The detection of the signal is also done using a coupling to the nuclear magnetic dipole moment. Knowing the wavefunction, we can compute the expectation value of the nuclear magnetic moment, $\bar{\mu}$, at any time. The component which is along the direction x' is given by

$$\langle \mu_{x'} \rangle = \gamma \hbar \sum_{j,k} a_j^* a_k \langle \Psi_j | I_{x'} | \Psi_k \rangle e^{-i(\omega_k - \omega_j)t}. \tag{2.25}$$

The total *nuclear magnetization* from N such nuclei, $M_{x'}$, can be written in terms of the ensemble average

$$M_{x'} = \gamma \hbar N \sum_{j,k} \langle a_j^* a_k \rangle \langle \psi_j | I_{x'} | \psi_k \rangle e^{-i(\omega_k - \omega_j)t}.$$

The set of values $\langle a_j^* a_k \rangle$ are, of course, the elements of the density matrix.

A time-dependent magnetization will generate an *electromotive force* (EMF, a voltage) $V(t)$, in a nearby inductor by Faraday's law of induction. If this inductor is the same one used above for excitation, then by reciprocity,

$$V(t) \propto \frac{dM_{x'}}{dt}. \quad (2.26)$$

A signal measured this way must arise from terms above where $j \neq k$. In thermal equilibrium $\langle a_j^* a_k \rangle$ will be zero for all $j \neq k$; after all, one cannot expect to continually extract electrical power in equilibrium. The role of the excitation is to disturb the thermal equilibrium so that a signal can be observed.

A common method to measure NQR signals is the pulse method where a relatively large AC magnetic field ($B_1 \approx 1$ to 100 G) is applied for a short time ($\tau_p \approx 1$ to 100 μ s), after which the EMF induced in the coil is detected. The other extreme is to continuously supply a low level AC magnetic field ($B_1 < 1$ G). In that case the transitions produced are balanced against those of thermal relaxation processes and a dynamic equilibrium is obtained. Then the steady state EMF induced by the nuclei which is in phase with the current in the inductor is equivalent to an electrical resistance, and that which is out of phase a reactance. Instrumentation will be discussed in more detail in the next section.

NQR is usually performed one transition at a time and hence any of these problems can be treated using the "effective spin 1/2" formalism [19, 20]. However, it is useful to consider what happens explicitly for the two common cases of $I = 1$ and $I = 3/2$ without using that formalism.

2.2.3.1 Example—Spin 1

For $I = 1$, the three energy levels and the corresponding wavefunctions are illustrated in Figure 2.3. For the sake of example, assume the transition labeled ν_+ is to be excited exactly on resonance ($\Delta\omega = 0$), and take $\phi = 0$. Then $\Omega = \gamma B_1 c_x$ and

$$\begin{aligned} a_+(t) &= a_+(0) \cos \frac{\Omega}{2} t + i a_0(0) \sin \frac{\Omega}{2} t \\ a_0(t) &= a_0(0) \cos \frac{\Omega}{2} t + i a_+(0) \sin \frac{\Omega}{2} t \\ a_-(t) &= a_-(0), \end{aligned} \quad (2.27)$$

which is exactly what one gets if one rotates the nucleus by an angle $\Omega t/2$ about the x -axis. Similar expressions are obtained for the other two transitions involving the other two axes. Such rotations are often conveniently treated using exponential operators. It is interesting that for spin 1 a simultaneous excitation of two transitions can also be described as a simple rotation of the spin [21].

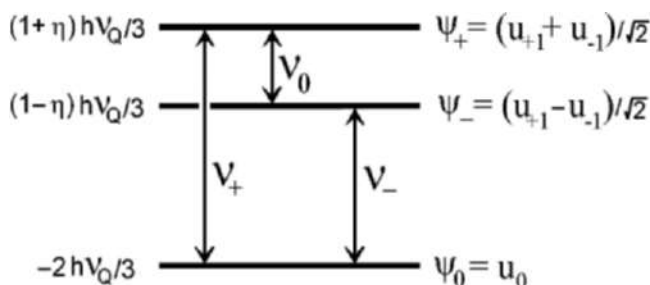


Figure 2.3 Energy levels and transitions for spin 1.

Starting from thermal equilibrium, the EMF after a time t will be

$$V(t) \propto c_x \omega_+ \left(\langle a_+^*(0)a_+(0) \rangle - \langle a_0^*(0)a_0(0) \rangle \right) \sin \Omega t \cos \omega_+ t, \quad (2.28)$$

which reaches a maximum at $\Omega t = \pi/2$ when the nucleus has been rotated by $\pi/4$. The term in parentheses is the population difference between the two levels determined by the Boltzmann distribution. For ^{14}N typical energy level splittings correspond to a temperature equivalent of about 0.1 mK and hence the thermal equilibrium population difference at room temperature is only about 1 part in 10^7 .

The motion of the spin in the absence of the AC field is not easy to visualize. The simple “counter rotating” picture obtained below for $I = 3/2$ does not apply even though one can use it to some extent to form a mental picture. The classical motion of a quadrupole system is discussed by Raich and Good [22].

Note that Ω depends on sample orientation and so for powder (or polycrystalline) samples one will have a broad distribution of values. This inherently large inhomogeneity in the “effective B_1 ” (here $B_{1\text{eff}} = B_1 c_x$) occurs for NQR of powder samples, but does not occur for NMR.

2.2.3.2 Example—Spin 3/2

The energy levels of the spin 3/2 system are doubly degenerate. The energy levels were given above and the corresponding wavefunctions can be written

$$\begin{aligned}\Psi_{\pm 3/2} &= \cos \delta u_{\pm 3/2} + \sin \delta u_{\mp 1/2} \\ \Psi_{\pm 1/2} &= \cos \delta u_{\pm 1/2} - \sin \delta u_{\mp 3/2}\end{aligned}\quad (2.29)$$

where $\sin \delta = [(\rho - 1)/2\rho]^{1/2}$ with $\rho = (1 + \eta^2/3)^{1/2}$ and the only non-zero transition frequency is $\nu = \rho \nu_Q$. In general all four transitions are allowed. However, it is always possible to create a new set of wavefunctions from linear combinations of states with the same energy. In particular,

$$\Psi'_{+3/2} = A\Psi_{+3/2} + B\Psi_{-3/2}; \quad \Psi'_{-3/2} = A\Psi_{-3/2} - B\Psi_{+3/2} \quad (2.30)$$

and similarly for $\Psi'_{\pm 1/2}$. Furthermore, a combination where only two of the four transitions are allowed can always be found. Once this has been done, the transformed spin 3/2 problem can be solved as two independent problems involving just two energy levels each [23]. The resulting classical picture for spin 3/2 NQR is that of an NMR experiment in an effective magnetic field involving the simultaneous measurement of two sets of (spin 1/2) nuclei, which are identical except for the sign of their gyromagnetic ratio. In the absence of the excitation one visualizes two sets of otherwise identical nuclei, precessing in opposite directions. Such a picture is a result of the degeneracy and generalizes to other half-integer spins.

The similarity between the classical picture used for NMR and that for spin 3/2 NQR leads to the use of “rotating reference frame” terminology for NQR even though it is perhaps not entirely appropriate.

2.2.4 The Effect of a Small Static Magnetic Field

The application of a small static magnetic field is sometimes advantageous and at other times it may simply be unavoidable. By “small” it is meant that the nuclear Zeeman interaction can be treated as a perturbation. In what follows, calculations will be carried out in the principal axes reference system. The Hamiltonian representing the Zeeman interaction can then be written

$$\mathcal{H}_z = -\gamma \hbar B_0 (c_x I_x + c_y I_y + c_z I_z), \quad (2.31)$$

where the directional cosines c_i may not be the same as those used previously. Any case can be treated numerically without difficulty, however it is worth taking a detailed look at spin 1 and spin 3/2 as representatives of what happens for integer and half-integer spins.

2.2.4.1 Spin 1

For the case of spin 1 with asymmetry parameter $\eta \neq 0$, there is no first-order shift in the energy levels. Using standard second-order perturbation theory the changes in the three transition frequencies are:

$$\Delta v_+ = \left(\frac{\gamma B_0}{2\pi v_Q} \right)^2 \left(\frac{3}{2} \frac{c_z^2}{\eta} + \frac{c_y^2}{(1-\eta/3)} + 2 \frac{c_x^2}{(1+\eta/3)} \right) v_Q \quad (2.32)$$

$$\Delta v_- = \left(\frac{\gamma B_0}{2\pi v_Q} \right)^2 \left(-\frac{3}{2} \frac{c_z^2}{\eta} + 2 \frac{c_y^2}{(1-\eta/3)} + \frac{c_x^2}{(1+\eta/3)} \right) v_Q \quad (2.33)$$

$$\Delta v_0 = \left(\frac{\gamma B_0}{2\pi v_Q} \right)^2 \left(3 \frac{c_z^2}{\eta} - \frac{c_y^2}{(1-\eta/3)} + \frac{c_x^2}{(1+\eta/3)} \right) v_Q, \quad (2.34)$$

where v_Q is as defined above. These are valid provided $\Delta v_0 \ll v_0$.

When $\eta = 0$, degenerate perturbation theory must be used and to lowest order one finds

$$\Delta v_{\pm} = \mp \frac{\gamma B_0}{2\pi} c_z \quad (2.35)$$

$$\Delta v_0 = 2 \frac{\gamma B_0}{2\pi} c_z, \quad (2.36)$$

a result which can also be used when $\eta \neq 0$ if the first calculation yields $\Delta v_0 \gg v_0$. The intermediate case where $\Delta v_0 \approx v_0$ is more complicated and will not be treated here.

For larger magnetic fields or when a more precise result is needed, the exact but more cumbersome solutions given by Muha can be used [24].

2.2.4.2 Spin 3/2

NQR in the presence of a small magnetic field is a principal method used to determine the asymmetry parameter η for spin 3/2.

The energy levels for spin 3/2, and for half-integer spins in general, will be degenerate regardless of the value of η and hence degenerate perturbation theory must be used. The four energy levels which result for spin 3/2, in the form presented by Brooker and Creel [25], become

$$E_{\pm 3/2} = \frac{h v_Q \rho}{2} \pm \frac{h v_0}{2\rho} \left[(\rho - 1 + \eta)^2 c_x^2 + (\rho - 1 - \eta)^2 c_y^2 + (2 + \rho)^2 c_z^2 \right]^{1/2} \quad (2.37)$$

$$E_{\pm 1/2} = -\frac{h v_Q \rho}{2} \pm \frac{h v_0}{2\rho} \left[(\rho + 1 - \eta)^2 c_x^2 + (\rho + 1 + \eta)^2 c_y^2 + (2 - \rho)^2 c_z^2 \right]^{1/2} \quad (2.38)$$

where $v_0 = \gamma B_0 / 2\pi$. In general all the transitions between these four levels are allowed. The four transitions shown in Figure 2.4 are of most interest. The highest and lowest frequency transitions, v_β and $v_{\beta'}$, will be somewhat "weaker" than the middle two. A computation of the transition probabilities is straightforward, though complicated enough that it will not be reproduced

here. The strength of each transition is a function of the relative orientations of the static magnetic field, the RF magnetic field, and the principal axes.

For multiple pulse measurements (described below) using a spin $3/2$ nucleus in a small magnetic field one can observe an additional effect called “slow beats” [26] due to the fact that all four of these transitions are excited and they are not independent of each other.

To separately determine ν_Q and η the transition frequencies can be measured as a function of sample orientation for single crystals or, less accurately, the spectral line shape (i.e., the frequency distribution) can be measured for powdered or polycrystalline samples [27, 28].

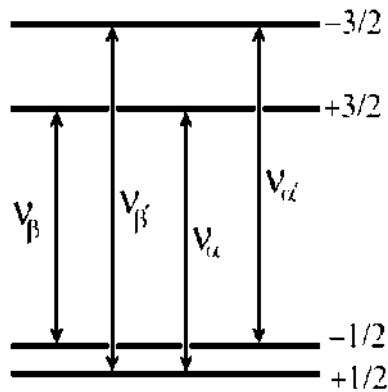


Figure 2.4 Energy levels and transitions for spin $3/2$ in a magnetic field aligned along the z -principle axis. The energy level splitting due to the magnetic field is greatly exaggerated.

2.2.5 Line Widths and Relaxation Times

In many cases the spectral line width in an NQR measurement is due to an inhomogeneous environment. That is, there is a distribution of frequencies due to small variations in the electric field gradients within the sample. The common causes for the inhomogeneity include impurities, crystal lattice defects, and even small thermal gradients within a sample. Inhomogeneous effects can be reduced through the use of carefully prepared samples and/or can be handled with pulsed methods and the spin echo techniques.

Two other important contributors to the spectral line width are dynamic effects due to motion at the atomic scale and nuclear magnetic dipole-dipole interactions. These are generally referred to as “homogeneous effects” since they apply equally to all the nuclei.

As is the case for NMR, there are several different relaxation times that can be measured. The so-called *spin-spin relaxation time*, T_2 , which may or

may not actually involve spin-spin interactions, characterizes the return of the ensemble to thermal equilibrium at some “spin temperature.” The *spin-lattice relaxation time*, T_1 , which is the inverse of the relaxation rate, characterizes the return of the ensemble of nuclei to thermal equilibrium with the surrounding crystal, usually called the “lattice.” The processes which determine T_1 involve exchange of energy between the nuclei and their surroundings—that is nuclear transitions are induced by the (random) fluctuations of the surroundings. In contrast, the interactions that are usually most effective for T_2 relaxation are those where there is no (net) gain or loss of energy from the nuclear ensemble. In general several mechanisms will contribute to the relaxation.

Typically only one of several possible transitions is excited and detected for NQR and so the phrase “the return to thermal equilibrium” is usually applied in the effective spin- $\frac{1}{2}$ sense. That is, the thermal ensemble includes just the two nuclear energy levels used, with the remaining levels now belonging to the lattice. This can give rise to relaxation characterized by multiple exponentials. A nice derivation of the effect for Nb ($I = 9/2$) is given by Chen and Slichter [29].

2.2.5.1 Spin-Lattice Relaxation and Temperature-Dependent Frequency Shifts

The coupling between the nuclei and the surrounding crystal will be due to time-dependent magnetic and/or electric quadrupole interactions. Magnetic interactions include those due to paramagnetic impurities and, in metals, the conduction electrons. A much weaker magnetic interaction can occur via a time-dependent spin-spin interaction. For materials with two readily available isotopes (e.g., Cl, Cu, Ga, Br, Rb, Sb, etc.), whether the relaxation is dominated by magnetic or electric quadrupole interactions can usually be determined by comparing the ratio of the relaxation times to the ratios of the magnetic dipole and electric quadrupole moments, respectively, for the two isotopes.

The contribution to the relaxation by the conduction electrons in metals is due to the so-called *Korringa result*, just as in NMR [30]. Hence, this contribution is very sensitive to changes in the electron density of states at the Fermi level, such as what one expects near superconducting phase transitions [31]. Korringa relaxation is also evident in some semiconductors [32]. Paramagnetic impurities generally contribute a constant to the rate, as they do for NMR.

In many NQR measurements of non-metals, the spin-lattice relaxation time and the temperature coefficient of the NQR frequency are both a result of lattice dynamics. This can be understood using the simple model proposed by Bayer [33]. Consider an electric quadrupole Hamiltonian that has been rotated about the y -axis by a small angle β . The new Hamiltonian (in the old principal axis coordinates) is given by

$$\begin{aligned} \mathcal{H}_Q = \frac{\nu_Q}{6} & \left[\left(\frac{3}{2} \cos^2 \beta - \frac{1}{2} + \frac{\eta}{2} \sin^2 \beta \right) (3I_z^2 - I^2) \right. \\ & + (3 - \eta) \sin 2\beta (I_z(I_+ + I_-) + (I_+ + I_-)I_z) \\ & \left. + \frac{1}{4} (3 \sin^2 \beta + \eta (1 + \cos^2 \beta)) (I_+^2 + I_-^2) \right] \end{aligned} \quad (2.39)$$

and if β represents a small, rapid oscillation about an equilibrium at $\beta = 0$, then one can expand and take a time average to determine the average coupling. Keeping the lowest non-zero terms one gets an average of

$$\mathcal{H}_Q = \frac{\nu_Q}{6} \left[\left(1 - \langle \beta^2 \rangle \frac{3 + \eta}{2} \right) (3I_z^2 - I^2) + \frac{1}{2} \left(\eta + \langle \beta^2 \rangle \frac{3 + \eta}{2} \right) (I_+^2 + I_-^2) \right]$$

and one can expect that $\langle \beta^2 \rangle$ increases with temperature. The time-dependent terms, with RMS amplitude $\langle \beta^2 \rangle^{1/2}$, can give rise to nuclear transitions and hence contribute to increase the relaxation rate $1/T_1$.

The theory of the dependence of the NQR frequency on temperature has been further developed by a number of authors [34–36]. While there are exceptions, near room temperature one can expect a temperature coefficient of order 1 kHz/K for most materials. Since NQR lines are often narrower than 1 kHz, even a small temperature change can be significant, and a small temperature gradient across the sample can significantly broaden the NQR line.

2.2.5.2 Spin-Spin Interactions

Nuclear magnetic dipole interactions between nuclei in a solid can produce some broadening of an NQR line, as happens for NMR. In an NMR experiment, the broadening due to the spin-spin interaction can be substantially reduced using a *magic angle spinning* (MAS) measurement. Spinning the sample is not effective for NQR and can make matters worse.

One way to estimate the size of the spin-spin interaction is to consider the size of the magnetic field due to a neighboring nucleus, typically of order 1 Gauss in solids, and then to treat the problem as in Section 2.2.4. It is easy to predict, quite correctly, that the effects for integer spin and half-integer spin will be very different. Except in a few isolated cases, the indirect dipole-dipole coupling (*e.g.*, J-coupling), one of the cornerstones of analysis for high resolution NMR spectroscopy, is not important for pure NQR work.

The method of moments developed by van Vleck for NMR [37], adapted to the NQR case, is often used to estimate the broadening due to the spin-spin interaction. As is the case for NMR, there are separate calculations for unlike

spins and like spins. For NQR there is an additional case for spins that are otherwise alike, but for which the directions of the principal axes are different. This latter case is sometimes referred to as “semi-like.” In the semi-like case the nuclear energy levels are degenerate, as is the case for like spins, however the geometry is more complicated.

One common way to compare the different situations is to compute the second moment for the somewhat artificial case of a cubic lattice of one type of nucleus. Such a comparison for several different cases is shown in Table 2.1. The characteristic decay time will be proportional to the inverse of the square root of the second moment.

Table 2.2 Results of some second moment calculations for NQR for the case of like nuclei in a cubic lattice of edge d . Results are in units of $\gamma^4 \hbar^4 / d^6$.

| Spin | Condition | Second Moment | Ref. |
|------|---------------|---------------|------|
| 1 | $\eta = 0$ | 28.2 | 40 |
| 1 | $\eta \neq 0$ | 22.1 | 40 |
| 3/2 | $\eta = 0$ | 60.0 | 38 |
| 5/2 | $\eta = 0$ | 108.1 | 39 |

For spin 1 with $\eta \neq 0$ the first-order dipole coupling to unlike nuclei is zero and second-order calculations are necessary. For ^{14}N NQR when there are nearby hydrogen nuclei, the second-order coupling to the hydrogen nuclei can actually be larger than the coupling between (like) ^{14}N nuclei. A detailed derivation for this case is given by Vega [40].

In many cases, the addition of a small magnetic field can change “semi-like nuclei” into “unlike nuclei,” resulting in a significant increase in the spin-spin relaxation time.

2.3 INSTRUMENTATION

The basic physics for NQR signal detection is the same as for NMR signal detection. Hence, NQR spectrometers are similar to NMR spectrometers in design [41]. Of course NQR does not require a large external magnetic field and associated field control circuitry. High speed sample spinning, often used for NMR, is also not appropriate for NQR and will not be present. Since magnetic field homogeneity and spinning are not at issue, sample size is limited only by the available RF power and convenience.

Early NQR and NMR instruments were largely based on relatively simple oscillator designs including the super-regenerative oscillator [42], the

marginal oscillator [43], and the self-limiting “Robinson” oscillator circuit [44]. All of these are generally referred to as *continuous wave* (CW) techniques. For all of these oscillators the frequency is determined by an LC resonant circuit with the sample placed within (or near) the inductor L . The frequency is scanned by changing the capacitance C , either mechanically or electrically. Modern versions of these simple and inexpensive designs are still useful, particularly when searching for a signal over a broad range of frequencies and/or where small size is important [45]. Increasingly, however, computer-controlled pulsed spectrometers, similar to those now used for NMR, are employed for NQR. The sample is also within (or near) an inductor which is part of a tuned circuit, though the frequency is now determined by a separate reference oscillator.

For well-built NQR spectrometers, the principal source of electrical noise is the thermal noise from the LC tuned circuit. For best signal-to-noise ratios, care should be taken to minimize the resistive losses (i.e., maximize the quality factor) for that circuit. The signal-to-noise expected from an NQR measurement can be roughly estimated using expressions for an NMR measurement using the same nucleus at the same frequency [46–48].

In addition to the more common designs, several alternative techniques for NQR detection have been recently proposed, a few of which are also discussed below in Section 2.3.4.

2.3.1 CW Spectrometers

The use of a *marginal oscillator* for nuclear magnetic resonance originated with Pound and Knight [49, 50]. A number of transistorized versions of that circuit have appeared [51–54]. The marginal oscillator, as its name implies, uses just enough feedback to sustain low-level oscillations. That is, just enough energy is supplied by an active device (e.g., a transistor) as is lost and the behavior of the active device is still relatively linear. When additional energy is absorbed by the nuclei the level of oscillation can change significantly. The Robinson circuit, also now developed as a transistorized version for NQR [55], uses an additional bit of circuitry to maintain the level of feedback at a fixed value. The Robinson design is particularly useful for scans over a large frequency range.

The *super-regenerative spectrometer* is essentially a super-regenerative radio receiver but designed to detect the induced EMF from the nuclei rather than distant radio stations. An excellent explanation of how a super-regenerative receiver functions is presented by Insam [56]. In the super-regenerative circuit, the feedback condition is alternated between two states, one which maintains oscillations and one which does not. When switched from the non-oscillating or “quenched” state to the oscillating state, the time for the oscillations to build up to a predetermined level will depend on the

initial signal. That is, if one assumes an exponential growth in voltage starting at a value $V(0)$ and with a time constant τ , the time t to grow to a level $V_0 > V(0)$ is given by $t = \tau \ln(V_0/V(0))$.

Hence, in the presence of an induced EMF plus noise the oscillations will build up to the predetermined level sooner than with noise alone. The quenching signal may be generated by separate circuitry or one can design circuits which self quench. Due to the nonlinearity of the detection process (e.g., the logarithm above), one should not expect to obtain accurate line shapes with this type of spectrometer.

For the continuous wave (CW) techniques, and particularly for powder samples, additional sensitivity is often achieved using a set of external magnetic field coils which are switched on and off, combined with phase sensitive (“lock-in”) detection. Typically 10–100 G fields are used at 10–100 Hz. When the magnetic field is on (with any polarity), the NQR signal is broadened sufficiently so that it is unobservable. Effectively, the magnetic field alternately turns the NQR signal on and off and only the change in the signal are recorded. Thus, all baseline errors are removed. Note that a similar technique is used for CW-NMR (usually with a sinusoidal magnetic field) resulting in a derivative signal. For NMR the magnetic field shifts the signal in frequency a bit rather than destroying it.

As an alternative to an on/off magnetic field, the frequency of an NQR oscillator circuit can be modulated electronically using a varicap diode or similar device as part of the LC tuned circuit. With phase sensitive detection, one obtains a derivative signal (in the limit of small modulation) though often with significant baseline problems.

2.3.2 Pulsed Spectrometers

The electronics of pulsed NQR spectrometers is virtually identical to that of broad-band NMR spectrometers except without a large magnet. In fact, many pulsed NQR spectrometers are also used (with a magnet) as broad-band NMR spectrometers and vice versa. Since the pulsed method is much more versatile than the CW techniques, the vast majority of modern NQR measurements are made using pulse methods. Many of the pulse techniques began as NMR techniques and have been adapted to the NQR environment. Since significant inhomogeneous broadening is common in NQR (See section 2.2.5), one of the most important techniques is the use of spin-echoes, and related multiple-pulse techniques, for the study of these broadened lines.

A basic computer-controlled single channel pulsed NQR spectrometer is shown schematically in Figure 2.5. As is the case for NMR, the signals are often recorded in *quadrature*. That is, signals, which are in phase (cosine-like) and 90° out of phase (sine-like) with a stable reference source, are

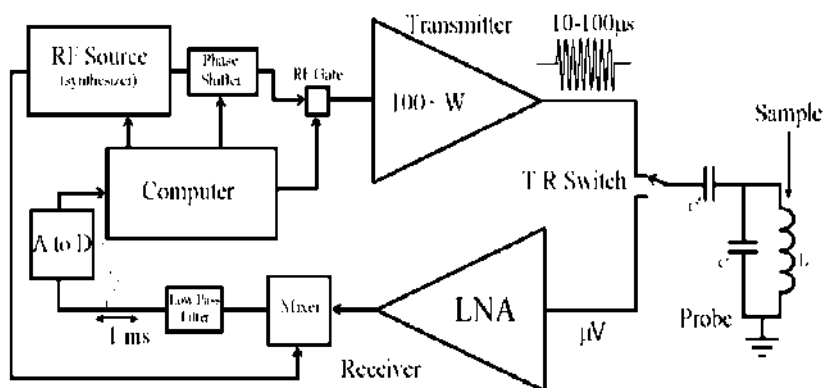


Figure 2.5 Schematic of a simple computer-controlled pulsed NQR spectrometer.

simultaneously recorded in two channels. Due to their treatment under Fourier transform, and some carryover from CW-NMR terminology, these two signals are also sometimes referred to as the “real” and “imaginary” signals and/or “absorption” and “dispersion” signals, respectively. After heterodyning and filtering, the recorded signals have a frequency which is the difference between that of the RF reference and that of the nuclear magnetization. In many modern spectrometers, the analog to digital conversion is done before heterodyning, with the mixing and filtering performed digitally.

The transmit/receive (T/R) switch shown is usually implemented using passive circuitry. One common circuit is based on the scheme developed by Low and Tarr [57], which uses semiconductor diodes and quarter wavelength transmission lines. At frequencies below about 10 MHz, common in NQR, the quarter wavelength transmission lines are replaced with lumped circuit equivalents. Other tuned circuits using diodes can also be employed [58].

While the low noise amplifiers (LNAs) are protected from damage by such a passive T/R circuit, the receiver will be overdriven and there will be some “dead time” following the pulse while the receiving circuitry recovers. At lower frequencies this is exacerbated by the ringing of the LC tuned circuit containing the sample. When this ringing is a bad enough, additional circuitry can be added to damp the oscillations, such as a “Q-switch,” and/or one can switch the phase of the applied RF pulse by 180° for a short time just before the RF is turned off. The latter approach can be quite demanding on the high power amplifier.

The simplest pulsed experiment is the application of a single pulse with a duration τ_p set to maximize the signal (1 to 100 μs typically). This is referred to as a 90° or $\pi/2$ pulse in analogy to the NMR case, though the simple classical picture, that this corresponds to a rotation of the nucleus by 90° , is

not valid. For powders, slightly longer pulses (approximately 30% longer) are used, compared to oriented single crystals, since many of the crystallites have a less than optimal orientation [59, 60]. The time-dependent signal after the pulse is referred to as the *free induction decay* (FID). If the spectral line shape is of interest, or in the rare case that there is more than one spectral line within the excitation band width (~ 10 kHz) then the signal will be Fourier transformed.

Simple spin-echoes are often very useful. The simplest is a two pulse measurement sometimes referred to as the *Hahn echo* with a 90° pulse, a time delay τ , a 180° pulse (twice the duration of a 90° pulse), followed by acquisition. The echo signal appears a time τ after the second pulse. All time-independent inhomogeneous interactions will be “refocused” by such a pulse sequence. Figure 2.6 illustrates FID (one pulse) and simple echo (two pulse) signals using one of the Br NQR transitions of ZnBr_2 .

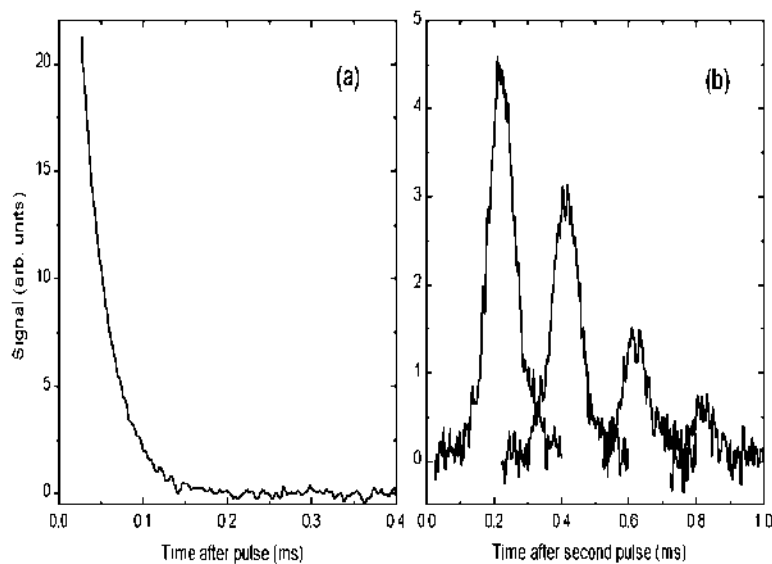


Figure 2.6 Room temperature pulse NQR signals from the 79.75 MHz ^{81}Br transition in a powder sample of ZnBr_2 showing (a) a free induction decay (FID) after a single pulse and (b) echoes obtained using a two-pulse sequence for four different delay times ($\tau = 0.2, 0.4, 0.6,$ and 0.8 ms).

As is the case for NMR, phase shifts are often applied to the RF pulses and they are often labeled as they are in NMR. That is, a “ $\pi/2_x$ ” pulse and a “ $\pi/2_y$ ” pulse are 90° out of phase with each other. Phase cycling during signal averaging, in order to remove the effects of some spectrometer imperfections, is also common [61].

In the case of weaker signals, spin-echoes may be reformed many times using *steady state free precession* (SSFP) [62, 63] or *spin-lock spin-echo*

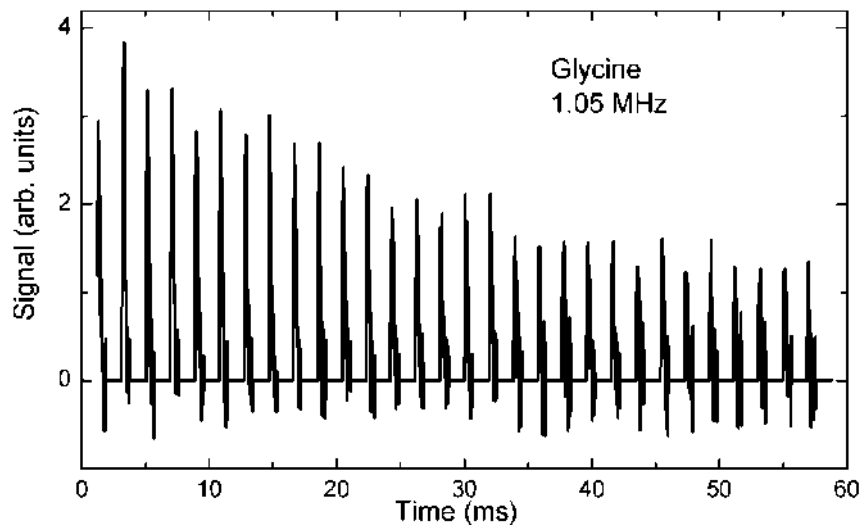


Figure 2.7 Multiple ^{14}N spin-echo signals from a spin-lock spin-echo (SLSE) pulse train. Data courtesy of J.B. Miller.

(SLSE) *pulse trains* [64, 65]. An example of such a measurement is shown in Figure 2.7.

Some more advanced work on pulse techniques includes the simultaneous excitation of two (or more) NQR transitions on the same nucleus [66–68] and various techniques to improve on the inherently inhomogeneous effective B_1 field for powder samples [69–71].

2.3.3 Field Cycling NQR Spectrometers

Field cycling spectrometers are often used to improve the sensitivity, particularly for low frequency NQR measurements and also in cases of low natural abundance. There are several different types of field cycling measurements referred to as NQR measurements – the most common are pulsed double resonance techniques where the actual measurement is an NMR measurement.

In a field cycling spectrometer the sample is alternatively subjected to a large magnetic field and a small (or zero) magnetic field. Since large magnetic fields are difficult to turn on and off rapidly, this is commonly achieved by physically moving the sample. Using pneumatics, this can be routinely accomplished over a distance of about 1 m in about 100 ms or less.

In its simplest form, the sample is placed in a very high magnetic field to obtain a large nuclear splitting and hence a large population difference. After

equilibrium is reached, the magnetic field is reduced and RF is applied at the NQR frequency, the magnetic field is reintroduced, and an NMR measurement is performed. This method can be applied to half-integer spins directly [72] or for any spin using double resonance [73]. For the latter, ^1H is most often used as the second nucleus since it is easily observed using NMR.

For double resonance one relies on “contact” between the two nuclei some time during the measurement. Contact here refers to the case where the nuclear energy level splittings for the two nuclei match and the nuclei are physically close enough so that they can interact (e.g., via the nuclear magnetic dipole interaction). That match can occur either in the presence or absence of RF irradiation(s). When there is a match, there is efficient transfer of energy between the two types of nuclei in the same way there is transfer of energy between two weakly coupled, identical pendulums.

In an alternative form useful for compounds that contain hydrogen, the large polarizations that can be achieved for ^1H in a high magnetic field can be transferred, in part, to the nucleus to be measured and then a traditional NQR measurement is made. While not as sensitive, this technique has the advantage that a highly uniform magnetic field is not required for the NMR measurement. For example, initial exposure to the nonuniform magnetic field of permanent magnets can be used to obtain a large, though non-uniform, initial ^1H polarization, which can then be transferred to ^{14}N prior to an NQR measurement [74].

2.3.4 Some Less Common NQR Detection Schemes

The direct NQR techniques mentioned above all rely on Faraday’s law of induction. Since the signal is generated by the time rate of change of the magnetic flux, these techniques lose sensitivity at low frequencies. In contrast, in a growing number of cases it is possible to detect the magnetic flux directly, rather than its time derivative. At present, these alternative detection schemes are difficult to implement on a routine basis.

A *superconducting quantum interference device*, or SQUID, is sensitive to magnetic flux and can have a very low noise level. For use as a pure NQR detector, the time-dependent nuclear magnetization is detected after a perturbation. Unlike the NMR case, however, there is no static nuclear magnetization. NQR signals have been detected using a SQUID at frequencies as low as few tens of kHz up to about 1 MHz [75–78].

A second flux detection technique recently proposed for NQR utilizes an optical transition in an alkali metal vapor in a way that is very sensitive to magnetic fields [79]. It is, in essence, a form of optically detected electron paramagnetic resonance (EPR) in a very weak static magnetic field. For NQR detection the time-dependent resonant magnetic field is supplied by the precession of the nearby nuclear magnetic moments to be detected.

A disadvantage for many pulsed NQR measurements at lower frequencies is the “dead time” after an applied pulse. Eles and Michal [80] have recently developed a method for spin 3/2 using a strong excitation at half the resonant frequency yielding a two-photon excitation, followed by traditional detection. The advantage is that the excitation frequency is well-separated from the receiver frequency, thus allowing the dead time to be virtually eliminated.

Another interesting NQR technique, which does not rely on magnetic flux at all was recently reported [81]. A close relative of *perturbed angular correlation* (PAC) techniques, the β -decay is measured from radioactive ^8Li nuclei after they are implanted in a material using a polarized beam. The β particles are then emitted in a direction determined by the nuclear polarization. A resonant sinusoidal magnetic field alters the nuclear polarization and thus affects the β count rate. While the number of isotopes available for such studies may be limited, it is noted that only about 10^7 nuclei are required for this technique, far fewer than are required for other NQR techniques.

2.4 INTERPRETATION OF COUPLING CONSTANTS

The contribution of the electric quadrupole field (eq in e^2qQ) can be computed for a known charge distribution surrounding a nucleus. From that the coupling constant can be estimated and compared to experiment. With modern computational techniques for materials, the largest uncertainty is often that due to the uncertainty in nuclear electric quadrupole moment, Q . For many measurements, however, of most importance are the relative changes from one situation to another, and not the absolute values. For example, one might be concerned with the differences in bonding between two similar compounds, one may be studying structural changes in the lattice during a phase transition, or one might be concerned with general correlations between NQR and other properties [82].

There are three broad situations encountered for electric quadrupole field calculations. The easiest to handle are molecular crystals where the charge distribution near the nucleus is predominantly determined by covalent bonds. For those compounds, relatively straightforward molecular computations can be made and one can expect only a small “solid effect” due to the stacking of molecules within the crystal structure. The two other cases are for ionic and metallic materials, respectively.

The electric quadrupole field at the origin due to a point charge of magnitude 1 (in cgs units) at a position $(x_1, x_2, x_3) = (x, y, z)$ relative to a nucleus at the origin is found by taking the second derivatives of the usual Coulomb potential. That computation gives

$$V_{ij} = \frac{1}{r^3} \left(\frac{3x_i x_j}{r^2} - \delta_{ij} \right),$$

where r is the distance to the origin. Since superposition applies, the field from a charge distribution is computed as the sum of the contributions from all the charges involved. Due to the $1/r^3$ dependence and charge neutrality within a unit cell, the most important contributions are those due to charges near the nucleus.

2.4.1 Molecular Crystals and Covalently Bonded Groups

Electron wavefunctions, and hence quadrupole coupling constants, can be easily computed using *ab initio* computation techniques. To understand and describe trends, however, it is often convenient to describe the electron wavefunctions in covalently bonded systems using a *linear combination of atomic orbitals* (LCAO) approach. Since filled electron (atomic) shells have a spherical charge distribution, only the outer electrons need be considered. There is also a response of the inner core electrons to the presence of an electric field gradient, which is quite important but which is ignored for the moment.

Consider an occupied electronic p_z -orbit which is (quite generally) described by a wavefunction ψ , as

$$\psi = \left(\frac{1}{2} \sqrt{\frac{3}{\pi}} \cos \theta \right) f(r) \quad (2.40)$$

where $f(r)$ is the (separately normalized) radial part of the wavefunction and, of course, $\cos \theta = z/r$. Then, for example,

$$\begin{aligned} V_{zz} &= -e \int_{r=0}^{\infty} \int_{\phi=0}^{2\pi} \int_{\theta=0}^{\pi} \psi^* \frac{3 \cos^2 \theta - 1}{r^3} \psi r^2 \sin \theta d\theta d\phi dr \\ &= -\frac{3e}{2} \int_{r=0}^{\infty} \frac{1}{r^3} r^2 |f(r)|^2 \int_{\theta=0}^{\pi} \cos^2 \theta (3 \cos^2 \theta - 1) \sin \theta d\theta dr \\ &= -\frac{4e}{5} \int_{r=0}^{\infty} \frac{1}{r^3} r^2 |f(r)|^2 dr = -\frac{4e}{5} \left\langle \frac{1}{r^3} \right\rangle \equiv e q_p \end{aligned} \quad (2.41)$$

and similarly for other terms and other orbitals. Note that $\langle 1/r^3 \rangle \approx 1/a_0^3$, where a_0 is the Bohr radius, so $V_{zz} \approx 10^{18}$ V/cm/cm. Values of $\langle 1/r^3 \rangle$ from nonrelativistic [83] and relativistic [84] atomic calculations are available.

For a more general combination of atomic orbitals the following should be noted [85, 86]. First, s-orbitals are spherical and do not contribute. Furthermore, cross-terms involving s-orbitals and p-orbitals, and p-orbitals and d-orbitals are zero due to symmetry within the integral. Cross-terms between s- and d-orbitals are usually neglected. For molecular wavefunctions using the

LCAO-MO picture, the contributions from orbitals on other atoms will be small.

Hence, with a_x^2 , a_y^2 , and a_z^2 the respective weights for p_x , p_y , and p_z contributions to the wavefunction from orbitals on the atom in question, one gets

$$\begin{aligned} V_{zz} &= e q_p \left[3a_z^2 - (a_x^2 + a_y^2 + a_z^2) \right] / 2 \\ V_{xx} &= e q_p \left[3a_x^2 - (a_x^2 + a_y^2 + a_z^2) \right] / 2 \\ V_{yy} &= e q_p \left[3a_y^2 - (a_x^2 + a_y^2 + a_z^2) \right] / 2 \end{aligned} \quad (2.42)$$

and note that $a_x^2 + a_y^2 + a_z^2 \leq 1$ though the entire wavefunction must be normalized. If there is a small s or d contribution to the wavefunction, the largest impact on the electric field gradient is likely via the reduction in the weights for the p-orbitals. The total electric field gradient is computed using the sum of the contributions from all the occupied valence wavefunctions.

2.4.2 Ionic Crystals

In principle, the computation of the electric field gradient in an ionic material is straightforward. The ions are replaced by point charges and the appropriate lattice sums are performed [87]. To achieve accurate values and reasonably fast convergence, it is necessary to take some care in the way the sum is computed.

To understand why care must be exercised, consider the following inaccurate method. First the contribution from all the negative charges is added out to a large distance R . Then, the contributions from the positive charges are added, again out to the distance R . The two sums are then subtracted from one another. Such a technique fails since the quadrupole field falls as $1/r^3$ but the number of neighboring ions in a spherical shell a distance r away grows as r^2 . Hence, the total contribution falls as $1/r$, and the individual sums tend to diverge. The net result is the relatively small difference between two very large values. Furthermore, the use of an arbitrary cut-off R does not guarantee that the total calculation is charge neutral, which can lead to a significant systematic error.

To obtain accurate values and rapid convergence, terms in these lattice sums should be grouped appropriately. A simple method which has rapid convergence is to use a sum over conventional unit cells where the nucleus in question has been centered. In addition, ions of charge q which are on the boundary of n conventional unit cells are included in all of the unit cells, but with a charge q/n for each [88]. The use of a conventional unit cell ensures that charge neutrality and the symmetry of the crystal are included at every step. The field produced from each neighboring unit cell will be that of an electric dipole, or more often a higher order multipole, which will fall off much faster with distance than that of a point charge.

For numerical computations terms of comparable magnitude should be grouped together. Symbolically, the appropriate lattice sum would then be

$$V_{ij} = \sum_{\text{all } R} \left\{ \sum_{\substack{\text{unit cells at} \\ \text{distance } R}} \left[\sum_{\substack{\text{ions in conven-} \\ \text{tional unit cell}}} \frac{q}{r^3} \left(\frac{3x_i x_j}{r^2} - \delta_{ij} \right) \right] \right\} \quad (2.43)$$

where r is the total distance from the origin to the ion and q is the appropriate, possibly fractional, charge for that ion. Alternative approaches include the explicit use of multipole expansions and/or the Fourier transformation of the lattice.

Field gradients computed using this type of point charge model for the ions will certainly need to be corrected as discussed below in Section 2.4.4.

2.4.3 Metals

A very simple model for a metal is the “uniform background lattice,” where the conduction electrons are considered to be uniformly distributed and the remaining positive ions are treated as point charges [89]. To achieve convergence for the electric quadrupole field, charges near the origin need to be avoided, however. Metals with narrow conduction bands can often be treated using the tight binding model, which is treated as in Section 2.4.1. To go much beyond these simple models the problem becomes very complicated very quickly and will depend on the specific metal being considered. The interested reader is referred to the review articles by Kaufmann and Vianden [90] and by Das and Schmidt [91].

For simple metals the temperature dependence of the quadrupole coupling often varies as the 3/2 power of the (absolute) temperature. That is

$$v_Q(T) = v_Q(0) \left(1 - \alpha T^{3/2} \right), \quad (2.44)$$

where α is a constant. This temperature dependence is associated with the changes in the electronic structure in the presence of thermal vibrations [92].

2.4.4 Sternheimer Shielding/Antishielding

The slight rearrangement of the core electrons in the presence of an electric field gradient has so far been neglected. A series of works by Sternheimer [93] has shown, however, that the effects on the observed quadrupole coupling constant can be far from negligible. There are two Sternheimer shielding factors which are usually considered, one associated with charges which are on the atom (or ion) in question, R , and one associated with more distant charges, γ_∞ . These factors are often negative and are then referred to as “antishielding” factors. If eq_{atomic} is the magnitude of the computed electric

field gradient associated with electrons on the atom (e.g., the valence electrons) and eq_{ext} is that due to charges on other atoms, then the observed value eq_{obs} is predicted to be

$$eq_{\text{obs}} = eq_{\text{atomic}} (1 - R) + eq_{\text{ext}} (1 - \gamma_{\infty}) . \quad (2.45)$$

More rigorously the atomic and external terms should be combined as tensor, rather than scalar, quantities. Table 2.3 shows a selection of typical shielding values for γ_{∞} .

Table 2.3 Typical Sternheimer factors for several ions.

| Atom/Ion | γ_{∞} |
|------------------|-------------------|
| Na | -3.7 |
| Na ⁺ | -3.7 |
| Al ²⁺ | -1.8 |
| Cl ⁻ | -60 |
| Br ⁻ | -110 |
| Rb ⁺ | -50 |
| I ⁻ | -160 |

Agreement between γ_{∞} values computed using different methods is no better than $\pm 10\%$ and in many cases much worse. It is clear, however, that the correction can be quite large. Computed values for R can be so dependent on the specific electronic configuration used that one is prone to wonder about the utility of having such values. In the majority of cases, R is of order 0.1.

Of course, a rigorous *ab initio* computation of the electronic structure of a material (including the core electrons, band structure effects, etc.) will not require these additional corrections. Computer codes available for electronic structure calculations are often optimized for computations of energies, rather than electron densities, and hence any quadrupole coupling constants produced from such programs should be used with caution.

2.5 SUMMARY

NQR is a radio frequency spectroscopy akin to wide line NMR but without a large magnet. NQR uses nuclei with spin $I > \frac{1}{2}$ to probe the environment in a material. The NQR frequency will be determined by the (time-averaged) distribution of electric charge in the vicinity of a nucleus, and that distribution depends on the material being investigated. The quadrupole coupling constant, the relaxation times after an excitation, and the effects of small magnetic fields, along with modeling and comparison to other similar materials, are used to extract information about the material.

Bibliography

For additional general information, interested readers should consult one or more of the following:

- Nuclear quadrupole resonance spectroscopy, T.P. Das and E.L. Hahn, Supplement 1 of *Solid State Physics* (Academic Press, NY, 1958).
- Nuclear quadrupole resonance spectroscopy, E. Schempp and P.J. Bray, Chapter 11 of *Physical Chemistry, An Advanced Treatise, Vol IV, Molecular Properties*, D. Henderson (ed.), pages 521–632 (Academic Press 1970).
- Nuclear quadrupole resonance spectroscopy, J.A.S. Smith, *J. Chem. Education*, Vol 48, Nos. 1–4, pages 39–49, A77–A89, A147–A148, A159–170, and A243–A252, (1971).
- Nuclear quadrupole resonance in inorganic chemistry, Yu. A. Buslaev, E.A. Kravchenko, and L. Kolditz, published as Volume 82 of *Coordination Chemistry Reviews* (Elsevier, Amsterdam, 1987).
- Nuclear Quadrupole Coupling Constants*, Lucken E.A.C (Academic Press, London and New York, 1969).
- Principles of Nuclear Magnetism*, A. Abragam (Oxford Univ. Press, Oxford, 1961).
- Principles of Magnetic Resonance*, 3rd Ed., C.P. Slichter, (Springer-Verlag, Heidelberg, 1989).
- Experimental Pulse NMR – A Nuts and Bolts Approach*, E. Fukushima and S.B.W. Roeder (Addison-Wesley Publishing, Reading, MA, 1981).

REFERENCES

- [1] Pound, R.V. (1950) *Phys. Rev.* **79**, 685-702.
- [2] Dehmelt, H.G. & Kruger, H. (1950) *Naturwiss.* **37**, 111-112.
- [3] Das, T.P. & Hahn, E.L. (1958) *Nuclear Quadrupole Resonance Spectroscopy, Supplement 1 of Solid State Physics*, Seitz F. & Turnbull D. (eds) (New York, Academic).
- [4] Ohte, A., Iwaoka, H., Mitsui, K., Sakurai, H. & Inaba, A. (1979) *Metrologia***15**, 195-199.
- [5] Huebner, M., Leib, J. & Eska, G. (1999) *J. Low Temp. Phys.* **114**, 203-230.
- [6] Garroway, A.N., Buess, M.L., Miller, J.B., Suits, B.H., Hibbs, A.D., Barrall, G.A., Matthews, R. & Burnett, L.J. (2001) *IEEE Trans. Geosci. Remote Sens.* **39**, 1108-1118.
- [7] Segel, S.L. (1978) *J. Chem. Phys.* **69**, 2434-2438.
- [8] Thyssen, J., Schwerdtfeger, P., Bender, M., Nazarewicz, W. & Semmes, P.B. (2001) *Phys. Rev. A* **63**, 022505:1-11.
- [9] Gerginov, V., Derevianko, A. & Tanner, C.E. (2003) *Phys. Rev. Lett.* **91**, 072501:1-4.
- [10] Slichter, C.P. (1990) *Principles of Magnetic Resonance*, 3rd Ed., (Heidelberg, Springer-Verlag)
- [11] Bain, A.D. & Khasawneh, M. (2004) *Concepts Magn. Reson.* **22A**, 69-78.
- [12] Butler, L.G. & Brown, T.L. (1981) *J. Magn. Reson.* **42**, 120-131.
- [13] Hiayama, Y., Butler, L.G. & Brown, T.L. (1985) *J. Magn. Reson.* **65**, 472-480
- [14] Cohen, M.H. (1954) *Phys. Rev.* **96**, 1278-1284.
- [15] Bersohn, R. (1952) *J. Chem. Phys.* **20**, 1505-1509.
- [16] Wang, T-C. (1955) *Phys. Rev.* **99**, 566-577.

- [17] Suits, B.H. & Slichter, C.P. (1984) *Phys. Rev. B* **29**, 41-51.
- [18] Sundfors, R.K., Bolef, D.I. & Fedders, P.A. (1983) *Hyperfine Interactions* **14**, 271-313.
- [19] Lee, Y.K. (2002) *Concepts Mag. Reson.* **14**, 155-171.
- [20] Vega, S. (1978) *J. Chem. Phys.* **68**, 5518-5527.
- [21] Sauer, K.L., Suits, B.H., Garroway, A.N. & Miller, J.B. (2001) *Chem. Phys. Lett.* **342**, 362-368; (2003) *J. Chem. Phys.* **118**, 5071-5081.
- [22] Raich, J.C. & Good Jr. R.H. (1963) *Am. J. Physics* **31**, 356-362.
- [23] Bloom, M., Hahn, E.L. & Herzog B. (1955) *Phys. Rev.* **97**, 1699-1709.
- [24] Muha, G.M. (1980) *J Chem Phys* **73**, 4139-4140; (1982) *J. Magn. Reson.* **49** 431-443.
- [25] Brooker, H.R. & Creel, R.B. (1974) *J. Chem. Phys.* **61**, 3658-3664.
- [26] Bloom, M. (1954) *Phys. Rev.* **94**, 1396-1397.
- [27] Creel, R.B., von Meerwall, E.D. & Brooker, H.R. (1975) *J. Magn. Reson.* **20**, 328-333.
- [28] Sunitha, Bai N., Reddy, N. & Ramachandran, R. (1993) *J. Magn. Reson. A* **102**, 137-143.
- [29] Chen, M.C. & Slichter, C.P. (1983) *Phys. Rev. B* **27**, 278-292.
- [30] Korrington, J. (1950) *Physica* **16**, 601-610.
- [31] For Example see Martindale, J.A., Barrett, S.E., Durand, D.J., O'Hara, K.E., Slichter, C.P., Lee, W.C. & Ginsberg, D.M. (1994) *Phys. Rev. B* **50**, 13645-13652.
- [32] Matsamura, M., Saskawa, T., Takabatake, T., Tsuji, S., Tou, H. & Sera, M. (2003) *J. Phys. Soc. Japan* **72**, 1030-1033.
- [33] Bayer, H. (1951) *Z. Physik* **130**, 227-238.
- [34] Kushida, T., Benedek, G.B. & Bloembergen, N. (1956) *Phys. Rev.* **104**, 1364-1377.
- [35] Schempp, E. & Silva, P.R.P. (1973) *Phys. Rev. B* **7** 2983-2986; (1973) *J. Chem. Phys.* **58**, 5116-5119.
- [36] Alexander, S. & Tzalmona, A. (1965) *Phys. Rev.* **138**, A845-A855.
- [37] van Vleck, J.H. (1948) *Phys. Rev.* **74**, 1168-1183.
- [38] Abragam, A. & Kambe, K. (1953) *Phys. Rev.* **91**, 894-897.
- [39] Nagel, O.A., Ramia, M.E. & Martin, C.A. (1996) *Appl. Magn. Reson.* **11**, 557-566.
- [40] Vega, S. (1973) *Advances in Magn. Reson.* **6**, 259-302.
- [41] Suits, B.H. (1994) in Trigg G. L. (ed.) *Encyclopedia of Applied Physics, Vol. 9*, 71-93 (VCH Publishers).
- [42] Roberts, A. (1947) *Rev. Sci. Instrum.* **18**, 845-848.
- [43] Pound, R.V. & Knight, W.D. (1950) *Rev. Sci. Instrum.* **21**, 219-225.
- [44] Robinson, F.N.H. (1959) *J. Sci. Instrum.* **36**, 481-487.
- [45] Kim, S.S., Mysoor, N.R., Carnes, S.R., Ulmer, C.T. & Halbach, K. (1997) In *Proceedings of the 16th Digital Avionics Systems Conference (DASC)*, Irvine, CA, (IEEE, New Jersey), pp. 2.2-142.2-23.
- [46] Hill, H.D.W. & Richards, R.E. (1968) *J. Phys. E: Sci. Inst. Series 2*, **1**, 977-983.
- [47] Hoult, D.I. & Richards, R.E. (1976) *J. Magn. Reson.* **24**, 71-85.
- [48] Hoult, D.I. (1973) *Prog. NMR Spec.* **12**, 41-77.
- [49] Pound, R.V. & Knight, W.D. (1950) *Rev. Sci. Instrum.* **21**, 219-225.
- [50] Pound, R.V. (1952) *Prog. Nucl. Phys.* **2**, 21-50.
- [51] Viswanathan, T.L., Viswanathan, T.R. & Sane, K.V. (1968) *Rev. Sci. Instrum.* **39**, 472-475; (1970) *Rev. Sci. Instrum.* **41**, 477-478
- [52] Zikumaru, Y. (1990) *Z. Naturforsch.* **45a**, 591-594.
- [53] Sullivan, N. (1971) *Rev. Sci. Instrum.* **42**, 462-465.
- [54] Offen, R.J. & Thomson, N.R. (1969) *Phys. Educ.* **4**, 264-267.
- [55] Robinson, FNH. (1982) *J. Phys. E: Sci. Instrum.* **15**, 814-823.
- [56] Insam, E. (2002) *Electronics World* **108**(1792) 46-53.
- [57] Lowe, I.J. & Tarr, C.E. (1968) *J. Phys. E: Sci. Instrum.* **1**, 320-322.
- [58] McLachlan, L.A. (1980) *J. Magn. Reson.* **39**, 11-15.
- [59] Bloom, M., Hahn, E.L. & Herzog, B. (1955) *Phys. Rev.* **97**, 1699-1709.
- [60] Vega, S. (1974) *J. Chem. Phys.* **61**, 1093-1100.

- [61] Stejskal, E.O. & Schaefer, J. (1974) *J. Magn. Reson.* **13**, 249-251.
- [62] Bradford, R., Clay, C. & Strick, E. (1951) *Phys. Rev.* **84**, 157-158.
- [63] Rudakov, T.N., Mikhaltsevitch, V.T., Flexman, J.H., Hayes, P.A., & Chisholm, W.P. (2004) *Appl. Magn. Reson.* **25**, 467-474.
- [64] Marino, R.A. & Klainer, S.M. (1977) *J. Chem. Phys.* **67**, 3388-3389.
- [65] Cantor, R.S. & Waugh, J.S. (1980) *J. Chem. Phys.* **73**, 1054-1063.
- [66] Grechishkin, V.S., Anferov, V.P. & Ja., N. (1983) *Adv. Nucl. Quadrupole Reson.* **5** 1; Greschishkin, V.S. (1990) *Z. Naturforsch.* **45a**, 559-564.
- [67] Sauer, K.L., Suits, B.H., Garroway, A.N. & Miller, J.B. (2001) *Chem. Phys. Lett.* **342**, 362-368; (2003) *J. Chem. Phys.* **118**, 5071-5081.
- [68] Furman, G.B. & Goren, S.D. (2002) *Z. Naturforsch.* **57a** 315-319.
- [69] Miller, J.B., Suits, B.H., Garroway, A.N. (2001) *J. Magn. Reson.* **151**, 228-234.
- [70] Miller, J.B. & Garroway, A.N. *Appl. Magn. Reson.* **25**, 475-483.
- [71] Ramamoorthy, A. & Narasimhan, P.T. (1990) *Z. Naturforsch.* **45a** 581-586.
- [72] Ivanov, D. & Redfield, A.G. (2004) *J. Magn. Reson.* **166**, 19-27.
- [73] Slusher, R.E. & Hahn, E.L. (1968) *Phys. Rev.* **166**, 332-347.
- [74] Luznik, J., Pirnat, J. & Trontelj, Z. (2002) *Sol. State Commun.* **121**, 653-656.
- [75] Hürlimann, M.D., Pennington, C.H., Fan, N.Q., Clarke, J., Pines, A. & Hahn, E.L. (1992) *Phys. Rev. Lett.* **69**, 684-687.
- [76] TohThat, D.M. & Clarke, J. (1996) *Rev. Sci. Instrum.* **67**, 2890-2893.
- [77] Augustine, M.P., TohThat, D.M. & Clarke, J. (1998) *Solid State Nucl. Magn. Reson.* **11**, 139-156.
- [78] Greenberg, Ya.S. (1998) *Rev. Mod. Phys.* **70**, 175-222; 2000 *Rev. Mod. Phys.* **72**, 329.
- [79] Savukov, I.M., Seltzer, S.J., Romalis, R.V. & Sauer, K.L. (2005) *Phys. Rev. Lett.* **95**, 063004:1-4.
- [80] Eles, P.T. & Michal, C.A. (2005) *J. Magn. Reson.* **175**, 201-209.
- [81] Salman, Z., Reynard, E.P., MacFarlane, W.A., Chow K. H., Chakhalian, J., Kreitzman, S.R., Daviel, S., Levy, C.D.P., Poutissou, R. & Kiefl, R.F. (2004) *Phys. Rev. B* **70**, 104404:1-7.
- [82] Weiss, A. & Wigand, S. (1990) *Z. Naturforsch.* **45a**, 195-212.
- [83] Fischer, C.F. (1977) *The Hartree-Fock Method for Atoms* (Wiley & Sons, NY).
- [84] Lindgren, I. & Rosén, A. (1974) *Case Studies Atomic Phys.* **4**, 197-298.
- [85] Townes, C.H. & Dailey, B.P. (1949) *J. Chem. Phys.* **17**, 782-796.
- [86] Schempp, E. & Bray, P.J. (1970) Vol. IV, Chap. 11 of Henderson D (ed.) *Physical Chemistry: An Advanced Treatise*, Academic Press, New York, London.
- [87] Hutchings, M.T. in Seitz, F. & Turnbull, D. (eds.) (1964) *Solid State Physics* **16** (Academic Press, New York and London), 227-273.
- [88] Frank, F.C. (1950) *Philos. Mag.* **41**, 1287-1289.
- [89] de Wette, F.W. & Schacher, G.E. (1965) *Phys. Rev.* **137**, A92-A94.
- [90] Kaufmann, E.N. & Vianden, R.J. (1979) *Rev. Mod. Phys.* **51**, 161-214.
- [91] Das, T.P. & Schmidt, P.C. (1986) *Z. Naturforsch.* **41a** 47-77.
- [92] Jena, P. (1976) *Phys. Rev. Lett.* **36**, 418-421.
- [93] Sternheimer, R.M. (1951) *Phys. Rev.* **84**, 244-253; 1951 *Phys. Rev.* **86**, 316-324; 1954 *Phys. Rev.* **95**, 736-750; 1986 *Z. Naturforsch.* **41a**, 24-36.